

100
1908 - 2008



UNIVERSITEIT VAN PRETORIA
UNIVERSITY OF PRETORIA
YUNIBESITHI YA PRETORIA

Gold compounds with anti-HIV and immunomodulatory activity

Pascaline N. Fonteh

s28594267

MSc. Biochemistry, cum laude, 2008, University of Johannesburg,
former Rand Afrikaans University

Submitted in partial fulfilment of the degree

Philosophiae Doctor Biochemistry

In the Faculty of Natural and Agricultural Sciences

University of Pretoria

Pretoria

2nd December 2011

100
1908 - 2008



UNIVERSITEIT VAN PRETORIA
UNIVERSITY OF PRETORIA
YUNIBESITHI YA PRETORIA

SUBMISSION DECLARATION

I Pascaline N. Fonteh hereby declare that this thesis which is herewith submitted to the Faculty of Natural and Agricultural Sciences for the degree of *Philosophiae* doctor Biochemistry at the University of Pretoria is my own work and has not been previously submitted for a degree at this or any other tertiary institution.

Date: _____

Signature _____

Plagiarism Declaration:

UNIVERSITY OF PRETORIA
FACULTY OF NATURAL AND AGRICULTURAL SCIENCES
DEPARTMENT OF BIOCHEMISTRY

Full name: _____ Student number: _____

Title of the work _____

Declaration

1. I understand what plagiarism entails and I am aware of the University's policy in this regard.
2. I declare that this _____ (e.g. essay, report, project, assignment, dissertation, thesis etc) is my own, original work. Where someone else's work was used (whether from a printed source, the internet or any other source) due acknowledgement was given and reference was made according to departmental requirements.
3. I did not make use of another student's previous work and submit it as my own.
4. I did not allow and will not allow anyone to copy my work with the intention of presenting it as his or her own work.

Signature _____ Date _____

TABLE OF CONTENT

DEDICATION	VI
ACKNOWLEDGEMENTS	VII
PREFACE	VIII
PUBLICATIONS: _____	VIII
AWARDS: _____	VIII
CONFERENCES: _____	VIII
SUMMARY	IX
LIST OF FIGURES	X
LIST OF TABLES	XII
LIST OF IMPORTANT ABBREVIATIONS	XIII
CHAPTER 1	1
INTRODUCTION _____	1
CHAPTER 2	5
LITERATURE REVIEW AND BACKGROUND _____	5
2.1 HIV AND AIDS _____	5
2.1.1 Epidemiology _____	6
2.1.2 Mode of Transmission _____	7
2.1.3 HIV Genome Organisation and Structure _____	7
2.1.4 Life Cycle and Course of Infection _____	8
2.1.5 HIV and the Immune System _____	11
2.1.6 Vaccine Development _____	13
2.1.7 Therapy _____	14
2.1.7.1 HIV reverse transcriptase and inhibitors _____	14
2.1.7.2 HIV protease and inhibitors _____	16
2.1.7.3 HIV integrase and inhibitors _____	17
2.1.7.4 Viral entry and inhibitors _____	19
2.1.7.5 Cytostatic inhibitors and virostatic combinations _____	20
2.1.7.6 Novel targets _____	22
2.1.8 Therapy Complications and the Need for Novel Drug Development _____	23
2.1.8.1 Viral resistance to available drugs _____	23
2.1.8.2 Drug toxicity to host _____	24
2.1.8.3 Other limitations _____	24
2.1.8.4 Cure limitations _____	25
2.1.8.5 Local needs _____	25
2.2 DRUG DEVELOPMENT _____	26
2.3 METALLODRUGS _____	27
2.3.1 Brief Background _____	27
2.3.2 Gold Compounds as Metallodrugs _____	28
2.3.2.1 Gold compounds as anti-rheumatoid arthritic agents _____	29
2.3.2.2 Gold compounds as anti-cancer agents _____	29
2.3.2.3 Gold compounds as anti-malarial agents _____	30
2.3.2.4 Gold compounds as anti-HIV agents _____	31
2.3.3 Some Anti-HIV Mechanisms of Gold Compounds _____	31
2.3.3.1 Ligand exchange reactions _____	31
2.3.3.2 Stripping of peptides from class II MHC _____	32
2.3.3.3 Modulation of cytokine production _____	33
2.3.4 Side Effects of Gold-Based Therapy _____	33
2.4 HYPOTHESIS AND MAIN RESEARCH QUESTIONS _____	34
2.4.1 Were the Gold Compounds Drug-Like? _____	34

2.4.2 What were the Effects of the Gold Compounds on Host Cells and Whole Virus? _____	34
2.4.3 Could the Gold Compounds Inhibit Viral Enzymes, and How? _____	35
2.5 SCREENING STRATEGY AND METHODOLOGY _____	36
2.5.1 Drug-likeness Studies _____	38
2.5.2 The Effect of the Compounds on Host Cells and on Whole virus. _____	38
2.5.3 The Effects of the Compounds on Viral Enzymes _____	39
2.5.4 Statistical Analysis _____	40
2.6 OTHER RESEARCH OUTCOMES _____	40

CHAPTER 3 _____ **41**

GOLD COMPOUNDS: STRUCTURE AND DRUG-LIKENESS _____ **41**

SUMMARY _____ **41**

3.1 INTRODUCTION _____	41
3.2 COMPOUNDS _____	44
3.2.1 The Gold(I) Phosphine Chloride-containing Complexes – Class I _____	45
3.2.2 The Bis(phosphino) Hydrazine Gold Chloride-containing Complexes – Class II _____	47
3.2.3 The gold(I) Phosphine Thiolate-based Complexes - Class III _____	49
3.2.4 The gold(III) Tscs-based Complexes – Class IV _____	50
3.2.5 The Gold(III) Pyrazolyl-based Complex – Class V _____	52
3.3 MATERIALS AND METHODS _____	53
3.3.1 NMR Studies for Stability Determination _____	53
3.3.2.1 Human intestinal absorption prediction model _____	55
3.3.2.2 Aqueous solubility prediction model _____	55
3.3.2.3 Blood brain barrier penetration prediction model _____	56
3.3.2.4 Cytochrome P4502D6 prediction model _____	56
3.3.2.5 Hepatotoxicity prediction model _____	56
3.3.2.6 Plasma protein binding prediction model _____	57
3.3.2.7 Currently available ARV drugs as Controls for ADMET predictions _____	57
3.3.3 Shake Flask Method for Lipophilicity Measurement _____	57
3.4 RESULTS AND DISCUSSION _____	58
3.4.1 NMR Profiles _____	58
3.4.1.1 ³¹ P and ¹ H NMR chemical shifts of the gold(I) phosphine chloride complex TTC3 _____	58
3.4.1.2 ³¹ P and ¹ H NMR chemical shifts of the BPH gold(I) chloride complex EK231 _____	59
3.4.1.3 ³¹ P and ¹ H NMR chemical shifts of the gold(I) thiolate complexes MCZS3 and PFK174 _____	59
3.4.1.4 ¹ H NMR chemical shifts of the gold(III) thiosemicarbazone complex, PFK7 _____	60
3.4.1.5 ¹ H NMR chemical shifts of the gold(III) pyrazolyl complex, KFK154b _____	60
3.4.1.6 Summary of NMR Stability Profiles _____	61
3.4.2 <i>In silico</i> ADMET Predictions _____	62
3.4.2.1 Prediction of human intestinal absorption _____	62
3.4.2.2 Prediction of aqueous solubility _____	66
3.4.2.3 Prediction of blood brain barrier penetration _____	66
3.4.2.4 Prediction of cytochrome P450 2D6 inhibition _____	67
3.4.2.5 Prediction of hepatotoxicity _____	68
3.4.2.6 Prediction of plasma protein binding ability _____	68
3.4.2.7 Drug-likeness summary for the compounds _____	69
3.4.3 Shake Flask Method of Lipophilicity Determination _____	70
3.5 CONCLUSIONS _____	70

CHAPTER 4 _____ **73**

COMPOUND-INDUCED HOST CELL RESPONSES AND EFFECTS ON WHOLE VIRUS _ **73**

SUMMARY _____ **73**

4.1 INTRODUCTION	74
4.2 MATERIALS AND METHODS	77
4.2.1 Cells	77
4.2.1.1 Isolation of primary cells from whole blood	77
4.2.1.2 Culturing of continuous cell lines	78
4.2.2 Compound Preparation	79
4.2.3 Cell Viability Assays	79
4.2.3.1 HTS dye assays for determining cell viability	80
4.2.3.2 Effect of the compounds on cell viability by flow cytometry	81
4.2.4 Effect of the Compounds on Cell Proliferation	83
4.2.4.1 Compound effects on the proliferation of PBMCs by use of CFSE	83
4.2.4.2 Compound effects on the proliferation profile of TZM-bl cells by RT-CES assessment	85
4.2.5 Virus Infectivity Inhibition Ability of Compounds by Luciferase Gene Expression Assay	86
4.2.6 Effects of Compounds on Immune System Cells Using Multi-parametric Flow Cytometry	88
4.2.7 Experimental Summary	90
4.3 RESULTS AND DISCUSSION	91
4.3.1 Cell Viability Determination	91
4.3.2 Cell Proliferation Determination	94
4.3.2.1 Monitoring proliferation using CFSE	94
4.3.2.2 Monitoring proliferation using a RT-CES device	96
4.3.3 Inhibition of Viral Infectivity by Determining Luciferase Gene Expression from TZM-bl Cells	100
4.3.4 Effects of Compounds on T Cell Frequency and on Inflammation	103
4.4 CONCLUSION	110
CHAPTER 5	114
COMPOUND EFFECTS ON VIRAL ENZYMES	114
SUMMARY	114
5.1 INTRODUCTION	115
5.2 MATERIALS AND METHODS	117
5.2.1 Direct Enzyme-Based Assays	117
5.2.1.1 RT inhibition assay	117
5.2.1.2 PR inhibition assay	118
5.2.1.3 IN inhibition assay	119
5.2.2. Molecular Modelling to Predict Potential Binding Sites	120
5.2.2.1 Ligand preparation	121
5.2.2.2 Receptor preparation	122
5.2.2.3 Docking with CDOCKER	124
5.2.2.4 Ligand minimization	125
5.2.2.5 Energy calculations and analysis of minimized poses (Scoring)	125
5.2.2.6 Summary of methods used	126
5.3 RESULTS AND DISCUSSION	126
5.3.1 Direct Enzyme Assays	126
5.3.1.1 HIV RT and PR activity	126
5.3.1.2 HIV IN activity	128
5.3.2. Molecular Modelling for Predicting Binding Interactions with Enzyme Active Sites.	129
5.3.2.1 Binding modes between ligands and RT sites	131
5.3.2.2 Binding modes of ligands to the HIV PR site	139
5.3.2.3 Binding modes of the ligands with HIV IN sites	140
5.4 CONCLUSION	145
CHAPTER 6	147

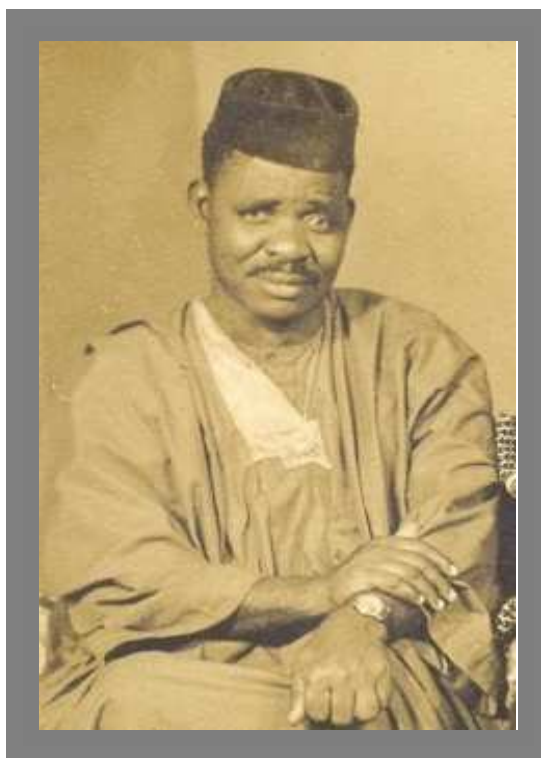
CONCLUDING DISCUSSION & FUTURE WORK	147
6.1 COMPOUNDS: STRUCTURE AND DRUG-LIKE PROPERTIES	148
6.2 EFFECTS OF COMPOUNDS ON HOST CELLS AND WHOLE VIRUS	149
6.3 EFFECTS OF COMPOUNDS ON VIRAL ENZYMES	151
6.4 ANSWERS TO RESEARCH QUESTIONS	151
6.4.1 Were the Compounds Drug-like?	152
6.4.2 What Were the Effects of the Compounds on Host cells and Whole Virus?	152
6.4.3 Were the Compounds Capable of Inhibiting Viral Enzymes and How?	152
6.4.4 Other Questions	152
6.4.4.1 Did complexation enhance anti-viral activity?	152
6.4.4.2 Was activity class and oxidation state related?	153
6.4.4.3 What was the effect of complexation on drug-likeness?	153
6.5 RECOMMENDATIONS	154
6.5.1 Bioassays should be Complemented with <i>In Silico</i> Molecular Modelling Studies	154
6.5.2 Incorporate Real Time Techniques in Drug Discovery Studies	154
6.5.3 The Need for Therapies to Inhibit Immune Activation	154
6.5.4 Test the Prodrug in Bioassays	155
6.5.5 Management of DMSO Compound Stocks	155
6.6 NOVEL CONTRIBUTIONS	157
6.7 FUTURE WORK	158
6.7.1 Structural Modification To Improve Solubility and Activity	158
6.7.3 Determine the Oxidation State of Gold Within Cells	159
6.7.4 RT-CES Analysis	159
6.7.5 Combination Studies of PFK7 and PFK8 with dNTP Analogues.	159
6.7.6 Determine if Compounds with Anti-proliferative Effects can Prevent T Cell Activation	159
6.7.7 Determine Viral Core Protein (p24) Secretion as Measure for Viral Infectivity	160
6.7.8 Cell Cycle Analysis to Determine the Phase Affected by Cytostatic Compounds	160
6.7.9 Preselect T Cells Prior to Treatment	160
6.7.10 Docking Considerations	160
6.8 CONCLUSION	161
CHAPTER 7	162
REFERENCES	162
CHAPTER 8	180
APPENDIX	180
8.1 CHAPTER 2	180
8.1.1 Statistical Definitions	180
8.2 CHAPTER 3	181
8.2.1 NMR chromatograms	181
8.2.1.1 The effect of water on the NMR spectra of gold complex TTC3	181
8.2.1.2 The ³¹ P and ¹ H NMR spectra of MCZS3	182
8.2.1.3 The ¹ H spectra of PFK7	183
8.2.1.4 The ¹ H NMR spectra of KFK154b after 24 h and 7 days	184
8.3 CHAPTER 4	184
8.3.1 Viability Assay Optimisations	184
8.3.1.1 MTT data optimisation	185
8.3.1.2 MTS data optimisation	187
8.3.1.3 Lactate dehydrogenase assay optimisations	188
8.3.1.4 Viability optimisation using flow cytometry and propidium iodide	190
8.3.2 CFSE Incubation Time and Stimulant Optimization	190
8.3.2.1. Time optimisation	190
8.3.2.2 Stimulant optimisation	191
8.3.3 Other Flow Cytometry Optimisations	192
8.3.3.1 Gating optimisation	192

8.3.3.2 Stimulant optimization _____	193
8.3.4 RT-CES Analyser Repeats _____	195
8.3.5 Infectivity Studies, CC ₅₀ and IC ₅₀ _____	197
8.3.6 Immune System Cells: Function Determination _____	197
8.3.6.1 Differences in CD4+ and CD8+ cell frequency. _____	197
8.3.6.2 ELISA data _____	198
8.4 CHAPTER 5 _____	200
8.4.1 Anti-RT Inhibitory Ability of Previously Anti-RT Complexes as Controls. _____	200
8.4.1.1 Poor aqueous solubility and solvent (DMSO) associated solubility limitations _____	200
8.4.1.2 NMR stability profile _____	201
8.4.1.3 Compound age and solvent used at synthesis _____	202
8.4.1.4 Poor stereochemical interaction with the RNase H site of RT _____	202
8.4.1.5 Other concerns and future perspectives _____	203
8.4.2 IN 3'P and ST Inhibitory Assay _____	203
8.4.3 Molecular Modelling _____	204
8.4.3.1 Summary of docked poses for each receptor _____	204
8.4.3.2 Structure of amino acids _____	205
8.4.3.3 Molecular surface diagram of TTC10 in the RNase H site of RT _____	206
8.4.3.4 KFK154B binding to 3LP3 in the presence of Mn ²⁺ ions _____	207
8.4.3.5 Molecular surface diagram of PFK5 and PFK7 with the LEDGF binding site of IN _	207
8.4.3.6 Molecular surface diagram of PFK7 with the sucrose binding site of IN _____	208
GLOSSARY _____	209

DEDICATION

To my **GOD** and **LORD ALMIGHTY** for giving me the strength, supreme guidance, the means and the understanding to have pursued this project to this point.

To my late dad **Papa Lucas Che Fonteh** (1927 - Jan 1981); for your believe in the education of your children and for being our “Fo-nteh” or main rock. It’s been 30 years since you left us to be with the LORD and despite the fact that I vaguely remember you, the zeal to keep your legacy alive still burns in me and I always wish I had known you better. RIP daddy.



Papa Lucas Che Fonteh (1927 - 1981)

And

To my late niece/sister/champion/adviser **Isabella A. Ade-Tamungang** (Nov. 1974 - Feb 2011): your zeal for success and passion in everything you did made you my role model. I know your next project was pursuing a Ph.D, by dedicating this to you, I hope it somehow fulfils that plan you had on earth. I will forever miss you. Words can’t express how hurt I was finding out that your death could have been avoided. Only the Good LORD knows why and I continue to praise HIM even in my pain. RIP Issa.

ACKNOWLEDGEMENTS

The contribution(s) of the following people and institutions were instrumental in the realisation of this project, to whom I express sincere gratitude and appreciation:

- Prof. Debra Meyer, my supervisor, for being an influential, insightful critic, persistent guide and mentor throughout the planning and execution phases.
- The Project AuTEK Biomed team (Mintek and Harmony Gold) for financial support and for access to the compounds screened herein and to the chemists who undertook the design and synthesis of these compounds (Dr. Frankline Keter, Telisha Traut, Dr. Erik Kriel, Dr. Mabel Coyanis, Dr. Zolisa Sam, Prof. Bradley Williams and Dr. Judy Coates).
- The University of Pretoria for providing the platform for the execution of this work and for financial support.
- L'ORÉAL/UNESCO for the 2010 Women in Science Fellowships (for Women in Science in Sub-Saharan Africa).
- The South African National Research Foundation (NRF) for additional funding especially for flow cytometry instrumentation and reagents.
- Special thanks to the chemists who provided assistance with the interpretation of the NMR data, Dr. Frankline Keter, Mr. Mohammed Balogun and Ms Afag Elkhadir.
- Dr. Tessa Little for providing molecular modelling training and assistance.
- I would like to thank the staff at the Student Health Centre (University of Pretoria), the Kings Hope Development Foundation Clinic, the Fountain of Hope Hospital and the Steve Biko Academic Hospital for their assistance with obtaining blood samples.
- Special thanks to my mum and role model (Mami Susan Fonteh, for keeping dad's will for his children and your unconditional love and support), my brothers (Mathias, Alfred, Samuel) and sisters (Anne, Lucy, Judith, Marie) for their motivation, love and spiritual support.
- To Felix for his continual support, love and patience, my girls Khien and Ateh and my son, Fon, your little cries gave me a reason to push on.
- The HIV research team of 2008-2011 at the University of Pretoria, especially Aurelia Williams for being there throughout the laughs, tough times and the never to be forgotten fun memories in the laboratory and beyond.
- The Bungus and the friends whom I have found as family here in SA, especially my lady friends, Aurelie, Mercy, Alice and Tessy, for all the moral support when I needed it most.

Pascaline Fonteh

PREFACE

Portions of this thesis have been published in peer reviewed journals, and presented at both local and international conferences while other sections are under preparation for submission for peer review.

Publications

- Fonteh P., Keter K., Meyer D. (2010). HIV therapeutic possibilities of gold compounds. *Biometals*, 23; 185-196. **Review paper.**
 - Fonteh P, Keter K, Meyer D., (2011). New bis(thiosemicarbazone) gold(III) complexes inhibit HIV replication at cytostatic concentrations: potential for incorporation into virostatic cocktails. *Journal of Inorganic Biochemistry*, 105; 1173-1180. **Original Paper.**
- NB:** Please see copies of the review and original paper at the end of this thesis.
- Fonteh P. and Meyer D. (2011). The inhibition of HIV-1 infectivity of TZM-bl cells by gold(I) phosphine compounds is related to cytostasis, In preparation.

Awards

The following are awards received by Fonteh P. in the course of this study:

- Travel award by the World Gold Council to attend the Gold2009 Conference in Heidelberg, Germany (April 2009).
- L'ORÉAL/UNESCO fellowship award for Women in Science in Sub-Saharan Africa in March 2010 (awarded on the 30th of March 2010, in Johannesburg, South Africa)
- Scholarship award (conference registration) by the South African AIDS organising committee (April 2011) sponsored by SIDA, CDC and the Bill and Melinda gates Foundation to attend the 5th SA AIDS conference, Durban, South Africa, 7th-10th of June 2011.
- Travel support from NIH through the Infectious Disease Society of America (IDSA) and HIV Medical Association to attend the 49th IDSA meeting in Boston, MA, USA (20th-23rd October 2011).
- WhiteScience Travel support (16th August 2011) to attend the IDSA meeting in Boston, MA, USA.

Conferences

- Fonteh P. and Meyer D. 2009. Poster presentation entitled: Chrysotherapy: evaluating the anti-HIV activity of novel gold(I) compounds. Gold2009 Conference (26th-29th July 2009, Heidelberg, Germany).
- Fonteh P, 2010. Overview of research project on gold compounds as anti-HIV agents/Challenges of being a female scientist. Network of UNESCO Chairs "Women, Science and Technology" conference (20th-30th March 2010, Johannesburg, South Africa).
- Fonteh P., Meyer D., 2010. Poster presentation titled: Cytostasis: a novel anti-HIV mechanism of gold(III) bithiosemicarbazone compounds to remedy drug resistance. The 5th SA AIDS Conference (7th-10th June 2011, Durban, South Africa).
- Fonteh P. 2011. Experiences as a L'ORÉAL/UNESCO fellow: impact on the realisation of the PhD project. Workshop on the promotion of women in science in Africa (29th-30th June 2011).
- Fonteh P., Meyer D. Poster presentation entitled: The inhibition of HIV-1 infectivity of TZM-bl cells by gold(I) phosphine compounds is related to cytostasis. The 49th IDSA meeting, Boston, MA, USA (20th-23rd October 2011).

SUMMARY

GOLD COMPOUNDS WITH ANTI-HIV AND IMMUNOMODULATORY ACTIVITY

by

PASCALINE N. FONTEH

Supervisor: **Prof. Debra Meyer**

Department: **Biochemistry**

Degree: **Ph.D Biochemistry**

The human immunodeficiency virus (HIV) and acquired immune deficiency syndrome (AIDS) that subsequently develops remain major health concerns even after three decades since the first cases were reported. Successful therapeutic measures to address HIV/AIDS consist mostly of combinations of drugs targeting viral enzymes including reverse transcriptase (RT), protease (PR) and integrase (IN) as well as entry steps of the viral life cycle. The remarkable benefits (e.g. improved quality of life) derived from the use of these agents are unfortunately limited by toxicity to the host and the development of drug resistant viral strains. Drug resistance limits the repertoire of drug combinations available. Unfortunately, because latent forms of the virus exists, therapy has to be life-long and with new infections occurring every day, resistant strains tend to spread. To circumvent these problems, new drugs that inhibit resistant strains or work against new viral targets have to be developed. The history of gold compounds as potential inhibitors of HIV prompted this study in which twenty seven compounds consisting of gold(I), gold(III) and precursors from five classes were tested for drug-likeness, anti-HIV and immunomodulatory effects using wet lab and *in silico* methodologies. Cytotoxicity determination was done using viability dyes and flow cytometry. Cell proliferation profiles were monitored using the carboxyfluorescein succinimidyl ester dye dilution technology and a real time cell analyser for confirming viability dye findings. The compounds' effects on viral enzymes was determined using direct enzyme assays and *in silico* molecular modelling techniques. ^1H and ^{31}P nuclear magnetic resonance spectroscopy studies for determining stability revealed that the backbone chemical shifts of the compounds were relatively unchanged after one week (-20 and 37 °C) when dissolved in dimethylsulfoxide. Eight of the gold compounds had drug-like properties comparable to clinically available drugs when *in silico* predictions were performed. The 50% cytotoxic dose of the compounds in human cells was between 1 and 20 μM (clinically relevant concentrations for gold compounds). Three gold(I) compounds inhibited viral infectivity at non-toxic concentrations and two gold(III) compounds did so at cytostatic (anti-proliferative mechanism that is also anti-viral) concentrations. In the immunomodulatory assay, cytokine levels were altered by five compounds with one gold(I) and a gold(III) compound significantly reducing the frequency of CD4+ cells (an anti-viral function) from HIV+ donors ($p= 0.005$ and 0.027 respectively) when multi-parametric flow cytometry was performed. Inhibition of RT activity was predicted in *in silico* studies to be through interactions with the ribonuclease (RNase) H site although with poor stereochemical orientation while favourable binding predictions with the IN cofactor binding site were observed for some gold(III) complexes. Compounds predicted to interact with the RNase H site of RT and the IN cofactor site require structural modification to improve drug-likeness and binding affinity. The drug-like compound(s) which inhibited viral infectivity and lowered CD4+ cell frequency have potential for incorporation into virostatic cocktails (combination of cytostatic and directly anti-viral agent). Cytostatic agents are known to be less prone to drug resistance and because they lower CD4+ cell frequency, such compounds can potentially limit HIV immune activation.

LIST OF FIGURES

CHAPTER 2		5
FIGURE 2.1: GLOBAL VIEW OF HIV INFECTIONS (2008).	_____	6
FIGURE 2.2: CHANGES IN THE INCIDENCE RATE OF HIV INFECTIONS FROM 2001 TO 2009 FOR SELECTED COUNTRIES	_____	7
FIGURE 2.3: SCHEMATIC REPRESENTATION OF HIV GENOME.	_____	8
FIGURE 2.4: THE STRUCTURE OF A MATURE HIV VIRION.	_____	8
FIGURE 2.5: KEY ASPECTS OF THE LIFE CYCLE OF HIV.	_____	9
FIGURE 2.6: A SCHEMATIC REPRESENTATION OF THE TYPICAL TIME COURSE OF HIV PATHOGENESIS.	_____	11
FIGURE 2.7: AN ILLUSTRATION OF THE MECHANISMS OF DEPLETION OF HIV SPECIFIC CD4+ T CELLS DURING INFECTION.	_____	12
FIGURE 2.8: RIBBON REPRESENTATION OF HIV-1 RT IN COMPLEX WITH ACTIVE SITE INHIBITORS.	_____	15
FIGURE 2.9: STRUCTURAL REPRESENTATION OF SOME RT INHIBITORS CURRENTLY IN CLINICAL USE.	_____	16
FIGURE 2.10: STRUCTURE OF HIV PR.	_____	17
FIGURE 2.11: STRUCTURE OF SOME HIV PR INHIBITORS IN CLINICAL USE.	_____	17
FIGURE 2.12: STRUCTURAL AND FUNCTIONAL DOMAINS OF IN.	_____	18
FIGURE 2.13: STRUCTURE OF SOME IN INHIBITORS.	_____	18
FIGURE 2.14: VIRAL ENTRY PROCESS AND SOME ENTRY INHIBITORS.	_____	19
FIGURE 2.15: THE ANTI-VIRAL AND CYTOSTATIC MECHANISM OF VIROSTATIC AGENTS	_____	21
FIGURE 2.16: STRUCTURE OF HYDROXYUREA, AN IMPORTANT CYTOSTATIC AGENT.	_____	22
FIGURE 2.17: STRUCTURE OF IN-LEDGF COMPLEX.	_____	23
FIGURE 2.18: DRUG DISCOVERY PHASES	_____	26
FIGURE 2.19: STRUCTURE OF SOME IMPORTANT GOLD COMPOUNDS IN MEDICINE.	_____	29
FIGURE 2.20: SCHEMATIC REPRESENTATION OF THE SCREENING STRATEGY	_____	37
CHAPTER 3		41
FIGURE 3.1: SYNTHETIC SCHEME FOR THE PHOSPHINE CONTAINING LIGANDS.	_____	45
FIGURE 3.2: THE CHEMICAL STRUCTURE OF HYDRAZINE	_____	47
FIGURE 3.3: SYNTHETIC DISPLAY FOR THE BPH GOLD(I) COMPLEXES.	_____	47
FIGURE 3.4: THE STRUCTURES OF INTERMEDIATE REAGENTS USED FOR THE SYNTHESIS OF AURANOFIN ANALOGUES	_____	49
FIGURE 3.5: SYNTHETIC SCHEME FOR THE BISTHISEMICABARZONATE COMPLEXES	_____	51
FIGURE 3.6: SYNTHETIC SCHEME FOR TETRA-CHLORO-(BIS-(3,5-DIMETHYLPYRAZOLYL)METHANE)GOLD (III)CHLORIDE.	_____	52
FIGURE 3.7: ABSORPTION AND BBB PENETRATION POINT PLOT OF THE COMPOUNDS AND ARV DRUGS IN THE CLINIC.	_____	65
CHAPTER 4		73
FIGURE 4.1: A SCHEMATIC REPRESENTATION OF THE SETUP OF A FLOW CYTOMETER.	_____	81
FIGURE 4.2: SCHEMATIC REPRESENTATION OF THE MECHANISM INVOLVED IN FLUORESCENT LABELLING OF CELLS WITH CFDA-SE.	_____	84
FIGURE 4.3: THE PRINCIPLE OF CELL PROLIFERATION MONITORING USING THE RT-CES ANALYSER.	_____	86
FIGURE 4.4: VIABILITY PROFILE OF PBMCs TREATED WITH THE COMPOUNDS AND ANALYSED USING FLOW CYTOMETRY.	_____	93
FIGURE 4.5: REPRESENTATIVE PROLIFERATION HISTOGRAMS SHOWING PROLIFERATION PATTERNS OF CFSE STAINED PBMCs.	_____	94
FIGURE 4.6: THE EFFECT OF THE COMPOUNDS ON PBMC PROLIFERATION.	_____	95
FIGURE 4.7A: TYPICAL TITRATION PROFILE OF TZM-BL CELLS.	_____	97
FIGURE 4.7B: EFFECT OF COMPOUNDS ON TZM-BL CELL GROWTH PATTERN MONITORED BY AN RT-CES ANALYSER.	_____	98
FIGURE 4.7C: THE EFFECT OF COMPLEX PFK8 ON THE PROLIFERATION OF TZM-BL CELLS MONITORED BY RT-CES ANALYSIS.	_____	100
FIGURE 4.8: THE EFFECT OF THE COMPOUNDS ON INFECTIVITY AND VIABILITY OF TZM-BL CELLS.	_____	101
FIGURE 4.9: THE EFFECT OF COMPLEX PFK7 ON RNR PRODUCTION FROM PBMCs.	_____	103
FIGURE 4.10: REPRESENTATIVE FACS PLOTS SHOWING THE HIERARCHICAL GATING STRATEGY FOR IFN- γ AND TNF-A DETECTION.	_____	104

FIGURE 4.11: THE EFFECT OF THE COMPOUNDS ON CD4+ CELLS FREQUENCY AND CYTOKINE PRODUCTION.	106
CHAPTER 5 114	
FIGURE 5.1: REVERSE TRANSCRIPTASE COLORIMETRIC TEST PRINCIPLE	118
FIGURE 5.2: BINDING SITE SPHERE IN THE CATALYTIC CORE DOMAIN OF IN (2B4J).	124
FIGURE 5.3: SUMMARY OF METHODS USED IN DETERMINING THE EFFECT OF THE COMPOUNDS ON VIRAL ENZYMES.	126
FIGURE 5.4: HIV IN INHIBITORY ACTIVITY OF REPRESENTATIVE COMPOUNDS FROM DIFFERENT CLASSES.	129
FIGURE 5.5: ANNOTATED STRUCTURES OF TTC3 AND TTC24 AND IMPORTANT GROUPS.	132
FIGURE 5.6: PREDICTED BINDING PREDICTIONS OF TTC10 AND TTC24 TO THE RNASE H SITE IN THE PRESENCE OF Mn ²⁺	134
FIGURE 5.7: PREDICTED BINDING INTERACTIONS OF TTC10 TO THE RNASE H SITE IN THE ABSENCE OF Mn ²⁺ .	137
FIGURE 5.8: PREDICTED BINDING INTERACTIONS OF TTC24 WITH THE SITE CLOSE TO THE POLYMERASE/NNRTI SITE (3LP2).	138
FIGURE 5.9: ANNOTATED STRUCTURES OF LIGANDS PFK5 AND PFK7.	141
FIGURE 5.10: PREDICTED INTERACTIONS OF LIGANDS PFK5 AND PFK7 WITH THE LEDGF BINDING SITE.	142
FIGURE 5.11: PREDICTED BINDING INTERACTIONS OF LIGANDS WITH THE SUCROSE BINDING SITE OF IN.	144
CHAPTER 8 180	
FIGURE A3.1: THE EFFECT OF WATER ON THE ¹ H PROFILE OF THE GOLD(I) PHOSPHINE CHLORIDE COMPLEX, TTC3.	181
FIGURE A3.2: THE ³¹ P AND ¹ H NMR OF MCZS3 ON DAY ZERO.	182
FIGURE A3.3: ¹ H NMR SPECTRA OF PFK7.	183
FIGURE A3.4: ¹ H NMR OF KFK154B	184
FIGURE A4.1: MTT VIABILITY OPTIMISATION ASSAYS WITH PBMCs.	186
FIGURE A4.2: MTS VIABILITY OPTIMISATION ASSAYS ON PBMCs	187
FIGURE A4.3: VIABILITY PATTERN OF PM1 CELLS TREATED WITH COMPOUNDS AND DETERMINED WITH MTS.	188
FIGURE A4.4: LDH CYTOTOXICITY ASSAY TEST PRINCIPLE.	189
FIGURE A4.5: CYTOTOXICITY PATTERN OF COMPOUNDS ON PBMCs DETERMINED USING THE LDH CYTOTOXICITY DETECTION KIT.	189
FIGURE A4.6: THE EFFECT OF THE COMPOUNDS ON THE VIABILITY OF PBMCs	190
FIGURE A4.7: TIME OPTIMISATION EXPERIMENTS FOR CFSE.	191
FIGURE A4.8: DIFFERENCES IN CELL PROLIFERATION PATTERN OF PBMCs IN THE PRESENCE AND ABSENCE OF STIMULANT AFTER 3 DAYS OF TREATMENT WITH COMPOUNDS.	192
FIGURE A4.9: LYMPHOCYTE IDENTIFICATION GATING.	193
FIGURE A4.10: STIMULANT AND TIME OPTIMISATION ASSAYS FOR ICCS EXPERIMENTS.	194
FIGURE A4.11: THE EFFECT OF REPRESENTATIVE COMPOUNDS ON THE PROLIFERATION OF TZM-BL CELLS USING AN RT-CES ANALYSER.	195
FIGURE A4.12: THE EFFECT OF REPRESENTATIVE COMPOUNDS ON THE PROLIFERATION OF TZM-BL CELLS USING AN RT-CES ANALYSER.	196
FIGURE A4.13: DIFFERENCES IN THE FREQUENCY OF PRODUCTION OF T LYMPHOCYTES FROM HIV+/- DONORS.	197
FIGURE A5.1: EFFECT OF COMPOUNDS ON HIV-1 IN ACTIVITY.	204
FIGURE A5.2: MOLECULAR SURFACE DIAGRAM OF TTC10 IN THE RNASE H ACTIVE SITE.	207
FIGURE A5.3: PREDICTED BINDING INTERACTIONS BETWEEN KFK154B AND THE RNASE H BINDING SITE OF RT.	207
FIGURE A5.4: MOLECULAR SURFACE DIAGRAM OF PFK5 AND PFK7 WITH THE LEDGF BINDING SITE OF HIV IN.	208
FIGURE A5.5: MOLECULAR SURFACE DIAGRAM OF PFK7 IN THE SUCROSE BINDING SITE OF IN.	208

LIST OF TABLES

CHAPTER 3 41

TABLE 3.1: THE GOLD(I) PHOSPHINE CHLORIDE COMPLEXES AND CORRESPONDING LIGANDS _____	46
TABLE 3.2: BPH GOLD(I) CHLORIDE-CONTAINING COMPLEXES _____	48
TABLE 3.3: GOLD(I) PHOSPHINE THIOLATE COMPLEXES. _____	50
TABLE 3.4: THE GOLD(III) THIOSEMICARBAZONATE COMPLEXES AND CORRESPONDING PRECURSORS. _____	51
TABLE 3.5: THE PYRAZOLYL GOLD(III) COMPLEX. _____	52
TABLE 3.6: ADDITIONAL COMPOUND STRUCTURAL INFORMATION. _____	53
TABLE 3.7: STABILITY PROFILE SUMMARY. _____	62
TABLE 3.8A: ADMET PREDICTION SCORES FOR THE COMPOUNDS. _____	63
TABLE 3.8B: ADMET PREDICTION DATA FOR CLINICALLY AVAILABLE ARV DRUGS. _____	64
TABLE 3.9: ADMET PREDICTION SCORES SUMMARY. _____	70

CHAPTER 4 73

TABLE 4.1: CELL-BASED ASSAY SUMMARY. _____	91
TABLE 4.2: CC ₅₀ VALUES INDICATING THE EFFECT OF THE COMPOUNDS ON THE VIABILITY OF PBMCs AND THE PM1 CELL LINE. _____	92
TABLE 4.3: A SUMMARY OF THE EFFECT OF THE COMPOUNDS ON IMMUNE CELL FUNCTION. _____	109
TABLE 4.4: SUMMARY OF THE VARIOUS EFFECTS CAUSED BY THE COMPOUNDS TO THE DIFFERENT CELL TYPES. _____	111

CHAPTER 5 114

TABLE 5.1: A SUMMARY OF THE PROTEIN DATA BANK CRYSTAL STRUCTURES USED FOR MOLECULAR MODELLING. _____	123
TABLE 5.2: THE EFFECT OF THE COMPOUNDS ON HIV RT AND PR ACTIVITY _____	127
TABLE 5.3: SUMMARY OF COMPOUNDS THAT INHIBITED HIV RT, PR AND IN IN DIRECT ENZYME BIOASSAYS. _____	130
TABLE 5.4: SUMMARY OF PREDICTED BINDING FREE ENERGY VALUES AND RELEVANT BOND DISTANCES AFTER MOLECULAR MODELLING _____	132

CHAPTER 8 180

TABLE A2.1: DESCRIPTION OF STATISTICS CALCULATIONS THAT WERE IMPLEMENTED IN THIS STUDY. _____	180
TABLE A4.1: CC ₅₀ AND IC ₅₀ FOR INFECTIVITY OF THE COMPOUNDS IN TZM-BL CELLS _____	197
TABLE A4.2: THE EFFECT OF THE COMPOUNDS ON IFN- γ AND TNF- α SECRETION FROM PBMCs. _____	198
TABLE A4.3: COMPARISON OF CYTOKINE PRODUCTION LEVELS BETWEEN ICCS (CD4+ CELLS) AND ELISAs (PBMCs). _____	199
TABLE A5.1: ANTI-RT ACTIVITY OF COMPLEXES WITH PRIOR RT ACTIVITY. _____	200
TABLE A5.2: NUMBER OF SUCCESSFULLY DOCKED POSES OF COMPOUNDS WITH DIFFERENT ENZYMES AND SITES. _____	205
TABLE A5.3: TABLE OF AMINO ACID STRUCTURES. _____	206

LIST OF IMPORTANT ABBREVIATIONS

3'	3 prime
5'	5 prime
3'P	3 prime Processing
5-CITEP	1-(5-chloroindol-3-yl)-3-hydroxy-3-(2H-tetrazol-5-yl)-propenone
Å	Armstrong
ADMET	Adsorption, Distribution, Metabolism, Excretion, Toxicity
AIDS	Acquired Immune Deficiency Syndrome
AlogP	Atom-based logarithm of Partition coefficient
ART	Antiretroviral Therapy
ARV	Antiretroviral
BBB	Blood Brain Barrier
BPH	Bis(Phosphino) Hydrazine
CC ₅₀	50% Cytotoxic Concentration
CCD	Catalytic Core Domain
CCR5	Chemokine Receptor 5
CD4	Cluster of Differentiation 4
CD8	Cluster of Differentiation 8
cDNA	Complementary Deoxyribonucleic Acid
CDOCKER	CHARMm-based Docker
CFSE	CarboxyFlourescein Succinimidyl Ester
CHARMm	Chemistry at Harvard Macromolecular Mechanics
CI	Cell Index
CTLs	Cytotoxic T Lymphocytes
CXCR4	CXC chemokine receptor 4
CYP	Cytochrome P450
d ₆ -DMSO	Deuterated Dimethylsulfoxide
DMEM	Dulbecco's Modified Essential Medium
DMSO	Dimethylsulfoxide
dNTPs	Deoxynucleotide Triphosphates
DS	Discovery Studio
ELISA	Enzyme Linked ImmunoSorbent Assay
FACS	Fluorescence-Activated Cell Sorter
FCS	Fetal Calf Serum
FITC	Flourescein Isothiocyanate
FMO	Fluorescent Minus One
GS	Gentamycine Sulphate
HAART	Highly Active Antiretroviral Therapy
H-bond	Hydrogen bond
HIA	Human Intestinal Absorption
HIV	Human Immunodeficiency Virus
HTS	High Throughput Screening
HU	Hydroxyurea
hu-PBL-SCID	human-Peripheral Blood Lymphocytes-Severe Combined Immunodeficiency
IC ₅₀	Inhibitory Concentration 50%
ICC	Intracellular Cytokine
ICCS	Intracellular Cytokine Staining
IFN-γ	Interferon gamma
IL	interleukin
IN	Integrase
ION	Ionomycin
kcal/mol	kilocalorie per mole
LDH	Lactate Dehydrogenase

LEDGF	Lens Epithelium Derived Growth Factor
Log P	Logarithm of Partition coefficient
LTR	Long Terminal Repeat
Mabs	Monoclonal Antibodies
MD	Molecular Dynamics
MHC	Major Histocompatibility Complex
MTS	3-(4,5-dimethylthiazol-2-yl)-5-[3-(3-carboxymethoxyphenyl)-2-(4-sulfophenyl)-2H-tetrazolium
MTT	3-(4,5-dimethylthiazol-2-yl)-2,5-diphenyltetrazolium bromide.
NF- κ B	Nuclear Factor Kappa Beta
NMR	Nuclear Magnetic Resonance
NNRTIs	Non Nucleoside Reverse Transcriptase Inhibitors
NRTIs	Nucleos(t)ide Reverse Transcriptase Inhibitors
P value	Probability value
PBMCs	Peripheral Blood Mononuclear Cells
PBS	Phosphate Buffered Saline
PDB	Protein Data Bank
PHA-P	Phytohemagglutinin-Protein
PI	Propidium Iodide
PMA	Phorbol Myristate Acetate
PPB	Plasma Protein Binding
ppm	parts per million
PR	Protease
PSA	Polar Surface Area
QUANTUMm	Quantum Mechanics and Molecular Mechanics
RA	Rheumatoid Arthritis
RNase H	Ribonuclease H
RNR	Ribonucleotide Reductase
RPMI	Rosewell Park Memorial Institute
RT	Reverse Transcriptase
RT-CES	Real Time Cell Electronic Sensing
SAR	Structure Activity Relationship
sdf	Structural Data Files
SIV	Simian Immunodeficiency Virus
ssRNA	Single Stranded Ribonucleic Acid
ST	Strand Transfer
TNF- α	Tumour Necrosis Factor alpha
tRNA	transfer Ribonucleic Acid
Tscs	Thiosemicarbone(s)
U	Units
U3	Untranslated 3'
U5	Untranslated 5'
UNAIDS	Joint United Nations Programme on HIV/AIDS
UV	Ultraviolet

CHAPTER 1

INTRODUCTION

Infection with HIV and the subsequent acquired syndrome continue to be global health and socio-economic concerns. Although there has been declining trends with respect to new infections and the number of deaths from HIV/AIDS related illnesses over recent years (UNAIDS, 2010), HIV remains a major health threat. Sub-Saharan Africa is the hardest hit area having up to 68% of the world's total number of infected people (UNAIDS, 2010). HIV affects the immune system depleting it of crucial T helper cells (CD4+ lymphocytes) needed by both the humoral and cellular arms of the immune system, thereby rendering the individual immunocompromised. This depletion leads to an AIDS state characterised by wasting, morbidity, a host of opportunistic infections and ultimately mortality if not treated. To combat HIV/AIDS, therapies that increase the lifespan of infected individuals have been developed. The strategy of these therapies is reduction of viral load and the prevention of further loss of CD4+ cells (Lori *et al.*, 2007). The use of highly active antiretroviral therapy (HAART) which is the combination of a PR inhibitor or a non nucleoside RT inhibitor (NNRTI) and two nucleos(t)ide RT inhibitors (NRTIs, Pommier *et al.*, 2005) has been paramount in this approach of lowering viral load and preventing CD4+ cell loss. More recently drugs targeting the viral IN and antagonists to the CCR5 receptor of host cells were approved as first line treatment or salvage therapy for the treatment-experienced patients (McColl and Chen, 2010) increasing the range of available drugs. While these developments have greatly improved the standard of living of HIV/AIDS patients by decreasing morbidity and mortality (Hogg *et al.*, 1999, Palella *et al.*, 1998), these drugs have limitations which include problems of toxicity, uncomfortable side effects (such as nausea, vomiting and diarrhoea, Montessori *et al.*, 2004) and the development of drug resistance by the virus (Chen *et al.*, 2004, Skillmann *et al.*, 2002). Other limitations are accessibility to treatment and the lack of infrastructure to monitor treatment especially in resource limited settings (developing countries, Lever, 2005b).

On the other hand, the development of a viable cure has not been achieved (Heagarty, 2003) but encouraging advances have been made. For example an HIV infected man who received stem cell transplantation from a donor homozygous for the *chemokine receptor 5* (CCR5) delta32 gene as treatment for acute myeloid leukemia was cleared of the virus (Hutter *et al.*, 2009). A mutation in the CCR5 gene is known to confer resistance against infections caused by HIV since the CCR5 co-receptor is involved in viral entry into cells. Another recent development towards a cure was the report from a group of Australian scientists who successfully cleared an HIV-like virus from mice by boosting the function of cells vital to immune responses (Pellegrini *et al.*, 2011). The authors showed that interleukin-7 (IL-7) which is important for immune activation and homeostasis could lower the expression of the

suppressor of cytokine signalling 3 (Socs3) gene leading to increased cytokine production and T cell function. This, the authors suggested, may have enhanced innate anti-viral mechanisms.

In the field of prevention, an encouraging advancement was the recent report on an antiretroviral (ARV) vaginal gel containing the anti-viral drug, tenofovir, which resulted in moderate protection against HIV infection. A 39% lower risk of acquisition and up to 54% reduction of infection in women who achieved the best adherence was observed while blocking infection from herpes at the same time (Abdool Karim *et al.*, 2010). This was a significant breakthrough especially because women are the most susceptible group in contracting new HIV infections (Quinn and Overbaugh, 2005). A recent breakthrough in prevention were the findings from the HIV Prevention Trial Networks (www.htpn.org, accessed 5/06/2011) in the study known as HPTN 052 which reported that the early administration of ARVs to infected men and women reduced the risk of HIV transmission to their partners by 96%. Other measures to curb infection have been intensive education and campaigns which have shown benefits in countries such as Uganda (Lever, 2005b).

Vaccine development has also been slow but has gained renewed interest after findings of limited protection from HIV infection were reported in the RV144 trial in Thailand (Rerks-Ngarm *et al.*, 2009).

While HAART has been a success story, the mentioned limitations such as toxicity and the development of resistant viral strains and the transmission thereof, are amongst the drawbacks which could eventually render this therapy ineffective. In addition, the identification of latent reservoirs of HIV-1 in patients on HAART (Finzi *et al.*, 1997) was one of the earliest limitations observed during therapy such that treatment has to be life-long. Because of the toxicity problems that are also associated with HAART, patients find it difficult to comply to prescriptions by physician (Ren and Stammers, 2005, Chen *et al.*, 2004). As a result, suboptimal doses of the drugs are taken, further enhancing resistance problems since optimal viral suppression is not attained. Identifying potential drug candidates that can be used in combination with or to supplement HAART with the goal of finding those with tolerable side effects that can also work against resistant strains is crucial. In this study, the possibility of using gold-based compounds as anti-HIV agents was investigated.

The focus here was mainly on bioactivity testing of gold-based compounds synthesized and provided by chemists from the Project AuTEK Biomed Consortium (Mintek and Harmony Gold, South Africa). The compounds were tested on the HIV-1 subtype C strain because it is the most prevalent subtype in Southern Africa (HIV clades are geographically distributed, Schiavone *et al.*, 2008). Currently, subtype C infected patients are administered subtype B specific drugs. This leads to the emergence of resistant viral forms similar to those seen for subtype B as well as others not seen for the B subtype strain (Kantor and Katzenstein, 2004), which further complicates treatment and treatment options. By testing the compounds against

subtype C strains, the likelihood that more specific inhibitors could be identified which would eventually reduce the resistance burden seen when drugs designed for the subtype B strain are used was increased.

Gold compounds have medicinal properties that have mainly been exploited for the treatment of rheumatoid arthritis (Ahmad, 2004, Best and Sadler, 1996, Sutton, 1986). These compounds also show activity against cancers and microorganisms including the malaria parasite (Khanye *et al.*, 2010, Gabbiani *et al.*, 2009, Sanella *et al.*, 2008, Navarro *et al.*, 2004, Navarro *et al.*, 1997) and HIV (reviewed by Fonteh *et al.*, 2010). This laboratory previously contributed evidence in a proof of concept study on the effect of gold compounds against HIV enzymes (RT and PR, Fonteh *et al.*, 2009, Fonteh and Meyer, 2009).

The scope of this research was further extended here by determining how comparable the gold compounds were to known drugs with regards to functional groups and physical properties (drug-likeness), effects on host cells in cell-based assays (to determine compound effects on host cells and whole virus), and on viral enzymes (direct enzyme bioassays and *in silico* to determine binding modes). In addition to the sixteen compounds previously tested in the proof of concept studies (Fonteh and Meyer 2008), eleven new ones were included in this study resulting in twenty-seven compounds that span five different chemical classes based on synthetic precursors used.

Binding mode interactions of the compounds with the RNase H site of RT and the IN cofactor site showed favourable enthalpic contributions but require structural modifications of the compounds to enhance activity. An outstanding novel observation of this study was the identification of the mechanism by which three compounds (designated PFK7, PFK8 and EK207) inhibited cellular infectivity by a dual subtype C strain of HIV-1. Inhibition of infectivity was not as a result of the compounds' interaction with viral surface components but rather was as a result of the compounds' cytostatic effect which was observed using the dye dilution technology of carboxyfluorescein succinimidyl ester (CFSE) and the impedance (resistance) technology of a real time cell electronic sensing (RT-CES) device. The cytostatic mechanism (anti-proliferative effect on the cell rather than on the virus) was further confirmed for complexes PFK7 and EK207 using multi-parametric flow cytometry where the frequency of CD4+ cells from peripheral blood mononuclear cells of HIV infected individuals was significantly reduced ($p = 0.0049$ and 0.027 respectively). The ability of these compounds (PFK7 and EK207) to reduce T cell numbers could be interpreted to mean that the compounds were capable of blocking viral replication as a result of the ability to prevent antigen presenting cells from activating T cells, a finding which has been shown for gold and other metal compounds (De Wall *et al.*, 2006). Compounds which have a cytostatic mechanism of action and which lower CD4+ cell numbers (such as hydroxyurea) have demonstrated a significant role in HIV research both *in vitro* (Clouser *et al.*, 2010, Lori *et al.*, 2005, Mayhew *et al.*, 2005) and in clinical trials (Lori *et al.*, 1997, Frank, 1999, Rutschmann *et al.*, 1998, Federici *et al.*,

1998). The cytostatic effect of hydroxyurea is also known to be as a result of the inhibition of ribonucleotide reductase (RNR) which is an enzyme involved in converting ribonucleotides to dNTPs (DNA building blocks, Lori, 1999). At 10 μ M PFK7 also inhibited RNR significantly ($p = 0.003$). Combining these agents with compounds that directly target the virus is known to result in the overall restoration of immune parameters in infected patients and to a better resistance profile compared to HAART (Lori *et al.*, 2007). Three of the twenty seven compounds (PFK7, PFK8 and to a lesser extent EK207) have the potential of being combined with compounds that directly target the virus and function in the new emerging class of combination therapy known as virostatics. Such a combination stands a better chance in managing HIV since drug resistance (which this combination minimises) has become the greatest threat to HAART. In addition, the drug-like properties that were seen for complexes PFK7 and PFK8 (drug score of 6 out of 7) makes these cytostatic agents highly favoured as potential components of virostatic cocktails.

In chapter 2, general background and literature review of topics relevant to this study is provided. This is followed by three chapters that provide detailed information on each of the main research aims which were (1) determining the drug-likeness of the compounds (chapter 3), (2) the effect of the compounds on immune system cells and whole virus (chapter 4) and (3) effect on viral enzymes (chapter 5). An overall conclusion on the study is then provided (chapter 6), followed by a comprehensive list of references (chapter 7). Supplementary data is provided in the appendix (chapter 8) followed by a glossary with definitions for uncommon words. Finally, copies of two published manuscripts containing information obtained during this study are provided.

CHAPTER 2

LITERATURE REVIEW AND BACKGROUND

2.1 HIV AND AIDS

HIV is a primate lentivirus belonging to the *Retroviridae* family and affects cells of the immune system ultimately leading to AIDS (Gonzalez *et al.*, 2009, Campbell and Hope, 2008). Two viral types exist, HIV-1 and HIV-2 both being enveloped retroviruses (Campbell and Hope, 2008, Lever, 2005). HIV-1 found worldwide is more pathogenic than HIV-2 but both cause similar illnesses (Lewthwaite and Wilkins, 2005). Patients with HIV-2 have lower viral loads, slower CD4 decline and lower rates of vertical transmission (Lewthwaite and Wilkins, 2005), not seen in HIV-1 infection. The nucleic acid sequences of the two types are only 40% similar (Lever, 2005b). HIV is closely related to another primate lentivirus, the simian immunodeficiency virus (SIV). HIV-1 is similar to SIV found in a group of chimpanzees while HIV-2 is more closely related to SIV found in sooty mangabey monkeys (Lemey *et al.*, 2003, Sharp *et al.*, 1995). The former virus (HIV-1, which is the focus of this study) has a high genetic variability and has been classified into major (M), outlier (O), and non-M/O (N) groups (Sanabani *et al.*, 2006). Group M has nine subtypes ranging from A-J which include subtypes A, B, C, D, F, G, H, J and K as well as circulating recombinant forms (CRFs), Carr *et al.*, (1998). The most prevalent strain worldwide and in Southern Africa is the subtype C strain (Nkolola and Essex, 2006, Wouter *et al.*, 1997).

Infection with HIV if not treated culminates in death from infections that lead to AIDS defining diseases like candidiasis, cryptosporidiosis, cytomegalovirus, *Pneumocystis carinii* pneumonia, toxoplasmosis and tuberculosis (Pozio and Morales, 2005). The AIDS state stems from the depletion of CD4+ T helper lymphocytes (Rambaut *et al.*, 2004) which are critical for effective immune function. AIDS, which is usually the last battle between HIV and the body's immune system, occurs when there is a drop of the total CD4+ T cell count to approximately 200 cells/ μ L of blood (World Bank, 1997). In addition to CD4 T cells, the virus also infects other cells that express cell surface receptors that allow for viral entry such as the CD4 and chemokine co-receptors consisting of CCR5 or CXCR4 (CXCR4), Dragic *et al.*, (1996), Choe *et al.*, (1995).

In the next subsections, the epidemiology, transmission modes, structure, life cycle and the course of HIV-1 infection will be provided. This will be followed by information on vaccine development, HIV's effect on the immune system, available therapy and information on the need for new drug development. Finally, the research hypothesis will be stated and the main research questions introduced. HIV will be used throughout this document to refer to HIV-1.

2.1.1 Epidemiology

The global view of HIV infections in 2009 according to the UNAIDS report of 2010 has not changed significantly compared to the previous year where an average of 33.4 million people were living with the virus worldwide as detailed in Figure 2.1. A revision of the 2008 statistics showed that 32.8 million people were living with the virus, which is within the uncertainty range of the previous estimate. According to these statistics, Sub-Saharan Africa still bears the greatest burden with regards to the number of infected people (with 22.4 of the total 33.4 million worldwide estimate in 2008) and new infections.

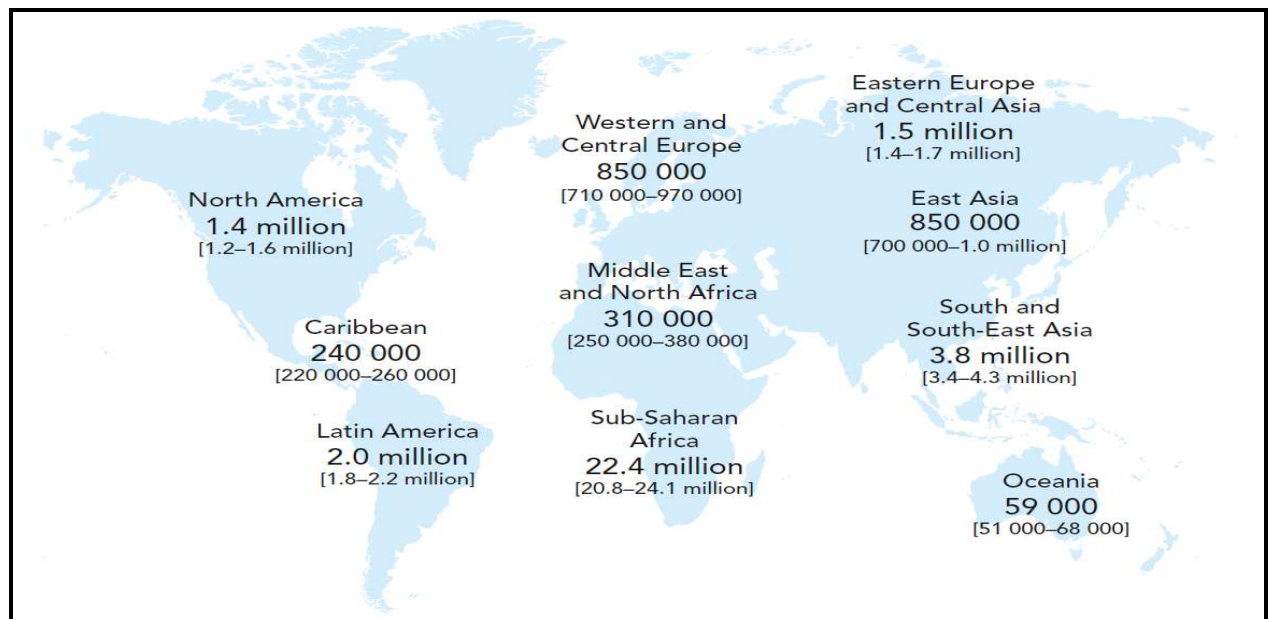


Figure 2.1: Global view of HIV infections (2008). An average of 33.4 million adults and children were living with HIV (UNAIDS report, 2009).

The good news according to the 2010 report is that although up to 32.8 million people are infected globally, there were declining trends in new infections in 2009 where only 2.1 million were noted compared to 2001 where 3.1 million people were newly infected. Figure 2.2 shows the changes in the incidences of new infections over 2001 to 2009. In 33 countries including South Africa there has been decreasing incidence of newly infected people by >25% from 2001 to 2009 (Figure 2.2). Not only are new infections decreasing but the death rate from HIV is also decreasing across the spectrum due to increased access to antiretroviral agents. The decrease in new infections has been attributed to an overall combination of factors including the impact of prevention efforts (UNAIDS report, 2010).

The lack of survey data in some instances and the absence of diagnostic test for very early detection of HIV are factors that limit the determination of the actual infection rate such that only estimates are obtained. In addition, while the rate of infection is declining in some regions, statistics show that the reverse is true for others such as parts of Asia (Figure 2.2) with an increasing rate of >25%. These findings suggest that the battle is still on and more effort than ever has to be directed to researching solutions for managing and preventing HIV infection.



Figure 2.2: Changes in the incidence rate of HIV infections from 2001 to 2009 for selected countries (http://media.economist.com/images/images-magazine/2010/11/27/st/20101127_stm958.gif, accessed 02/02/2011).

2.1.2 Mode of Transmission

HIV is transmitted through bodily fluids and mostly sexually (homosexual or heterosexual), but also occurs vertically from mother to child, through blood transfusion and sometimes through unidentified means (Monavi, 2006). Sexual transmission is the most important route since it is the most common means of transmission of HIV (Walker *et al.*, 2003). Vertical transmission is common in developing countries in pregnancy and at birth or during breast-feeding (Lewthwaite and Wilkins, 2005). Injection drug use is also one of the ways by which HIV is transmitted and although it is relatively low in countries such as the United Kingdom, its prevalence can be up to 50% in others such as Eastern Europe, Vietnam, India and China (Lewthwaite and Wilkins, 2005).

2.1.3 HIV Genome Organisation and Structure

The HIV genome consists of nine genes that encode 15 viral proteins (Gotte *et al.*, 1999). These include the group-associated antigen (*gag*) encoding structural core proteins, a polymerase (*pol*) portion encoding the enzymatic proteins PR, RT, IN, and an envelope (*env*) frame encoding the receptor binding protein. The genome codes for two regulatory proteins (Tat and Rev) and four accessory proteins (Vif, Vpr, Vpu and Nef) required for proper virion replication. A schematic representation of the viral genome is shown in Figure 2.3. Two long terminal repeats (LTRs) flank both the 5' and 3' ends of the proviral DNA genome. The 5' LTR includes the HIV promoter and enhancer sequences that regulate viral gene expression. The genome constantly undergoes variation as a result of mutational and evolutionary pressures and pressure from the immune system such as those exerted by viral specific CD8+ T lymphocytes, which also leads to escape mutants (Sanabani *et al.*, 2006, Karlsson *et al.*, 2003).

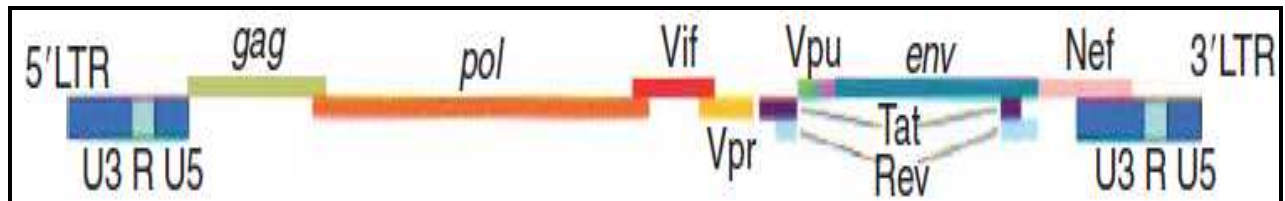


Figure 2.3: Schematic representation of HIV genome. Replication genes (*pol*, *vif*, *nef*, *tat*, *rev*, *vpu*, *vpr*) and assembly genes (*gag* and *env*) are represented. The figure was taken from Schiavone *et al.*, (2008).

The structure of HIV (shown in Figure 2.4) described by Turner and Summers (1999) consist of an enveloped lipid bilayer derived from the host membrane, contains exposed surface glycoproteins (gp120) and is anchored to the virus by the transmembrane protein (gp41). A matrix shell comprising approximately 2000 copies of the matrix protein (MA, p17) lines the inner surface of the viral membrane, and a conical capsid core shell comprising \pm 2000 copies of the capsid protein (CA, p24) is located in the centre of the virus. The capsid particle encloses two copies of the unspliced viral genome, which is stabilized as a ribonucleoprotein complex with approximately 2000 copies of the nucleocapsid protein (NC, p7), and also contains the three essential virally encoded enzymes namely: RT (p66/p51), PR (p11) and IN (p31). The unspliced viral genome consists of two similar RNA molecules approximately 10 kb in length (Coffin *et al.*, 1997).

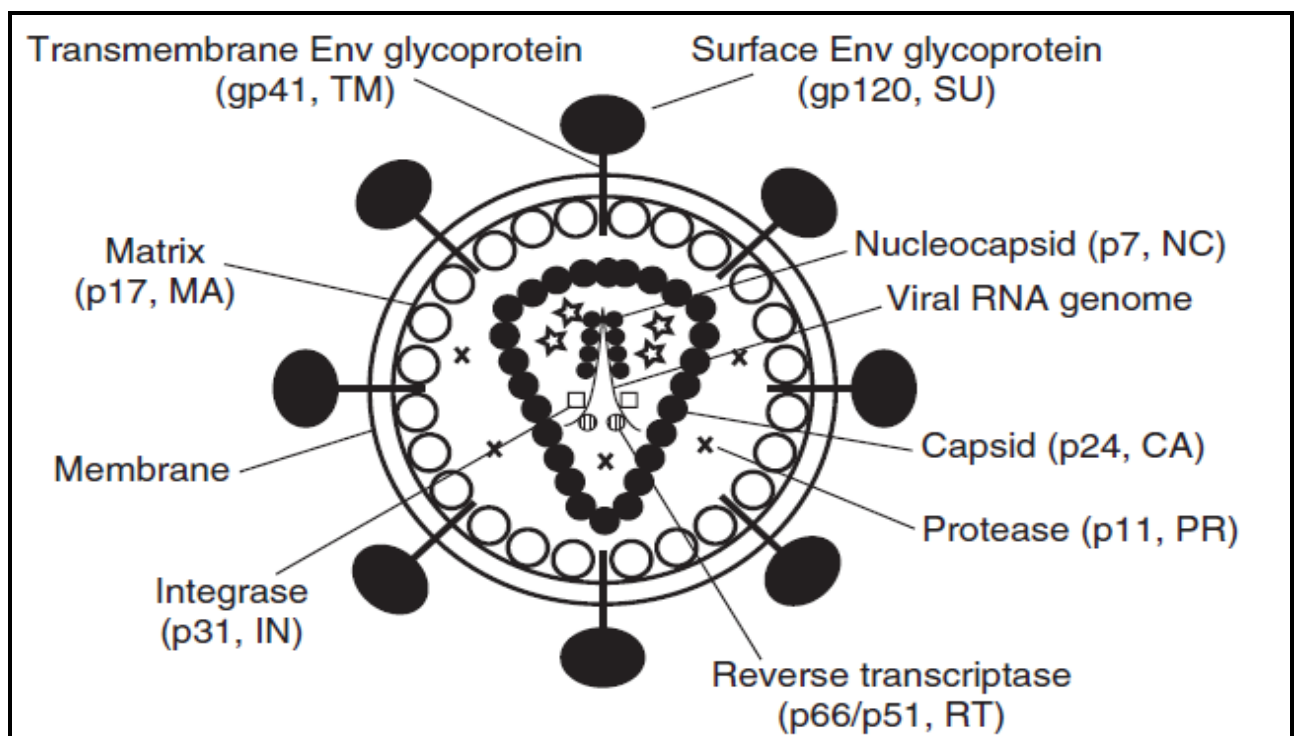


Figure 2.4: The structure of a mature HIV virion. The figure shows important viral proteins and their arrangement within the virion. This figure was taken from, Adamson and Freed (2007).

2.1.4 Life Cycle and Course of Infection

The life cycle of HIV involves three main steps including (1) entry and integration, (2) transcription and translation and finally (3) budding (Lever, 2005). Figure 2.5 shows the key aspects of the life cycle as well as selected drug targets namely; (a) virus fusion, (b) reverse transcription, (c) proteolytic processing, (d) 3' processing and (e) strand transfer (ST) steps.

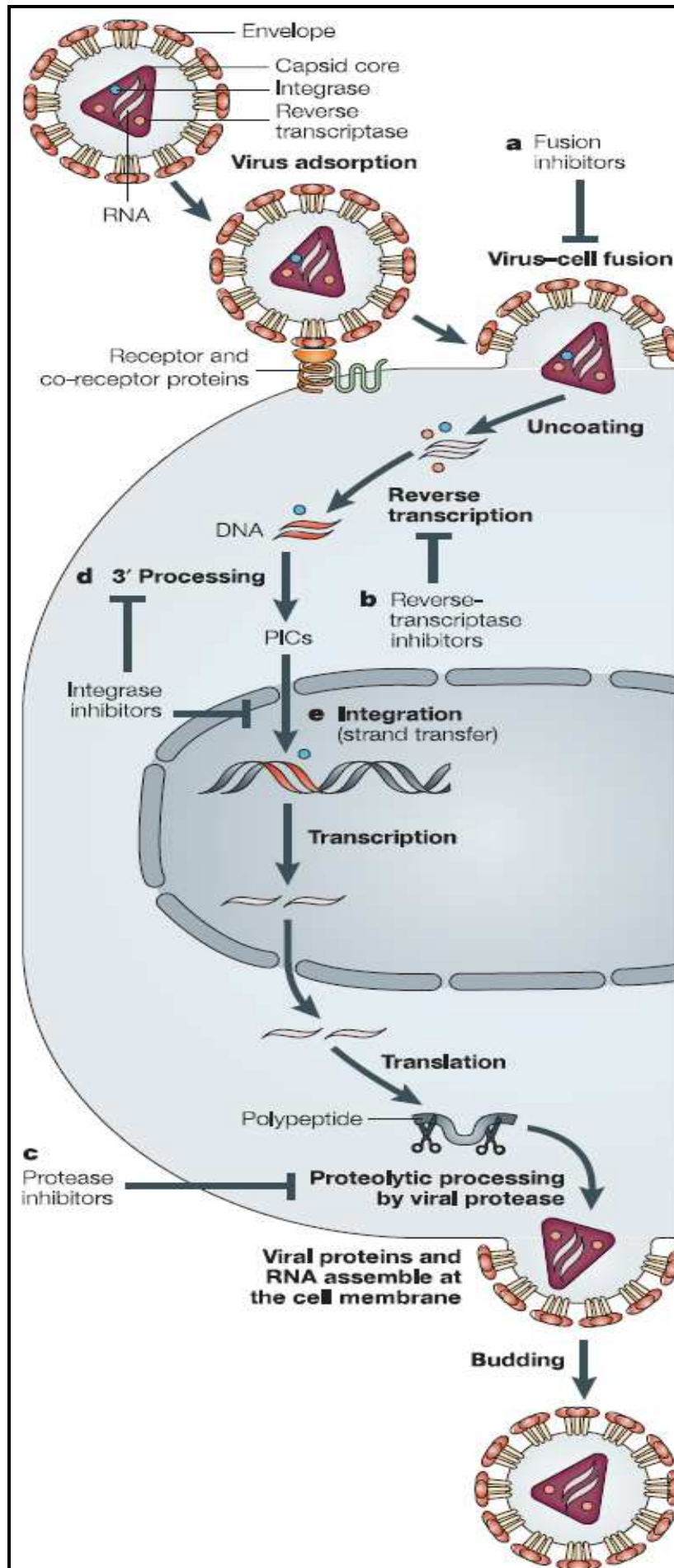


Figure 2.5: Key aspects of the life cycle of HIV. Important drug targets are also shown. The figure was taken from Pommier *et al.*, (2005).

In the **entry and integration** steps of the life cycle, the virion bearing two copies of ribonucleic acid (RNA) binds to CD4+ receptors and chemokine co-receptors (CCR5 or CXCR4) on the cell surface. This is followed by fusion where the viral core is inserted into the host cell followed by uncoating and the release of viral contents within the cytoplasm of these cells. The viral RNA is reverse transcribed by RT to a complementary deoxyribonucleic acid (cDNA) strand, which is subsequently transported into the nucleus as the pre-integration complex (PIC). Here it is integrated into the host genomic deoxyribonucleic acid (DNA) by the viral enzyme, IN.

Transcription of the viral DNA leads to the production of viral genomic RNA and **translation** of viral proteins that are then processed and assembled in the cytoplasm by HIV PR. HIV PR further catalyses the maturation of the viral particles through proteolytic processing into infectious virions which then **bud** off from the cells

As the virus replicates and makes new copies, the course of infection in the infected individual is the gradual loss and destruction of naive and memory CD4+ T cells leading to AIDS which is the final stages of the infection course (shown in Figure 2.6, Forsman and Weiss, 2008). The primary acute infection stage (4-8 weeks) is characterised by high plasma viremia and low CD4+ cells and the absence or very little HIV specific antibodies. The viremia drops as cytotoxic T lymphocytes (CTLs) develop leading to an individual viral set point in the course of chronic infection (5-15 years).

In the final stages of infection, when opportunistic infections like tuberculosis and infections from *Pneumocystis*, *Cytomegalovirus* (CMV), cerebral *Toxoplasma* or *Candida* occur (CD4+ count usually around 200 cells/ μ L of blood, World Bank, 1996), the viral load increases and CD4+ count continues to decrease ultimately leading to AIDS and death over a time course of 2-3 years. A striking new finding is the blow that the virus causes on the human body's largest lymphoid "organ" i.e. the gut and mucosal tissues, which is the significant depletion of mucosal CD4+ cells (Paiardini *et al.*, 2008, Brenchley *et al.*, 2006) not seen when circulating CD4+ cells in peripheral blood are sampled (Figure 2.6). This in turn could be the cause of the severe chronic immune activation noted throughout the course of infection such that recommendations for novel therapies aimed at targeting immune activation have been proposed (Forsman and Weiss, 2008). Other notable changes observed in lymphoid tissues are generalised lymphadenopathy, tonsillar enlargement and splenomegaly noted in early infection (Kilby, 2001). These features are associated with lymphocyte proliferation and the recruitment of inflammatory cells from the circulation. The enlargement gradually decreases in a majority of patients after seroconversion but may persist in others. In advance disease (and in the absence of treatment), the architecture of the lymphoid tissues changes resulting in an involution and lymphadenopathy becomes less prominent (Pantaleo *et al.*, 1993).

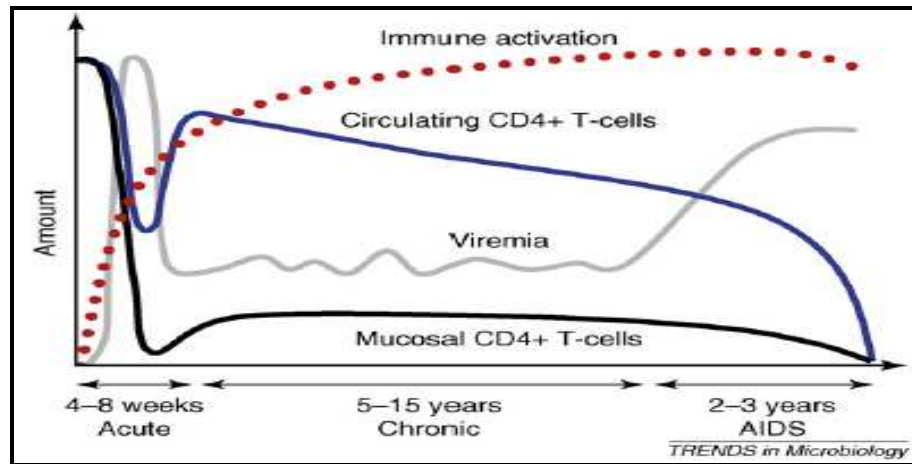


Figure 2.6: A schematic representation of the typical time course of HIV pathogenesis. The time course of adaptive immune responses in relation to viremia levels from acute infection to AIDS defining conditions is also depicted. The figure was taken from Forsman and Weiss (2008).

2.1.5 HIV and the Immune System

Infection with HIV triggers both B-cell (humoral) and T-cell (cell mediated) immune responses. These adaptive immune responses which unlike immediate and non specific innate immune responses, develop over days or weeks after exposure to the antigen as a result of clonal expansion and differentiation of B and T lymphocytes (McMichael and Dorrell, 2005). These responses unfortunately fail to clear the infection (McMichael and Dorrell, 2009, Young, 2003). The CD4+ T cell subset which tends to be depleted in HIV infection is important in the adaptive immune response since these cells recognise antigen presented by major histocompatibility complex (MHC) class II and respond by turning on B lymphocytes to secrete antibodies against the antigen (humoral response). After recognising antigen, the CD4+ T cell gets activated and produces a heterogeneous group of proteins (cytokines) that are secreted to exert an effect on target cells (Goldsby *et al.*, 2000) and which aid in the stimulation and recruitment of the CD8+ T cell subset or CTLs. Along with the decrease in CD4+ T cells in HIV infection, is the corresponding increase in CD8+ T cells (Musey *et al.*, 1997, Koup *et al.*, 1994). The latter targets and lyses virally infected cells through recognition of the foreign antigen bound by host proteins (Goepfert, 2003). In addition to killing the infected CD4+ cells, CTLs also release cytokines and chemokines which tend to block viral entry into other CD4+ cells (McMichael and Dorrell, 2009). The CTLs just like the antibodies play a critical role in the control of the infection.

Infection with HIV also kills CD4+ cells by direct cytopathic effect of the virus or through means which trigger apoptosis (a normal process for the elimination of unwanted cells), Young, (2003). This direct cytopathic effect of CD4+ T cells by the virus is one of the means by which the virus evades the immune system since by killing these cells, they also destroy immune effectors (Gougeon, 2005). The interaction of Fas ligand (which is a cell surface molecule belonging to the tumour necrosis factor family) on CTL surfaces with Fas molecules on the target cells e.g. CD4+ cells is also one of the ways by which apoptosis and lysis of the infected cells occurs (Garcia *et al.*, 1997) and constitutes an indirect cytopathic means.

Figure 2.7 (taken from Gougeon, 2005) is an illustration of how HIV depletes the immune system of T helper cells as elaborated above. Through cognate interaction (cell-to-cell contact), CD4+ T cells recognise antigen from an antigen-presenting cell (APC, in this case a dendritic cell, DC) bearing MHC II complex. This interaction could either lead to apoptosis (direct or indirect viral cytopathic effect or CTL response), anergy (no response by the immune system) or to an activation state driven by cytokines such as IL-2 in the clonal expansion phase. Associated with this activation is the susceptibility to infection and destruction through activated T cell autonomous death (ACAD) and activation induced cell death (AICD) by virions. Proapoptotic virion particles such as gp120, Tat, Nef, Vpr or Vpu also cause HIV-protein mediated apoptosis. Following the massive cell death that occurs after activation (in the contraction phase, Figure 2.7) is the resulting loss of antigen specific CD4+ T cells. At this point cytokines such as IL-7 and IL-15 may rescue T cells from death, allowing for memory T cell generation. A fraction of the cells at this point still contain a reservoir of proviral DNA that is hidden from the immune system.

Given the central role played by the T helper cells on both the humoral and cellular arms of the immune response, it is easy to envision how their depletion as a result of the direct and indirect cytopathic effects and the CTL response can eventually lead to immune failure, opportunistic infections and death. It is therefore not surprising that targeting CD4+ T cell activation is now being recommended for novel HIV therapies (Forsman and Weiss, 2008) and has been shown to be effective in several clinical trials and studies (Lori *et al.*, 2005, Lori *et al.*, 1997, Frank, 1999, Rustchman *et al.*, 1998). In addition, the role played by cytokines such as IL-7 in this sequence of events in rescuing T cells further elaborates its significance in boosting immune parameters as seen in the mice cleared of an HIV-like virus (Pellegrini *et al.*, 2011).

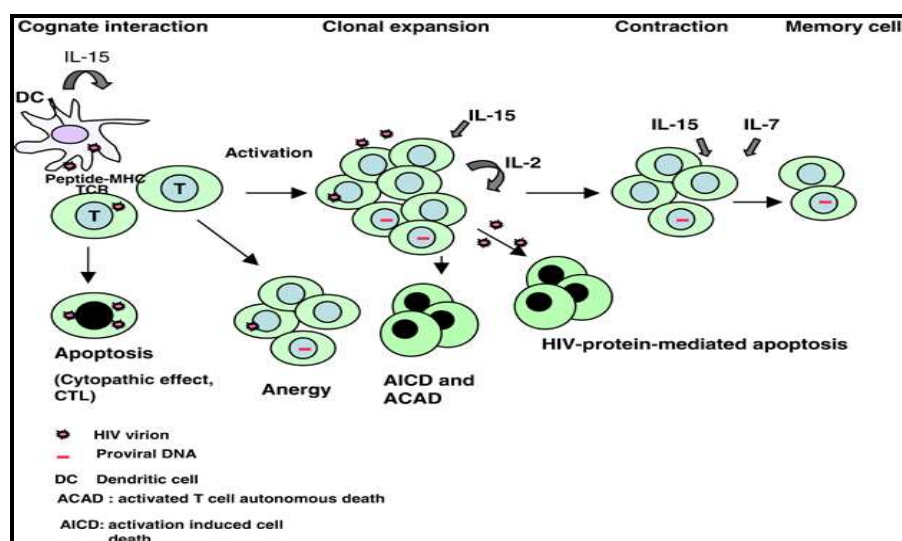


Figure 2.7: An illustration of the mechanisms of depletion of HIV specific CD4+ T cells during infection. Upon recognition of antigen, T cells are either killed by direct viral cytopathic effect or CTL response. Some cells undergo a state of anergy (no response) while others become activated and are destroyed through AICD and ACAD or by HIV-protein mediated apoptosis. Cytokines such as IL7 and IL-15 secreted in the course of the activation may rescue the cells allowing for memory T cell generation. This figure was taken from Gougeon (2005).

2.1.6 Vaccine Development

There is no doubt that an effective vaccine remains the most practical way of addressing and preventing new infections from HIV. Traditional vaccine strategies such as those that have been effective for pandemics like smallpox, polio, measles and yellow fever depended on the production of neutralising antibodies (Arrode-Bruses *et al.*, 2010). The prevention and control of HIV infection on the other hand strongly depends on the development of high-frequency, broadly targeted, polyfunctional T-cell responses specific to the virus (Johnston and Fauci, 2008, Betts *et al.*, 2006). Unfortunately efforts towards such a vaccine have not kept pace with basic scientific research except for some exciting advances that were made in 2009. These include the first partial protection in humans from an HIV vaccine in the RV144 trial in Thailand (Rerks-Ngarm *et al.*, 2009). In this trial, four priming injections of a recombinant canarypox vector vaccine (ALVAC-HIV [vCP1521]) and two booster injections of a recombinant gp120 subunit vaccine (AIDSVAX B/E) were evaluated in a randomised trial involving 16,402 healthy men and women. Vaccine efficacy of up to 31.2% was observed. Other developments include evidence for significant vaccine induced control of SIV in non-human primates (Hansen *et al.*, 2009) with others that involved the use of live-attenuated SIV/HIV (Mansfield *et al.*, 2008, Johnson *et al.*, 1997). The risk that pathogenic forms of such vaccines can redevelop makes them ineligible for human use (Arrode-Bruses *et al.*, 2010). The identification of a new target for broadly neutralising antibodies on HIV's surface (Walker *et al.*, 2009) was also a significant move towards vaccine development. Recent findings on vaccine development reported by BBC News on Health, May 11th 2011 (<http://www.bbc.co.uk/news/health-13362927>) by US researchers suggests protection of 13 of 24 rhesus macaques monkeys from infection with SIV. This exciting new finding involved the use of a genetically modified form of rhesus cytomegalovirus (CMV) engineered to produce antigens to attack SIV. Again safety concerns are an issue here in terms of translating these findings to humans considering that the CMV virus is disease causing.

While preventative vaccines studies are being pursued, the development of therapeutic vaccines needed to boost the immune system of people already living with the virus is also gaining grounds. Following reports that indicated the induction of protective anti-viral immunity in hu-PBL-SCID (mice model appropriate for HIV research) mice upon the adoptive transfer of autologous dendritic cells loaded *in vitro* with aldrithiol-2 (AT-2)-inactivated HIV-1 (Lapenta *et al.*, 2003, Yoshida *et al.*, 2003), *in vivo* toxicity and efficacy studies were performed (Lu *et al.*, 2004). This first *in vivo* study on the toxicity and efficacy of an HIV therapeutic vaccine resulted in viral suppression and HIV specific immunity after immunisation by 90% in 8 of 18 subjects, with the only clinical manifestation being the increase in size of peripheral lymph nodes (Lu *et al.*, 2004). The efficacy of this vaccine still had to be proven in a randomized trial with appropriate controls (Lu *et al.*, 2004). In a recent report by Garcia *et al.*, (2011), using the same AT-2-inactivated HIV-1 vaccine, with the inclusion of a control arm, weak HIV-1 specific

T cell responses were observed unlike the sustained responses observed by Lu *et al.*, (2004). The differences in the responses in the two trials was not clear but might be related to the inactivation method of the virus used for the treatments (Garcia *et al.*, 2011). Four therapeutic DNA vaccines with promising activity were presented at the XVIII International AIDS Conference in Vienna (Austria, 2010). The identification of a therapeutic vaccine for HIV will be advantageous over current medication because of the associated reduced toxicity (Fiorentini *et al.*, 2010).

These recent advances in both preventative and therapeutic vaccines call for more investment in vaccine development. In the case of preventative vaccines, the immediate aim should be to increase the efficacy that has been demonstrated by the live attenuated SIV vaccine in non-human primates while focusing on ways to minimise the development of pathogenic strains; also a main concern in the CMV engineered vaccine. In addition, focusing on the development of vaccines that can illicit neutralising antibodies in the long term (Koff, 2010) is also desired so as to maintain extended protection.

2.1.7 Therapy

The US Food and Drug Administration (FDA) has approved a total of 25 ARV drugs for the treatment of HIV infection (de Béthune, 2010). These available drugs belong to six different classes and include; eight NRTIs, four NNRTIs, ten PR inhibitors and one IN inhibitor which all target viral enzymes, a fusion inhibitor which prevents the fusion of the viral envelope with the host cell membrane and a CCR5 inhibitor which blocks the interaction of the virus with one of its receptors on the host cell (De Clercq, 2009). Until recently, therapy largely involved the virally encoded targets RT, IN, PR, and gp41 (Adamson and Freed, 2010) and has only more lately been expanding to include viral-host protein interactions and cellular targets. The combination of these drugs (mostly RT and PR inhibitors) in what is known as HAART has led to substantial improvement in the clinical management of HIV infection in terms of delaying disease progression, prolonging survival and improving quality of life (Antiretroviral Therapy Cohort Collaboration, 2008). This simultaneous use of multiple drugs is required because of the ease with which HIV can develop drug resistance to any single inhibitor (Simon *et al.*, 2006, Temesgen *et al.*, 2006). In the following subsections, the various viral targets and structural examples of some of the drugs targeting each will be discussed followed by a brief discussion on novel targets that are being explored as future therapeutic intervention points.

2.1.7.1 HIV reverse transcriptase and inhibitors

The RT enzyme of HIV is a heterodimer consisting of 66- and 51-kDa subunits (Fields, 1996) and is involved in converting viral RNA to cDNA. This multifunctional enzyme is involved in RNA dependent polymerisation, DNA dependent polymerisation, strand displacement synthesis and strand transfer, and degrades the RNA strand in the RNA/DNA hybrid (Schultz

and Champoux, 2008). It performs these functions through its **polymerase function** (for which there are two classes of inhibitors, the NRTI and NNRTIs) and an **RNase H function** that is unique to the C terminus of the p66 subunit (Su *et al.*, 2010). The polymerase domain of the enzyme is found in the N-terminal two-thirds while the RNase H domain is in the C-terminal one-third (Telesnitsky and Goff, 1993) of the p66 subunit. The polymerase function requires either RNA or DNA as the template (Sarafianos *et al.*, 2009). In addition, like most DNA polymerases, it needs a primer and makes use of a host transfer RNA (tRNA) as primer (tRNA_{Lys3}). RNase H activity is required for processing the tRNA primer to begin minus-strand DNA synthesis and degradation of viral RNA during synthesis followed by preparation of the polypurine tract DNA-RNA hybrid which serves as the primer for positive strand DNA synthesis (Fields, 1996, Hansen *et al.* 1988). All these processes (reviewed by Sarafianos *et al.*, 2009) result in the copying of a single stranded RNA to a double stranded DNA (Schultz and Champoux, 2008).

The crystal structure of RT in complex with some active site inhibitors are shown in Figure 2.8 while the structures of some **RT inhibitors** in clinical use (NRTIs and NNRTIs) are provided in Figure 2.9. The earliest inhibitor of HIV was the NRTI, azidothymidine (AZT) which initially had potential as an anti-cancer agent (Wlodawer and Vondrasek, 1998). Although RNase H inhibitors have been described, none has yet been approved for clinical use (Sarafianos *et al.*, 2009). NRTIs function by terminating the elongation of the growing cDNA strand and thus function like deoxynucleotide triphosphate (dNTPs) or analogues of the natural substrates of DNA synthesis. These inhibitors lack the 3'-OH normally present in the natural substrates and act as chain terminators when incorporated into viral DNA by RT (Sarafianos *et al.*, 2009). Examples are zidovudine and didanosine (shown in Figure 2.9). NNRTIs on the other hand are allosteric inhibitors that inhibit the polymerase function by binding to a pocket that is approximately 10 Å close to the NRTI site, (Sarafianos *et al.*, 2009, Gotte, 2006). The structures of two NNRTIs (nevirapine and delavirdine) are shown in Figure 2.9.

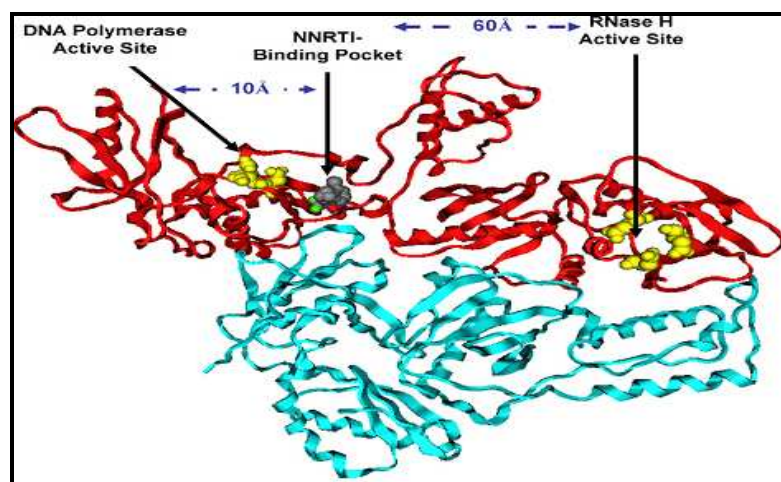


Figure 2.8: Ribbon representation of HIV-1 RT in complex with active site inhibitors. The DNA polymerase, the NNRTI binding pocket and the RNase H active site are shown, all within the p66 domain (red). The p51 subunit is shown in green. This figure was taken from Sluis-Cremer and Tachedjian, (2008).

The importance of these NNRTIs and the NRTIs in HAART is significant. The NRTIs form the basis of HAART with at least two of them usually included in combination with one NNRTI or a PR inhibitor (Pommier *et al.*, 2005). Unfortunately, the greatest shortcoming with HAART therapy amongst others is not only the high genetic diversity of HIV within an individual patient resulting from high replication and frequent recombination events. The error prone nature of RT (Simon *et al.*, 2006, Svarovskaia *et al.*, 2003) also results in the development of viral strains resistant to RT inhibitors and other drug targets. In addition these drugs like most of the other classes of HAART drugs are toxic, with adverse effects ranging from lactic acidosis to hepatotoxicity (Montessori *et al.*, 2004). More details on these limitations will be provided in the next section.

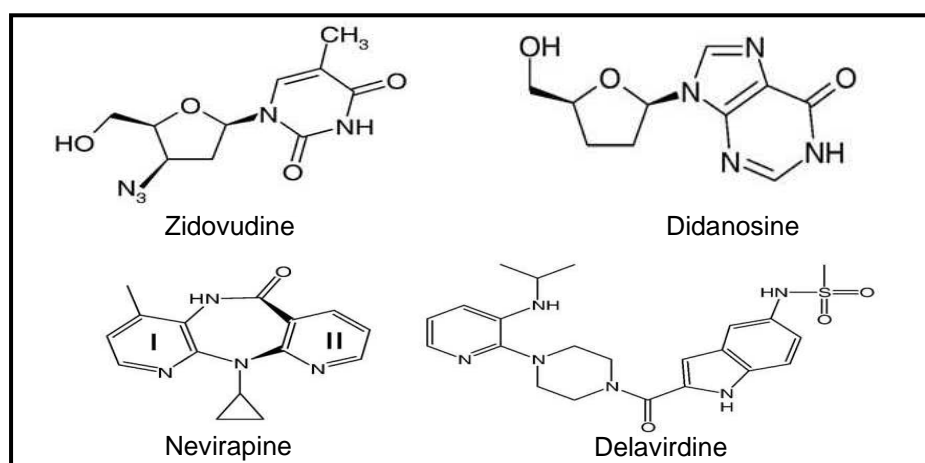


Figure 2.9: Structural representation of some RT inhibitors currently in clinical use. Zidovudine and didanosine are examples of NRTIs while delavirdine and nevirapine are NNRTIs. This figure was adapted from Sarafianos *et al.*, (2009).

2.1.7.2 HIV protease and inhibitors

HIV protease is an aspartic PR that is involved in the processing of the viral gag and gag/pol polyproteins (Debouck, 1992), a step that is necessary for the production of infectious virions. It does so by hydrolysing the polyproteins to functional protein products that are necessary for viral assembly and subsequent activity. This maturation process occurs as the virion buds from the cell. A functional HIV PR enzyme exists as a dimer of identical 99 amino acids with a twofold axis of symmetry through the substrate binding site (Purohit *et al.*, 2008). This enzyme is very important in HAART therapy since its inhibition prevents the formation of infectious virions (Wlodawer and Vondrasek, 1998). A crystal structure of HIV PR is shown in Figure 2.10 with two catalytic residues (Asp25 from each monomer) shown as ball and stick diagrams. The early knowledge of the crystal structure of HIV PR facilitated structure-based drug design for this target (Wlodawer and Vondrasek, 1998).

The structures of two of the ten clinically approved **PR inhibitors** are shown in Figure 2.11 namely ritonavir and indinavir. Both inhibitors have hydroxyl groups (boxed) that are important in the formation of hydrogen bonds with the active site aspartates (Wlodawer and Erickson, 1993). Resistance to PR inhibitors is also common and develops rapidly because of the site-specific mutations that occur in the enzyme at one or more locations (Rose *et al.*,

1996, Baldwin *et al.*, 1995). This is also linked to the high error rate of RT since the nucleotide sequence of PR ends up changing over generations. Toxicity (e.g. hepatotoxicity), is also a common adverse effect associated with the use of PR inhibitors (Montessori *et al.*, 2004).

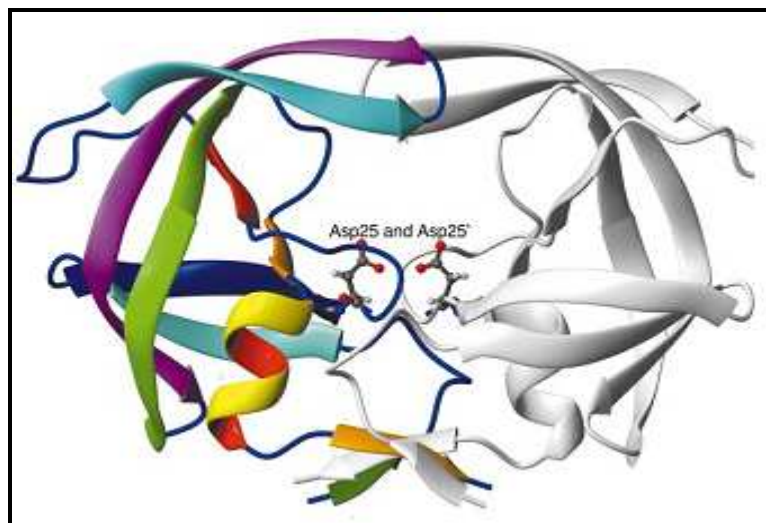


Figure 2.10: Structure of HIV PR. Catalytic residues Asp25 from each monomer are shown in ball and stick notation just below the binding site pocket (Adapted from Zoete *et al.*, 2002).

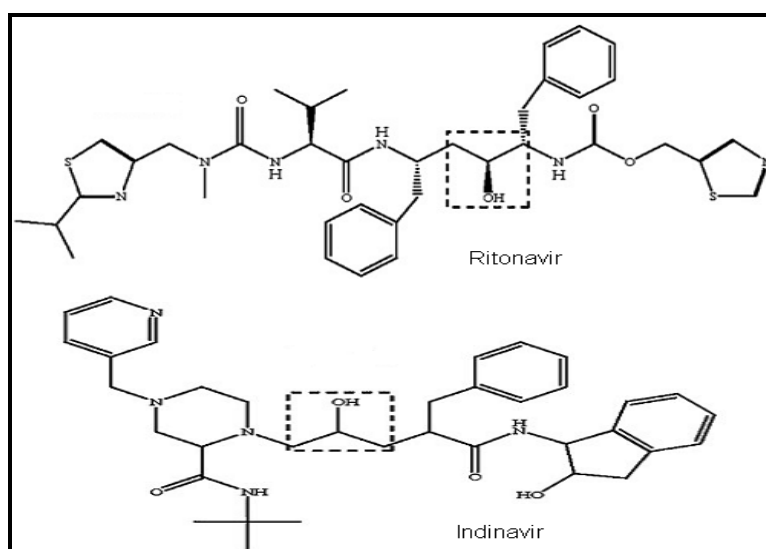


Figure 2.11: Structure of some HIV PR inhibitors in clinical use. The boxed hydroxyl group in both inhibitors is critical in forming hydrogen bonds with the active site aspartates. This figure was adapted from Wensing *et al.*, (2010).

2.1.7.3 HIV integrase and inhibitors

HIV IN is an attractive drug target because there are no homologues in eukaryotic systems that could negatively affect host cell viability (Dolan *et al.*, 2009). The enzyme is a DNA recombinase that catalyses two endonucleolytic reactions (Michel *et al.*, 2009). These are the **3'processing (3'P) reaction** in which IN cleaves a dinucleotide from each of the 3' ends of viral cDNA thereby exposing a 3'-OH group at each end and the **strand transfer reaction** where the enzyme generates a double-strand break in the host DNA and joins the newly formed ends to the viral 3' ends by transesterification (Engelman *et al.*, 1991). Host DNA repair proteins then remove the two nucleotide overhangs and fill in the DNA gaps to complete the integration reaction (Yoder and Bushman, 2000). The enzyme consists of three

structural and functional domains (shown in Figure 2.12). The N-terminal zinc-binding domain (residues 1-49), which is required for 3' P and ST *in vitro*, binds viral DNA sequences and promotes IN multimerisation (Engelman *et al.*, 1993), the central catalytic core domain (CCD; residues 50-212) binds specifically to viral DNA and the C-terminal domain (residue 213-288) that interacts with RT (Eijkelenboom *et al.*, 1999).

IN inhibitors were only recently approved for anti-viral therapy with one of the greatest limitations having been the fact that the crystal structure of full length IN or in complex with DNA has not yet been resolved (Savarino, 2007). The first drug raltegravir has already been successfully used in the clinic (Chirch *et al.*, 2009). Even though the enzyme represents an attractive HIV drug target, resistance (Wielens *et al.*, 2010) and cross resistance problems between raltegravir and a second IN inhibitor in clinical trials (elvitegravir) have already been reported (Marinello *et al.*, 2008). Figure 2.13 portrays the structures of raltegravir and elvitegravir and two other compounds, 5-CITEP (1-(5-chloroindol-3-yl)-3-hydroxy-3-(2H-tetrazol-5-yl)-propenone) and a diketo acid B which have demonstrated *in vitro* inhibition of IN.

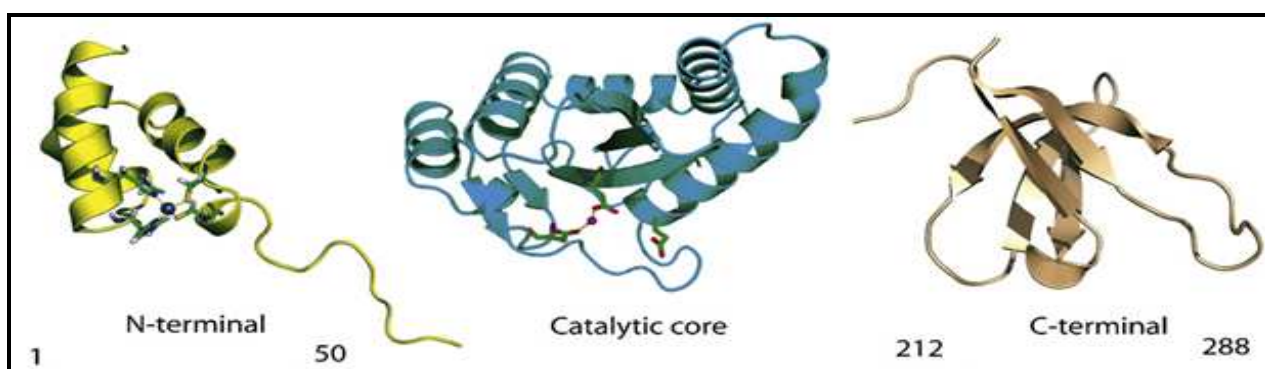


Figure 2.12: Structural and functional domains of IN. The N-terminal domain which is also the zinc binding domain consisting of residues 1-49, the CCD consisting of residues 50-212 which binds specifically to viral DNA and the C-terminal domain which interacts with RT and consist of residues 213-288. Residue numbers for each of the domains are shown (but not for RT and PR above) since the structure of full length IN has not been resolved. The figure was adapted from Mouscadet *et al.*, (2010).

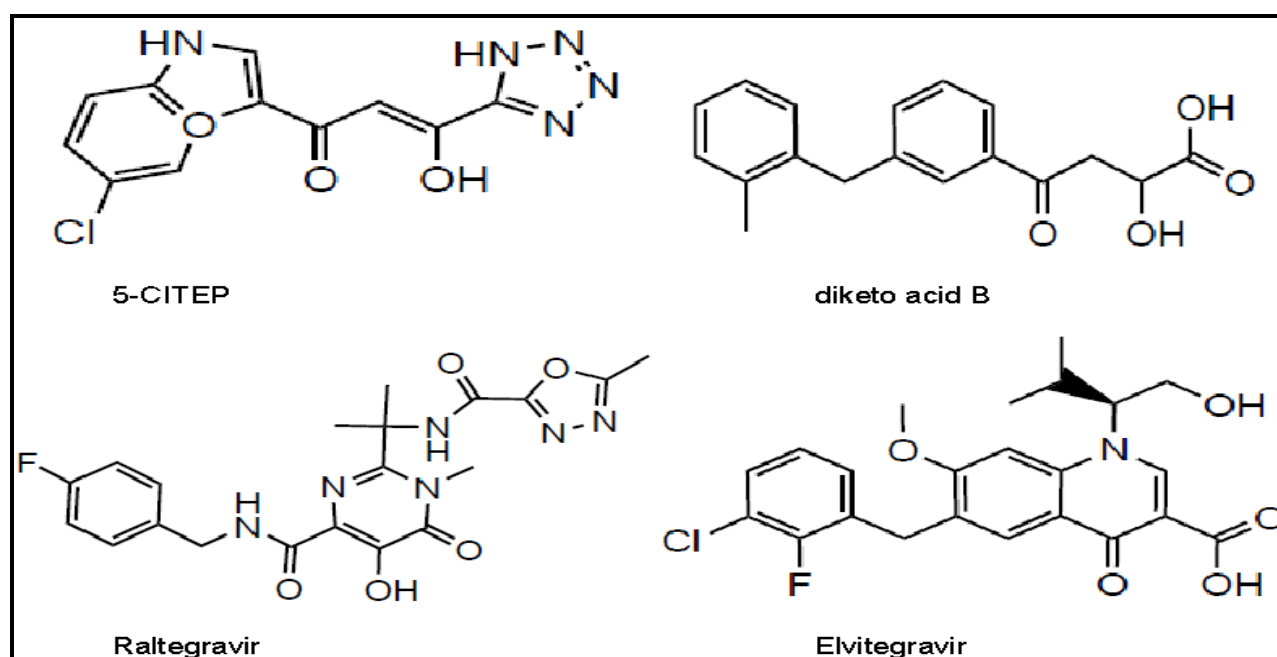


Figure 2.13: Structure of some IN inhibitors. The clinically approved raltegravir and elvitegravir are shown. 5-CITEP and the diketo acid B have inhibited IN *in vitro*. This figure was taken from Savarino, (2007).

2.1.7.4 Viral entry and inhibitors

The viral entry process is a complex multistep event that involves (a) attachment to host cells and CD4 binding, (b) co-receptor binding and finally (c) membrane fusion (see Figure 2.14A, reviewed by Tilton and Doms, 2010). Entry is initiated by the attachment of gp120 found on the viral surface with the CD4 receptor of the host cell. This is followed by conformational changes involving the V3 loop (on gp120) of the virus, allowing for binding with the co-receptor (Huang *et al.*, 2005 Trkola *et al.*, 1995). The gp41 fusion peptide is then inserted into the host membrane followed by the formation of a six-helix bundle that brings both viral and host membranes together. This leads to the formation of a fusion pore allowing for the entry of HIV capsid into the host cell.

Entry inhibitors consist of compounds that prevent one of the multistep processes involved in entry i.e. attachment and CD4 binding, co-receptor binding and fusion. Two entry inhibitors (maraviroc and enfuvirtide) have been approved for the treatment of HIV infection and a number of new drugs are in development (Tilton and Doms, 2010). The currently approved entry inhibitors block CCR5 binding e.g. maraviroc and fusion e.g. enfuvirtide (structures shown in Figure 2.14B). These drugs are ideal for patients harbouring strains resistant to RT and PR and can therefore serve as salvage therapy. Such drug types are also recommended for use in microbicides (Tilton and Doms, 2010) since they can prevent entry.

Resistance to entry inhibitors is also possible since the viral envelope which is targeted either directly or indirectly has high diversity and can vary between patients (Tilton and Doms, 2010). Mutations indicative of resistance have been seen in patients on enfuvirtide (Xu *et al.*, 2005, Poveda *et al.*, 2004).

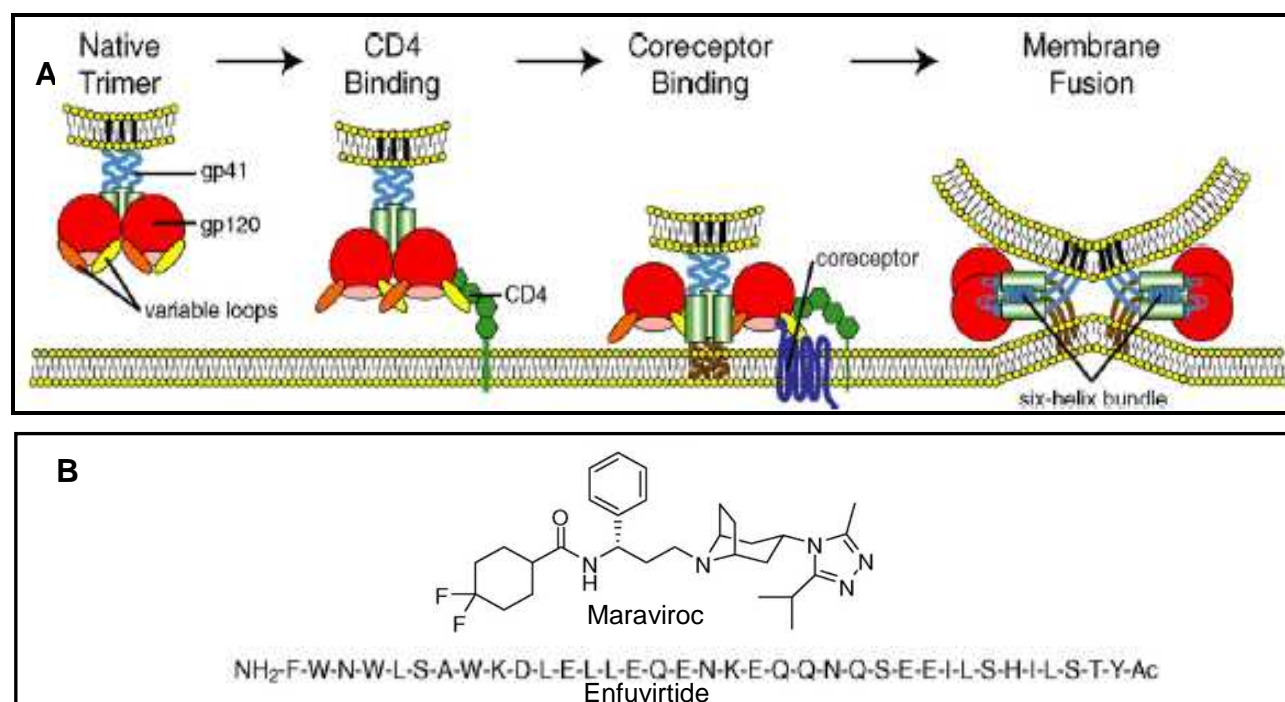


Figure 2.14: Viral entry process (A) and some entry inhibitors (B). The molecular structure of the CCR5 antagonist maraviroc and that of the fusion inhibitor, enfuvirtide are shown in B. This figure was taken from Tilton and Doms, (2010).

2.1.7.5 Cytostatic inhibitors and virostatic combinations

Drugs used in the clinic for HIV treatment have until recently, largely focused on those that target the virus directly. The problem with such medication is the rapid development of drug resistant strains of the virus (Simon *et al.*, 2006, Svarovskaia *et al.*, 2003, Holmes *et al.*, 1992). In order to address drug resistance, recent research efforts have aimed at indirectly inhibiting the virus through cellular targets (Lori *et al.*, 2005, Mayhew *et al.*, 2005, Lori *et al.*, 2007, Lori, 2008). Compounds that cause a cytostatic effect on cells such as hydroxyurea (HU), trimidox and didox have been shown *in vitro* and all the way to clinical trials (Lori, 2008, Mayhew *et al.*, 2005, Lori *et al.*, 2005, Lori, 1999, Lori *et al.*, 1997) to be less prone to resistance when compared to the current HAART combinations. Cytostasis is the ability of an agent to prevent cell growth and multiplication. Hydroxyurea has a history in the hematology field for the treatment of myeloproliferative disorders and cancers (Lori, 1999) because of its cytostatic effects. The cytostatic effect of HU lowers dNTP pools within the cells resulting in a reduction in viral replication since the virus requires host dNTPs for synthesising viral cDNA. HU is known to inhibit RNR which normally converts ribonucleotides to dNTPs (Lori, 1999) and specifically reduces the synthesis of deoxyadenosine triphosphate (dATP, Slabaugh *et al.*, 1991, Bianchi *et al.*, 1986). For this reason, it is often combined with adenosine dideoxynucleoside analogues e.g. didanosine (ddI). In this combination, HU lowers the concentration of the natural substrate needed for DNA synthesis (i.e. dATP) thereby increasing the concentration of the analogue (ddI) leading to an overall decrease in viral replication. Other ways by which HU inhibits HIV is through its immune modulating effects in which case the compound decreases CD4 T cell numbers, reducing the number of activated cells that are primed for killing by HIV. There are concerns that such agents may be very toxic especially when administered to already immunocompromised individuals (Lori *et al.*, 2005). However, even though HU alone may be toxic (to very sick people) compelling evidence now suggests that the combination of HU or HU-like agents with compounds that have a direct anti-viral effect such as ddI, results in the boosting of immune parameters such as CD4+ cell increases and decreases in viral load. This combination forms what is now considered a new and emerging class of anti-HIV agents known as virostatics and defined by Lori *et al.*, (2007, 2005) as the combination of a drug directly inhibiting virus e.g. ddI (*viro*) and one indirectly inhibiting virus (*static*) e.g. HU.

The anti-viral and cytostatic mechanism of virostatics is illustrated in Figure 2.15A and B and the structure of HU is provided in Figure 2.16. Didanosine is clinically used as a NRTI and its structure was provided earlier in Figure 2.9. In the anti-viral mechanism (A), in the absence of treatment, more viral particles are produced and upon treatment with HU, there is a decrease in viral particles. In the absence of treatment (cytostatic mechanism, B), proliferation increases and so does viral particles but upon treatment with HU, there is a

decrease in viral particles and an optimal number of CD4+ cells. The combination of the anti-viral and cytostatic effects results in an overall shift to an optimal state.

Virostatic cocktails have shown promising results both *in vitro* and in clinical trials (Clouser *et al.*, 2010, Lori *et al.*, 2005, Mayhew *et al.*, 2005, Lori *et al.*, 1997, Frank, 1999, Rutschmann *et al.*, 1998, Federici *et al.*, 1998). The outstanding advantage is the observed improved resistance profile, which makes this combination unique over current HAART schedules.

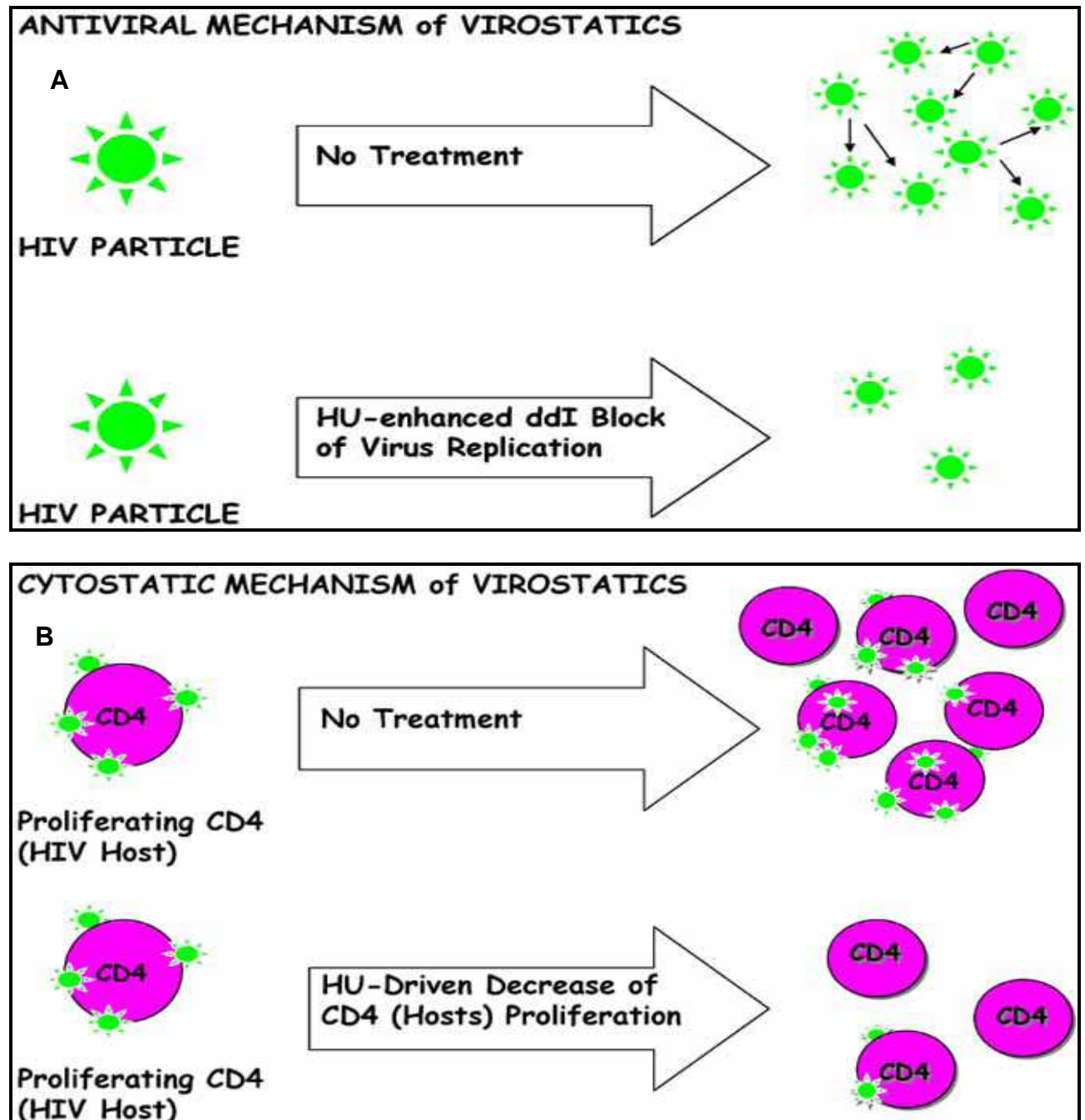


Figure 2.15: The anti-viral and cytostatic mechanism of virostatic agents. In (A), in the absence of treatment, the virus makes more copies of itself and upon treatment with HU-ddI combination, less viral particles are present. In B, in the absence of treatment, the virus divides more as the cells get activated and proliferation increases but upon treatment with HU, the number of viral particles reduces and the CD4 cell number shifts to an optimal but intermediate level. These figures were taken from Lori *et al.*, (2007).

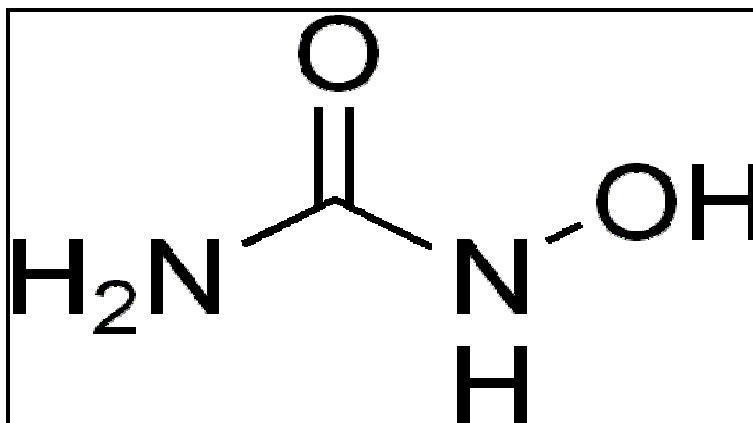


Figure 2.16: Structure of hydroxyurea, an important cytostatic agent. The figure was taken from <http://upload.wikimedia.org/wikipedia/commons/c/c9/Hydroxyurea.png> (accessed on the 5/05/2011).

2.1.7.6 Novel targets

Until a cure is developed for HIV, sustained continual development of anti-viral therapy is required since it is the only lifeline for infected individuals. The driving force for novel drug development is the resistance problems associated with HAART (Adamson and Freed, 2010). Identifying new therapeutic targets for inhibiting the virus is important and as such new ones are continually being sought. In addition to exploring new viral targets, viral host protein interactions and cellular targets are also being explored (Adamson and Freed, 2010). Novel targets relevant to this study include the RNase H site of RT and the IN cofactor or lens epithelium derived growth factor (LEDGF) or p75 binding site which are both post entry targets (Adamson and Freed, 2010). The RNase H site as mentioned earlier is involved in the reactions that result in the conversion of viral RNA to cDNA during the reverse transcription process. There are currently no known RNase H inhibitors in the clinic but a lot of research into their possible use is ongoing. RNase H is a viable target because point mutations within its domain have shown that its endonuclease activity is required for viral infectivity (Kirschberg *et al.*, 2009).

LEDGF on the other hand is a cellular cofactor involved in the integration process by tethering IN to the chromosome of infected cells (Poeschla, 2008, Maertens *et al.*, 2003). Various studies have shown that by inhibiting the LEDGF-IN (protein-protein) interaction, the integration process catalysed by IN can be allosterically blocked (Christ *et al.*, 2010). The cofactor interacts with the enzyme's catalytic core domain using its C terminal integrase binding domain (IBD). The structure of the LEDGF-IN complex is shown in Figure 2.17. Only the IBD of LEDGF is shown.

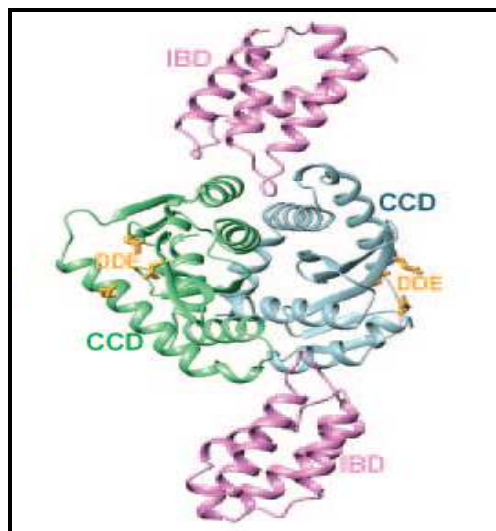


Figure 2.17: Structure of IN-LEDGF complex. The cofactor interacts with the CCD of IN using the IBD. The CCD of IN chains A and B are coloured green and blue. The integrase binding site of LEDGF is coloured purple. Yellow sticks represent the catalytic triad of IN active site. The LEDGF binding site is different from the catalytic site. This figure was taken from Cherepenov *et al.*, (2005).

2.1.8 Therapy Complications and the Need for Novel Drug Development

Treatment with antiretroviral therapy (ART) has greatly improved and prolonged the lives of infected individuals. This development has unfortunately been met with numerous challenges. The major ones which include toxicity to the host and resistance to drugs by the virus will be discussed together with some of the adverse effects that stem from the use of these drugs.

2.1.8.1 Viral resistance to available drugs

Drug resistance has been noted for all the known inhibitors of HIV i.e. those aimed at viral enzymes (RT, PR and IN) as well as those aimed at viral entry. This has been attributed to a number of factors. The extensive genetic variation that the virus has within an individual host particularly in the hypervariable regions of the *env* genes (Holmes *et al.*, 1992) means that different variants of the virus easily develop. Furthermore, the error prone nature of RT during the viral genome copying process also facilitates the development of resistance (Simon *et al.*, 2006, Svarovskaia *et al.*, 2003). The enzyme is known to make ~ 0.2 errors per genome during each replication cycle (Preston *et al.*, 1988). These errors end up causing mutations in the structure of RT, IN, PR as well as the viral envelope over generations of replication with the result being resistance to all the inhibitors of these targets. This is further enhanced by the high replicative ability that the virus has with a viral generation time of ~ 2.5 days, producing ~ 10^{10} - 10^{12} new virions everyday (Perelson *et al.*, 1996). In addition, recombination and natural selection pressures further propagate evolution and genetic diversity and thus increases resistance (Rambaut *et al.*, 2004). The fact that most HAART drugs were developed for subtype B viral strains means that specificity for non-B subtypes is reduced. The result of this is the development of resistant strains by non-B subtypes that are different from those seen in

the subtype B strain, in addition to those normally present in subtype B strains (Kantor and Katzenstein, 2004). Resistance problems are also further complicated by cross resistance to the same class of compounds e.g. NNRTI (Johnson *et al.*, 2005) and to the recently approved raltegravir and elvitegravir (a second IN inhibitor in phase III trials, Marinello *et al.*, 2008). The identification of drugs that target non viral targets (e.g. those that inhibit ribonucleotide reductase or which lower immune activation by preventing antigen presenting cells from activating T cells) may arguably be the best remedy in curbing the rampant resistance problems associated with all classes of drugs currently used in HAART combinations and in salvage therapy. More specifically the use of virostatic combinations (please see section 2.1.7.5 for details on this) which reduce the development of viral resistance, may be the way forward.

2.1.8.2 Drug toxicity to host

Toxicity to the host is a major limitation of ARV agents and is evident in many ways that result in adverse clinical manifestations. Some toxicity examples include hepatotoxicity from the RT inhibitors (NRTIs and NNRTIs) and PR inhibitors, PR inhibitor-associated retinoid toxicity (reviewed by Montessori *et al.*, 2004) and mitochondrial toxicity caused by NRTIs which all lead to a whole host of clinical manifestations that can be deadly (Montaner *et al.*, 2003). The fact that therapy is life-long means toxicity problems cannot be ruled out during HAART. Other clinical complications from HAART, provided by Yeni (2006) include complications from NRTIs that lead to subcutaneous lipoatrophy peripheral neuropathy, lactic acidosis and pancreatitis with the former two being life threatening conditions. Complications from NNRTIs could be skin rashes and toxic hepatitis and these usually occur during the onset of treatment. With regards to PR inhibitors, the major adverse effects are the accumulation of visceral fat and hyperlipidemia. A link between the duration of HAART and the incidence of myocardial infarction has also been observed.

2.1.8.3 Other limitations

Other limitations of HAART that end up affecting treatment and treatment schedules are: (1) intolerable side effects such as bloating, nausea, diarrhoea (which may be temporary or may be throughout therapy, Carr and Cooper, 2000), fatigue, headaches and nightmares (Montessori *et al.*, 2004). These effects usually lead to poor adherence. Poor adherence means suboptimal doses of the drugs are taken such that virus escape mutants result leading to increased drug resistance. (2) The costs involved in acquiring the drugs limits availability in resource restricted settings such as Sub-Saharan Africa where the infection burden is the highest. (3) Unfavourable drug-drug interactions resulting from the combination therapy and (4) the presence of latent forms of the virus in patients on HAART (Finzi *et al.*, 1997) prevents

complete eradication. This last complication is the reason why therapy has to be life-long since upon discontinuation, the latent forms emerge and start replicating.

2.1.8.4 Cure limitations

In 2009, the New England Journal of Medicine published a report of a man who was cured of HIV after receiving stem cells transplanted from a donor homozygous for the *CCR5* delta32 gene as treatment for acute myeloid leukaemia (Hutter *et al.*, 2009). Infection with HIV requires the presence of the CD4+ receptor and the *CCR5* co-receptor. People with a 32 bp deletion in their *CCR5* allele are reportedly resistant to HIV infection. Although possible, treating HIV infected people through this means has significant costs implications and finding the right donor could be very challenging as well. An important outcome of the study was the awareness of the significance of the *CCR5* co-receptor in HIV infectivity that has encouraged investigations into identifying *CCR5* inhibitors. Findings by Pellegrinii *et al.*, (2011) in which the clearing of an HIV-like virus (by the boosting of immune functions) from mice through the suppression of the *Socs3* gene by IL-7 still require significant research to translate to useful clinical application. As mentioned before, the identification of latent forms of the virus during treatment (meaning the virus can not be completely eradicated with HAART, Finzi *et al.*, 1997) was one of the earliest shortcomings. Upon termination of treatment, these latent forms emerge and start replicating.

2.1.8.5 Local needs

In the South African context, identifying novel therapy specific to the subtype C strain is very important because this strain (which is prevalent in this part of the world, Nkolola and Essex, 2006, Wouter *et al.*, 1997) has not been as widely studied as the subtype B virus found in developed countries. Currently administered medications were synthesised using the subtype B viral strain and even though these drugs are active against non B strains e.g. C, effectiveness is less with a resultant increase in the incidence of mutations (Kantor and Katzenstein, 2004). In addition, the cost of current medication cannot be met by the poor (Ford *et al.*, 2007) making the identification of local, more effective and potentially cheaper therapies a necessary endeavour. This was one of the reasons that led to the creation of the Project AuTEK Biomed Consortium which is affiliated with two mining companies in South Africa (Mintek and Harmony Gold) and South African universities. The idea here was that the natural availability of pure gold deposits in South Africa could be exploited for possible health benefits by using gold in synthesising potential drugs.

Taken together, all the shortcomings in managing HIV and AIDS, coupled with the fact that no available vaccine or cure has been discovered necessitates the continuous search and identification of novel treatment options that can be used to supplement or replace currently available drugs. In the next section, an introduction to the drug development process will be

provided followed by a discussion on the use of metals in medicine with specific emphasis on gold-based compounds.

2.2 DRUG DEVELOPMENT

Drug development and discovery can be a very tough and long process both scientifically and financially for the pharmaceutical industry and it can typically take up to a decade for a drug to go through the different phases of drug discovery (Fishman and Porter, 2005), which are shown in Figure 2.18. These phases include the lead or target discovery phase during which important molecular targets are identified. This phase can typically take a year to several years (Fishman and Porter 2005). This is followed by the preclinical phase where toxicity, efficacy and dose response is determined using both *in silico* and *in vitro* techniques and involves technologies that range from traditional high throughput screening (HTS) to affinity selection of large libraries, fragment-based techniques and computer-aided design (Keseru and Makara, 2006). In phase I/II, biomarkers and response to treatment are monitored together with adverse responses and efficacy in humans. Successful candidates which go through these preliminary phases are finally entered into phase III/IV, a phase which involves the prediction of adverse responses and efficacy monitoring at a larger scale and finally approval and clinical application of the successful drug candidate.

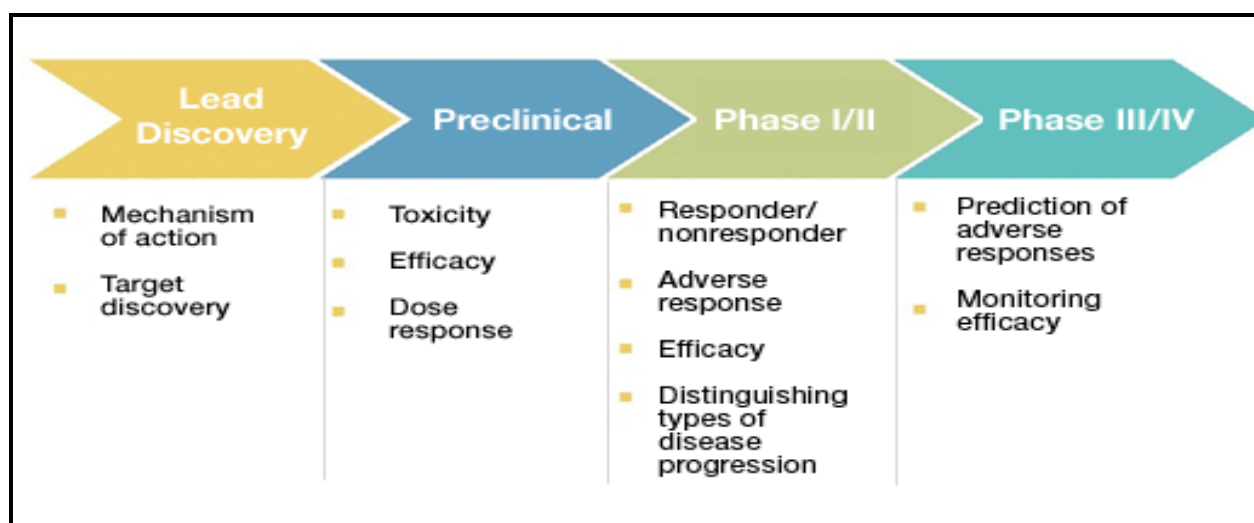


Figure 2.18: Drug discovery phases: a typical drug discovery phase diagram. This figure was taken from www3.bio-rad.com (accessed 26/01/2011)

In the course of the discovery process, drug-like properties which include; absorption, distribution, metabolism, excretion and toxicity (ADMET) are monitored. Compounds that are drug-like are defined as those compounds that have sufficiently acceptable ADMET properties to survive through the completion of human Phase I clinical trials (Lipinski, 2000). Identifying drug-like compounds has become increasingly important after it was observed in the late 1990s that the main causes of late-stage failures in drug development were as a result of poor pharmacokinetics and drug toxicity (Lombardo *et al.*, 2003, van de Waterbeemd and Gifford,

2003). The introduction of ADMET screens in the early phases of drug discovery avoids loss in expenditure by pharmaceutical companies downstream the discovery process when it becomes apparent that the compounds are not drug-like.

In the past, focus on determining binding to the active site was a strong priority in discovery for medicinal chemists where HTS and traditional medicinal chemistry techniques were employed (Kerns and Di, 2008). The focus in modern day drug discovery is on structure activity relationships (SAR, Di and Kerns 2003). The latter has been enhanced by the development of virtual (*in silico*) screening techniques, which have been emerging in the past decade and are now perceived as complementary approaches to experimental HTS (Desai *et al.*, 2006). Coupling experimental HTS and virtual screening with structural biology, promises to enhance the probability of success in the lead identification stage of drug discovery. The combinations of these techniques have not only led to increased output but through SAR or rational drug design studies, medicinal chemists can easily correlate pharmacological and biological properties (Kerns and Di, 2008). The earliest impact of this was the decrease in late failures from 39% in 1998 to 10% in 2000 (Kola and Landis, 2004).

While it is important that drugs should go through the various phases of drug design to ensure safety and efficacy, identifying a perfect drug has never been achieved in the pharmaceutical industry (Joshi, 2007). As such, finding drugs that are tolerable such that management and patients could eventually benefit has been the trend. In this regard, physician intervention at the point of administration is an important point to consider during therapy.

2.3 METALLODRUGS

2.3.1 Brief Background

With close to three decades that have passed since the discovery of HIV as the causative agent of AIDS, many investigators have dedicated enormous efforts to finding promising drug leads, both synthetic and natural (De Clercq, 1995) to supplement existing treatments. Although many potential medicinal products (crude extracts and single molecules) have shown efficacy against HIV *in vitro* and *in vivo* (Gambari and Lampronti, 2006), mostly organic synthetic agents have been clinically approved. Advances in inorganic chemistry suggest a significant role of metals especially those of the transition metal series as being important in synthetic medicinal chemistry (Rafique *et al.*, 2010). These advances are facilitated by the inorganic chemists' knowledge on coordination chemistry and redox properties of metal ions (Kostova, 2006). In addition, the wide scope that metals have in interactions with biological systems means that they could easily be accommodated in drugs. This ease of interactions results from the fact that metals easily lose electrons and get converted to an ionic state, which is soluble and electron deficient (Orvig and Abrams, 1999). In this state, metals tend to interact with proteins and DNA which are electron rich (Orvig and

Abrams, 1999). An example is iron, contained in the protein haemoglobin which binds to oxygen. Others are manganese, copper, zinc and iron that are incorporated into enzyme structures producing metalloenzymes which facilitate important chemical reactions in the body (Orvig and Abrams, 1999).

Metal-based drugs or metallodrugs have a history dating back to the earliest times (Higby, 1982) have advantages over traditional organic medicine. The drugs make use of metal-drug synergism where there is enhancement of the activity of the parental drug after complexation which is chemical reaction involving a metal and an organic moiety (ligand) with the metal (Navarro, 2009, Beraldo and Gambino, 2004). This activity enhancement is thought to be as a result of structural stabilisation from the coordination/complexation of the metal to the organic moiety (Navarro, 2009) or the ligand to form what is known as a complex. The metal complex or coordination complex as defined by Rafique *et al.*, (2010) is a structure consisting of a central atom, bonded to a surrounding array of molecules or anions.

In some cases, complexation with metals has been reported to lead to decreases in toxicity of the metal ions since the organic portion of the drug makes it less available for unwanted interactions that could lead to toxicity (Sánchez-Delgado and Anzellotti, 2004). Coordination may also lead to significant reduction in drug resistance because of improved specificity (West *et al.*, 1991, Kostova, 2006). The metals in metallodrugs form covalent bonds and ionic forces, unlike organic molecules, which form van der Waal forces and hydrogen bonding. Since these covalent and ionic forces are stronger, the drugs tend to stay at the active site longer thereby increasing efficacy and resulting in a synergistic effect from the organic and metal moieties (Navarro, 2009).

Some metals with medicinal properties are iron, ruthenium and silver, among others (reviewed by Rafique *et al.*, 2010). A typical example of a medicinally significant metal-based compound is cisplatin (a platinum-based drug), an anti-cancer agent. The discovery of this compound renewed interest in medicinal inorganic chemistry (Fricker, 2007, Zhang and Lippard, 2003). Gold-based metallodrugs also exist and are the focus of this study.

2.3.2 Gold Compounds as Metallodrugs

The use of gold in medicine (known as chrysotherapy) dates back to 2500 BC in ancient China (Fricker, 2007) probably mostly from anecdotal evidence. Its modern day application goes as far back as 1890 when Robert Koch discovered $[\text{KAu}(\text{CN})_2]$ as a bacteriostatic agent effective against the tubercle bacillus (Navarro, 2009). This led to the subsequent use of gold compounds for the treatment of tuberculosis (Berners-Price and Sadler, 1996) without success and later for the treatment of rheumatoid arthritis (RA) for which remission has been largely successful. In the following subsections, the activity of gold compounds both *in vitro* and *in vivo* will be discussed with emphasis on the anti-rheumatoid arthritic, anti-cancer, anti-malarial and anti-HIV effects.

2.3.2.1 Gold compounds as anti-rheumatoid arthritic agents

Rheumatoid arthritis is an inflammatory disease characterized by progressive erosion of the joint resulting in deformities, immobility and a great deal of pain (Fricker, 1996). It is an autoimmune disease that causes progressive destruction of the connective tissue in joints (Sutton, 1986). As early as 1935, Jacques Forrester reported on the beneficial effects that gold salts had in slowing down RA (Sutton, 1986). Some gold compounds that have been used for the treatment of RA are the thiolate compounds in which the gold is coordinated to sulphur-containing ligands. The earliest gold compounds used for the treatment of RA were the injectable thiolates; aurothioglucose (also called solganol) and aurothiomalate (also called myochrisin). Auranofin (also called radiura) is orally administered and was identified as a potential anti-rheumatoid arthritic agent in 1972 (Sutton *et al.*, 1972) and was later approved for clinical use. This compound has better pharmacokinetic properties and reduced toxicity than the injectable drugs. The structures of the thiolate compounds (aurothioglucose, aurothiomalate and auranofin) are shown in Figure 2.19. A fourth compound which is of medical importance (also represented in Figure 2.19) is the bis(diphos)gold(I) chloride compound which demonstrated promising anti-cancer activity and will be discussed in the next subsection.

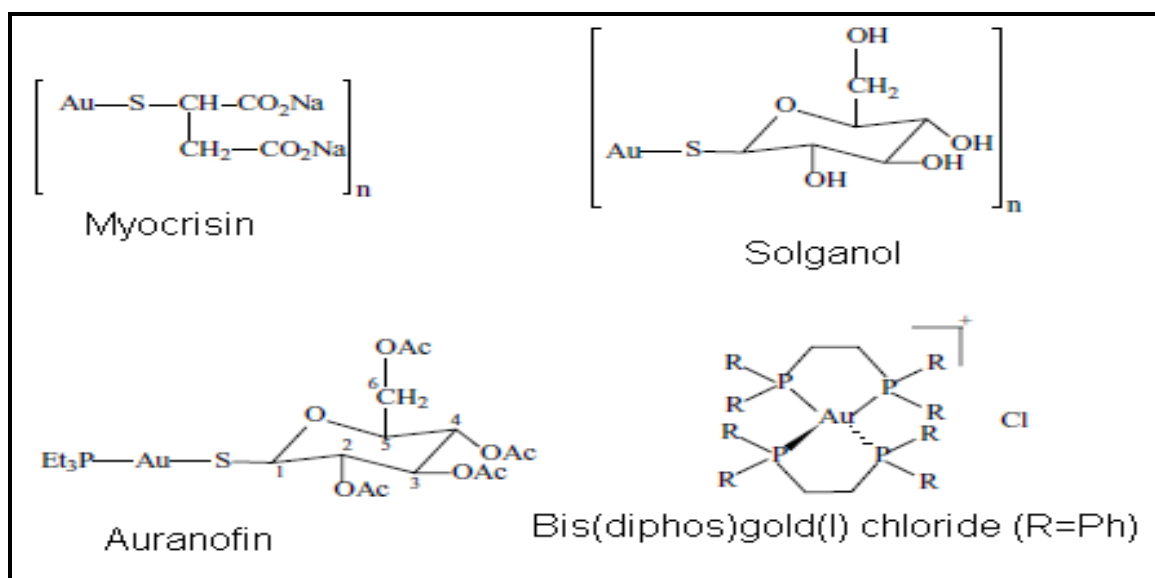


Figure 2.19: Structure of some important gold compounds in medicine. Thiolate compounds coordinated to Au through a S atom include myocrisin, solganol and auranofin. Myocrisin and solganol are injectable drugs while auranofin is orally available. The bis(diphos)gold(I) chloride is also represented as Au(DPPE) chloride (Adapted from Ahmad, 2004).

2.3.2.2 Gold compounds as anti-cancer agents

The discovery of cisplatin and its derivatives as anti-cancer drugs prompted the search for other metal containing anti-cancer agents (Arnesano and Natile, 2009). Early studies showed that the anti-rheumatoid arthritic agent, auranofin was toxic to some tumour cells in culture and *in vivo* against P388 leukaemia (Lorber *et al.*, 1979) but because of inactivity *in vivo* on most cancer cells, further testing was not pursued. A bis(diphos) gold(I) chloride

containing compound, $\text{Au}(\text{DPPE})_2\text{Cl}$ (Figure 2.19) known in full as [1,2-bis(diphenylphosphino)ethane]gold(I) chloride was reported in the 80s as having promising anti-tumour activity (Fricker, 1996, Berners-Price *et al.*, 1986, Mirabelli *et al.*, 1986) but latter dropped because of pre-clinical toxicity (Hoke *et al.*, 1989). This compound and auranofin are both gold(I) complexes.

Since gold(III) complexes are similar to cisplatin isostructurally and isoelectrically (Bruni *et al.*, 1999), these complexes were favoured for anti-cancer testing. Despite the similarity, little literature information existed on the use of gold(III) complexes as anti-cancer agents (Tiekink, 2002) up to the late 1990s. The reason for this is because of the high redox potential and poor stability that these compounds have in the biological milieu (Fricker, 1996). It has only been in the last decade that gold(III) complexes with promising anti-cancer activity *in vitro* have been identified leading to a rekindled interest. This is attributed to the identification and coordination to more stable ligands that are not readily reduced. Ligands such as polyamines, terpyridines, and phenathrolines are favoured (Milacic and Dou 2009). Some examples of stable gold(III) complexes that employed stabilising ligands are $[\text{Au}(\text{cyclam})](\text{ClO}_4)\text{Cl}_2$, $[\text{Au}(\text{terpy})\text{Cl}]\text{Cl}_2$ and $[\text{Au}(\text{phen})\text{Cl}_2]\text{Cl}$ (where terpy = terpyridine and phen = phenathroline) which were active against the A2780 ovarian cancer cell line and on a cisplatin resistant variant (Marcon *et al.*, 2002, Messori *et al.*, 2000). The gold(III) porphyrins are other examples which are stable in the presence of glutathione and exerted higher potency than cisplatin to human cervix epitheloid cancer cells (Che *et al.*, 2003). These new gold(III) compounds which have demonstrated greater efficacy than cisplatin require further pharmacological testing (Nobili *et al.*, 2010) to establish their possible role in anti-cancer therapy.

2.3.2.3 Gold compounds as anti-malarial agents

Since the landmark report by Navarro *et al.*, (1997) on the anti-malarial activity of a Au-CQ complex (CQ=chloroquine) and their 2004 report (Navarro *et al.*, 2004) further supporting these findings, other authors (Khanye *et al.*, 2010, Gabbiani *et al.*, 2009, Sannella *et al.*, 2008) have also shown that gold-based compounds demonstrate such activity. Khanye *et al.*, (2010) investigated the anti-malarial activity of gold(I) thiosemicarbazone-based complexes against the malarial cysteine protease, falcipain 2. The authors showed that there was an enhanced efficacy of the gold(I) thiosemicarbazone-based complexes against CQ sensitive (D10) and CQ-resistant (W2) strains compared to the parent ligand through the inhibition of falcipain 2. Gabbiani *et al.*, (2009) also reported on the anti-plasmodial activity of a panel of metal complexes consisting of one mononuclear gold(III) complex (Aubipy where bipy represents bipyridenes) and three dinuclear gold(III) complexes. In another report, Sanella *et al.*, (2008) showed that auranofin which is a potent inhibitor of mammalian thioredoxin reductases (which causes severe oxidative stress) was capable of inhibiting the growth of the malaria parasite which is known to be sensitive to oxidative stress. This interesting revelation which displays

the potent antiplasmodial effect of auranofin (a drug already in clinical use for the treatment of RA) has the advantage of lowering costs in drug discovery in the emerging field known as drug repositioning.

2.3.2.4 Gold compounds as anti-HIV agents

Various reports on the *in vitro* activity of gold compounds as anti-HIV agents have been recounted by various authors (Sun *et al.*, 2004, Traber *et al.*, 1999, Tepperman *et al.*, 1994, Okada *et al.*, 1993, Blough *et al.*, 1989). *In vivo* activity has also been reported (Lewis *et al.*, 2011, Yamaguchi *et al.*, 2001, Shapiro and Masci, 1996). Shapiro and Masci noted an increase in the CD4+ count of an HIV positive patient who was being treated for psoriatic arthritis with auranofin. Since the natural progression of HIV is characterised by a decrease in CD4+ count and considering the patient was not on anti-HIV medication, the assumption was that auranofin must have caused the improvement in the patient's status. The anti-HIV activity of gold-based compounds was reviewed by Fonteh *et al.*, (2010) as part of this PhD project and the full article is provided at the end of this thesis. The activity of these compounds is linked to their inhibition of HIV RT (Blough *et al.*, 1989, Okada *et al.*, 1993, Sun *et al.*, 2004), immunomodulatory effects (Yamaguchi *et al.*, 2001, Traber *et al.*, 1999) and also to infectivity inhibition (Okada *et al.*, 1993). In their 1996 report, Shapiro and Masci postulated that the remission that was observed for the HIV patient might have been as a result of inhibition of RT by auranofin or to the fact that proliferating cells were able to escape viral cytopathic effects. More recently, Lewis *et al.*, (2011) demonstrated remission of a primate lentiviral infection through the restriction of viral reservoirs in a monkey AIDS model when auranofin was administered.

2.3.3 Some Anti-HIV Mechanisms of Gold Compounds

Gold-based metallodrugs have been used for the treatment of RA and have shown activity against cancers and a wide range of microorganisms including HIV as discussed above. This implies that these compounds have various mechanisms by which they function. In the next subsections, the mechanism of action of gold-based compounds will be discussed with particular focus on anti-HIV modes of action.

2.3.3.1 Ligand exchange reactions

Ligand exchange reaction is one of the mechanisms by which gold-based compounds interact with biological materials for example in the interaction with the sulphhydryl group of cysteine residues in the active site of proteins (Shaw III, 1999, Sadler and Guo, 1998). This is because gold readily binds to atoms of relatively low electronegativity such as sulphur, phosphorus or carbon (Parish and Cottrill, 1987). Another notable observation that suggested that gold in gold complexes undergoes ligand exchange reactions was the identification of

Au(CN)₂ (a metabolite of gold compounds) in the urine of most patients after the administration of gold drugs and very minute amounts of the administered complex (such as auranofin and solganol, Elder *et al.*, 1993). This observation meant that the drugs are prodrugs and that the active form was not the one administered but was produced as a result of the original compound being converted to the active form through ligand exchange reactions (Shaw III, 1999).

Ligand exchange reactions were implicated in the inhibition of HIV infectivity by aurothioglucose (AuTG) and aurothiomalate which did so through the formation of the reactive species bis(thiolato) gold(I) with acidic thiol groups exposed on the surface proteins of the virus (Okada *et al.*, 1993). The bis(thiogluocse)gold(I) - bisAuTG reactive intermediate is formed upon the addition of AuTG to thiol ligands (such as thioglucose) that are capable of interacting with thiol groups of cysteinyl residues on the surface of proteins (Shaw III, 1999). In their work, Okada *et al.*, (1993) demonstrated that the bisAuTG intermediate could undergo ligand exchange with thiol groups exposed on the surface of viral proteins. BisAuTG, was able to protect MT-4 cells from infection and lysis by HIV-1_{NL4-3} (Okada *et al.*, 1993). Inhibition of viral entry or infectivity was reportedly through its reaction with Cys⁵³² on gp160, a viral coat protein. BisAuTG was much more active than AuTG but unfortunately, lacked activity against more virulent strains of HIV.

The inhibition of RT as seen for Au(CN)₂ (Tepperman *et al.*, 1994) was also attributed to ligand exchange reactions where gold binds to sulfhydryl groups in the active site of RT (Allaudeen *et al.*, 1985).

2.3.3.2 Stripping of peptides from class II MHC

De Wall *et al.*, (2006) suggested that metal-based compounds such as gold compounds prevent the progress of autoimmune diseases like RA by stripping peptides from class II MHC proteins. Class II MHC proteins are essential for normal immune system function but also drive many autoimmune responses. This is done through the binding of peptide antigens in endosomes and presenting them on the cell surface for recognition by CD4+ T cells (Watts, 1997). The findings by De Wall *et al.*, (2006) that metals can strip peptides from class II MHC supports the hypothesis of Best and Sadler (1996) that gold has the ability to alter MHC class II peptides. Ultimately, a small molecule inhibitor such as a gold-based compound could therefore potentially block an autoimmune response by disrupting MHC-peptide interactions. De Wall and colleagues (2006) proposed this mechanism based on the identification of noble metal complexes as allosteric inhibitors of class II MHC proteins. The authors also showed that the noble metal inhibitors were able to block the ability of antigen presenting cells from activating T cells. This proposed mechanism might also be related to how gold compounds inhibit HIV. Considering that immune activation results in increased viral replication and decrease in CD4+ count (Forsman and Weiss, 2008), compounds that block

this activation might reduce viral replication and hence slow disease progression. The metal ions shown to possess this property shared similar characteristics such as being able to form square planar, four coordinate complexes which are isoelectric (i.e. having d^8 electronic configuration). A typical example of a metal complex with these characteristics is the platinum-based complex, cisplatin. Gold(III) compounds form similar complexes to cisplatin and are favoured over gold(I) complexes for such a mechanism.

2.3.3.3 Modulation of cytokine production

Chrysotherapy has been shown to reduce the production of IL-6 and IL-8 in serum (Madhok *et al.*, 1993) and cells such as monocytes (Crilly *et al.*, 1994), macrophages (Yanni *et al.*, 1994) and synovial cells (Loetscher *et al.*, 1994). IL-6 and IL-8 are all cytokines under nuclear factor kappa beta (NF- κ B) regulation. This nuclear factor is also known to be a potent activator of HIV gene expression through the triggering of the transcription of viral genes. Gold compounds possibly act by down regulating NF- κ B leading to a reduction in the production of these cytokines. The result is prevention of activation of the transactivator *Tat* gene which in turn prevents explosive increase in HIV replication (Traber *et al.*, 1999).

In another report, weekly treatment of LP-BM5 murine leukemia virus-infected mice with aurothiomalate resulted in prolonged survival (Yamaguchi *et al.*, 2001). LP-BM5 murine leukemia virus causes a disease in mice that presents as immunosuppression and lymphoproliferation with features similar to AIDS. The mice had less cervical lymph node swelling and generally had fewer abnormalities in the expression of cell surface markers such as CD4.

2.3.4 Side Effects of Gold-Based Therapy

Like many medications, clinically available gold compounds demonstrate toxicity and various side effects. The side effects are strongly linked to the ligand used in synthesising the particular gold complex (Ott, 2009). Systemic toxicity e.g. nephrotoxicity is one of the noted toxicological effects of gold compounds (Nobili *et al.*, 2010). Side effects noted in the course of gold therapy develop after the drugs have accumulated in the body and these effects affect the skin, blood, and kidney and occasionally cause liver toxicity (Parish and Cottrill, 1987). Side effects on the skin include rashes, dermatitis and stomatitis (Ott, 2009). Major side effects such as proteinuria and thrombocytopenia have been reported (Taukumova *et al.*, 1999, von dem Borne *et al.*, 1986, Tosi *et al.*, 1985). The majority of the noted side effects have been linked to the polymeric (injectable) gold compounds. The reason for this is because these compounds take up to two months to reach a steady state in blood and generally have a very long half life (Parish and Cottrill., 1987). Only 70% of gold drugs are excreted after 10 days of administration (Jones and Brooks, 1996). Gold is rapidly cleared from the blood and distributed to various tissues like the kidneys where it causes the already mentioned

nephrotoxicity. The orally available monomeric auranofin is much more tolerable but then has lower efficacy than the injectable drugs (Jones and Brooks, 1996) while $\text{Au}(\text{CN})_2$ is known to accumulate in cells with relatively low cytotoxicity (Zhang *et al.*, 1995).

The ability of gold-based compounds to alter MHC II peptide complex is thought to result in both the advantageous and disadvantageous qualities these drugs have (Best and Sadler, 1996). Depending on the type of interaction (i.e. binding to MHC protein directly or to the peptide directly) that the gold drugs make with the MHC II peptide complexes, therapeutic (inhibition of specific T cells) or side effects (stimulation of new set of T cells) could result respectively. Gold-induced dermatitis is known to result from significant lymphocyte proliferation in response to gold therapy (Verwilghen *et al.*, 1992). Gold-specific T cell clones that proliferate when exposed to either gold(I) or gold(III) *in vitro* have been isolated from patients who developed hypersensitive reactions to gold therapy (Romagnoli *et al.*, 1992).

While these limitations are a concern, it should be noted that some patients tolerate the drugs more than others and because of the popularity that these drugs have in providing long lasting remission from rheumatoid arthritis (De Wall *et al.*, 2006, Merchant, 1998) their therapeutic effect cannot be ruled out.

2.4 HYPOTHESIS AND MAIN RESEARCH QUESTIONS

The important role that gold plays in medicinal inorganic chemistry (section 2.3) coupled with the need for identifying novel compounds that could serve as anti-HIV agents prompted research into identifying gold-based anti-HIV agent(s). The research **hypothesis** was that: gold-containing compounds can inhibit HIV replication directly through action on viral enzymes and indirectly through action on host cells (e.g. immune modulation) and can serve as drug leads for further analysis and development. To investigate this hypothesis, the following main research questions were asked.

2.4.1 Were the Gold Compounds Drug-Like?

The mentioned side effects of gold-based drugs (section 2.3.4) suggest that for consideration as treatment, there was a need to determine how drug-like the compounds in the current study were. This need was further supported by the fact that one of the major reasons for late failures in drug development stems from the lack of drug-like or ADMET properties (Lombardo *et al.*, 2003, van de Waterbeemd and Gifford, 2003). A very important drug-like property that was also investigated was the stability of the compounds in the dimethylsulfoxide (DMSO) solvent used for dissolution over time.

2.4.2 What were the Effects of the Gold Compounds on Host Cells and Whole Virus?

There is no point in developing a drug for human use if the source material is toxic to human cells. Primary cells and continuous cell lines represent an easy way of determining

drug interactions with host cells in an inexpensive manner prior to animal studies which are more costly and involve complex ethical issues (Allen *et al.*, 2005). As noted earlier, gold-based compounds such as AuTG and the reactive intermediate bisAuTG were capable of preventing viral infectivity of host cells (Okada *et al.*, 1993). Aurothiomalate was shown to enhance CD4⁺ cell frequency in a mouse AIDS model and prolonged the life of the mice after weekly treatments (Yamaguchi *et al.*, 2001). Based on this background, the effects of the compounds on immune system cells and on cell lines susceptible to HIV infection were also investigated. The cell-based analysis included; determining cytotoxicity (i.e. if the compounds had adverse effects that could lead to interference with structures and processes essential for cell survival) and monitoring of compound effect on cell proliferation (increasing cell number) patterns. Additionally the effect of the compounds on viral infectivity and immune system cells (frequency of CD4⁺ and CD8⁺ cells from both HIV positive and negative donors and the effect on inflammation by assessing IFN- γ and TNF- α levels within the CD4⁺ and the CD8⁺ cells) was also investigated. The effect of the compounds on T cell frequency and on the inflammation caused by HIV will be referred to as immunomodulatory effects which are defined as immunological changes in which one or more immune system molecules (such as IFN- γ and TNF- α) are altered through suppression or stimulation.

2.4.3 Could the Gold Compounds Inhibit Viral Enzymes, and How?

Current anti-HIV medications inhibit three important viral enzymes i.e. HIV RT, PR and IN. Viral resistance has become a major problem for compounds that target these enzymes. The identification of new inhibitors for existing drug resistant viruses or inhibitors that can inhibit important viral functions catalysed by these enzymes that are not blocked by existing drugs (Himmel *et al.*, 2009) is important. In this project, tests to identify inhibitors of these enzymes were performed in direct enzyme assays (where compound effect on purified enzyme was studied in the presence of substrate). These direct enzyme assays provide information on whether a compound inhibits a viral enzyme or not, but does not provide information on the type of binding site interactions that occur or information on whether the compound is an active site or allosteric inhibitor. In order to probe the binding interactions of the compounds with viral enzymes, *in silico* computer aided screening also known as docking was performed. Docking refers to procedures aimed at identifying orientations of small molecules called ligands in the binding pocket of a protein or a receptor and to predict the binding affinity between the two (Krovat *et al.*, 2005). Through this method, compounds with the potential to inhibit specific enzyme functions such as the polymerase or RNase H function of RT could be identified. In addition, medicinal chemistry information can be obtained that should aid in rational drug design such as information on functional group preference for enzyme active sites.

2.5 SCREENING STRATEGY AND METHODOLOGY

In a proof of concept study, sixteen compounds were tested for toxicity to human cells, cellular uptake, HIV RT and PR inhibition, and for effects on the production of the viral core protein, p24 (Fonteh *et al.*, 2009, Fonteh and Meyer 2009, Fonteh and Meyer, MSc. Dissertation, 2008). These compounds consisted of four ligands and eleven gold complexes. The compounds demonstrated stability in DMSO solution after one week when ^{31}P and ^1H NMR spectra were obtained. Uptake into both primary cells and continuous cell lines were demonstrated by inductively coupled plasma atomic emission spectrometry (ICP-AES, Traoré and Meyer, 2001) as positive. Eight of the complexes significantly inhibited HIV-1 RT at concentrations of 25 and 250 μM and three of the eight did so at 6.25 μM . In a fluorogenic substrate assay against HIV-1 PR, four of the gold complexes demonstrated inhibitory activity at 100 μM . The gold compounds were selectively toxic to cell lines but not to primary cells. One of the complexes (EK231) significantly ($p=0.0042$) reduced p24 production at a non-toxic concentration of 25 μM .

Present Study: Based on the inhibitory effects of the gold compounds on RT and PR, the present study was initiated. Important questions such as the drug-likeness of the gold compounds, effects on host cells (immunomodulatory and whole virus) and binding interactions with viral targets such as RT and PR were desired. The effect of the compounds on the activity of a third viral enzyme, IN, was also sought.

Eleven new compounds were included in the new study leading to a total of twenty seven compounds (eight ligands or gold compound precursors and nineteen complexes) consisting of five classes (I – V) which were based on the ligand types used for synthesis. The classes included; (I) gold(I) phosphine chloride-containing complexes, (II) the bis(phosphino) hydrazine gold(I) chloride-containing complexes, (III) the gold(I) phosphine thiolate-based complexes, (IV) the gold(III) Tscs-based complexes and (V) a gold(III) pyrazolyl-based complex. In addition to determining drug-likeness, the compounds' effect on immune system cells was also determined. Direct enzyme assays were performed to determine the compounds' effects on viral enzymes (RT, PR and IN) followed by *in silico* binding predictions to determine active site binding modes. To establish whether the different ligand types (and oxidation states i.e. +1 or +3) conferred unique class properties that could be exploited for further therapeutic use, activity and drug-likeness was compared.

Strategy: A schematic overview of the screening strategy that was used is shown in Figure 2.20. In the figure, twenty seven compounds from five classes (I-V) were tested for drug-likeness, effects on host cells and viral enzymes followed by statistical analysis for differences between controls and treatments.

In this report, the gold compound precursors (the ligands) and complexes are collectively referred to as the compounds. In the molecular modelling section in Chapter 5, the terminology used for the compounds will be ligands, to comply with molecular modelling

terminology for the complementary partner molecule that binds or interacts with a receptor. All the compounds tested here were received through Project AuTEK Biomed for bioscreening. Detailed synthesis (chemistry information) is not important for this work and is reported elsewhere but the basic chemical characteristics of the compounds are provided in chapter 3.

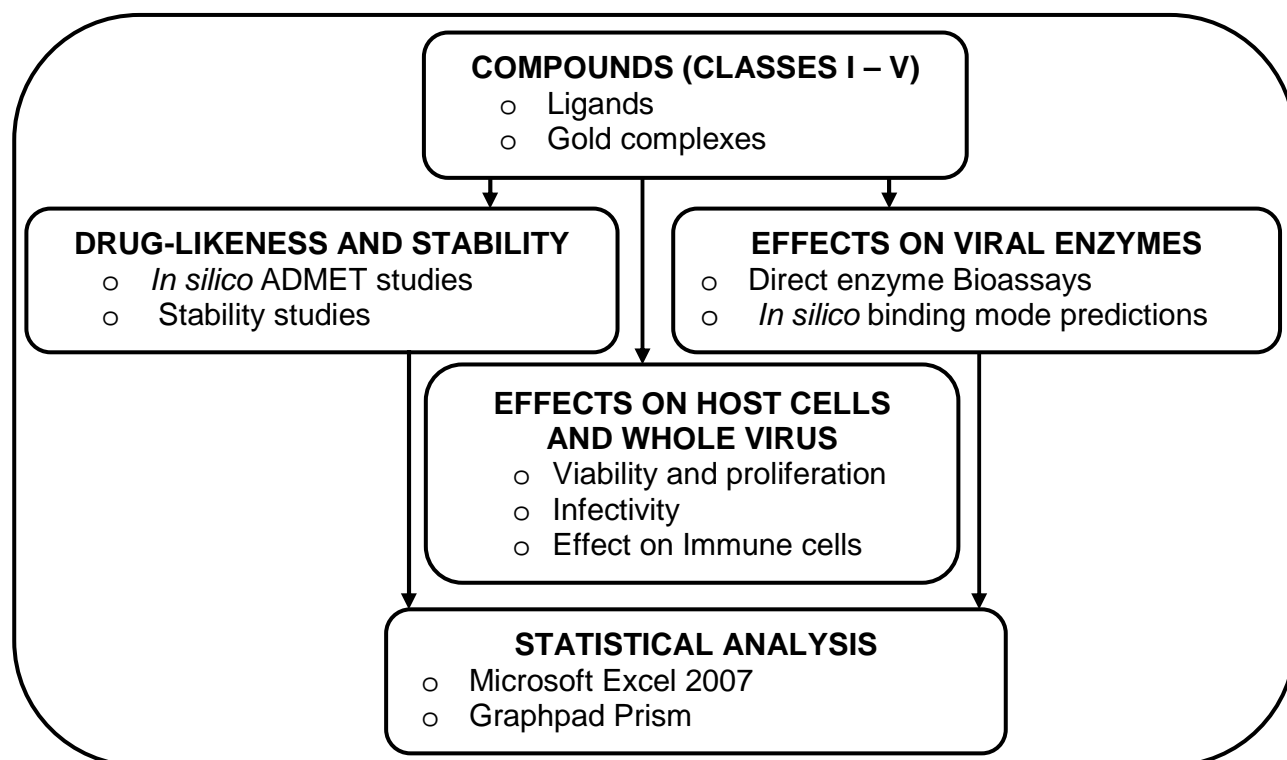


Figure 2.20: Schematic representation of the screening strategy. Twenty seven compounds from five classes (I – V) were tested for drug-likeness, and for effects on host cells and viral targets.

In silico techniques were used in this study, for optimisation and as complementary approaches to *in vitro* experimental assays. This is because the compounds tested had already been synthesised using traditional medicinal chemistry knowledge such as analysis of available biological data and chemical structure (Ohlstein *et al.*, 2000), lipophilicity and anti-viral activity of the relevant ligands and the history of gold-based compounds as anti-HIV agents. Other considerations were the fact that complexation of the ligands with gold and other metals usually led to an enhanced synergistic medicinal effect. Therefore, the screening approach was not rational drug design-based, where *in silico* predictions precede synthesis and experimental analysis. However, as soon as ADMET predictions were determined, the more favourable drug-like compounds were prioritised for further screening. Compounds with less favourable ADMET predictions were only tested further with the hope that efficacious compounds based on beneficial experimental data can be recommended for structural modification to improve activity.

Preliminary assays included determining the ADMET properties and enzyme inhibitory effects of the compounds. This was done using *in silico* drug-likeness predictions and *in vitro* cytotoxicity studies as well as direct enzyme assays respectively with emphasis on high throughput screening (96 well plate formats for analysis). Subsequent assays included determining the immunomodulatory effects of the compounds, effect of compound on ability to

prevent whole virus from infecting host cells (infectivity) and *in silico* enzyme mechanistic studies. In most cases, especially for the non HTS such as immunomodulatory studies, only compounds with favourable ADMET properties or which had shown activity in the direct enzyme assays were tested.

Methodologies: Methodologies employed were standard biochemical techniques and included: (1) Nuclear magnetic resonance spectroscopy which was used in determining the stability of the compounds by monitoring structural changes from spectral chemical shifts, (2) spectrophotometric studies for determining absorbance (related to activity) after colour reaction in viability dyes and for the colorimetric RT and IN assays, (3) flow cytometry for determining the properties of single cells in suspension such as scatter, viability, proliferation and immune state, (4) fluorescent-based methods for monitoring the fluorescence of a fluorogenic HIV PR substrate, (5) luminescent methods for determining the luminescence of the luciferase gene product used in measuring infectivity levels and (6) *in silico* techniques for predicting drug-likeness and the bindings modes of the compounds to enzyme active sites using protocols in Discovery Studio® (DS) (Accelrys®, California, USA). In the next subsections, more details on what each of the main research questions entailed is provided.

2.5.1 Drug-likeness Studies

The drug-likeness of the compounds was determined using *in vitro* cytotoxicity techniques and *in silico* ADMET predictions. *In vitro* methods included the determination of the compound's effect on the viability of human cells. This was assessed by monitoring the optical density of viability dyes by spectrophotometry and fluorescence properties of stained cells by flow cytometry as well as by monitoring the effect of the compounds on the proliferation of these cells. The *in silico* predictions involved the use of the ADMET protocol in the DS® software program (Accelrys®, California, USA) to predict human intestinal absorption (HIA), aqueous solubility, blood brain barrier (BBB) penetration, cytochrome P450 (CYP) inhibition, plasma protein binding (PPB) and hepatotoxicity. In addition, predictions for lipophilicity and polar surface area (hydrogen bonding ability) were also deduced. Stability studies were performed by storing the compounds at different temperatures and monitoring structural changes using NMR spectroscopy. This is important because structural stability means the original chemical entity obtained at the point of synthesis still has the same characteristics. Additionally, stability information can lead to deductions on shelf life.

2.5.2 The Effect of the Compounds on Host Cells and on Whole virus.

To investigate the effects of the compounds on host cells and whole virus, cell-based assays were performed. The assays included viability studies and proliferation studies to determine cytotoxicity, viral infectivity inhibition studies and the effect of the compounds on

immune cell frequency and cytokine production. Inhibition of infectivity was measured as a reduction in luciferase reporter gene expression in the TZM-bl reporter cell line.

The immunomodulatory assays were done using a multi-parametric flow cytometry assay to determine the production of the important bio-molecules such as cytokines that are altered during infection. For this project the intracellular production of two representative cytokines within T cells (CD4+ and CD8+) was monitored. Only representative cytokines were chosen because of the complexity of the immune system. These were; (1) the anti-inflammatory cytokine, interferon gamma (IFN- γ). This cytokine although also labelled as a pro-inflammatory because of its bimodal role in HIV (causes both enhancement and suppression of HIV replication, Alfano and Poli, 2005), was evaluated in this study as an anti-inflammatory cytokine. IFN- γ is known to prevent systemic inflammation and has been associated with a decrease in HIV disease progression and pathogenesis (Ghanekar *et al.*, 2001, Francis *et al.*, 1992). The second cytokine (2) was tumour necrosis factor alpha (TNF- α) which is a pro-inflammatory cytokine that is known to promote systemic inflammation and which has been associated with HIV disease progression *in vivo* (Caso *et al.*, 2001). In addition, the choice of TNF- α as a representative pro-inflammatory cytokine was based on the fact that it is a prototype of pro-inflammatory cytokines and activates the production of other pro-inflammatory cytokines such as IL-1 (Barrera *et al.*, 1996).

Proliferation studies simultaneously provide information about cell viability and mechanistic information such as mode of cell death (apoptosis, necrosis or cytostasis). In addition, proliferation patterns provided clues on the possible stimulatory or inhibitory effects the compounds could have on T cell proliferation (i.e. if the compounds could have therapeutic benefits or if they could have adverse side effects, Best and Sadler, 1996). These were performed using the flow cytometric carboxylfluorescein succinimidyl ester dye dilution technology and the xCelligence impedance-based technology on an RT-CES device.

2.5.3 The Effects of the Compounds on Viral Enzymes

The inhibition of three viral enzymes was performed using direct enzyme bioassays. These assays involve combining of recombinantly purified enzymes and their substrates in the presence of the compounds followed by activity monitoring either spectroscopically by measurement of absorbance from a colour reaction (for RT and IN) or by fluorescence measurement (PR). A complementary *in silico* assay using molecular modelling (docking) was performed for compounds which showed promise in the direct enzyme assays so as to predict the type of inhibitory mechanism involved as well as to confirm direct enzyme assay findings. With regards to inhibitory mechanism, it was necessary to know if compounds which inhibited these enzymes in the bioassays did so by binding to the active site or if they were allosteric inhibitors. In the case of RT, since the enzyme has both a polymerase and an RNase H

function, it was important that the exact function inhibited by the compound be determined. For IN, knowledge of whether the compounds interacted with the DNA binding or LEDGF binding site was necessary.

2.5.4 Statistical Analysis

Statistical analyses were performed using Microsoft® Office Excel® 2007 (Microsoft Corporation, Washington, USA) and Graphpad Prism® (San Diego, California, USA). Some of the calculations that were performed included: standard error of means (SEM), p values, correlation coefficients, means, standard deviations, medians, CC_{50} s and IC_{50} s. Detailed explanations of what the statistical terminologies mean are provided in the appendix, chapter 8 (Table A2.1 where A= appendix)

For this project, assays were performed at least 4 times and up to 6 times for experiments that needed optimisation unless stated otherwise.

2.6 OTHER RESEARCH OUTCOMES

Other research outcomes include publications, awards (travel and fellowships) and the presentation of results at conferences. More details on these are provided in the preface section of this document, after acknowledgments (on page VIII).

CHAPTER 3

GOLD COMPOUNDS: STRUCTURE AND DRUG-LIKENESS

SUMMARY

Background: Drug-likeness characteristics of compounds that are newly synthesised for biological testing or which are part of virtual libraries have to be investigated early in the drug development process. The compounds (twenty seven in total: eight precursors and nineteen complexes) tested in this study were synthesized and characterized by chemists of the Project AuTEK Biomed consortium. The compounds consisted of four gold(I) phosphine chloride complexes and four complementary ligands, four bis(phosphino) hydrazine (BPH) gold(I) chloride complexes, six gold(I) thiolate complexes, four gold(III) thiosemicarbazone complexes and corresponding ligands and a gold(III) pyrazolyl complex. These compounds were analysed for stability and similarity to known drugs with regards to chemical structure.

Materials and Methods: ^{31}P and ^1H NMR spectra were obtained to determine the stability of representative complexes from each class. Drug-likeness studies were performed using *in silico* prediction models for ADMET and lipophilicity in the Discovery Studio Software package from Accelrys. The *in silico* lipophilicity predictions were compared to those obtained using the traditional shake flask method and to those obtained for available anti-HIV agents.

Results and Discussion: The ^{31}P NMR chemical shifts of a gold(I) phosphine chloride complex (TTC3), and a BPH gold(I) complex (EK231), remained stable after one week analysis dissolved in deuterated (d_6)-DMSO and stored at $-20\text{ }^\circ\text{C}$ and $37\text{ }^\circ\text{C}$ respectively. In the ^1H NMR spectra of complexes TTC3, MCZS3, PFK174 and PFK7, a water peak on day zero suggested inherent hygroscopic abilities which became prominent after 24 h and on day 7 (attributable to the hygroscopic nature of DMSO). The water peak appeared to have no discernible effect on structure since the backbone chemical shifts of most of the complexes were maintained but aqueous solubility appeared to be affected especially for complexes MCZS3 and PFK174. Of the nineteen gold complexes analysed, acceptable drug-like properties were predicted for eight and these findings were comparable to those of existing drugs. There was good correlation between experimental (shake flask) and *in silico* lipophilicity prediction values for two of the complexes; thus confirming the *in silico* findings.

Conclusion: Compounds with satisfactory drug-like properties which also demonstrate inhibitory activity (chapter 4 and 5) will be recommended as leads for further testing. Those with poor properties which end up being inhibitory will be recommended for optimisation by structural modification to increase drug-likeness while maintaining or improving potency.

Keywords: Compound structure, drug-likeness, *in silico*, ADMET properties, stability.

*chemical notation does not use space

Various transition metals have been exploited for therapeutic activity and have wide application in medicine ranging from the treatment of arthritis and cancers to microorganism infections (reviewed by Rafique *et al.*, 2010). These metal-based drugs which are chemically synthesised complexes containing the relevant metal coordinated to suitable ligands form what is also known as metallodrugs. The metal of interest in this study is gold which is chemically represented as Au. Gold is a transition metal element with an atomic weight of 197 and is a member of group IB on the periodic table. Gold exists in three oxidation states which are gold(0) or metallic gold, gold(I) and gold(III). Gold(III) and gold(I) are easily reduced to gold(0) in the presence of reducing agents and in the absence of stabilizing ligands (Merchant, 1998). Gold(0) is the least active (Merchant, 1998).

The ligands used play a crucial role in the synthesis of gold or metal-based complexes not only because complexation confers stability, but in some cases leads to better activities and/or reduced toxicities (Pelosi *et al.*, 2010, Beraldo and Gambino, 2004). Since ligands can be chemically modified to accommodate different functional groups or atoms, a diversity of possibilities with regards to complex types is possible. This diversity is further enhanced by the fact that the d orbital of metals are in the process of filling such that different coordination complexes can be formed (Rafique *et al.*, 2010). This is the advantage that inorganic medicinal chemistry has over organic medicinal chemistry (Fricker, 2007) since a diverse number of chemical entities can be synthesised.

Gold-containing complexes are well known for their application as anti-rheumatoid arthritic agents (Champion *et al.*, 1990, Fricker, 1996) but also show activity against various microorganisms including HIV (reviewed by Fonteh *et al.*, 2010). In this project, the interest in synthesizing new gold-based complexes was not only sparked by the need for identifying novel therapy for the treatment of HIV infection but also by the history of these complexes with regards to anti-HIV activity. The earliest limitation of gold-based complexes that had activity against HIV was the fact that inhibition in direct enzyme assays could not be correlated in cell-based assays. This was because the compounds could not be readily taken up by cells and thus could not reach therapeutic levels to inhibit viral targets within the cell in cultures (Zhang *et al.*, 1994). A typical example is the injectable gold(I) thiolate complex, aurothioglucose, which inhibited RT in cell-free assays (Okada *et al.*, 1993) but together with its metabolites could not be taken up by cells.

Phosphine-containing ligands have better membrane permeability profiles (Gandin *et al.*, 2010). The phosphine complexes screened here which were fourteen in total, included four gold(I) phosphine chloride-based complexes (P-Au-Cl) designated TTC3, TTC10, TTC17 and TTC24, four BPH gold(I) chloride-containing complexes (P-Au-Cl) designated EK207, EK208, EK219 and EK231 and six gold(I) phosphine thiolate-containing complexes (S-Au-P) designated MCZS1, MCZS2, MCZS3, PFK174, PFK189 and PFK190. The sulphur-containing ligand in the S-Au-P complexes is known to readily bind to gold (Abdou *et al.*, 2009). This

ease of binding to gold is a property that is displayed during ligand exchange reactions when these compounds interact with sulfhydryl groups in cysteine residues of proteins (Roberts *et al.*, 1996, Bernners-Price *et al.*, 1996, Allaudeen *et al.*, 1985). In the fourteen complexes, the gold atom formed strong covalent bonds with the ligands through coordination with S and P. Covalent bonds formed with S, P and C result in complexes with good stability and longer shelf life (Parish and Cottrill, 1987).

The oxidation state of any metal is a critical factor in considering chemotherapeutic applications (Thompson and Orvig, 2003). Gold(I) complexes are generally preferred because of their stability and because they are less toxic than gold(III). The use of hard donor ligands such as N and O which result in relatively stable gold(III) complexes (Milacic and Dou 2009) has led to the synthesis of more physiologically stable gold(III) complexes. Gold(III) complexes with anti-HIV activity have been reported with their stability linked to the ligand choice (Sun *et al.*, 2004). Five of the compounds tested in this study were gold(III) complexes and consisted of four gold(III) thiosemicarbazone-based complexes designated PFK7, PFK8, PFK41 and PFK43 and a gold(III) pyrazolyl complex designated KFK154b. Gold(III) gives rise to complexes that are isoelectric and isostructural like those of platinum (Bruni *et al.*, 1999) and have thus been analysed for anti-cancer activity (Gabbiani *et al.*, 2007, Messori *et al.*, 2004, Che *et al.*, 2003, Marcon *et al.*, 2002) because of the anti-cancer activity associated with cisplatin (a platinum-based metallodrug). The choice of Tscs as ligands for gold(III) synthesis was not only motivated by the fact that these compounds consist of mixed donor atoms (N,S) that resulted in considerably stable gold(III) complexes. It was also because Tscs-based complexes have previously shown anti-HIV activity (Pelosi *et al.*, 2010, Mishra *et al.*, 2002, Pandeya *et al.*, 1999) and it was thus envisaged that complexation with gold will enhance this activity as a result of the conferred stabilisation of the compound after complexation.

In summary, the factors that were considered during synthesis (so as to increase the drug-likeness of the complexes) included the compounds' potential for inhibiting HIV, potential for stability in biological media and lipophilic tendencies. Studies in the late 1990s indicated that poor pharmacokinetics and toxicity ranked high among the causes of late-stage failures in drug development (van de Waterbeemd and Gifford, 2003, Lombardo *et al.*, 2003). This finding dictated that methods to eliminate non drug-like compounds early in drug discovery were essential. In addition to *in vitro* HTS assays that have been developed to determine drug-likeness, *in silico* computational methods have been emerging as complementary approaches (Desai *et al.*, 2006). Besides aiding in optimising the drug discovery process, computational tools also help in the identification of leads from large libraries according to certain restrictions such as ideal lipophilicity values. Here, the use of computational screening (e.g. ADMET predictions) was mainly for optimisation and to complement findings from biological assays as well as to prioritise hits based on drug-likeness.

In *in vitro* HTS assays, the ability to easily retrieve and test compounds is a priority and compounds are typically dissolved in DMSO and stored until needed (Ellson *et al.*, 2005). Unfortunately DMSO is highly hygroscopic and easily absorbs water from the atmosphere. In a DMSO solution, water accelerates degradation of compounds and causes precipitation thereby affecting product concentration (Ellson *et al.*, 2005). This could lead to problems ranging from underestimated activity, variable data, inaccurate SAR, discrepancies in enzyme and cell-based assays and inaccurate *in vitro* ADMET data (Di and Kerns, 2006). *In vitro* ADMET refers to drug-likeness properties determined in culture (e.g. using caco-2 cells for cellular permeability determination, Egan and Lauri, 2002) unlike *in silico* ADMET which refers to computational predictions. To investigate whether the structural composition of the compounds was still intact (compared to when synthesised) and the effect of solvent on storage and stability, NMR profiles of representative complexes in *d6*-DMSO were obtained. This is because the only information on compound stability that could be obtained from the *in silico* ADMET predictions studies was that of plasma protein binding ability. It was therefore important that stability in the solvent used in dissolving the complexes be determined using the alternative NMR procedure.

In the next sections, the structures and chemical names of the compounds will be provided as well as brief summaries of the synthetic procedures and references to publications and reports containing detailed information on synthesis. Stability and storage issues will then be addressed as well as the ADMET predictions for drug-likeness. This will be followed by information on lipophilicity determination to confirm *in silico* predicted values for two of the complexes using the traditional shake flask method. In addition, the ADMET findings will be compared to the “Lipinski’s rule of five” which states that poor absorption or permeation is more likely when there are > 5 H-bond donors, >10 H-bond acceptors, the molecular weight (*M_r*) is > 500 and when the calculated log *P* is > 5 (Lipinski *et al.*, 1997). The “five” in the name of the rule does not refer to the number of rules but to the fact that each property is described in multiples of 5. According to the rule, a compound with values which exceed any two of the properties has particularly poor absorption or solubility. “Lipinski’s rule of 5” forms a model that has been widely used for the prediction of passive intestinal absorption (Egan and Lauri, 2002, Lipinski *et al.*, 1997).

3.2 COMPOUNDS

The gold complexes that were tested in this study have been grouped according to the ligand types that were used during synthesis. The different ligand structures within and between groups contributed to the diversity of the gold complexes. In some cases the corresponding ligands were also tested as controls to verify the effect of complexation. This was however not possible in all cases because not all the ligands were stable enough for

biological testing as observed and stated by the chemists e.g. the BPH ligands were prone to decomposition even under inert conditions but not upon complexation (Kriel *et al.*, 2007).

3.2.1 The Gold(I) Phosphine Chloride-containing Complexes – Class I

The gold(I) phosphine chloride class of compounds consisted of four ligands and four complementary gold(I) phosphine complexes. The ligands are designated TTL3, TTL10, TTL17 and TTL24 while the complementary complexes are represented as TTC3, TTC10, TTC17 and TTC24 respectively. The structures, identification codes and full chemical names are shown in Table 3.1. Synthesis involved the production of ligands starting from commercially available 2-(diphenylphosphino)benzaldehyde (Traut and Williams, 2006). This was followed by complexation of the synthesised phenethyl amine or *N,N*-dimethyl-ethane-1,2-diamine-containing phosphine ligands with (THT)AuCl (where THT=tetrahydrothiophene) as gold starting material (Traut and Williams, 2006, shown in Figure 3.1A and B). Characterisation was then performed using ^{31}P NMR. In all cases, the coordination of the gold to the ligand was by covalent interaction with P. The synthesis and characterization of these compounds has been published (Williams *et al.*, 2007).

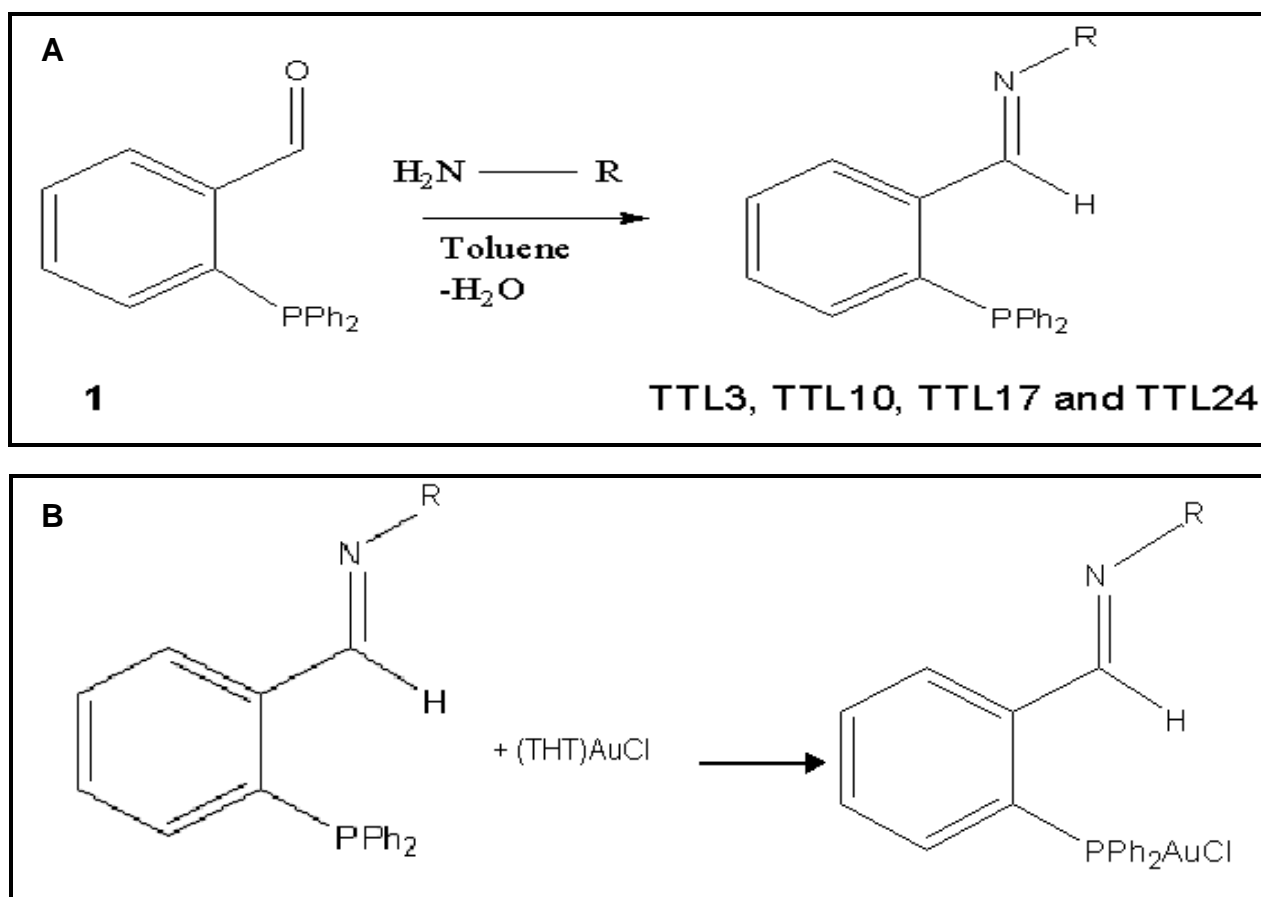
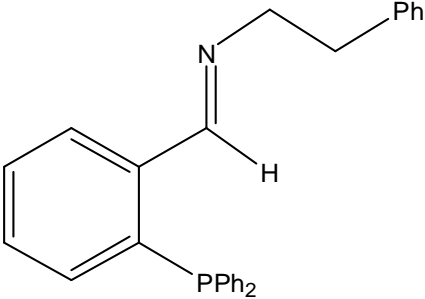
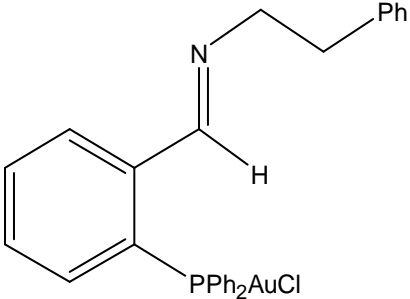
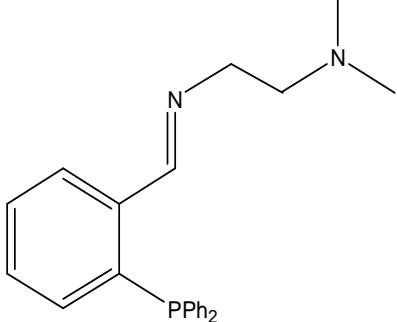
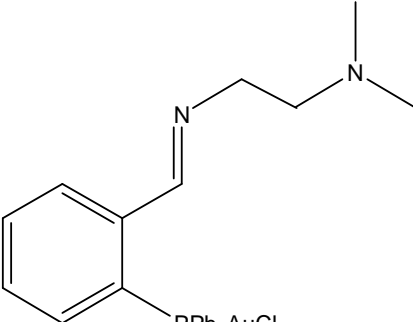
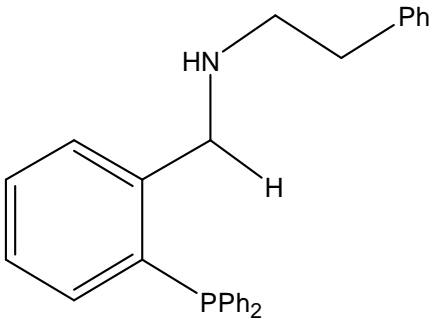
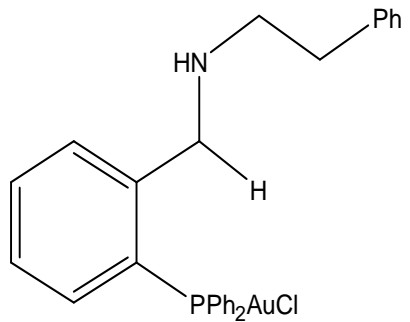
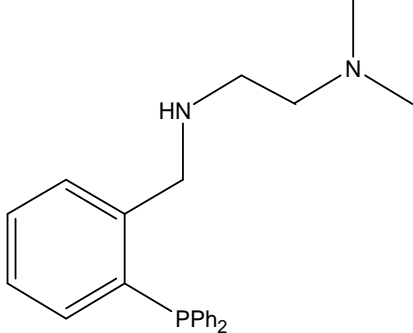
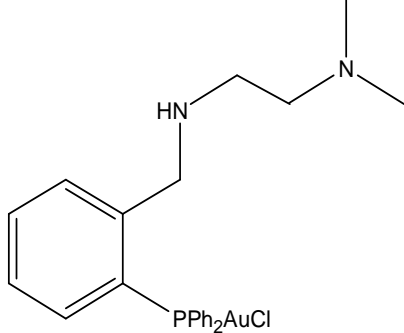


Figure 3.1: Synthetic scheme for the phosphine containing ligands. In A, the ligand synthetic route is shown starting from commercially available 2-(diphenylphosphino)benzaldehyde (**1**). In B, the synthetic route for the corresponding gold(I) complexes using the relevant ligands is shown and involves reactions with (THT)AuCl. R= Phenylethyl (TTL3 and TTL17), R= *N,N*-dimethyl-ethane-1,2-diamine (TTL10, TTL24). These figures were adapted from Traut and Williams (2006).

Table 3.1: The gold(I) phosphine chloride complexes and corresponding ligands (Class I). Ph represents a phenyl ring and the asterisk refers to ligand. The ligands are organic precursors used in the synthesis of the complexes.

Compound structure, code and name	Compound structure, code and name
 <p>TTL3*: (2-diphenylphosphanyl-benzylidene)-phenethyl amine</p>	 <p>TTC3: Benzyl-(2-diphenylphosphanyl-benzylidene)-phenethyl-amine gold(I)chloride</p>
 <p>TTL10*: <i>N'</i>-(2-diphenylphosphanyl-benzylidene)-<i>N,N</i>-dimethyl-ethane-1,2-diamine</p>	 <p>TTC10: <i>N'</i>-(2-diphenylphosphanyl-benzylidene)-<i>N,N</i>-dimethyl-ethane-1,2-diamine gold(I) chloride</p>
 <p>TTL17: 2-diphenylphosphanyl-benzyl)-phenethyl-amine</p>	 <p>TTC17: 2-diphenylphosphanyl-benzyl)-phenethyl-amine gold(I) chloride</p>
 <p>TTL24: <i>N'</i>-(2-diphenylphosphanyl-benzyl)-<i>N,N</i>-dimethyl-ethane-1,2-diamine</p>	 <p>TTC24: <i>N'</i>-(2-diphenylphosphanyl-benzyl)-<i>N,N</i>-dimethyl-ethane-1,2-diamine gold(I) chloride</p>

3.2.2 The Bis(phosphino) Hydrazine Gold Chloride-containing Complexes – Class II

The BPH gold(I) chloride group consisted of four gold(I) complexes designated: EK207, EK208, EK219 and EK231. The structure of the hydrazine (backbone structure) for these complexes is shown in Figure 3.2. Synthesis, characterization and analysis for purity were performed by Kriel *et al.*, (2007). The authors prepared bisphosphinohydrazine ligand precursors using published methods followed by reaction with either dimethylsulphidegold(I) chloride ((Me₂S)AuCl) or (THT)AuCl to produce the corresponding BPH gold(I) complexes (shown in Figure 3.3 A and B and in Table 3.2).

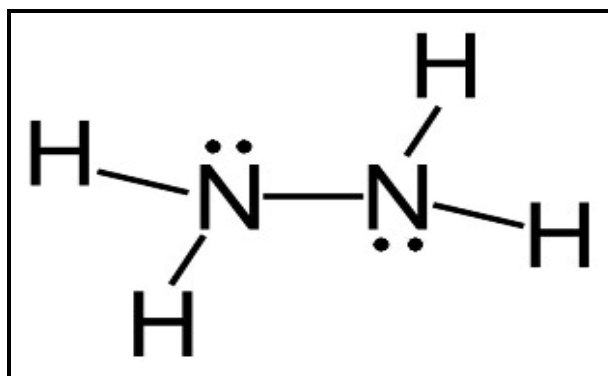


Figure 3.2: The chemical structure of hydrazine (N₂H₄). Hydrazine has two lone pairs of electrons which make it very reactive. The figure was taken from <http://toxipedia.org/display/toxipedia/Hydrazine> (accessed on the 26/04/2011).

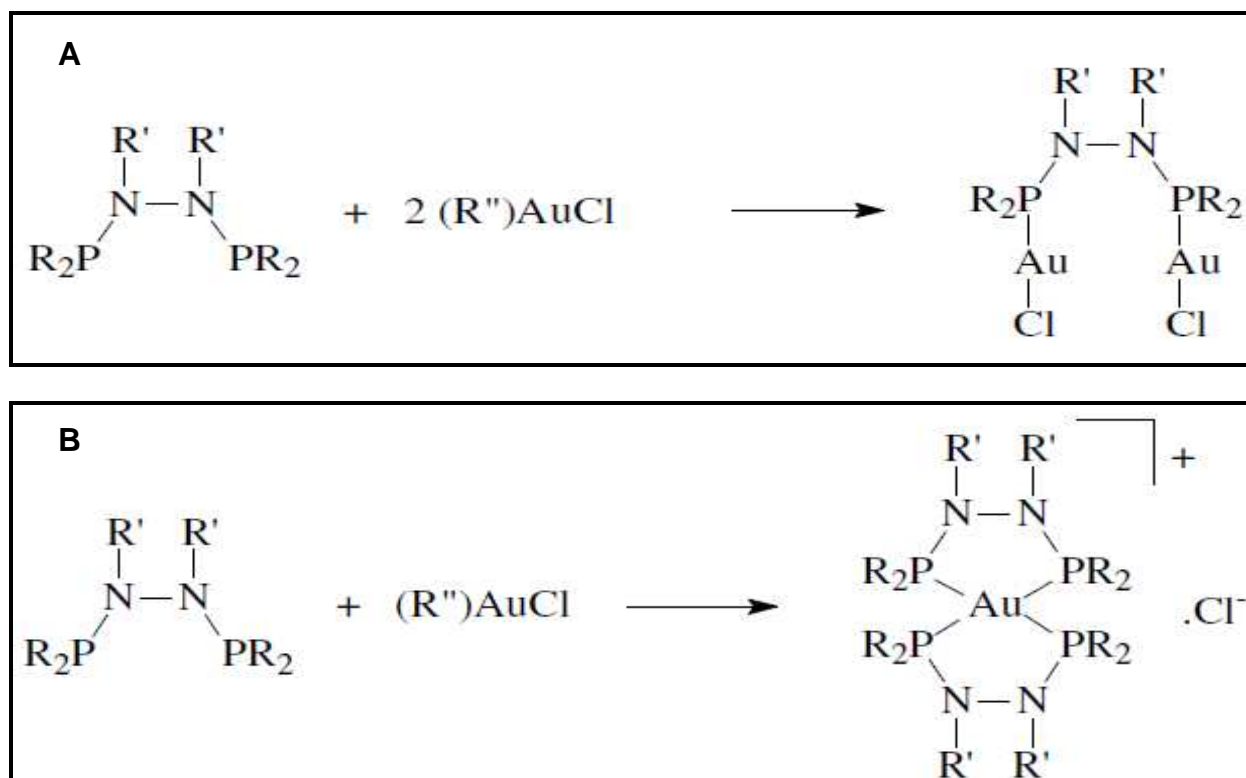


Figure 3.3: Synthetic display for the BPH gold(I) complexes. In (A), R = Ph, R' = Et (EK207), R = PhOMe, R' = Et (EK219), R = Me₂NPh, R' = Et (EK231) and in (B), R = Ph, R' = Et (EK208). In B, R'' = THT or SMe₂ (dimethylsulphide). The figures were taken from Kriel *et al.*, (2007).

Table 3.2: BPH gold(I) chloride-containing complexes, Class II. Ph represents a phenyl ring, Et an ethyl group, Me a methyl group and MeO a methoxy.

Compound structure, code and name	Compound structure, code and name
<p>EK207: Bis(diphenylphosphino)-1,2-diethylhydrazine di(gold chloride)</p>	<p>EK208: Bis [bis (diphenylphosphino)-1,2-diethylhydrazine] gold chloride</p>
<p>EK219: Bis (di (4-methoxyphenyl) phosphine)-1,2-diethylhydrazine di(gold chloride)</p>	<p>EK231: Bis(di(N,N-dimethyl aniline)phosphine)-1,2-diethylhydrazine di(gold chloride)</p>

A complex with similar structure to those in this group and to EK208 is the four coordinate gold complex, [1,2-bis(diphenylphosphino)ethane]gold(I) chloride ($\text{Au}(\text{DPPE})_2\text{Cl}$, please refer to Figure 2.19 for the structure) which was reported in the mid 80s to have promising anti-tumour activity (Fricker, 1996, Berners-Price *et al.*, 1986, Mirabelli *et al.*, 1986). This complex, in which a phosphine ligand was incorporated, demonstrated activity against leukaemia cells as well as on other tumour models (Berners-Price *et al.*, 1986, Mirabelli *et al.*, 1986). It was however not entered into clinical trials due to cardiotoxicity problems encountered during pre-clinical toxicology studies (Hoke *et al.*, 1989). The toxicity that was observed for this compound was attributable to the high lipophilicity of the phosphine moieties and the ethane backbone which resulted in non specific uptake. The newly synthesized analogues (EK207, EK208, EK219 and EK231) in this study were thus modified through the use of nitrogen heteroatoms to replace the lipophilic ethane bridge present in the parent compound ($\text{Au}(\text{DPPE})_2\text{Cl}$) by employing a hydrazine bridge instead. It was hoped that the hydrophilic nature of the nitrogen heteroatoms will increase the hydrophilicity of the compounds rendering them more selective and drug-like (Kriel *et al.*, 2007). Although the initial aim of synthesis was to test for anti-cancer activity (explored by Kriel *et al.*, 2007), the potential of gold-based compounds as inhibitors of HIV prompted the inclusion of these compounds for testing in this project.

3.2.3 The gold(I) Phosphine Thiolate-based Complexes - Class III

The gold(I) phosphine thiolate group consisted of auranofin designated MCZS2 which is an orally available anti-arthritis agent (Ahmad 2004, Sutton, 1986) that has shown anti-HIV activity *in vivo* (Lewis *et al.*, 2011, Shapiro and Masci, 1996) and two analogues represented by identification codes MCZS1 and MCZS3. The synthesis of MCZS1 and MCZS3 was reported in an AuTEK Biomed communiqué by Sam in 2005. Synthetic intermediates consisting of 2,3,4,6-tetra-O-acetyl-1-thio-B-D-glucopyranose, 1,3,5-triaza-7-phosphaadamantane (PTA), (PTA)AuCl and [MePTA]⁺[CF₃FO₃]⁻AuCl (where CF₃FO₃ = trifluoromethanesulfonate) were prepared according to literature procedures (see Figure 3.4 for structures). In the case of MCZS1, 2,3,4,6-tetra-O-acetyl-1-thio-B-D-glucopyranose was reacted with (PTA)AuCl while synthesis of MCZS3 involved the reaction of 2,3,4,6-tetra-O-acetyl-1-thio-B-D-glucopyranose with [MePTA]⁺[CF₃FO₃]⁻AuCl. Synthesis was followed by characterisation using ³¹P NMR. MCZS2 (purchased from Biomol International L.P. (Pennsylvania, USA) was also provided by the AuTEK Biomed group (Mintek, South Africa). The molecular structures, codes and names of the complexes are represented in Table 3.3. This class also included three additional complexes designated PFK174, PFK189 and PFK190 whose structures cannot be disclosed because they are currently part of a patent application for promising anti-cancer activity. The main distinction that the latter has over the former (shown in Table 3.3) is the bimetallic property (containing two gold atoms).

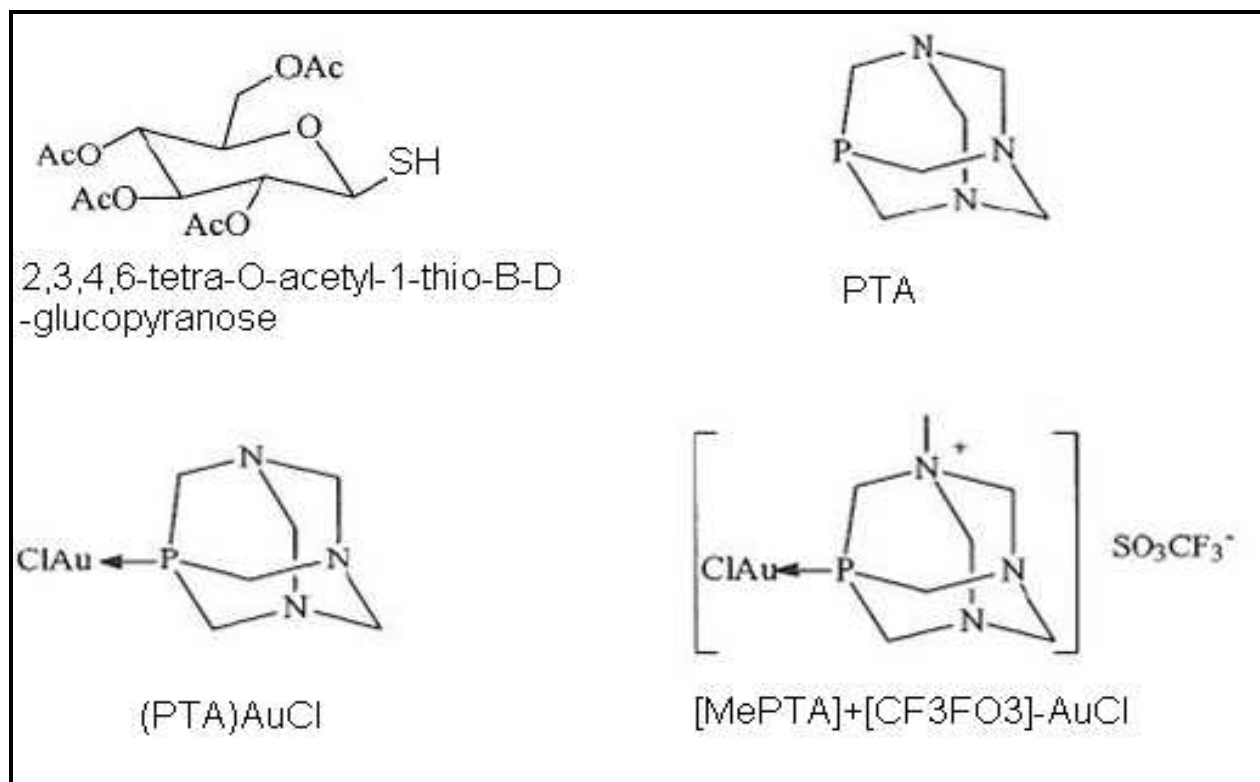
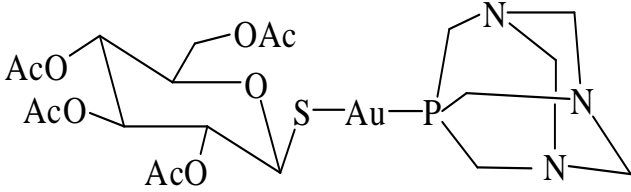
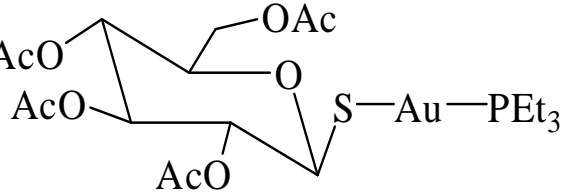
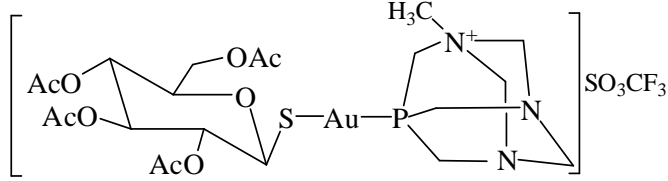


Figure 3.4: The structures of intermediate reagents used for the synthesis of auranofin analogues (MCZS1 and MCZS3). The figure was adapted from Sam, (2005).

Table 3.3: Gold(I) phosphine thiolate complexes. The structures, code names and full chemical names are represented. Ac represent and acetyl group and Et an ethyl group.

Compound structure, code and name	Compound structure, code and name
 <p>MCZS1: (2,3,4,6-tetra-O-acetyl-1-thio-B-D-glucopyranosato-S)-(1, 3, 5-triaza-7-phosphaadamantane) gold (I)</p>	 <p>MCZS2: (2,3,4,6-tetra-O-acetyl-1-thio-B-D-glucopyranosato-S-) (triethylphosphine) gold (I)</p>
 <p>MCZS3: (2,3,4,6-tetra-O-acetyl-1-thio-B-D-glucopyranosato-S)-(1, 3, 5-triaza-7-phosphaadamantane)gold (I) (+1) trifluoromethanesulphonate(-1)</p>	

3.2.4 The gold(III) Tscs-based Complexes – Class IV

The Tscs compounds included ligands PFK5, PFK6, PFK38 and PFK39 and their corresponding complexes designated PFK7, PFK8, PFK43 and PFK41 respectively. The synthesis and anti-HIV activity has been compiled in a manuscript that has been accepted for publication by the Journal of Inorganic Biochemistry (Fonteh *et al.*, 2011). The gold starting material, $\text{HAuCl}_4 \cdot 4\text{H}_2\text{O}$, was synthesised using procedures reported by Block (1953) while the bis(Tscs) ligands (PFK5, PFK6, PFK38 and PFK39) were synthesised according to methods by West *et al.*, 1997. This was followed by the complexation reaction which led to the production of PFK7, PFK8, PFK43 and PFK43 (the synthetic route is shown in Figure 3.5). Synthesis was followed by characterisation using ^1H NMR, infrared spectroscopy and microanalysis (Fonteh *et al.*, 2011). The structures of the ligands and complexes are shown in Table 3.4. These compounds unlike the first two classes (phosphine and the BPH containing compounds) and MCZS1, MCZS2 and MCZS3 were newly synthesised and tested for the first time in this study for anti-HIV activity. The complexes also differ from the first three classes in the oxidation state which is +3 unlike +1. Although Bottenus *et al.*, (2010) recently reported the synthesis of complex PFK8, the synthetic protocol used is different from that described by Fonteh *et al.*, (2011).

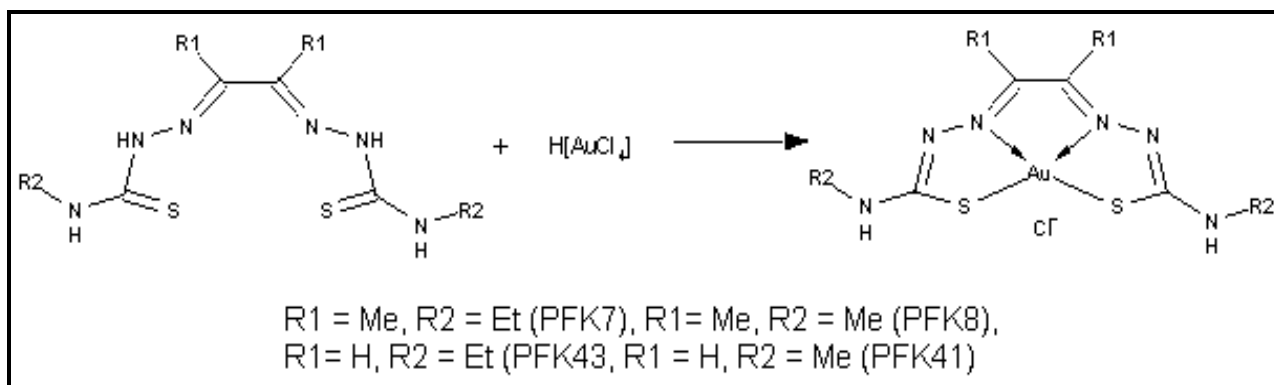


Figure 3.5: Synthetic scheme for the bisthiosemicarbazonate complexes (PFK7, PFK8, PFK43 and PFK41). The complexes were synthesised from the respective ligands (PFK5, PFK6, PFK38 and PFK39). This figure was taken from Fonteh *et al.*, (2011).

Table 3.4: The gold(III) thiosemicarbazonate complexes and corresponding precursors. The asterisk represents ligands. (Fonteh *et al.*, 2011).

Compound structure, code and name	Compound structure, code and name
<p>PFK5*: diacetyl-bis-(N⁴-ethylthiosemicarbazone)</p>	<p>PFK7: diacetyl-bis-(N⁴-ethylthiosemicarbazonate)gold(III)chloride</p>
<p>PFK6*: diacetyl-bis-(N⁴-methylthiosemicarbazone)</p>	<p>PFK8: diacetyl-bis-(N⁴-methylthiosemicarbazonate)gold(III)chloride</p>
<p>PFK38*: diglyoxal-bis-(N⁴-methylthiosemicarbazone)</p>	<p>PFK43: diglyoxal-bis-(N⁴-methylthiosemicarbazonate)gold(III)chloride</p>
<p>PFK39*: diglyoxal-bis-(N⁴-ethylthiosemicarbazone)</p>	<p>PFK41: diglyoxal-bis-(N⁴-ethylthiosemicarbazonate)gold(III)chloride</p>

3.2.5 The Gold(III) Pyrazolyl-based Complex – Class V

The last class (V) consisting of only one member is the gold(III) pyrazolyl-based complex designated KFK154b. The synthesis, purity and characterization, activity on HIV RT and PR was reported by Fonteh *et al.*, (2009). Synthesis involved reacting $\text{H}[\text{AuCl}_4]$ with bis(3,5-dimethylpyrazolyl)acetic acid as shown in the synthetic reaction in Figure 3.6. The structure of the complex is shown in Table 3.5.

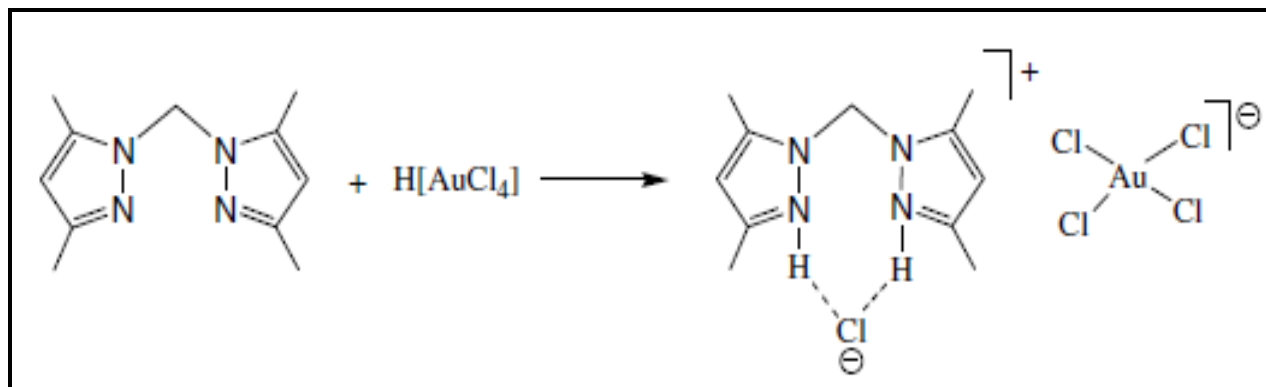


Figure 3.6: Synthetic scheme for tetra-chloro-(bis-(3,5-dimethylpyrazolyl)methane)gold (III)chloride. The Figure was taken from Fonteh *et al.*, (2009).

Table 3.5: The pyrazolyl gold(III) complex, (Fonteh *et al.*, 2009).

Compound structure, code and name
<p>KFK154b: Tetra-chloro-(bis-(3,5-dimethylpyrazolyl)methane)gold (III)chloride</p>

In Table 3.6 important additional information on the compounds is provided and includes relative Mr, the number of rotatable bonds and the number of hydrogen bond (H-bond) donors (counted as number of hydrogens attached to N or O) and acceptors (approximated as the number of N or O atoms). Some of these parameters were incorporated by Lipinski *et al.*, in 1997 in coining the rule of 5 regarding absorption (one of the drug-like parameters). The number of rotatable bonds is related to molecular flexibility and gives an idea of the number of conformations that can be generated (Höltje *et al.*, 2003) to allow it to interact with an active site in receptor/ligand interactions (covered in chapter 5). For ease of reference, the compounds tested in the proof of concept study (mentioned in chapter 2 section 2.5) will sometimes be referred to as “compounds tested in prior study” from here onwards. These are the first fifteen and last compound in Table 3.6. Tables 3.1 to 3.6 will be referenced throughout this report to refer to the different compounds in the different classes.

Table 3.6: Additional compound structural information. Molecular formula, Mr, the number of rotatable bonds, H-bond donors and acceptors are shown. The ligands are shaded in gray. The various classes of the compounds are also represented.

Class	Compound code	Molecular formula	Mr (g/mol)	Rotatable bonds	H-bond donors	H-bond acceptors
I	TTL3	C27 H24 N P	393.17	7	0	2
	TTC3	C27 H24 Au Cl N P	625.10	8	0	1
	TTL10	C23 H25 N2 P	360.18	7	0	3
	TTC10	C23 H25 Au Cl N2 P	592.11	8	0	2
	TTL17	C27 H26 N P	395.18	8	1	2
	TTC17	C27 H26 Au Cl N P	627.12	9	1	1
	TTL24	C23 H27 N2 P	362.19	8	1	3
	TTC24	C23 H27 Au Cl N2 P	594.13	9	1	2
II	EK207	C28 H30 Au2 Cl2 N2 P2	920.06	11	0	2
	EK208	C56 H64 Au Cl N4 P4	1148.34	18	4	4
	EK219	C32 H38 Au2 Cl2 N2 O4 P2	1040.10	15	0	6
	EK231	C36 H50 Au2 Cl2 N6 P2	1092.23	15	0	6
III	MCZS1	C20 H31 Au N3 O9 P S	717.12	11	0	13
	MCZS2	C20 H34 Au O9 P S	678.13	14	0	10
	MCZS3	C22 H34 Au F3 N3 O12 P S2	881.09	13	0	15
IV	PFK5	C10 H20 N6 S2	288.12	9	4	4
	PFK7	C10 H18 Au Cl N6 S2	518.04	4	2	4
	PFK6	C8 H16 N6 S2	260.09	7	4	4
	PFK8	C8 H14 Au Cl N6 S2	490.01	2	2	4
	PFK38	C8 H16 N6 S2	232.06	7	4	4
	PFK43	C8 H14 Au Cl N6 S2	461.98	2	2	4
	PFK39	C6 H12 N6 S2	260.09	9	4	4
	PFK41	C6 H10 Au Cl N6 S2	490.01	4	2	4
V	KFK154b	C11H20AuCl5N4	582.5	2	2	1

In addition to screening the gold-based complexes, four platinum-based complexes of the Tscs ligands (PFK5, 6, 38 and 39, Table 3.4) were also assayed for HIV inhibitory effects. The platinum-based complexes had no inhibitory effect on the activity of HIV RT and PR both *in vitro* and *in silico*. A manuscript describing synthesis of these Pt-based compounds and possible reasons for the lack of activity on RT and PR enzymes is in preparation (by Keter *et al.*).

3.3 MATERIALS AND METHODS

In the materials and methods section of this chapter and in chapter 4 and 5, the principles or background of the techniques employed will also be provided.

3.3.1 NMR Studies for Stability Determination

Compounds for HTS are normally dissolved in DMSO. The hygroscopic nature of DMSO could unfortunately lead to stability issues. To investigate the structural stability of the complexes, NMR spectra of the complexes dissolved in DMSO was obtained on immediate dissolution and later at 24 h and after one week at two relevant temperatures (storage and

physiological). The fact that many nuclei have magnetic properties that arise from the spin of subatomic particles (protons and neutrons) in their nucleus makes it possible to observe their spectra which results from the overall spin. In some nuclei such as ^{12}C , ^{16}O and ^{32}S , the overall spin cancels out while in others such as ^1H , ^{13}C , ^{19}F and ^{31}P , it does not, such that an overall spin and therefore spectra are produced. Gold unfortunately does not have a useful NMR nucleus (Shaw III, 1999). NMR characterisation of gold complexes therefore makes use of the presence of other magnetic nuclei such as ^1H and ^{31}P .

A minimum of 10 mg/mL of representative gold complexes (TTC3, EK231, MCZS3, PFK7, PFK174 and KFK154) from each class was subjected to ^1H and or ^{31}P NMR spectra analysis (300 MHz Anova Varian spectrometer, Varian Inc., Oxford, England) following dissolution in *d*₆-DMSO (newly opened to minimise the presence of water). The spectra obtained were labelled day zero spectra. Day zero samples and a duplicate were then stored at -20 and 37 °C respectively and analysed again after 24 h and on day 7 to determine compound stability over this time period compared to day zero. ^1H chemical shifts of the complexes were referenced to the signals of the residual proton peak of the NMR solvent while those of ^{31}P were referenced to a phosphorous standard (85% H_3PO_4) and quoted in parts per million (ppm).

Due to concerns that compound stability and precipitation from solution could be significantly enhanced over longer periods of storage in DMSO, dissolved compounds were generally not stored for longer than one week before use in bioassays. It has been shown that compounds dissolved in DMSO are capable of precipitating out of solution by the third week (Waybright *et al.*, 2009). Since the compounds were not used beyond a week after dissolution in DMSO, NMR spectroscopy studies were therefore limited to one week. Another precautionary measure to sustain stability was the fact that the compounds were maintained in desiccated forms at -20 °C and only working stocks sufficient for use within a week were prepared.

3.3.2 *In Silico* ADMET Predictions

In order to perform the ADMET predictions, 2D sketches of the compounds were drawn in ChemDraw (CambridgeSoft, PerkinElmer Inc., USA) and saved as structural data files (sdf) or molecular (mol) file formats which are formats compatible with the Discovery Studio® (Accelrys®, California, USA) computational software package that was used for the predictions. Prior to initiating the runs, a compound preparative phase was performed. This involved checking and correcting valencies, adding hydrogens, applying force fields and geometry optimisation through energy minimization. The energy minimisation was performed using a CHARMM (Chemistry at Harvard Macromolecular mechanics) force field which updates the coordinates of the molecule (based on reference values, Höltje *et al.* 2003) and adds energy properties. By using these computations, the structures were given more relaxed

and better geometries with energy minima. The computational predictions were performed on an LG Intel® Core™ 2 Duo CPU 2.2 GHz processor, 1.97 GB RAM with Windows XP professional version 2002 operating system which are the minimum system requirements recommended by DS® for such studies.

The ADMET protocol in DS® which aids in the prediction of aqueous solubility, BBB penetration, CYP inhibition, hepatotoxicity, HIA and PPB of the compounds was used for predicting drug-likeness. This protocol includes the models by Egan *et al.*, (2000) and Egan and Lauri, (2002) for HIA which incorporates AlogP98 (atom-based log P or lipophilicity) and polar surface area (PSA, related to the H-bonding ability). Also included are the models of Cheng and Merz, (2003) for aqueous solubility, Egan and Lauri, (2002) for BBB penetration, Susnow and Dixon, (2003) for CYP inhibition, Cheng and Dixon, (2003) for hepatotoxicity and Dixon and Merz, (2001) for PPB predictions. These models come with rankings for each ADMET descriptor that helps in predicting the confidence of the estimations. The various models were derived from diverse datasets of compounds with a wide range of chemical families from both the literature and those in clinical use, representative of each descriptor and subsequently validated using training sets.

Lipophilicity (presented as AlogP98 in the *in silico* studies and as Log P in the shake flask assay in sections 3.3.3) is applicable to all the ADMET parameters and is not a standalone property. Lipophilicity is used to assess biological parameters relevant to drug action such as lipid solubility, tissue distribution, receptor binding, cellular uptake, metabolism and bioavailability (Ghose *et al.*, 1998) which are all related to the ADMET descriptors. It is the driving force around transmembrane transport and additionally helps to determine pharmacological activity and toxicity (Gombar and Enslein, 1996). The importance of lipophilicity as a physicochemical property in drug design means it plays a major role in determining drug-likeness of potential compounds.

3.3.2.1 Human intestinal absorption prediction model

The HIA model was developed using 182 compounds in the dataset with descriptors that include AlogP98 and PSA (Egan *et al.*, 2000, Egan and Lauri, 2002). The model includes a 95% confidence ellipse and a robust 99% confidence ellipse in the ADMET PSA and AlogP98 plane. These ellipses define regions where well-absorbed (>90% absorbed) and poorly absorbed (<30% absorbed) compounds are expected to be found. Four prediction levels are provided to aid in the classification: 0 = good, 1 = moderate, 2 = poor and 3 = very poor absorption.

3.3.2.2 Aqueous solubility prediction model

A predictive model for aqueous solubility was determined by Cheng and Merz (2003) using a data set of 775 compounds with Mr between 70 and 800 g/mol. A validation set of

1665 compounds from Physician's desk References and Comprehensive Medicinal Chemistry databases were used and the findings from the predictions agreed with experimental values. Six solubility levels are described, 0 = extremely low ($\log(S_w) < -0.8$), 1 = very low but possible ($-0.8 < \log(S_w) < -6.0$), 2 = low ($-6.0 < \log(S_w) < -4.0$), 3 = good ($-4 < \log(S_w) < -2.0$), 4 = optimal ($-2.0 < \log(S_w) = 0.0$), 5 = too soluble ($0.0 < \log(S_w)$) and 6 = warning; molecules with one or more unknown AlogP98 type are present, where $\log S_w$ = solubility in water at 25 °C and pH 7.0.

3.3.2.3 Blood brain barrier penetration prediction model

The BBB penetration prediction also developed by Egan and Lauri (2002) incorporates the AlogP98 as well as PSA plane. Confidence ellipses were also used in the prediction and included a 95 and 99% ellipse. Although the data is interpreted similarly to those of the HIA ellipses, the planes are different from those used in the HIA model. The model was derived from over 800 compounds that are known to enter the central nervous system after oral administration. Four prediction levels within the ellipses were determined for this model and include: 0 = very high penetrant ($\log BB \geq 0.7$), 1 = high ($0 \leq \log BB < 0.7$), 2 = medium ($0.52 < \log BB < 0$), 3 = low ($\log BB \leq -0.52$), 4 = undefined, where $\log BB$ = logarithm of blood brain penetration.

3.3.2.4 Cytochrome P4502D6 prediction model

The model derived by Susnow and Dixon (2003) for predicting CYP inhibition was obtained from a diverse data set of 100 compounds using 2D chemical structures as input. The model classifies compounds as either 0 (non inhibitor, i.e. unlikely to inhibit the CYP2D6 enzyme with probability < 0.5) or 1 (inhibitor, likely to inhibit CYP2D6 enzyme with probability > 0.05) and provides an average value of confidence.

3.3.2.5 Hepatotoxicity prediction model

Drug induced liver injury is responsible for 5% of all hospital admissions and 50% of all acute liver failures (Ostapowicz *et al.*, 2002) making the identification of potential hepatotoxic compounds crucial during drug development. The training set of compounds that were employed by Cheng and Dixon (2003) for hepatotoxicity prediction was from a diverse set of compounds causing all types of liver injuries and spanning a wide range of chemical families. The resulting training set of compounds included 382 drug and drug-like compounds of various therapeutic classes known to exhibit liver toxicity. Using only 2D information of the compounds provided, the model predicts with $> 80\%$ accuracy, the potential for the occurrence of dose-dependent human hepatotoxicity of any compound. The model classifies compounds as either "toxic" (1) or "nontoxic" (0) and provides a confidence level indicator of the likelihood of the model's predictive accuracy.

3.3.2.6 Plasma protein binding prediction model

The ADMET PPB model derived by Dixon and Merz (2001) predicts the likelihood of a compound binding to carrier proteins in blood. The properties computed in this model include the AlogP98, unknown AlogP98 and the PPB levels. The classification levels include 0 = likelihood of a compound binding by <90%, 1 = likelihood of binding by > 90% and 2 = likelihood of binding by > 95%. These levels are scored based on the flagging of marker molecules in the compound.

3.3.2.7 Currently available ARV drugs as Controls for ADMET predictions

Currently available ARV drugs were used as controls for supporting the predictions as well as for providing data that could allow for commentary on the drug-like properties of the compounds studied here with respect to these available drugs. Molecular structures of the controls in the sdf format were obtained from the protein data bank (PDB, at <http://www.ncbi.nlm.nih.gov/pccompound>).

3.3.3 Shake Flask Method for Lipophilicity Measurement

In addition to using DS® to computationally determine the lipophilicity of the compounds, an experimental shake flask method was also used. This was employed to complement or confirm the theoretical predictions. The shake flask method is a traditional method for determining lipophilicity and involves the introduction of the test compound to two phases (n-octanol and water) into a separating funnel (Danielsson and Zhang, 1996). The funnel is then shaken for a period long enough for equilibrium to be achieved. The concentration of the compound of interest in each phase is determined after phase separation by measuring absorbance.

The confirmation assay was performed for two complexes only, PFK7 and PFK8 which were found to be soluble in both the octanol and water phases used for determining partition coefficient or lipophilicity. Solubility in both phases obviates one of the shortcomings of the shake flask method. This is because lipophilicity values are difficult to obtain for compounds which are very lipophilic or very hydrophilic since a proper ratio or partition coefficient between the two phases cannot be obtained.

The assay was performed using a modified shake flask method (Yousif *et al.*, 2009). Phosphate buffered saline (PBS, sterile filtered, pH 7.4) was used as the aqueous phase because it is more physiologically relevant while the organic (or lipid phase) was 1-octanol (Sigma Aldrich, Missouri USA, ≥ 99%). The physicochemical similarity of 1-octanol to lipids makes it a natural choice as a hydrophobic solvent (Ghose *et al.*, 1998). The complexes were dissolved in DMSO and diluted with PBS to a final concentration of 200 µM. An equal volume of 1-octanol was added to the solution and both fractions were subjected to shaking (45 rpm, 30 min) on an Intelli Mixer (Sky Line, Riga, Latvia). Once equilibrium had been attained, the

two phases (organic and aqueous phases) were separated after allowing the mixture to stand for 5 min. Serial 2 fold dilutions (200 to 0.625 μM) for each compound in both the 1-octanol and PBS phases were used as standards in determining the concentration of those of the test samples. Both the standards and different phases of each of the compounds were loaded onto 96 well plates (tissue culture grade, NuncTM, Roskilde, Denmark) and the absorbance obtained by UV-Vis spectroscopy at 375 nm using a Multiskan Ascent[®] spectrophotometer (Labsystems, Helsinki, Finland). Plots of the standard curves were used in obtaining the concentrations of the samples. Log P was defined and calculated as the logarithm of the ratio of the concentrations of the compound in the organic and aqueous phases ($\text{Log } P = \text{Log} \left\{ \frac{[\text{compound}_{(\text{org})}]}{[\text{compound}_{(\text{aq})}]} \right\}$ where org = organic phase and aq = aqueous phase).

3.4 RESULTS AND DISCUSSION

3.4.1 NMR Profiles

The NMR profiles of the complexes were obtained on day zero to serve as reference spectra and for comparison with those obtained at synthesis. Subsequently two more spectra were obtained at 24 h and after 7 days (stored at -20 and 37 °C) to determine stability w.r.t. the day zero sample. Because the characterisation of the structures had been performed and confirmed by the chemists, emphasis was placed on identifying any differences and changes in the spectra over time at these temperatures. When using NMR for stability analysis one expects spectra taken at different time points to exhibit peaks at the same chemical shifts irrespective of when they were collected. If there is a change in the observed shifts or appearance of new signals over time, this can be interpreted as possible degradation or the formation of new products. It should however be kept in mind that some structural changes which could have occurred over time may not be detectable by NMR either as a result of spectral overlap (resulting from similarity in backbone structures of breakdown products) or as a result of low sensitivity (Kenseth and Coldiron, 2004). In the next subsections, the outcomes from the NMR analysis for the different complexes that were analysed will be provided. The actual spectra are provided in the appendix for those complexes for which chemical shifts were observed.

3.4.1.1 ³¹P and ¹H NMR chemical shifts of the gold(I) phosphine chloride complex TTC3

The ³¹P NMR of TTC3 remained unchanged over 7 days at -20 and 37 °C with a consistent peak at 33.9 ppm. In the chemical shifts in the ¹H NMR were maintained except for the presence of a water signal at 3.3 ppm (Gottlieb *et al.*, 1997) which was present on day zero, becoming more prominent after 24 h and 7 days later and affecting resolution (Figure A3.1). The spectrum on day zero for this complex suggests that water was present in the compound even as a powder (Figure A3.1A). This means that the compound was hygroscopic (taking up some water from the atmosphere in the course of storage) which was further

compounded by DMSO's hygroscopic nature, evident from the more prominent water peak after 24 h and 7 days (Figure A3.1B and C). The increase in the water peak must have been enhanced by the fact that the same sample was intermittently opened and closed during the analysis times (24 h and 7 days later). The hygroscopic limitation associated with DMSO emphasises the importance of storing DMSO stocks and DMSO dissolved compounds in single use vials or under inert gas. By so doing, complications (e.g. compound precipitating out of solution) that can arise from having water in a DMSO solution of potential bioactive compounds can be avoided or reduced (unless in a case where the compound itself is hygroscopic).

3.4.1.2 ^{31}P and ^1H NMR chemical shifts of the BPH gold(I) chloride complex EK231

The ^{31}P NMR spectra for EK231 over 7 days and at the two different temperatures also remained unchanged with a consistent peak at 83.9 ppm. As was the case for TTC3, the water peak in the ^1H NMR (absent on day zero) was prominent after 24 h and at 7 days, increasing in area and height over this time. The rest of the shifts remained stable throughout the analysis except for a new peak at 2.4 ppm (after 24 h and on the 7th day) suggestive of the presence of acetone which was used in cleaning the NMR tubes.

The stability of this complex and that of TTC3 (seen in the ^{31}P NMR) is thought to be related to the stability conferred by the covalent bond between P of the phosphine ligand and gold (Parish and Cottrill, 1987).

3.4.1.3 ^{31}P and ^1H NMR chemical shifts of the gold(I) thiolate complexes MCZS3 and PFK174

The ^{31}P NMR peak for MCZS3 on day zero was absent possibly because of poor solubility (Figure A3.2A). This compound which was provided as a powder was noted to be hygroscopic absorbing water from the atmosphere. The poor solubility in DMSO may be as a result of precipitation of the compound out of solution due to the presence of water. In the ^1H NMR spectrum, the broad peak at 3.4 ppm is likely HDO (semi heavy water) resulting from d_6 -DMSO exchanging a deuterium atom with hydrogen atom of water (deuterium exchange). According to the spectrum, the backbone phosphine and acetylated sugar moieties are intact but impurities (including HDO and possibly H_2O) are evident (Figure A3.2B). Subsequent analysis after 24 h and 7 days was not done due to the evident poor solubility observed as precipitation which ended up limiting sample concentration for ^{31}P NMR analysis. In addition, since this compound did not show promising activity during inhibition studies (reported in chapter 4 and 5), the need to pursue stability and storage properties was considered not important for this study.

A ^{31}P NMR peak for PFK174 was also evidently absent and the reason for this was also ascribed to poor solubility. In the ^1H NMR spectra, a water peak was evident on day zero (inherent hygroscopic ability) but most of the ^1H shifts were poorly resolved. Similar to MCZS3,

the poorly resolved peaks probably arose from the poor solubility that was observed for this compound. At the minimum required concentration (10 mg/mL) for NMR analysis, the complex was visibly precipitating out of *d*6-DMSO. The fact that solubility (both in DMSO and in aqueous media) can affect bioassay reproducibility means that for this compound to be successfully used as a drug, it would require some form of modification to enhance solubility. Fortunately, it may not be necessary to do this for PFK174 and its analogues because outstanding inhibitory effects were not observed in the inhibition studies (discussed in chapters 4 and 5). This compound which is one of the bimetallic compounds in class III may however need further attention in determining its solubility especially for the anti-cancer project for which a patent application has been launched for the outstanding anti-cancer activity.

In the ^1H NMR spectrum the presence of a water peak at 3.3 ppm was also evident (day zero), subsequently becoming more prominent. This finding was similar to that observed the ^1H spectra of TTC3 and EK231 and was thought to be as a result of DMSO's hygroscopic nature after intermittent opening at the 24th hour and latter at 7 days.

The limited solubility observed for complexes MCZS3 and PFK174 in *d*6-DMSO and the observed absence of a ^{31}P peak may be related to the fact that these complexes contained water which is known to facilitate the precipitation of compounds out of DMSO solution (Ellson *et al.*, 2005). Alternatively, the presence of water in these complexes (which was more prominent than for the others) might have suppressed the ^{31}P NMR peaks to undetectable levels.

3.4.1.4 ^1H NMR chemical shifts of the gold(III) thiosemicarbazonate complex, PFK7

Only the ^1H NMR spectrum of PFK7 was obtained since the compound does not contain phosphorous as one of its atoms. With respect to the ^1H spectrum, the chemical shifts for this complex appeared stable over time except for the presence of the water peak at 3.3 ppm (Gottlieb *et al.*, 1997) on day zero which became more prominent at 24 h and 7 days at 37 °C (shown in Figure A3.3). The increase in the water peak after 24 h and 7 days was also attributed to DMSO's hygroscopic nature.

3.4.1.5 ^1H NMR chemical shifts of the gold(III) pyrazolyl complex, KFK154b

Only the ^1H NMR spectrum for this compound was obtained as well since there is no phosphorous environment. The water peak at 3.33 ppm seen on day zero for the other complexes and at 24 h and 7 days later at both -20 and 37 °C was absent for this complex. The only new peak that was observed appeared around 4.7 ppm after 24 h (Figure A3.4B) and was present on analysis on day 7 (Figure A3.4C). The peak at 4.7 ppm indicated the presence of impurities such as deuterated water (D_2O , Gottlieb *et al.*, 1997). It is not clear why the water peak at 3.33 ppm was absent at 24 h and after 7 days since all the samples were handled the same. The deuterated water peak at 4.7 ppm may have compensated for this or alternatively,

this compound did not have a hygroscopic tendency like the others did. According to the ^1H NMR of the compound, the backbone structure remained intact over the analysis time.

3.4.1.6 Summary of NMR Stability Profiles

Table 3.7 is a summary of the NMR profile changes that were observed. A water peak in the ^1H NMR spectrum (at 3.33 ppm, Gottlieb *et al.*, 1997) of complexes TTC3, EK231, MCZS3, PFK174 and PFK7 was the most visible change that was seen over time. A water peak was evident in the spectra of complexes TTC3, MCZS3, PFK174 and PFK7 (suggesting that these complexes had hygroscopic tendencies) on day zero and became prominent by 24 h and 7 days later. In the spectra of EK231, a water peak was visible at 24 h and at 7 days but not on day zero. The presence of water in DMSO solutions of compounds causes precipitation of dissolved compounds and can lead to concentrations disparities in *in vitro* tests. According to Ellson *et al.*, (2005), only minimal degradation can result probably explaining why all the compounds tested above remained relatively intact (as seen from the uniformity in ^1H and ^{31}P environments and the overall backbone structures) even in the presence of water. To minimise DMSO's effects in our samples, compounds were aliquoted and stored in single use vials. Compounds dissolved and stored at $-20\text{ }^\circ\text{C}$ for subsequent assays were also stored in single use volumes.

With regards to compound stability, the backbone structures of the compounds appeared to be maintained suggesting stability. The only new peaks were the water peak found in the spectra of complexes TTC3, MCZS3, PFK174 and PFK7 on day zero which became prominent at 24 h and 7 days. In the ^1H spectra of EK231 acetone was present as an impurity while a new peak in the spectrum of KFK154b at 4.7 ppm after 24 h and on day 7 following storage at $-20\text{ }^\circ\text{C}$ and at $37\text{ }^\circ\text{C}$ (Figure A3.4B) was suggestive of the presence of deuterated water (Gottlieb *et al.*, 1997). Poor solubility of PFK174 led to poorly resolved ^1H NMR and no ^{31}P shifts. It is possible that structural changes can appear especially at higher temperatures after longer time periods (has been seen for compounds stored at $4\text{ }^\circ\text{C}$ dissolved in DMSO). However, ^{31}P NMR shifts of some of these complexes after 4 months in DMSO at $-20\text{ }^\circ\text{C}$, (Fonteh and Meyer, 2008) maintained chemical shifts. The fact that the compounds in this study were never used for bioassays beyond one week (dissolved in DMSO), meant stability studies after one week were not necessary. Although the backbone structures of the compounds appeared to be maintained, compounds with inherent hygroscopic abilities e.g. TTC3, MCZS3, PFK174 and PFK7 can lead to varying data in bioassays resulting from precipitation in DMSO.

Table 3.7: Stability profile summary. ¹H and ³¹P NMR spectra of the complexes were acquired on immediate dissolution in *d*₆-DMSO, at 24 h, and 7 days later (stored at -20 and 37 °C). N/A is not applicable

Complex	¹ H NMR profile changes		³¹ P profile changes over time	Conclusion (overall backbone structure)
	Day zero	over time (24 h and 7 days)		
TTC3	H ₂ O peak	Increasing	Stable	Intact but compound may be hygroscopic
EK231		H ₂ O peak and acetone	Stable	No water peak on day zero but present after 24h
MCZS3	HDO and H ₂ O	Not done	Nil (limited solubility)	Intact but contains impurities and is hygroscopic
PFK174	H ₂ O peak	Increasing	Nil (limited solubility)	Poorly resolved ¹ H spectra. Compound may be hygroscopic
PFK7	H ₂ O peak	Increasing	N/A	Intact but compound may be hygroscopic.
KFK154b		New peak at 4.6ppm	N/A	Backbone intact with impurity at 4.6 ppm suggestive of D ₂ O.

3.4.2 *In silico* ADMET Predictions

Drug-likeness predictions for the compounds using the ADMET protocol in DS[®] are shown in Table 3.8A. Predictions for existing ARV drugs are shown in Table 3.8B and were included for comparison purposes with those of the compounds studied here. Auranofin/MCZS2 (a gold-based drug) was also used as reference since the literature contains information on its drug-likeness.

3.4.2.1 Prediction of human intestinal absorption

HIA was predicted to be good (0) to moderate (1) for sixteen of the compounds namely four of the phosphine compounds (TTL10, TTC10 and TTL24, TTC24), three of the gold(I) phosphine thiolate complexes (MCZS1, MCZS2 and MCZS3), the Tscs ligands and complementary gold(III) complexes (PFK5, PFK6, PFK38, PFK39 and PFK7, PFK8, PFK41, PFK43 respectively) and the gold(III) pyrazolyl complex KFK154B (Table 3.8A). Very low (3) HIA levels were predicted for three phosphine chloride compounds (TTL3, TTC3, and TTL17), the BPH gold(I) complexes (EK207, EK208, EK219 and EK231) and the bimetallic complexes; PFK174, PFK189 and PFK190 of class III (Table 3.8A). TTC17 was the only complex ranked to be low (2) in absorption. The compounds predicted to have poor HIA also meet some of the criteria of “Lipinski’s rule of five” which states that poor absorption or permeation is more likely when there are > 5 H-bond donors, >10 H-bond acceptors, the Mr is > 500 and the calculated log P is > 5 (Lipinski *et al.*, 1997). The BPH complexes (EK207, EK208, EK219, EK231) and the gold(I) thiolate complexes (PFK174, PFK189 and PFK190) as well as TTC3 with very low solubility predictions have molecular weights of >500 (Table 3.6) as well as lipophilicity values of >5 (Table 3.8A). TTL3 and TTL17 (phosphine compounds), predicted to have very low HIA (Table 3.8A), also met one of “Lipinski’s rule of five” by having lipophilicity predictions of >5.

Table 3.8A: ADMET prediction scores for the compounds. The shaded portions represent compounds with good drug properties. A Key to these predictors is presented as footnotes below the table. The assigned asterisk indicates the ligands or complex precursors.

Name	HIA	Aqueous Solubility Level	BBB Level	Hepatotoxicity	Hepatotoxicity Probability ^a	CYP2D6	CYP2D6 Probability ^a	PPB Level	AlogP98 (lipophilicity)	AlogP98 unknown	PSA 2D
TTL3*	3	0	4	1	0.86	1	0.831	2	7.6	0	11.3
TTC3	3	1	4	1	0.841	1	0.613	2	7.4	2	11.3
TTL10*	1	1	0	1	0.668	1	0.891	2	5.9	0	14.7
TTC10 ^b	1	1	0	1	0.516	1	0.782	2	5.7	2	14.7
TTL17*	3	1	0	1	0.94	1	0.861	2	7.1	0	12.8
TTC17	2	1	0	1	0.854	1	0.653	2	6.9	2	12.8
TTL24*	0	2	0	1	0.675	1	0.891	2	5.4	0	16.2
TTC24 ^b	0	2	0	1	0.523	1	0.782	2	5.2	2	16.2
EK207	3	0	4	1	0.841	0	0.435	2	8.6	6	6.7
EK208	3	1	4	1	0.887	1	0.554	2	7.4	4	6.7
EK219	3	0	4	1	0.953	0	0.475	2	8.5	6	42.4
EK231	3	0	4	1	0.748	0	0.415	2	9.2	6	20.1
MCZS1	0	4	4	0	0.052	0	0.356	0	0.1	2	123.9
MCZS2	0	4	4	0	0.086	0	0.306	0	1.4	2	113.9
MCZS3	1	4	4	0	0.046	0	0.336	0	-1.3	2	120.6
PFK174	3	0	4	1	0.801	0	0.326	2	12.8	4	33.2
PFK189	3	0	4	1	0.774	0	0.198	2	13.7	4	33.2
PFK190	3	0	4	1	0.827	0	0.386	2	15.2	4	33.2
PFK5*	0	4	3	0	0.132	0	0.386	0	1.1	0	73.9
PFK7	0	3	2	1	0.701	0	0.247	0	1.5	5	25.6
PFK6*	0	4	3	0	0.304	0	0.366	0	0.4	0	73.9
PFK8	0	3	2	1	0.86	0	0.108	0	0.8	5	25.6
PFK39*	0	4	3	0	0.384	0	0.079	0	0.3	0	73.9
PFK41	0	4	2	1	0.834	0	0.069	0	0.7	5	25.6
PFK38*	0	4	3	0	0.284	0	0.257	0	0.9	0	73.9
PFK43	0	3	2	1	0.794	0	0.118	0	1.4	5	25.6
KFK154B ^b	0	4	2	1	0.516	0	0.059	0	0.9	2	36.6

Absorption level: 0 = good, 1 = moderate, 2 = low, 3 = very low. **Aqueous Solubility level:** 0 = extremely low, 1 = possible, 2 = low, 3 = good, 4 = optimal. **BBB:** 0 = very high, 2 = medium, 3 = low, 4 = undefined. **Hepatotoxicity:** 0 = non-toxic, 1 = toxic, **CYP:** 0 = non-inhibitor, 1 = inhibitor. **PPB:** 0 = <90% binding, 2 = >95% binding. ^a = probability of occurring, the closer it is to 1 the higher the chance of the compound being hepatotoxic or inhibiting CYP and the closer it is to 0, the higher the probability of the compound not being hepatotoxic or inhibiting CYP. The **PSA** gives an indication of the H-bonding ability and was used together with AlogP98 in determining HIA (shown in Figure 3.7). ^b = 50 /50 chance of being either hepatotoxic or not. AlogP98 unknown represents the number of atoms in the compound with unknown AlogP98.

Table 3.8B: ADMET prediction data for clinically available ARV drugs. The key provided for the descriptors in Table 3.8A also apply here.

HIV drugs	Names	HIA level	Aqueous Solubility level	BBB Level	Hepato-toxicity	CYP 2D6	PPB level	Alog P98	Unknown AlogP98	PSA 2D
NRTIs	Lamivudine	0	4	3	0	0	0	-0.59	0	88.26
	Tenofovir	1	4	4	1	0	0	-0.91	0	133.53
	Emtricitabine	0	4	3	0	0	0	-0.68	0	88.26
	Tipranavir	3	1	4	1	0	2	7.38	0	105.72
	Zalcitabine	0	4	3	0	0	0	-0.99	0	88.26
	Stavudine	0	4	3	1	0	0	-0.32	0	80.51
	Didanosine	0	4	3	1	0	0	-0.84	0	87.79
NNRTIs	Entravirine	2	1	4	1	0	2	5.49	0	116.67
	Nevirapine	0	2	2	1	1	0	2.29	0	55.99
	Delavirdine	0	2	4	0	0	2	2.29	0	110.54
	Efavirenz	0	1	1	0	0	1	4.38	0	39.04
PR	Saquinavir	3	2	4	0	0	0	3.67	0	169.60
	Fosamprenavir	3	2	4	0	0	2	2.54	0	180.33
	Antazanavir	3	2	4	1	0	2	5.08	1	173.73
	Darunavir	2	2	4	0	0	0	2.63	0	142.21
	Ritonavir	2	2	4	1	1	2	5.24	0	145.95
	Amprenavir	1	3	4	0	1	2	2.43	0	133.28
IN	Raltegravir	2	3	4	0	0	0	0.36	0	148.09

The lipophilicity or AlogP98 values which were involved in the model development play a very significant role in determining HIA. According to Kerns and Di, (2008), compounds with ideal lipophilicity values (which should be $0 \geq 3$, unlike log P values of <0 [poor lipid bilayer permeability] and >3 [poor aqueous solubility]) also have good solubility patterns. This was observed for the Tscs-based compounds (PFK5, PFK7, PFK6, PFK8, PFK39, PFK41, PFK38 and PFK43), the gold(III) pyrazolyl complex (KFK154b) and two of the gold(I) phosphine thiolate complexes (MCZS1 and MCZS2, Table 3.8A). Compounds TTL10, TTC10 and MCZS3 were predicted to have moderate (1) lipophilicity values with those of TTL10 and TTC10 falling just above the recommended value for “Lipinski’s rule of five” while MCZS3’s value of -1.3 was out of the range indicated by Kerns and Di, (2008).

In Figure 3.7, point plots representing the AlogP98 and PSA ellipses in relation to HIA and BBB penetration for the compounds in this study (Figure 3.7A) and those of currently available ARVs (Figure 3.7B) are shown. Compounds predicted to have good HIA appear within the 95% ellipse (Figure 3.7A) which has an upper PSA limit of 131.4 while those with moderate absorption occupied the 99% absorption ellipse which has an upper PSA limit of 148.12. The poorly absorbed compounds appeared outside both the 95 and 99% ellipses of the AlogP98 versus PSA point plot. The AlogP98 versus PSA point plot for the currently available ARVs is shown in Figure 3.7B. On the list of currently available anti-HIV medication, at least 4 of the 18 compounds (22%) had very low HIA prediction levels (Table 3.8B) and this was mostly the PR inhibitors. This finding suggested that compounds with low absorption could still make it through the discovery process and be useful in a clinical setting. This is

probably because there are exceptions to the rule of five (Walters and Murcko, 2002) making these rules guidelines and not absolute requirements (van de Waterbeemd and Gifford, 2003). The point plots in Figure 3.7 also display BBB penetration ellipses for 95 and 99% confidence levels.

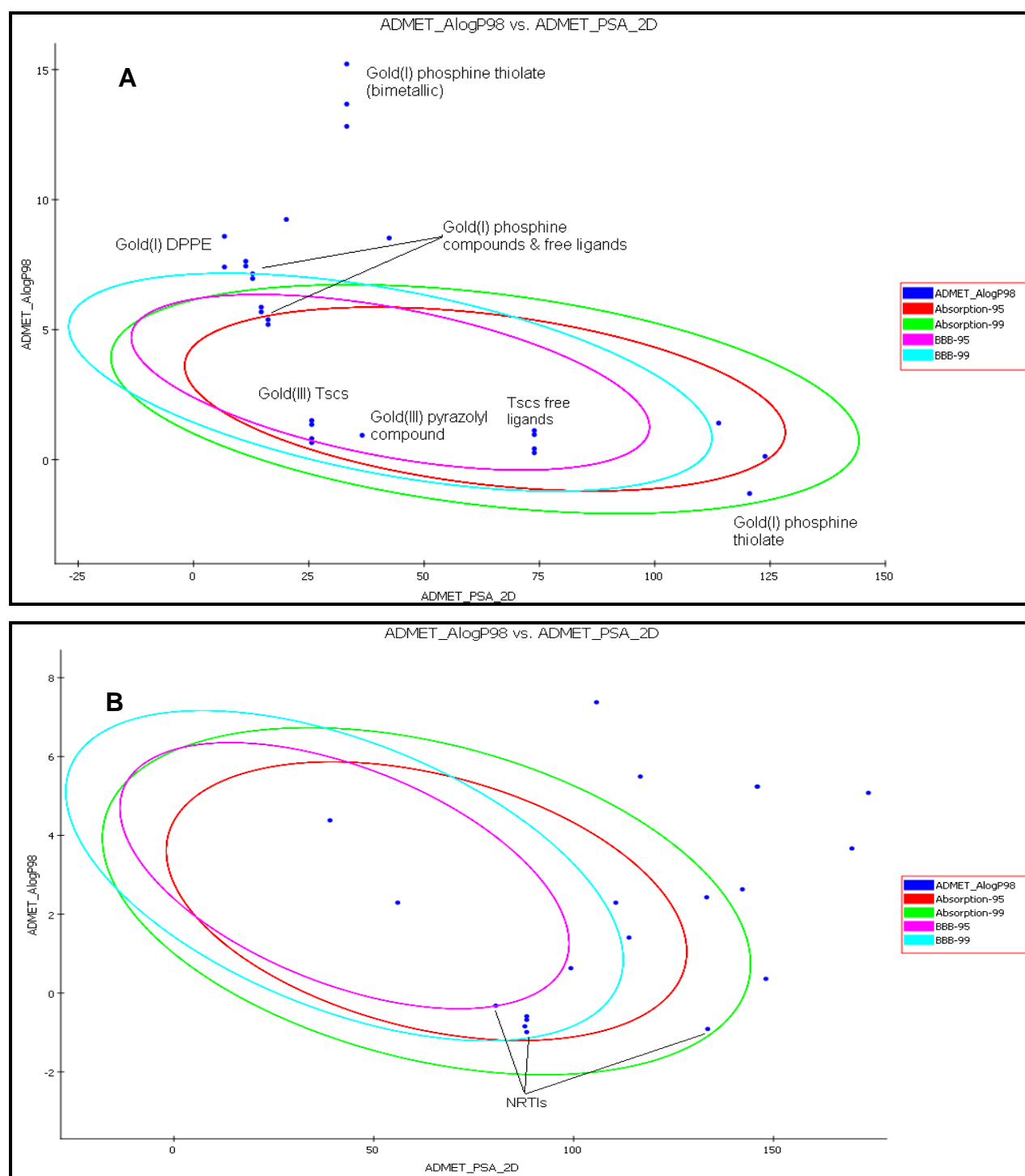


Figure 3.7: Absorption and BBB penetration point plot of the compounds (A) and ARV drugs in the clinic (B). AlogP98 is plotted against PSA. Except for the BPH gold(I) complexes, the gold(I) phosphine bimetallic thiolate complexes and two phosphine chloride compounds (TTL3 and TTC3), the rest of the compounds were predicted to have good HIA levels as they appeared within the 95 and 99% confidence ellipses (A). A total of 18 drugs from the different classes (NNRTIs, NRTIs, PR and IN inhibitors) of ARVs were analysed. Twelve of the drugs were predicted to have acceptable HIA levels and only 8 were predicted to have acceptable BBB penetration levels. A total of 58% of the controls were predicted to be outside the BBB ellipses while at least 37% were outside the HIA ellipses. Each dot on the figure represents a compound. The relative positions of the various classes of compounds are shown in A but only that of the NRTIs (dNTP analogues) in B because there was dispersion within the other groups of ARVs.

3.4.2.2 Prediction of aqueous solubility

Fourteen of the compounds were predicted to have aqueous solubility (25 °C, pH 7.0) in the drug-like category (Table 3.8A) which includes levels 2, 3 and 4 (Cheng and Merz, 2003). These were TTL24 and TTC24, the Tscs-based compounds (PFK5, PFK6, PFK7, PFK8, PFK38, PFK39, PFK41 and PFK43), the gold(I) phosphine thiolate complexes (MCZS1, MCZS2, MCZS3) and the gold(III) pyrazolyl complex (KFK154b). The rest of the compounds (the gold(I) phosphine chloride complexes and ligands, the BPH complexes, and the three gold(I) phosphine thiolates, PFK174, PFK189, and PFK190) had low to extremely low solubility levels. The extremely low aqueous solubility prediction for PFK174 was not surprising given that this compound was not soluble enough to give a visible ^{31}P NMR peak when the day zero samples were analysed (subsection 3.4.1.3).

It was notable that compounds with ideal aqueous solubility predictions generally had good absorption levels as seen in Table 3.8A i.e. good solubility = good oral absorption (Lipinski *et al.*, 1997). In addition, all the compounds with poor aqueous solubility also had very high AlogP98 or lipophilicity values suggesting that these compounds were very hydrophobic. Although attempts were made in increasing the hydrophilicity of the $(\text{Au}(\text{DPPE})_2\text{Cl})$ parent compound in the synthesis of its analogues (EK207, EK208, EK219 and EK231, see section 3.2.2) through the use of nitrogen heteroatoms to replace the lipophilic ethane bridge (Kriel *et al.*, 2007), it appears the N bridges were not sufficient in fine tuning the lipophilicity/hydrophilicity. This observation is consistent with findings by Kriel *et al.*, (2007) who noted that the addition of the N bridge in the synthesis of $\text{Au}(\text{DPPE})_2\text{Cl}$ analogues slightly improved selectivity but not sufficiently enough in the targeting of tumour cells over healthy cells. The observed poor aqueous solubility noted for the BPH gold(I) complexes suggested that these compounds would have to be very efficacious for further consideration as drugs and would probably require additional structural modification to improve aqueous solubility.

Only two of the eighteen currently available anti-HIV drugs which were tested as controls (Table 3.8B) had poor aqueous solubility predictions. This observation may be indicative of the importance of aqueous solubility as a drug-like property (Di and Kerns, 2006). Compounds with poor aqueous solubility affect bioassays by causing underestimated activity, reduced HTS hit rates, result in variable data, inaccurate SAR, discrepancies between enzyme and cell assays and inaccurate *in vitro* ADMET testing (Di and Kerns, 2006). While aqueous solubility is a required property, it is important that a balance be obtained because very high aqueous solubility which is usually associated with poor lipophilicity means compounds with such properties cannot be orally available.

3.4.2.3 Prediction of blood brain barrier penetration

Three of the phosphine ligands and corresponding gold(I) complexes (TTL10, TTC10, TTL17, TTC17, TTL24 and TTC24) were predicted to have very high BBB penetration levels

(0), while the thiosemicarbazone gold(III) complexes (PFK7, PFK8, PFK41 and PFK43) and the gold(III) pyrazolyl complex (KFK154b) had medium BBB penetration prediction levels of 2 (Table 3.8A). The Tscs ligands PFK5, PFK6, PFK39 and PFK38 had moderate BBB penetration. Complexation with gold appeared to improve BBB penetration for the complementary complexes. The rest of the compounds i.e. TTL3 and TTC3 from the phosphine chloride class, the BPH gold(I) complexes and the gold(I) phosphine thiolate complexes were predicted as having undefined (ranked 4) BBB penetration levels. These compounds also appeared outside the 99% ellipse (seen in Figure 3.7) while those with acceptable penetration levels were within the 95 and 99% confidence ellipses for BBB penetration. BBB penetration is important for anti-HIV agents to be able to combat infection and inhibit viral replication in the brain (Glynn and Yazdanian, 1998). Existing anti-HIV agents such as nevirapine are able to cross the BBB (this ability is attributed to its lipophilicity, Glynn and Yazdanian 1998). According to the predictions that were performed for the current anti-HIV drugs (Table 3.8B and Figure 3.7B), nevirapine had a BBB level of 2 (medium penetration) supporting the findings by Glynn and Yazdanian (1998). The majority of the HIV drugs either had low or undefined BBB penetration levels (Table 3.8B and Figure 3.7B) especially the PR inhibitors, a finding which has been confirmed by other authors (Enting *et al.*, 1998). This suggests that these drugs would be unable to arrest or reduce viral replication in the brain, a situation that has been shown to result in increased incidence of AIDS dementia (Marra and Booss, 2000). Except for TTL3 and TTC3, the phosphine chloride compounds (TTL10, TTC10, TTL17, TTC17, TTL24 and TTC24), the gold(III) thiosemicarbazone complexes (PFK7, PFK8, PFK41 and PFK43) and the gold(III) pyrazolyl complex (KFK154b) could be better inhibitors of HIV replication in the brain (BBB levels of 0 = very high and 2 = medium). While good BBB penetration predictions were observed for the phosphine chloride compounds (ligands and complexes), unfortunately aqueous solubility was very poor (except for TTL24 and TTC24). These compounds will therefore require further structural modification to fine tune lipophilicity/hydrophobicity so as to obtain ideal lipophilicity values. This observation confirms the ideology that finding a perfect drug is not easily achievable in drug discovery (Joshi, 2007).

3.4.2.4 Prediction of cytochrome P450 2D6 inhibition

Except for the phosphine chloride compounds of class I (Table 3.6) and the BPH gold(I) complex (EK208) which were predicted to be CYP inhibitors, none of the other compounds had such effects (Table 3.8A). This finding is promising for these compounds because inhibition of CYP is not desirable. CYP is involved in drug metabolism (Susnow and Dixon, 2003) and its inhibition could potentially block the metabolism of other drugs. Anti-HIV drugs are administered in combination and if one of the drugs is a CYP inhibitor, its metabolism and that of the other drugs will be compromised. This can lead to a reduction in bioavailability

resulting in enhanced mutation rate since suboptimal doses will end up in the circulation. Alternatively it could result in interactions that may lead to elevated blood levels of some of the drugs that are used such that unwanted and life-threatening side effects could ensue (Tanaka, 1998). Only three of the eighteen anti-HIV drugs for which ADMET predictions were determined had the potential of inhibiting CYP. These included the NNRTI, nevirapine and two PR inhibitors (ritonavir and amprenavir, Table 3.8B).

3.4.2.5 Prediction of hepatotoxicity

Hepatotoxicity prediction levels according to the ADMET protocol could either be 1= hepatotoxic, or 0 = non hepatotoxic. This ranking is further classified based on the likelihood of the toxicity occurring and represented by probability values (Table 3.8A). The closer the probability is to one, the higher the likelihood of the compound being hepatotoxic and the closer to zero, the higher the likelihood of it being non hepatotoxic. The phosphine compounds (TTL10, TTC10, TTL24 and TTC24), the gold(I) phosphine thiolate complexes (MCZS1, MCZS2 and MCZS3) and the Tscs ligands (PFK5, PFK6, PFK38 and PFK39) were predicted as non hepatotoxic (0). The rest of the compounds were hepatotoxic. The gold(III) pyrazolyl complex (KFK154b) was predicted as hepatotoxic but with a 0.516 probability (Table 3.8A). Eight of the eighteen anti-HIV medications on the control list (Table 3.8B) were predicted to be hepatotoxic. Although being hepatotoxic is not a drug-like property, because it can be clinically managed through physician intervention (Núñez, 2010), efficacious drugs with this property can make it through the drug discovery process and be clinically useful e.g. nevirapine in Table 3.8B.

3.4.2.6 Prediction of plasma protein binding ability

Eight gold complexes had a <90% chance of binding to plasma proteins. These were the gold(I) phosphine thiolate complexes, MCZS1, MCZS2 and MCZS2, the gold(III) thiosemicarbazonate complexes and complementary ligands (Table 3.4) and the gold(III) pyrazolyl complex (Table 3.5) with a classification of 0. This classification which also makes use of AlogP98 groups such compounds as having an AlogP98 of <4 (Table 3.8A). The gold(I) phosphine chloride complexes and free ligands (class I) and the BPH complexes (class II) as well as the gold(I) phosphine thiolate bimetallic complexes (PFK174, PFK189, PFK190) of class III on the other hand were predicted as having a > 95% chance of binding to plasma proteins and AlogP98>4. Compounds with a <90% chance of binding to plasma proteins, are more drug-like because the free drug will be able to stay in solution for penetration into tissue and will thus be able to reach the therapeutic target (Kerns and Di, 2008). Binding to plasma proteins tends to affect the concentration of a compound in bioassays involving the use of reagents such as fetal calf serum (FCS) and this could drastically affect *in vitro* efficacy (Lin *et al.*, 2008, Kageyama *et al.*, 1994). Compounds (e.g. those in class I, II and the three bimetallic

complexes of class III) with high PPB binding tendencies that inhibit in direct enzyme assays will have an increased likelihood of complete loss of activity in cell-based assays and *in vivo* (Kageyama *et al.*, 1994).

3.4.2.7 Drug-likeness summary for the compounds

Seven properties i.e. the six ADMET descriptors (HIA, aqueous solubility, BBB penetration, hepatotoxicity, PPB binding and CYP inhibition) and lipophilicity predictions were obtained for each of the twenty seven compounds in this study. These properties were used to construct an in-house drug score table (Table 3.9). According to the summary, only one gold complex (KFK154b) was predicted as having favourable properties for all ADMET descriptors (although with a 50% chance of being hepatotoxic) while seven complexes were positive for 6 out of 7 descriptors. Complex TTC24 and complementary ligand TTL24 had a score of 3 out of 7 with TTC24 having a 50% chance of being hepatotoxic. The least drug-like compounds were TTC3, its free ligand TTL3 and the BPH gold(I) complex EK208. With regards to classes, drug-like characteristics were common for three complexes from class III (MCZS1, MCZS2 and MCZS3), four from class IV (PFK7, PFK8, PFK41 and PFK43) and one from V (KFK154b). The predicted properties were similar when literature comparisons were made with those of the anti-arthritic gold complex, auranofin (also included here as MCZS2).

With regards to functional groups, the ligands played a very important role in the ADMET rankings for each class of compounds. For example, all the phosphine containing compounds which also had phenyl rings had significantly higher AlogP98 values (due to the hydrophobicity related to these rings) than the gold(I) phosphine thiolate complexes (MCZS1, MCZS2 and MCZS3) which have glucose rings and more H-bond acceptors and were less hydrophobic. The Tscs ligands of class IV (Table 3.4) which contain more H-bond donors (Table 3.6) tended to be less lipophilic (than the phosphine group of ligands) while the corresponding gold complexes (Table 3.4) had slightly higher but ideal values (Table 3.8A). The slightly higher values probably resulted from the fact that there was a decrease in the number of H-bond donors after complexation as seen in Table 3.6 where the free ligands had 4 H-donors and upon complexation only 2 were available. Some complexes e.g. the thiosemicarbazone complexes had better drug-like predictions than some currently available anti-HIV agents e.g. nevirapine (Table 3.8B). Nevirapine has the potential of inhibiting CYP which is not the case for eighteen of the 27 compounds in this study. A look at Table 3.9 also suggests that drug-like properties for the complexes were usually similar to those of the ligand precursors e.g. TTL3 and TTC3 which had a total score of 1 and the Tscs ligands and complexes a score of 6/7. The Tscs compounds, the gold(III) pyrazolyl compound and the gold(I) phosphine thiolate compounds containing 2,3,4,6-tetra-O-acetyl-1-thio-B-D-glucopyranose were the most drug-like.

Table 3.9: ADMET prediction scores summary. Compounds with a score of 0/7 were those predicted to be the least drug-like while those with a score of 6/7 were those predicted to be the most drug-like. Ligand precursors and corresponding complexes from different classes had similar scores suggesting that drug-likeness was related to ligand type.

Drug Score/7	Gold complex(s)		Free ligand(s)
	Gold(I)	Gold(III)	
0	TTC3, EK208		TTL3
1	TTC17 EK207, EK219, EK231, PFK174 PFK189, PFK190		TTL17
2	TTC10		TTL10
3	TTC24		TTL24
6	MCZS1, MCZS2 and MCZS3	PFK7, PFK8, PFK41 and PFK43, KFK154b	PFK5, PFK6, PFK39 and PFK38

3.4.3 Shake Flask Method of Lipophilicity Determination

In addition to using the DS® Client software package for predicting AlogP98 (lipophilicity) and its relation to other drug-like properties, lipophilicity determination was also done for gold complexes PFK7 and PFK8 using the traditional shake flask method. This method entails determining the concentration of the compounds in an aqueous and a lipid phase followed by calculating the logarithm of the partition coefficient (Log P) between the phases as a measure of lipophilicity. **Log P** values of **2.42±0.6** and **0.97±0.5** were obtained for complexes PFK7 and PFK8 respectively.

The slight differences between log P values obtained by the shake flask method and those from DS® (which were 1.5 and 0.8 for PFK7 and PFK8 respectively) might be as a result of the presence of the gold atom in the complexes. These atoms are not included in the ADMET AlogP98 protocol in DS®, because the program was designed from datasets involving organic molecules. This leads to 5 atoms (making the coordination sphere) for the gold(III) thiosemicarbazone complexes (PFK7, PFK8 - Table 3.4) and all the gold complexes to have unknown AlogP98 values (Table 3.8A). Atoms with unknown AlogP98 do not contribute to the AlogP98 calculation. However, this did not seem to have had a drastic effect on the AlogP predictions from DS® when compared to those from the shake flask method since very similar values were obtained. This observation was further supported by the fact that ideal lipophilicity predictions were obtained for auranofin which is a known orally available gold-based drug as a result of its lipophilic ability.

3.5 CONCLUSIONS

ADMET properties are required early on in drug discovery to help with prioritising lead compounds and for reducing late failures. While *in vitro* HTS methods can be implemented, *in silico* predictions (which are easily obtained) can serve as complementary approaches for substantiating the *in vitro* findings. In addition to using Discovery Studio for predicting ADMET parameters for the compounds in this study, NMR was also used for determining the stability

of representative complexes in *d6*-DMSO after storage at two different temperatures (-20 and 37 °C).

Backbone chemical shifts of the complexes generally appeared stable after storage at -20 and 37 °C as seen from ^{31}P and ^1H NMR spectra. The main changes appeared to be impurities such as acetone (spectrum of EK231) and D_2O peak in the ^1H spectrum of KFK154b. Another notable change was that of inherent hygroscopic abilities of four complexes while the ^{31}P and ^1H NMR spectra of MCZS3 and PFK174 could not be resolved because of poor solubility in DMSO (Table 3.7) stemming from the presence of water which is known to lead to compound precipitation when in DMSO (Ellson *et al.*, 2005).

With regards to drug-likeness predictions, twelve of the compounds (classes III, IV and V) had a score of 6 out of 7 (Table 3.9) which correspond with literature reports for auranofin (MCZS2), a clinically and orally available gold(I) complex that has been reported to restore the CD4+ count of an AIDS patient who was being treated for psoriatic arthritis (Shapiro and Masci, 1996). This compound was predicted to have ideal lipophilicity and HIA values. BBB penetration predictions for nevirapine also correlated with the experimentally determined findings of Glynn and Yazdanian (1997).

Another notable observation was the fact that ADMET properties, as expected, were dependent on the groups present in the compounds. For example the *N,N*-dimethyl-ethane-1,2-diamine moiety present in TTC10 and TTC24 appeared to confer better drug-like properties unlike the phenethyl-amine group present at a similar position in TTC3 and TTC17 (all complexes belonging to class I).

While some of the compounds were predicted as having favourable ADMET and Lipinski's properties, it should be noted that these are not absolute requirements and that there are exceptions that do go through to clinical application. For these reasons, where possible, all the compounds synthesised in this study were analysed in anti-HIV tests and the calculated/determined predictions here were not stringently used to filter out non drug-like compounds. The anticipation was that efficacious compounds with poor ADMET predictions could eventually be recommended for structural modifications through SAR studies to increase drug-likeness while maintaining therapeutic usefulness. Those with good drug-like properties on the other hand, which end up having therapeutic efficacy would be recommended for further testing.

Confirmatory tests between methods (*in silico* and shake flask for complexes PFK7 and PFK8) and with literature (for auranofin) suggested that the inorganic nature of the compounds did not seem to drastically affect ADMET predictions which were obtained from software that was developed for organic compounds (Fricker, 2007). The ADMET predictions of PFK7, PFK8 and the rest of the Tscs-based complexes and the shake flask findings form part of a publication from this project (Fonteh *et al.*, 2011).

Finding an ideal drug (based on *in silico* and experimental data) is always desirable, but not always possible (Joshi, 2007) as seen from the data for the currently available anti-HIV agents. What is important therefore is obtaining a balance with regards to efficacy and tolerability while ensuring appropriate physician intervention protocols at the point of administration.

CHAPTER 4

COMPOUND-INDUCED HOST CELL RESPONSES AND EFFECTS ON WHOLE VIRUS

SUMMARY

Background: The interaction of test agents with cells in culture is an important aspect of drug discovery because it mimics the *in vivo* scenario. In addition, it avoids the costs and ethical issues involved in working with animal models especially during the early stages when drug-like properties are still being investigated. In this study, the effect of the compounds on host cells and whole virus was evaluated by monitoring cell viability, cell proliferation, viral infectivity and immunomodulatory effects on relevant cell types.

Materials and Methods: Toxicity studies were done using spectrophotometric methods (measuring absorbance) and by flow cytometry (using the annexin V and propidium iodide kit) while proliferation studies were performed with carboxyfluorescein succinimidyl ester dye and a real time cell electronic sensing device. To determine if any of the compounds could prevent whole virus from infecting host cells, luminescence measurements of luciferase reporter gene expression (indicative of HIV *Tat*-responsive gene expression by engineered TZM-bl cells) were performed. The intracellular production of cytokines, IFN- γ and TNF- α within CD4+ and CD8+ cells, was evaluated using multi-parametric flow cytometry.

Results and Discussion: The 50% cytotoxic concentrations of most of the gold complexes were in the low micromolar range (between 1 and 20 μ M). Ten complexes had anti-proliferative effects on peripheral blood mononuclear cells (decreasing proliferation from the parent generation by >50%) with PFK7 being the most prominent followed by PFK190, PFK8 and EK207. Inhibition of viral infectivity was observed at non-toxic (cell viability was >80%) concentrations of complexes TTC24, EK207 and EK231 and cytostatic concentrations of PFK7 and PFK8 (seen by RT-CES analysis). CD4+ cell frequencies from PBMCs of twelve HIV infected donors were reduced by complexes EK207 and PFK7 ($p < 0.05$) further confirming the cytostatic abilities of these two complexes. The cytostatic ability of PFK7 was also shown to be as a result of significant ($p = 0.003$) inhibition of RNR enzyme. The production of the pro-inflammatory cytokine (TNF- α) was elevated in the same cells (CD4+) by the complementary ligand of PFK7 (PFK5) but not by complex PFK7 suggesting that complexation with gold resulted in a drug-like property. None of the complex precursors prevented infection of host cells, illustrating the importance of metal/gold complexation in these potential drugs.

Conclusion: Complexes TTC24, EK207, EK231 inhibited viral infectivity at non-toxic concentrations (but unfortunately had poor drug-like properties, chapter 3) suggesting that

structural modifications to improve drug-likeness may be required. PFK7 and PFK8 also inhibited viral infectivity but at cytostatic concentrations. Furthermore, EK207, PFK7 and PFK8 decreased PBMC proliferation while EK207 and PFK7 suppressed the frequency of CD4+ cells without altering cytokine production. Cytostasis is an anti-HIV mechanism which is also linked to decreases in CD4+ cell numbers and to inhibition of RNR. After modification to improve drug-likeness, complex EK207 and the drug-like complexes such as PFK7 and PFK8 which inhibit viral infectivity presumably as a result of cytostatic effects stand a chance of being incorporated into virostatic combinations which will offer better resistance profiles than existing drugs.

Keywords: viability, proliferation, infectivity inhibition, immunomodulation, cytostasis

4.1 INTRODUCTION

Test agents interacting in culture with cells are highly desirable in any drug discovery paradigm because they provide a means for ready, direct access and evaluation *in vitro* (Allen *et al.*, 2005). Drug-cell interactions are valuable in providing information about cytotoxicity, drug mechanism of action and allow for screening of potential therapeutic agents. With cell cultures, it is easy to manipulate the cells to mimic a disease state thereby making it possible for significant information about the effect of a test compound to be obtained (e.g. engineering cells to have surface receptors necessary for infectivity by HIV). *In vitro* analysis ensures that ethical issues related to drug testing in humans or animal models can be avoided in the initial stages of drug development research (Allen *et al.*, 2005) when safety is still a concern. The result of this is that, more safe drugs get into the more costly, late drug developmental phases (Donato *et al.*, 2008).

Two cell types were used in this study; primary cells and immortalized cell lines. Primary cells closely mimic the *in vivo* state and generate physiologically relevant data. These cells unfortunately tend to undergo senescence after a few divisions and cannot be maintained in culture indefinitely (Castilho *et al.*, 2008). Unlike the immortalised or continuous cell lines which are homogenous (Burdall *et al.*, 2003), primary cells usually contain a variety of cell types in the same mixture therefore requiring further manipulations (e.g. tagging of surface receptors with fluorescently labelled antibodies or sorting) if information on specific subsets is required. Immortalized cell lines facilitate high throughput screening since they are readily available and together with primary cells allow for extrapolation of information from *in vitro* data regarding the effect of potential drugs *in vivo*. Unfortunately, these cells could lose their genotype and/or phenotype as a result of continuous culturing (Burdall *et al.*, 2003). As such, strict culture conditions such as passage number have to be adhered to, to ensure phenotypic and genotypic stability.

The study of drug-like properties of new chemicals early in drug discovery has gained significant importance over the last decade due to the high rate of late drug failures during clinical trials (Hamid *et al.*, 2004) with toxicity and adverse effects being some of the reasons for the failures. While the *in silico* prediction models (covered in chapter 3) provides insights into potential toxicity and can significantly shorten the drug discovery time line (Lobell and Sivarajah, 2003), complementing these data with *in vitro* experimental studies is important because of the physiological relevance of the latter. Specific cell types are available for determining ADMET properties *in vitro*. Brain microvessel endothelial cells have been used in BBB penetration studies (Glynn and Yazdanian, 1998) and Caco-2 cells for cellular permeability (Egan and Lauri, 2002). Because cytotoxicity is one of the most critical and unpredictable of the drug-like properties and can be species and organ-specific (Ponsoda *et al.*, 1995), the focus here was on the toxicity component of ADMET.

In this study, both HIV uninfected and infected cells were used. When uninfected cells were used, compound cytotoxic effect could be monitored in the absence of viral cytopathic effect. When infected cells were used, it was also important to exclude toxicity by using non-toxic viral titres in addition to including viability dyes to exclude dead cells.

Various complementary assays were used in determining compound effect on cell viability. The reason for this is because of the multiple parameters that can influence cell death making the use of multiple markers to determine viability during early drug screening a necessity (Kepp *et al.*, 2011). Standard spectrophometric assays were used for determining cellular metabolism and have the advantage of being robust, inexpensive and can be easily applied in HTS (Kepp *et al.*, 2011). These included the tetrazolium dyes; 3-(4,5-dimethylthiazol-2-yl)-2,5-diphenyltetrazolium bromide (MTT) and 3-(4,5-dimethylthiazol-2-yl)-5-(3-carboxymethoxyphenyl)-2-(4-sulfophenyl)-2H-tetrazolium (MTS). These inexpensive 96 well format assays facilitated the determination of the 50% cytotoxic concentrations (CC_{50} s) of the compounds. This is because for determining CC_{50} , a wide range of concentrations (at least six or more) is required for producing a dose response curve. These assays are however susceptible to metabolic interference and can lead to false positive results (Kepp *et al.*, 2011, Boyd, 1989, Haselsberger *et al.*, 1996, Denizot and Lang 1986). For this reason, the assays were only used after thorough optimisation and only as preliminary viability screening assays. The more specific flow cytometric assay using annexin V and propidium iodide was used for validating viability dye findings. More background information on these assays will be provided in the materials and methods sections of this chapter.

Other approaches that were used to indirectly investigate viability included the use of proliferation assays such as the carboxyfluorescein succinimidyl ester dye dilution assay and impedance measurement by real time cell electronic sensing. In addition to providing information regarding the viability status of the cells, these assays also provide mechanistic information e.g. cytostasis or anti-proliferative effects of test agents. Various reports have

indicated the importance of anti-proliferative properties of test agents e.g. cytostatic anti-viral effect of HU which prevents immune activation by limiting proliferation (Lori *et al.*, 2005). For metal-based drugs, prevention of antigen presentation through stripping of peptide antigens from MHC class II molecules is one of the ways by which T cell activation is prevented (De Wall *et al.*, 2006).

Gold compounds with anti-proliferative or cytostatic effects which also inhibit viral replication have the potential of being incorporated into virostatic combinations (Lori *et al.*, 2005). This is a treatment strategy that is encouraged as a first-line combination to reduce the emergence of resistant strains and at a point when the patients are asymptomatic so as to avoid complications that could arise in advanced disease (Lori, 1999). On the other hand stimulation of lymphocyte proliferation may mean the compounds have the potential of being antigenic and may end up having adverse effects (Best and Sadler, 1996, Verwilghen *et al.*, 1992). Since in HIV infection, activation usually results in increased viral replication and progression to AIDS (Gougeon, 2005) this may mean such compounds will potentiate the chronic inflammation already present (Appay and Sauce, 2008). The side effects related to gold therapy have been linked to their ability to cause a stimulatory effect on the immune system leading to the production of pro-inflammatory cytokines (Lampa *et al.*, 2002). Such adverse effects previously seen in rheumatoid arthritis treatment are not manifested in all patients and some end up being cured by the use of gold-based drugs (Sigler *et al.*, 1974, Forrestier, 1935).

In HIV infection, there is immunodeficiency as a result of the loss of CD4+ cells, hyperactivity as a result of B cell activation as well as changes in cytokine production (Breen, 2002). Cytokine-based therapy has been reported to be an alternative approach to HAART since it allows for the manipulation of the immune system to attain beneficial results; exemplified for IL-2, which boosts CD4+ cell number (Alfano and Poli, 2001). Assessing the function of T lymphocytes (crucial immunological cells) is representative of the immune state and aids in the identification of correlates of protection and of disease (Heeney and Plotkin, 2006). The frequency of CD4+ and CD8+ cells as well as representative anti-inflammatory (IFN- γ) and pro-inflammatory (TNF- α) cytokine production levels was determined as a means of assessing the effect of the compounds on immune function and on the chronic inflammatory disease caused by HIV (Appay and Sauce, 2008). Gold compounds have been reported to have immunomodulatory effects (discussed in section 2.3.3.3). We envisaged similar properties for the compounds tested here and performed immunomodulatory assays as a means of ascertaining if the compounds could serve as immune therapies.

In the next sections, the effect of the compounds on cell viability, proliferation, viral infectivity and immunomodulation is described. For the inexpensive and HTS assays (such as viability using MTT and annexin V/PI, the proliferation assay using CFSE and in the infectivity assays), all the compounds were tested and only representatives from the various classes for

more expensive and non HTS assays (e.g. RT-CES and in the multi-parametric flow cytometry assay). The data from class representative compounds could be used to extrapolate or deduce similar responses for members of the same class especially since drug-likeness predictions suggested that there were similarities between groups (Table 3.8A, chapter 3).

4.2 MATERIALS AND METHODS

4.2.1 Cells

The primary cells, referred to as peripheral blood mononuclear cells were isolated from venous blood obtained from both HIV positive and negative donors. The cell lines PM1 (courtesy of Dr. Marvin Reitz, Lusso *et al.*, 1995) and TZM-bl (from Dr. John C. Kappes, Dr. Xiaoyun Wu and Tranzyme Inc, Takeuchi *et al.*, 2008, Wei *et al.*, 2002, Derdeyn *et al.*, 2000, Platt *et al.*, 1998) were obtained through the NIH AIDS Research and Reference Reagent Program, Division of AIDS, NIAID, NIH. The PM1 cell line obtained by transforming a neoplastic T-cell line, Hut 78 (Lusso *et al.*, 1995) to display CCR5 on its surface, is susceptible to infection by CXCR4 and CCR5 isolates and therefore ideal for expansion of progeny virus. The TZM-bl cells previously designated JC53-bl (clone 13) is a HeLa cell line engineered to stably express CD4, CXCR4 and CCR5. These cells were generated from JC.53 cells by introducing separate integrated copies of the luciferase and β -galactosidase genes under the control of the HIV-1 promoter (Platt *et al.*, 1998) and are highly sensitive to infection with diverse isolates of HIV-1.

4.2.1.1 Isolation of primary cells from whole blood

Ethics clearance for this research was obtained from both the Faculties of Natural and Agricultural Sciences and the Health Sciences Ethics Committees (University of Pretoria) with approval numbers EC080506-019 and 163/2008 respectively. Blood from HIV infected (HIV+) individuals was obtained from subjects attending routine check-up at clinics around Pretoria (South Africa) including the Kings Hope Development Foundation Clinic (Diepsloot), the Fountain of Hope Clinic (FOH, Pretoria Central) and the Steve Biko Academic Hospital's Division of Infectious Diseases. The University of Pretoria's clinic was the point at which uninfected (HIV-) blood samples were obtained from healthy volunteers. In sampling from HIV+ donors, blood was only obtained from volunteers who were not on antiretroviral therapy (ART) and generally had a CD4+ count of > 200 cells/ μ L of blood (the cut-off point used in South Africa as exclusion criteria from ART for people infected with HIV). It was important to collect blood from these treatment-naïve patients to avoid false conclusions regarding the compounds under study which might be resulting from residual effect of administered ART in the case where treatment-experienced donors were used.

Venous blood from consenting donors was collected in K₃ EDTA anti-coagulant Vacuette[®] tubes (Greiner Bio-one, Austria) and processed within 2 h. The separated plasma

portion (liquid portion containing clotting factors) was stored at -20 °C and the cell-containing fraction was diluted 1:1 with RPMI-1640 medium (Sigma Aldrich, Missouri USA) supplemented with antibiotics (10 mg/mL penicillin, 10 mg/mL streptomycin sulphate, 25 µg/mL fungizone and 1% v/v gentamycin sulphate). This was followed by standard Ficoll-Histopaque®-1077 (Sigma Aldrich, Missouri USA) density centrifugation. Briefly, two parts of the diluted blood was gently overlaid on one part of ficoll (Sigma Aldrich, Missouri USA) followed by 30 min of centrifugation (1610xg, 25 °c). The buffy coat (middle layer) containing the PBMCs was washed (866xg, 10 min, 25 °c) with incomplete medium (RPMI containing antibiotics only) to remove platelets and further treated with 5 mL of ammonium-chloride-potassium or ACK (150 mM NH₄Cl, 10 mM KHCO₃, 0.1 mM EDTA, pH 7.2) to disrupt and lyse any residual red blood cells. Following another wash step with incomplete RPMI-1640 medium (258xg, 10 min), the PBMCs were resuspended in complete RPMI-1640 medium which in addition to antibiotics, also contained 10% (v/v) heat-inactivated (56 °C, 30 min) fetal calf serum. A hemocytometer count was performed using trypan blue to determine the viability and concentration of the cells. A cell viability of > 90% was considered appropriate and the cells were resuspended at a suitable concentration as needed for the particular bioassay. Phytohemagglutinin-protein (PHA-P) also known as lectin from *Phaseolus vulgaris* was used as a stimulant for enhancing *in vitro* proliferation of primary cells while phorbol myristate acetate (PMA) and ionomycin (ION) were used for enhancing cytokine production (both stimulants were obtained from Sigma Aldrich, Missouri, USA). The cells were used to determine compound effect in one or more of the following assays: viability determination, proliferation or immune effects studies.

4.2.1.2 Culturing of continuous cell lines

Two types of continuous cell lines were used; the PM1 and the TZM-bl cell line. The PM1 suspension cell line were cultured in complete RPM1-1640 medium and subcultured at a concentration of approximately 5x10⁴ cells/mL every two days. The TZM-bl cells on the other hand are adherent cells and were subcultured in T-75 tissue culture flasks (Nunc™, Roskilde, Denmark) with approximately 10⁶ cells in 15 mL of complete Dulbecco's Modified Eagle Medium (DMEM) with L-glutamine, sodium pyruvate, glucose and pyridoxine (Gibco BRL Life Technologies, Grand Island, USA) containing antibiotics (10 mg/mL penicillin G, 10 mg/mL streptomycin sulphate, 25 µg/mL fungizone and 1%-v/v gentamycin sulphate) and 10% (v/v) heat inactivated FCS. The cells were sub-cultured every two or three days when confluency (surface area of the culture flask occupied by cells) was about 90%. Generally, a concentration of 1x10⁵ cells/mL was prepared for both the PM1 and the TZM-bl cells for experimental purposes unless stated otherwise.

4.2.2 Compound Preparation

Compounds were stored desiccated at -20 °C until needed for experiments. Sufficient quantities were dissolved in DMSO (Highveld Biologicals, Sandringham, South Africa) to a concentration of 20 mg/mL and stored as single use aliquots of 5 or 10 µL at -20 °C and used within a week. For bioassays, each of this was made up to 1 mg/mL with either phosphate buffered saline (PBS, pH 7.4) solution or growth medium (complete RPMI-1640 or DMEM) as required. The compounds were further diluted to experimental concentrations (0.02 - 200 µM) ensuring that the final DMSO concentration was ≤0.5% (v/v). This concentration of DMSO had no discernible effect on cell viability compared to controls.

4.2.3 Cell Viability Assays

Many *in vitro* cytotoxicity assays are available for determining cell viability. Some like the MTT and MTS assays, have the advantage of being adaptable to large scale screening relevant for most cells while others e.g. flow cytometry using annexin and propidium iodide (PI) provide additional information such as the mechanism of cell death. MTT (developed by Mosmann in 1983) is widely used for the quantitative assessment of cellular viability and proliferation but has shortcomings. Some of the draw backs are poor linearity with changing cell number, sensitivity to environmental conditions and the fact that it depend on the cells' metabolism of formazan (Boyd, 1989, Haselsberger *et al.*, 1996, Denizot and Lang 1986). In addition, some human cell lines metabolize these dyes very inefficiently, and in some cases such dyes are cytotoxic (Hertel *et al.*, 1996). Although MTT and MTS (Buttke *et al.*, 1993) are widely used, reported conditions and parameters of the assays vary widely and depend largely on cell type (Soman *et al.*, 2009, Young *et al.*, 2005). These limitations necessitated the inclusion of optimisation steps in the HTS assays (details for these are provided in the appendix in section 8.3) followed by the use of more specific confirmatory assays. Flow cytometry (using annexinV/PI and CFSE) as well as RT-CES analysis were used to corroborate MTT data. Although the flow cytometric method is more specific than the MTT viability dye, important criteria such as gating on the right population (inclusion of cell surface markers) and having the right forward scatter (FSC, which is related to size) and side scatter (SSC, related to granularity) scaling has to be adhered to. In the following subsections, HTS viability dye assays as well as flow cytometry methodologies are provided. An incubation time of 72 h was used because it is sufficient for monitoring early drug toxicity (Sussman *et al.*, 2002) but in the real time studies, proliferation (viability) was monitored for up to 7 days. Background information on all assays precedes protocols, all of which are followed by results and discussion.

4.2.3.1 HTS dye assays for determining cell viability

Several viability dyes (MTT, MTS and annexinV/PI) and a cytotoxicity kit for measuring lactate dehydrogenase release (details in the appendix, section 8.3.1), were compared during optimisation assays and a decision was made to use MTT and MTS for viability assessment. Both MTT (Sigma Aldrich, Missouri, USA) and MTS (Promega Corporation, WI, USA) are tetrazolium salts which function on the same principle. Dehydrogenase enzymes present in the mitochondria of viable cells convert these salts to a quantitative colorimetric formazan product that can be measured spectrophotometrically. In the case of MTT, the product is insoluble and requires a solubilisation step while for MTS, an additional coupling reagent (phenazine methosulfate-PMS), confers enhanced chemical stability leading to the formation of a stable solution. MTS was found to be easily metabolised by PBMCs probably because it is a more stable dye which could withstand the heterogeneity of PBMCs while either of the two dyes were easily metabolisable by the more homogenous cells lines (PM1 and TZM-bl). The MTT assay was done according to the protocol by Mueller *et al.*, (2004) with minor modifications including the removal of spent medium to exclude compound effect before dye addition. The same conditions were employed for the MTS assay.

Procedure: PBMCs (1×10^6 cells/mL) and PM1 cells (1×10^5 cells/mL) in complete RPMI-1640 medium were treated with various concentrations of the compounds (0.4-200 μ M) in cell culture grade 96 well plates (NuncTM, Roskilde, Denmark) and incubated (37 °C, 95% humidity, 5% CO₂) for 72 h. At the end of the incubation, the plates were centrifuged (258 x *g*, 10 min) and 150 μ L spent medium discarded and replaced with 50 μ L freshly prepared complete medium. Ten microlitres of MTS was added to the resuspended cells and reduction of the MTS tetrazolium compound to formazan was detected after colour development using a Multiskan Ascent[®] spectrophotometer (Labsystems, Helsinki, Finland) at 492 nm and 690 nm as reference wavelength. Readings were taken after 2 h of incubating with MTS in the case of the cell lines and 24 h later in the case of PBMCs. Viability percentages were determined relative to an untreated control of cells only.

When MTT was used, a similar protocol was implemented but with the inclusion of a solubilisation step. After incubating the cells with the compounds, 150 μ L of spent medium was discarded and replaced with an equivalent amount of freshly prepared complete medium. Then 20 μ L (5 mg/mL) of MTT was added to the cells and colour development analysed after 2 h (cell lines) or 24 h (PBMCs). This was followed by solubilisation of the formazan product using acidified isopropanol in a 1:9 ratio (1 part of 1 M HCl and 9 parts of isopropanol). Absorbance was measured at 550 nm and a reference wavelength of 690 nm on a Multiskan Ascent[®] spectrophotometer (Labsystems, Helsinki, Finland). In both cases (MTS or MTT), percentage viability was calculated using the formula:

$$\text{Viability (\%)} = \frac{\text{Absorbance of Sample} - \text{Absorbance of medium}}{\text{Absorbance of control} - \text{Absorbance of medium}} \times 100$$

CC₅₀ values were then graphically obtained after generating a dose response curve using Graphpad Prism® software (California, USA). Non-toxic concentrations (>50% viability) of the compounds obtained from viability assays were subsequently used in other cell-based assays and in the direct enzyme assays.

4.2.3.2 Effect of the compounds on cell viability by flow cytometry

Flow cytometry is a technology that simultaneously measures and then analyzes multiple physical characteristics of single particles, usually cells, as they flow in a fluid stream through a beam of light from a laser source. The properties measured include a particle's relative size (FSC), relative granularity or internal complexity (SSC), and relative fluorescence intensity). A schematic representation of the components of a typical flow cytometer is shown in Figure 4.1.

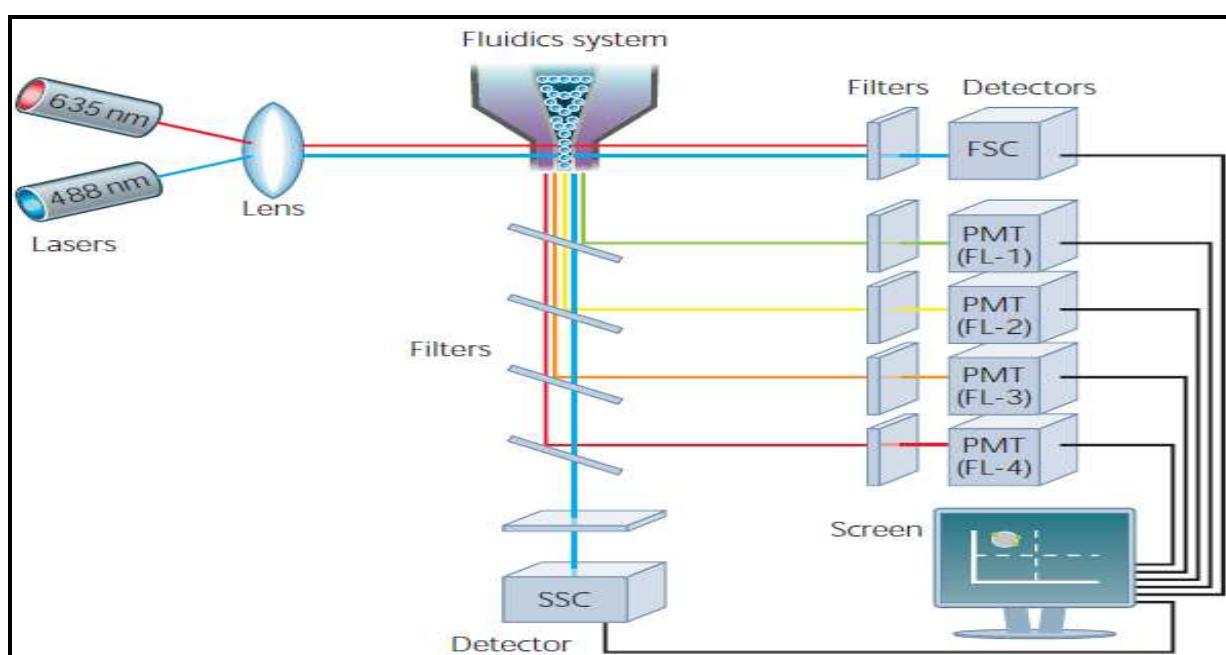


Figure 4.1: A schematic representation of the setup of a flow cytometer. Main components are lasers which generate light source, lenses which focus light onto sample, detectors for determining emitted light at specific wavelengths and this information is conveyed onto an output device represented by the screen. This figure was taken from www.ab-direct.com, accessed on the 25/04/2011

Unlike spectrophotometry (employed for the MTT and MTS assays), which measures absorption in a bulk volume, flow cytometry analyses single cells, making it more specific for determining cell viability and other cellular parameters. The major advantage of the dye assays is HTS but because of associated limitations, laborious and time consuming optimisation steps are usually required. Although the dye assays could have completely been left out, the fact that different parameters can influence cell death necessitated the use of multiple markers (Kepp *et al.*, 2011) and complementary assays to determine viability. While flow cytometry is more specific, care has to be taken to ensure that the right population (especially in a situation where different cell types are involved e.g. PBMCs) is identified and gated for analysis and that the FSC (particle's relative size) and SSC (relative granularity or

internal complexity) scales are accurate. Failure to follow these requirements could result in the analysis of a completely different population than that which is desired.

In this study, the cells of interest were the lymphocytes consisting predominantly of CD4⁺ and CD8⁺ subsets of CD3⁺ cells. To identify these cells from PBMCs, a CD45⁺ marker common on lymphocytes (Stelzer *et al.*, 1993) was used to determine their position on a FSC/SSC dot plot ensuring the exclusion of monocytes and neutrophils. In the viability and proliferation studies with annexin V/PI and CFSE respectively, no further immunophenotyping of surface molecules was necessary but for the immunomodulatory assay, a CD3⁺ marker for T cells was used followed by CD4⁺ and CD8⁺ to differentiate T cell subsets.

The annexin-V-fluorescein isothiocyanate (FITC) apoptosis detection kit (Becton Dickinson or BD BioSciences, California, USA) was used in determining the viability of the PBMCs using flow cytometry. The kit contains annexin V which stains cell surface phosphatidylserine indicating apoptotic cells and propidium iodide which stains the DNA of damaged cells indicating the presence of necrotic cells. Cells negative for both annexin V and PI were considered viable. In addition to being a complementary assay for the HTS viability assays, this assay provided information on the mode of cell death (necrosis or apoptosis) caused by the compounds.

Procedure: One millilitre of PBMCs (1×10^6 cells/mL) in complete RPMI medium was added to 1 mL of compound solutions in cell culture grade 24 well plates (NuncTM, Roskilde, Denmark). Since the CC₅₀ values obtained in the HTS assays only served as indicators of non-toxic concentrations, in this study, a decision was made to use compound concentrations that resulted in >60% viability (from MTT and MTS studies) for the flow cytometric analysis and other cell-based assays. This cut-off was considered sufficient in keeping toxicity to a minimum. After 72 h of incubating the PBMCs with various concentrations of the compounds, staining of the cells was performed using the annexin V/PI detection kit according to instructions by the manufacturer (BD Biosciences, California, USA). The cells were harvested by washing (500 x g, 5 min) twice with ice cold PBS (pH 7.4) and transferred to plastic flow tubes (BD Biosciences, California, USA). The cell pellet was resuspended in 100 µL of binding buffer followed by the addition of a pre-titrated amount or separation titre (minimum amount of dye to achieve good separation between positive and negative cell populations, which was 2 µL each in this case) of annexin V-FITC and PI solution. After gentle mixing, the tubes were kept on ice in the dark for 15 min followed by the addition of 400 µL of ice cold binding buffer. Controls used included untreated cells, an annexin positive and a PI positive control. The annexin positive control was obtained by treating cells with 10 µM of auranofin (an anti-arthritic gold(I) compound known to have anti-tumour activity) while PI positive cells were obtained by fixing cells in ice cold methanol for 5 min. An unstained control, the annexin as well as the PI positive controls were used for setting compensation (correcting for spectral emission overlap between different dyes to eliminate false positive or negative outcomes) and quadrant

specification. The samples suspended in 500 μL of binding buffer were subjected to flow cytometric analysis with 10,000 events collected per sample within 30 min of treatment. Ten thousand events were considered sufficient for discriminating apoptosis, necrosis and viability between treatments and controls for this assay (general criterion for determining the number of events that are enough for a flow cytometry assay, Roederer, 2008). Flow cytometric profiles were determined using a FACSAria (BD Biosciences, California, USA) with the FITC and peridinin chlorophyll protein-cyanin 5.5 (PerCp.Cy5.5) detectors used for the identification of apoptotic and necrotic cells respectively. The data was analysed using the FACSDiva software (BD Biosciences, California, USA) and FlowJo version 7.6.1 (TreeStar Inc., Oregon, USA).

4.2.4 Effect of the Compounds on Cell Proliferation

The proliferation of PBMCs and TZM-bl cells was monitored by flow cytometry using the CellTrace[™] CFSE kit (Molecular Probes, Oregon, USA) and by the use of a RT-CES analyser respectively. In addition to providing mechanistic information, proliferation assays also serve to confirm cell viability and can provide information on potential antigenicity of the compounds (i.e. if the compounds can cause lymphocyte proliferation, Lampa *et al.*, 2002, Verwilghen *et al.*, 1992).

4.2.4.1 Compound effects on the proliferation of PBMCs by use of CFSE

In its cell-free state, CFSE is non-fluorescent because of the presence of two acetate groups. This non-fluorescent form is designated CFDA-SE (carboxyfluorescein diacetate succinimidyl ester). The acetate groups however result in the compound being highly membrane permeable and allow the dye to rapidly shuttle across the plasma membrane of cells (the mechanism is shown in Figure 4.2). Once inside the cells, these groups are rapidly removed by intracellular esterases to yield highly fluorescent CFSE which binds covalently with proteins and is well retained within the cells (Graziano *et al.*, 1998). A fraction of the fluorescent conjugates are not stable and exit through the cell membrane while a highly stable proportion remains within the cells and is halved between daughter cells as they divide, allowing for proliferation monitoring by flow cytometry (Quah *et al.*, 2007, Lyons and Parish, 1994).

Procedure: Cell proliferation was monitored using the CellTrace[™] CFSE cell proliferation kit (Molecular Probes, Oregon, USA) from a “live gate” by simultaneous monitoring of viability using PI (BD BioSciences, California, USA). PI incorporation helps in the tagging and exclusion of dead cells which could potentially compromise proliferation data analysis. One microlitre of a 5 mM stock of CFSE was used in staining 1×10^7 cells/mL of PBMCs such that the final concentration of CFSE was 5 μM . Staining was done in PBS containing 5% (v/v) FCS as staining buffer for 15 min at 37 °C with gentle agitation every 5 min. The reaction was

quenched with 5 volumes of ice-cold complete RPMI-1640 medium with gentle mixing conditions for 5 min on ice. Unincorporated CFSE was removed by washing three times with ice cold complete RPMI-1640 medium and the stained cells were resuspended in the warm complete RPMI-1640 medium at 1×10^6 cells/mL.

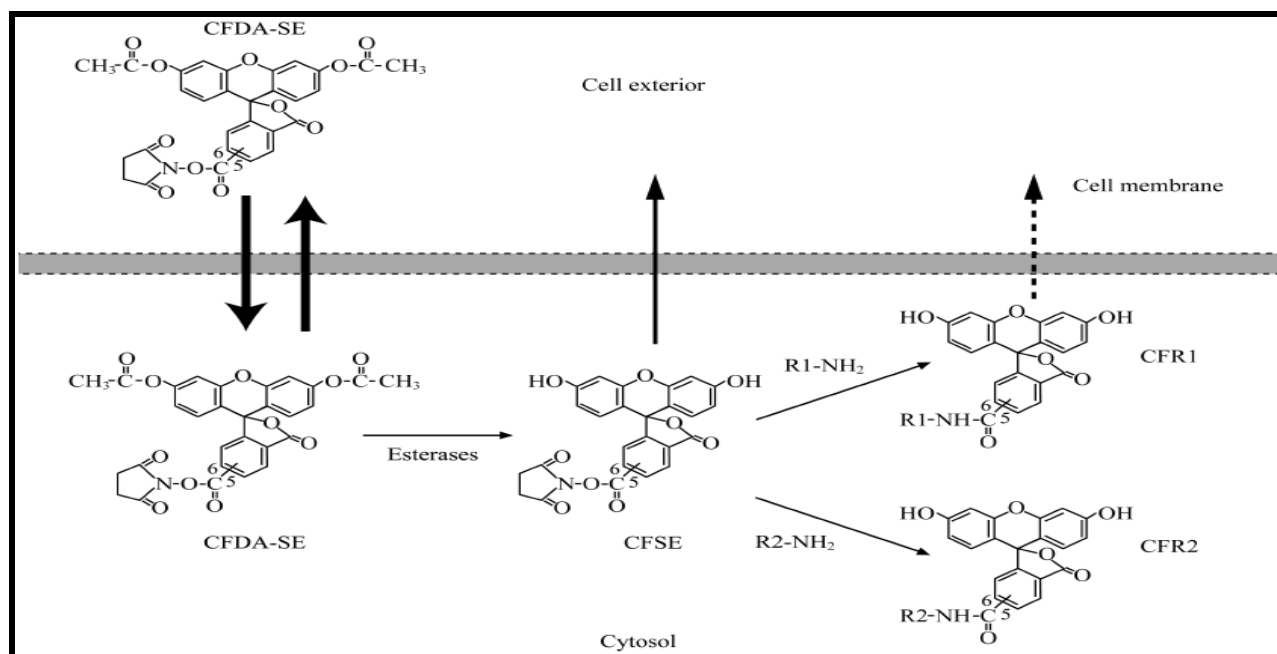


Figure 4.2: Schematic representation of the mechanism involved in fluorescent labelling of cells with CFDA-SE. The CFDA-SE readily taken up by the cell is converted to CFSE by intracellular esterases. The CFSE covalently binds to proteins (R1-NH₂ or R2-NH₂) and some exits the cell as CFR1 while some of it is retained as CFR2. (Figure was taken from Wang *et al.*, 2005).

To optimise the assay, various strategies were used. It was important to determine when incubations could be stopped and if compounds alone could affect cell proliferation or if stimulants were required for monitoring the effects of the compounds on cell proliferation. Details on these optimisations are provided in the appendix (section 8.3.2). Three days of incubating the compounds with cells stimulated with PHA-P (2 µg/mL) was considered optimal for subsequent tests. Three days (72 h) was used for this assay because by the 5th/6th/7th day, most of the cells had lost their fluorescence through proliferation (especially for treatments where anti-proliferative effects were absent). In addition to the fact that the data could be correlated with the annexin V/PI and the MTS viability data (which also involved 72 h incubations), adequate determination of dividing cells using CFSE can only be monitored after > 48 h in culture (Quah *et al.*, 2007) making 3 days ideal.

PHA-P (2 µg/mL) stimulated CFSE stained cells at a final concentration of 1×10^6 cells/mL were treated with different compound concentrations (those that had resulted in >60% viability in the MTS assay) for 72 h in 24 well plates. At the end of the incubation period, samples were harvested and washed twice with ice cold PBS. The samples were resuspended in 100 µL of PBS and a pre-titrated amount (2 µL) of PI was added to the cell suspension. This was incubated for 15 min on ice in the dark followed by the addition of 400 µL of ice cold PBS. Instrument controls for compensation setting included an unstained

control, CFSE stained cells (detected on the FITC detector) and dead cells stained with PI (detected on the PerCp-Cy5.5 detector). The samples were placed on ice and analysed within 1 h by the acquisition of 10,000 events on a FACS Aria (BD, California, USA) after compensation or exclusion of fluorescence spillover. Data analysis was done using the proliferation tool in FlowJo Version 7.6.1 (TreeStar Inc., Oregon, USA).

4.2.4.2 Compound effects on the proliferation profile of TZM-bl cells by RT-CES assessment

The xCelligence system (Roche Diagnostics, Mannheim, Germany) also referred to as a real time cell electronic sensing analyser, is a microelectronic biosensor system for monitoring cells. The system provides dynamic, real time, label-free cellular analysis for a variety of research applications in drug development, toxicology, cancer, medical microbiology and virology. Unlike standard end point assays such as MTT and flow cytometry, RT-CES allows for the capturing of more physiologically relevant data and complements these other techniques by providing additional information such as cytotoxicity start time (which will be difficult to identify in end point assays). The system uses plates known as E-plates which contain integral sensor electrode arrays that allow adherent cells (only) within each well to be monitored. The presence of cells in the wells of the E-plate affects the local environment leading to an increase in electronic impedance (resistance). The more the cells attach to the electrodes, the higher the electronic impedance which is measured as cell index (CI). Compound treated cells exhibited varying response patterns represented by CI changes which represent proliferating (increasing CI), cytotoxic (decreasing CI) or cytostatic (stable CI) behaviour of the cells when compared to untreated samples.

This assay has been described for the measurement of cytotoxicity (Boyd *et al.*, 2008, Xing *et al.*, 2006, Xing *et al.*, 2005) and can be used to determine other cellular parameters such as cell proliferation, cytotoxicity start time, cell recovery, and cell response patterns (Xing *et al.*, 2005) in real time. Figure 4.3 is a representative diagram showing the stages involved in the functioning of a RT-CES analyser. At point A where no cells are present (Figure 4.3), the CI is zero, but when cells are loaded into the well (1), the CI begins to increase gradually as the cells attach and divide (B). When a toxin or test agent is added (2), the cells can either carry on proliferating resulting in increasing CI (C) or could start dying resulting in decreasing CI (D). The effect of the test agent (stimulatory, cytostatic or toxic) could then be deduced based on the cell proliferation pattern relative to an untreated control.

Procedure: Before experiments were initiated, a cell titration experiment for the TZM-bl adherent cell line was performed in E-plates to establish ideal seeding concentrations. Based on the titration, a concentration of 10,000 cells/well was chosen for subsequent assays because it resulted in about 80% confluency after approximately 24 h (cell index was ~ 1.5) which was ideal for monitoring treatment effects. Proliferation profiles of these cells were established in the presence of selected compounds (TTL3, TTC3, EK207, MCZS2, KFK154B,

PFK5, PFK7 and PFK189) from each class and the assay was performed at least three times for each compound. Two hundred microlitres of 1×10^5 cells/mL was seeded into the microelectronic plates and allowed to adhere for 24 h. The cells were treated with three different concentrations of the compounds and proliferation or adhesion was automatically monitored every minute (short term) for 1 h and then every 30 min (long term) for 3 to 7 days. Short term monitoring allows for the identification of immediate and transient compound effects while long term monitoring allows sufficient time for the compounds to interact with the cells and modulate their targets and also allows for distinguishing cell response patterns (Abassi *et al.*, 2009).

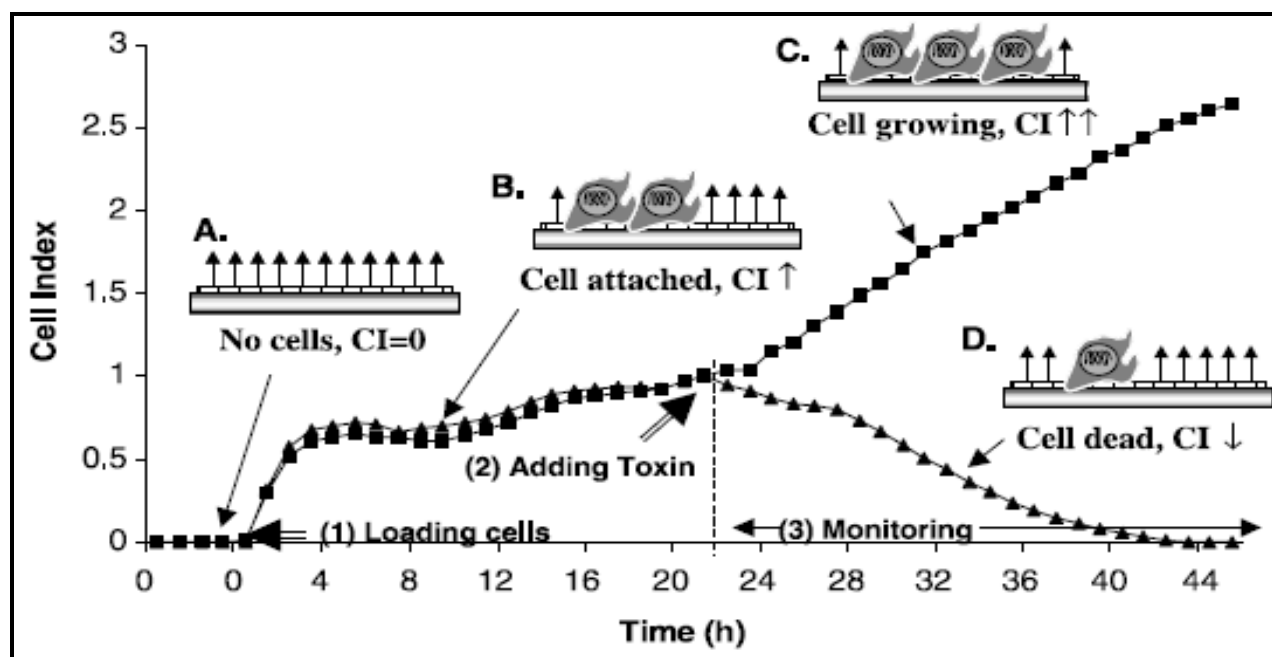


Figure 4.3: The principle of cell proliferation monitoring using the RT-CES analyser. A represents a point where no cell are present with a CI of 0, in B, cells had been added to the well and were beginning to attach and divide (the CI is steadily increasing). When a toxin is added, cells either die (D) or continue proliferating (C). This figure was taken from Xing *et al.*, (2006).

4.2.5 Virus Infectivity Inhibition Ability of Compounds by Luciferase Gene Expression Assay

The previous viability and cell proliferation assays were done using uninfected cells. Here and in the next section, the effect of the compounds on cells in the presence of virus is described. Infectivity assays measure the concentration of infective virus in a sample and in this case luciferase reporter gene expression was assessed. This assay was performed at the HIV Research Laboratory of the National Institute of Communicable Diseases (NICD, South Africa) according to the protocol described by David Montefiori (2004). The assay uses molecularly cloned pseudoviruses designed to undergo a single round of infection readily detectable in genetically engineered cell lines that contain a *lat*-responsive reporter gene such as luciferase and for this, the TZM-bl cell line was used. This reporter gene permits sensitive and accurate measurements of infection and the data obtained could be used to infer whether

the compounds could be viral entry inhibitors or if other pathways of the life cycle e.g. post entry steps were inhibited.

Procedure: Du151, an isolate of two phylogenetically distinct subtype C viral strains (Coetzer *et al.*, 2007), at a dilution that gave $50,000 \pm 15000$ relative light units (non-toxic tissue culture infectious dose - TCID) was pre-incubated with the compounds for 1 h. Following this incubation, 100 μ L of TZM-bl cells at a concentration of 1×10^5 cells/mL was added to the virus/compound mixture (final volume of 250 μ L) and further incubated for 48 h. At least six concentrations of the compounds were tested in 2 fold serial dilutions with the highest final concentration being 25 μ M. Controls included in the assay were a cell control (uninfected cells and growth medium), virus control (virus, growth medium and cells) and a positive inhibitor for infectivity known as BB pool (plasma with known virus neutralizing antibodies). At the end of the 48 hour incubation, 150 μ L of supernatant was removed from each well and discarded. Bright Glo substrate solution (100 μ L, Promega, Wisconsin, USA) was added to the wells followed by 2 min of incubation at room temperature. From each well, 150 μ L of the cell lysate was transferred to equivalent wells of a 96-well flat-bottomed black plate (NuncTM, Roskilde, Denmark) and luminescence was immediately obtained on a luminometer (PerkinElmer 1420 Multilabel Counter, Victor^{3TM}, Connecticut, USA) with the luciferase activity measured in relative light units. Infectivity inhibition was determined as a percentage using the formula = $100 - [(test\ wells - CC) / (VC - CC) \times 100]$, where CC represents cell control and VC represents virus control. The 50% inhibitory concentrations (IC₅₀) were graphically obtained after generating dose response curves (using Graphpad Prism® software, California, USA) representing percentage control inhibition values.

In addition to pre-incubating the virus and the compounds prior to the addition of cells, an alternative incubation strategy was performed which involved pre-incubating the cells with the compounds before adding virus. By using the virus/compound pre-incubation strategy above, it was tempting to conclude that compounds that inhibited viral infectivity did so by interacting with viral surface components. Pre-incubating cells with compounds prior to the addition of virus on the other hand helps in confirming or disproving this and allows for speculation on whether the compounds might have multiple modes of inhibiting infection of the cells. In the situation where both strategies result in similar levels of inhibition, one could conclude that inhibition was at multiple targets. However, if findings lead to different levels of inhibition, then it could be speculated that the compounds affected infectivity at the level of the virus or the cells. In general, such “time of addition studies” allows for commentary on whether a viral or cellular pathway was inhibited with the important variable being the exposure time.

Concurrent cell viability studies were also performed using MTT and the same experimental procedures (incubation time, final compound concentration and cell number) to determine the viability of the TZM-bl cells. This was important so as to eliminate compound toxicity in the infectivity studies since toxicity could be misinterpreted as infectivity inhibition.

4.2.6 Effects of Compounds on Immune System Cells Using Multi-parametric Flow Cytometry

Flow cytometry is the defining tool for immune system cell studies and is currently the only technology that can analyse complex components of the immune system for clinical significance (Mahnke and Roederer, 2007, Pala *et al.*, 2000). Because of the complexity of the T cell compartment, both phenotypically and functionally (Mahnke and Roederer, 2007), the frequency of immunological markers on cell surface alone are not reliable determinants of the immune state or the chronic inflammatory disease caused by HIV (Appay and Sauce, 2008). Monitoring the intracellular production of cytokines along with the phenotypic identity of a cell gives better insight about disease associations because the survival, growth, differentiation and effector function of cells and tissues are controlled by cytokines (Maino and Picker, 1998). The development of flow cytometers capable of measuring up to 20 parameters has widened the possibilities in this field (Mahnke and Roederer, 2007). Enzyme linked immunosorbent assays (ELISAs) can also be used for monitoring cytokines in culture supernatant but the method is impractical when large numbers of heterogeneous cells obtained *ex vivo* need to be analysed (Pala *et al.*, 2000). Because intracellular cytokine staining (ICCS) is an end point experiment, there was the concern that the cytokines being targeted might have been secreted before incubations were stopped. As a precautionary measure, culture supernatant from cells used for ICCS was collected and used to concurrently measure secreted cytokines using ELISAs with the hope of correlating the data with the ICCS data.

A multi-parametric ICCS flow cytometric analysis was performed to determine the effect of the compounds on the production of a representative pro-inflammatory cytokine, TNF- α (increases result in disease progression in HIV, Caso *et al.*, 2001) and an anti-inflammatory cytokine, IFN- γ (which has anti-viral effect, Dinarello, 2000). Simultaneous analysis of T-lymphocyte (CD3+, CD4+ and CD8+) subsets to determine cytokine levels with respect to T cell frequencies was also performed. A viability marker was included to aid in excluding dead cells. This is because false positive events resulting from antibody conjugates could bind non-specifically to dead cells resulting in misleading results (Mahnke and Roederer, 2007). Assays were performed for both HIV+ and HIV- donors so as to determine if the effects of the compounds (and therefore usefulness) on immune state was dependent or independent of infection status.

ICCS antibodies: The following monoclonal antibodies (Mabs) directed against T cell surface markers were used: CD3-pacific blue (detected on the 4',6'-diamidino-2-phenylindole or DAPI detector), CD4-phycoerythrin (PE), CD8-PerCP-Cy 5.5 as well as anti-human cytokine Mabs: anti-TNF- α -allophycocyanin (APC) and IFN- γ -FITC, all purchased from Pharmingen (BD BioScience, California, USA). The sixth fluorochrome conjugated antibody was an aqua fluorescent fixable amine reactive dye (Molecular Probes, Oregon, USA) for "live gating" to eliminate dead cells. This dye can permeate compromised membranes of necrotic cells and

react with free amines both in the interior and on the cell surface resulting in intense fluorescent staining. In contrast, only the cell surface amines of viable cells are available to react with the dye resulting in relatively dim staining. These fixable dyes help in preserving the live/dead discrimination in subsequent fixation steps in ICCS procedures during which pathogens are inactivated unlike PI which is not fixable.

ICCS Reagents: ION, PMA and PHA-P were obtained from Sigma Aldrich (Missouri, USA). Golgi stop reagent (containing monensin) as protein transport inhibitor and reagents for cell fixation and permeabilisation (Cytofix/Cytoperm and Perm/Wash, respectively) were purchased from Pharmingen/BD (California, USA).

Prior optimisation assays: Serious sensitivity issues limit the advantages of multi-parametric flow cytometry. These include cell autofluorescence in a specific region of the spectrum, the specificity or selectivity of the antibody conjugates and the presence of other antibody conjugates attached to the same cell that could result in spillover fluorescence into the same detector (Mahnke and Roederer, 2007). In order to curb these shortcomings, optimisation assays, which included Mabs titrations to determine optimal antibody concentrations were performed prior to actual experiments. Additionally, controls such as fluorescence minus one (FMO, to aid with proper gating) and compensation controls were included during data acquisition. Additional optimisation experiments were done for various conditions including the use of different stimulants (PHA-P or PMA/ION), different incubation times (6, 24, 48 and 72 h), and treatments (compounds only or compounds with stimulants). The optimisation data is shown in Figure A4.8. After the optimisations, PMA/ION stimulation in the last 6 of a 24 h treatment with the compounds was found ideal for monitoring ICC production. Stimulants were required to induce *in vitro* cytokine gene expression because unstimulated PBMCs spontaneously produce little or no cytokines (Baran *et al.*, 2001) making quantification difficult. The following detailed experimental conditions were used after the optimizations.

Procedure: PBMCs isolated from both HIV+ (12) and HIV- donors (13) were prepared at a concentration of 1×10^7 cells/mL in complete RPMI-1640 medium. The cells were incubated without or with the compounds (with at least one representative compound from each class) at concentrations ranging from 0.04 to 5 μ M for 24 h in V shaped 96 well plates (Nunc™, Roskilde, Denmark) with a final volume of 200 μ L and cell number of 1×10^6 cells/well. In the last 6 h of the incubation, activators of cytokine production, PMA (10 ng/mL) and ION (1 μ M) were added to the cells in the presence of 1 μ L of BD GolgiStop™ (containing monensin) for preventing cytokine secretion. At the end of the 24 h incubation, the plate was centrifuged and 150 μ L of culture supernatant from each well collected and stored at -20 °C for subsequent evaluation of secreted cytokines using ELISAs. The cells were blocked with 10% (v/v) FCS in PBS for 20 min at 4 °C to prevent nonspecific binding. Following two washes with staining buffer (PBS), the cells were stained with pre-titrated optimal concentrations of surface Mabs CD3-Pac blue (0.625 μ L), CD4-PE (2.5 μ L), CD8-PerCp-Cy5.5 (2.5 μ L) and the aqua

fluorescent fixable amine reactive dye (0.02 μ L) in 100 μ L reaction volumes for 20 min. The cells were washed twice with staining buffer and then fixed and permeabilised with Cytofix/Cytoperm solution for 20 min at 4 °C. Two more wash steps with Perm/Wash solution were performed and the pelleted cells were stained (30 min at 4 °C) for intracellular cytokines using pre-titrated FITC and APC conjugated Mabs against IFN- γ (0.05 μ L) and TNF- α (0.3 μ L) respectively. After two final wash steps with Perm/Wash, the cell pellet was resuspended in 150 μ L of PBS and transferred to flow tubes (BD BioSciences, California, USA). An equal amount of 6% (v/v) formaldehyde (Sigma Aldrich, Missouri USA) was added to the cells to maintain them in a fixed state. In addition to the FMOs and compensation (instrument) controls which were used for quadrant specification and for the exclusion of fluorescent spillovers, compulsory biological controls consisting of an unstained sample and a stained untreated control were included.

Flow cytometry acquisition and analysis: A six colour (multi-parametric) flow cytometry analysis was performed on a FACSAria (BD, California, USA) using FACSDiva software with a total of 30,000 events (3 times more than for the viability and proliferation assays since intracellular or rare events were being probed) collected per sample. Single cell cytokine production was evaluated after FSC and SSC gating of lymphocytes from the PBMCs population. The intracellular cytokines were determined from the CD4+ and CD8+ subpopulations of T cells (CD3+). FlowJo version 7.6.1 (TreeStar Inc., Oregon, USA) was used for data analysis and statistical evaluation was done using the stained untreated control sample as a reference for each treatment.

Statistical analysis: The frequency of CD4+, CD8+ and cytokine producing cells from untreated controls and those treated with the various compounds were expressed as a percentage. Statistical analysis was done using Graphpad Prism[®] (San Diego, California, USA). The Wilcoxon matched-pairs signed rank test was used in determining statistical significance between medians with a one way non-parametric statistical test used since the data did not meet normal distribution. Correlations were tested using the non-parametric Spearman correlation test. A p value of <0.05 was considered significant.

ELISA: The method and results for the ELISA performed for only 6 of the 12 HIV+ donors and 2 of the 13 HIV- donors is provided in the appendix (subsection 8.3.6.2).

4.2.7 Experimental Summary

Table 4.1 is a summary of the cell types (plus HIV status), incubation times and the concentration of compounds that were used for the various cell-based assays that have been described here. The viability of PBMCs and the PM1 cell line was monitored using MTS and the CC₅₀s of the compounds was determined from this assay. The TZM-bl adherent cell line was used for monitoring infectivity and concurrent viability using MTT (48 h) and for the RT-

CES analysis. The CC_{50} s data was subsequently used as a guide for determining non-toxic concentrations of the compounds needed in other assays.

Table 4.1: Cell-based assay summary. Cell types, cell HIV status and the various concentrations and incubations times used for the cell-based assays are shown. The asterisk (*) represents an adherent cell line unlike PM1 and PBMCs which are suspension cells. #. These were concentrations with >60% viability in MTS assay. HIV- cells were used for viability assays where only compound effect was determined. HIV+ cells were used for assays in which viral infectivity information was required and for determining compound effect on the inflammation caused by HIV.

Cell type	Assay type	HIV status	Time	[Compound] in μ M
PM1	MTS	HIV-	72 h	0.2 - 200
PBMCs	MTS	HIV-	72 h	0.2 – 200
	Annexin-V/PI	HIV-	72 h	0.04, 0.2, 2.5 or 5 [#]
	CFSE	HIV-	72 h	0.04, 0.2, 2.5 or 5 [#]
	Immune cell effect	HIV- & HIV+	24 h	0.04, 0.2, 2.5 or 5 [#]
TZM-bl*	RT-CES	HIV-	3-7 days	0.1, 5 and 10 μ M
	MTT	HIV-	48 h	0.8 - 25
	Infectivity	HIV+	48 h	0.8 – 25

4.3 RESULTS AND DISCUSSION

For ease of reference, data presentation always appears in the order of control samples (where applicable), followed by the gold(I) phosphine chloride complexes and corresponding ligands (class I), then the BPH gold(I) chloride complexes of class II, the phosphine gold(I) thiolate complexes of class III, the Tscs-based complexes and corresponding ligands of class IV and finally the pyrazolyl gold(III) complex of class V. Where only representative compounds were tested, the order of result presentation will still be maintained in terms of classes.

4.3.1 Cell Viability Determination

A crucial step in drug discovery is screening for non-toxic and hopefully efficacious concentrations at an early stage. The effect of the compounds on the viability of relevant cells types was monitored using the MTS dye as well as the annexin V FITC apoptosis kit (BD, California, USA). The concentration of compounds which caused 50% cytotoxicity of the PBMCs and the PM1 cell line was generally in the low micromolar range (between 1 and 20 μ M, Table 4.2). These are concentrations which are physiologically relevant for gold compounds (i.e. found in the serum or synovium of people on chrysotherapy, Stern *et al.*, 2005, Okada *et al.*, 1999, Yoshida *et al.*, 1999, Mascarenhas *et al.*, 1972). For this assay and all the cell-based assays, a percentage standard error of means (SEM) between experimental repeats of <20% was considered acceptable. This range is acceptable for these assays because of the inherent variabilities present in cell-based assays. For example opening and closing of incubator doors can cause slight temperatures fluctuations that can affect cell growth patterns (this was seen in the RT-CES assay and the expectation was that it was the

same for the end point assays). For the direct enzyme assays (chapter 4), a % SEM of <10% was considered acceptable because of the expected low variability in these assays.

Table 4.2: CC₅₀ values indicating the effect of the compounds on the viability of PBMCs and the PM1 cell line. The cells were treated with various concentrations (0.02-200 µM) of the compounds for 72 h followed by MTS treatment. ND refers to not done. Ligands are colour coded in grey while the superscript (a) refers to gold complexes with >10 µM CC₅₀.

Compounds	CC ₅₀ (µM)		Compounds	CC ₅₀ (µM)	
	PBMCs	PM1		PBMCs	PM1
TTL3	52±5.6	85.7±14	MCZS1 ^a	13±3.2	19.8±7.4
TTC3	4±1.3	ND	MCZS2	1.2±0.1	1.5±0.4
TTL10	65±10.1	88±7.1	MCZS3 ^a	19±1.8	12.6
TTC10	4.4±0.7	<3.1	PFK174 ^a	58±9.1	15±2.4
TTL17	21±6.8	35.5	PFK189 ^a	103±11.8	2.5±0.1
TTC17	3.7±0.9	43±5	PFK190 ^a	11±0.9	<0.4
TTL24	45.7±8.2	ND	PFK5	>200	>100
TTC24	4.6±0.4	4.8±0.1	PFK7	5.6±0.6	1.7±0.3
EK207	8.5±2.3	5.3±2.2	PFK6	>200	ND
EK208	6.6±1.5	6.1±0.2	PFK8 ^a	11.8±2.8	1.7±0.1
EK219	7.1±1.9	6.1±1.1	PFK39	<0.2	ND
EK231 ^a	50±8.9	29±4.8	PFK41	0.21±0.4	ND
			PFK38	<0.07	ND
			PFK43	0.07	ND
			KFK154B ^a	27±6.3	90±7.4

Although CC_{50s} were obtained for both PBMCs and PM1 cells, values determined using PBMCs were used as a model for further studies especially because subsequent assays mostly involved the use of the latter cell type. Gold complexes EK231, MCZS1, MCZS3, PFK174, PFK189, PFK190, PFK8 and KFK154b were generally less toxic with CC₅₀ of > 10 µM when PBMC viability was determined. The ligands had higher CC₅₀ values (less toxic) than the corresponding complexes except for two Tscs ligands (PFK39 and PFK38) which had CC₅₀ values of < 0.08. A decrease in toxicity after complexation has been reported in the literature for some Tscs ligands (Pelosi *et al.*, 2010) such that the latter findings were not surprising. The slightly higher toxicity that was generally observed for the other gold complexes compared to the ligands might be because of the fact that gold has a high affinity for sulphur and is known to undergo ligand exchange reactions with sulfhydryl groups in cysteine side chains of proteins (Shaw III, 1999, Sadler and Guo, 1998). If these interactions occur with the membrane or intracellular proteins it may be responsible for increased retention of the compound resulting in the observed increase in toxicity especially for the very lipophilic compounds (chapter 3, Table 3.8A) such as the gold(I) phosphine chloride complexes, the BPH gold(I) complexes and the bimetallic gold(I) phosphine thiolate complexes. In fact this kind of effect has been reported for the parent compound of the BPH gold(I) complexes, Au(DPPE)₂Cl, which demonstrated promising *in vitro* anti-cancer properties (Fricker, 1996, Berners-Price *et al.*, 1986, Mirabelli *et al.*, 1986) but led to cardiotoxicity problems in pre-

clinical studies (Hoke *et al.*, 1989). This would however not be the case for complexes such as the two of the phosphine thiolate complexes (MCZS1 and 2), the Tscs-based complexes and the gold(III) pyrazolyl complex which had ideal lipophilicity values and overall good ADMET qualities with a score of 6/7 (Table 3.8A). PF174, PFK189 and PFK190 demonstrated varying CC_{50} s in the PBMCs and PM1 population (Table 4.2) and these differences may be related to the poor aqueous solubility that was observed for these complexes during wet lab dissolution procedures corroborating the ADMET predictions in chapter 3 (Table 3.8A and 3.9).

Tests with the annexin V apoptosis detection kit (Figure 4.4) confirmed that concentrations of the compounds that resulted in >60% viability of PBMCs in the MTS assay were in fact not toxic (Figure 4.3) except for two complexes (PFK189 and PFK190). These two complexes caused < 50% viability of PBMCs at 5 μ M contrary to findings in the MTS assay (CC_{50} s were 103 ± 11.8 and 11 ± 0.9 μ M respectively, Table 4.2). Again, the poor aqueous solubility predicted in the *in silico* ADMET studies (chapter 3, Table 3.8A) and in wet lab assays might be responsible for this variation. Alternatively because the apoptotic mechanism cannot be identified in the MTS assay, cells in early apoptosis may still be able to metabolise MTS giving the overall impression that the compound was not toxic. Such variations were not surprising and support the idea that more than one parameter should be investigated when determining the toxicity of potential drugs (Kepp *et al.*, 2011).

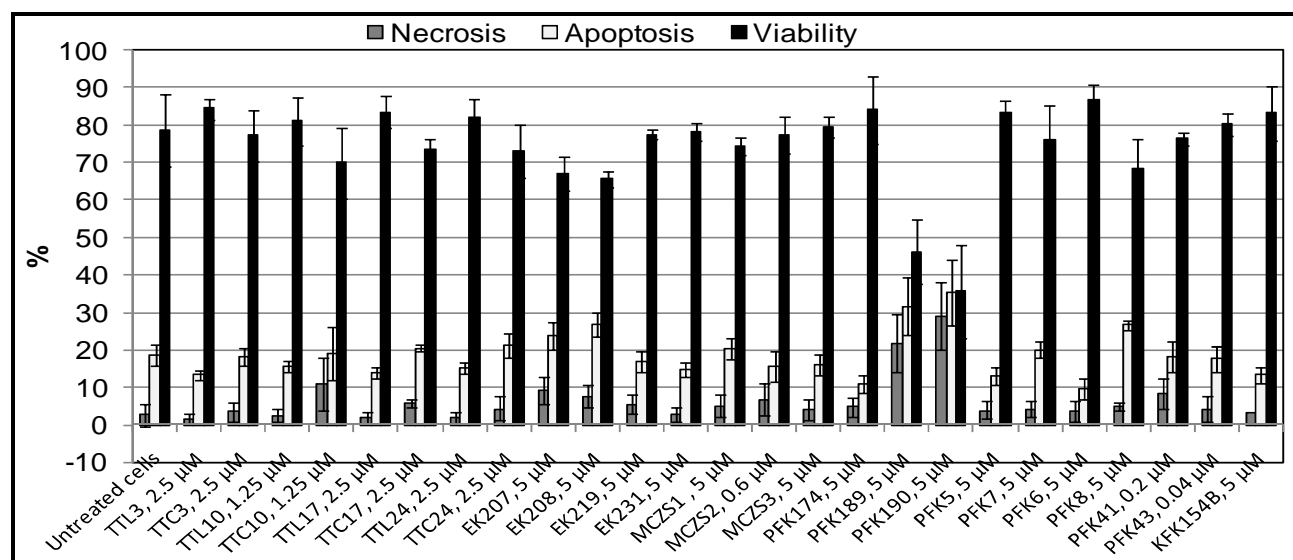


Figure 4.4: Viability profile of PBMCs treated with the compounds and analysed using flow cytometry. The cells were treated with the compounds for 72 h and stained with annexin V and PI for 15 min before flow cytometry analysis. Except for PFK189 and PFK190 which caused high apoptotic and necrotic abilities, all the other compounds did not significantly affect cell viability at the indicated concentrations (concentrations with >60% viability in MTS assay). Cells treated with ligands (e.g. TTL3, TTL10) had slightly more viable cells than those treated with corresponding complexes (e.g. TTC3, TTC10). The BPH gold complexes (EK207, and EK208) and the gold(III) thiosemicarbazone complex PFK8 were slightly more toxic than the rest. The percentage SEMs were <20%.

With regards to mode of cell death, the BPH gold(I) complexes, EK207 and EK208, the gold(III) thiosemicarbazone complex, PFK8, as well as complexes PFK189 and PFK190 caused the highest apoptotic cell death (>20%). Cell death by necrosis was generally below 10% for all treatments (except for PFK189 and PFK190) and untreated cells.

4.3.2 Cell Proliferation Determination

4.3.2.1 Monitoring proliferation using CFSE

The CellTrace™ CFSE kit from Molecular probes was used in determining the effect of the compounds on the proliferation of PBMCs. Representative cell proliferation histograms are shown in Figure 4.5. The various peaks in Figure 4.5 equate to different generations of daughter cells as they divide from the parent generation (orange coloured peak). The brightest peak (orange coloured) or parent generation or generation 0 consists of cells with the least proliferation while the dimmest peaks represent cells that proliferated the most (fluorescence intensity between 0 and 10^3 on the x-axis, Figure 4.5).

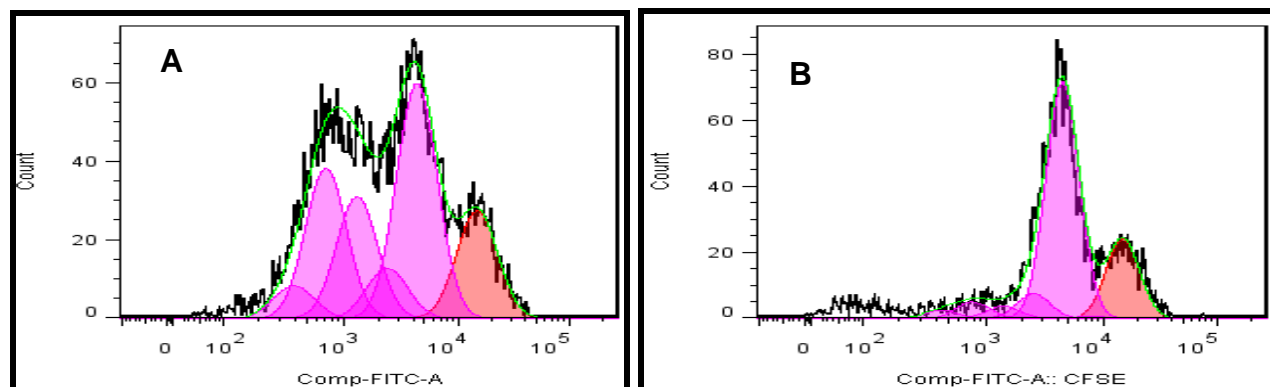


Figure 4.5: Representative proliferation histograms showing proliferation patterns of CFSE stained PBMCs. Various peaks represent generations with the brightest being cells that did not proliferate (orange colour) and the dimmest are cells that proliferated the most. In A, cells were treated with 2 $\mu\text{g/mL}$ of PHA-P and in B PHA-P stimulated cells were treated with gold complex EK208. EK208 was anti-proliferative.

The software (FlowJo version 7.6.1, TreeStar Inc., Oregon, USA) that was used in analysing the proliferation of the PBMCs indicated a total of eight generations but only 6 were visible enough (Figure 4.5A and B) since events in the dimmest generations were very few especially in Figure 4.5B due to compound (EK208) effect on cell proliferation. Because of the diminished number of events observed in generations 2, 3, 4, 5, 6, and 7 for the treated cells (Figure 4.5B), the first 3 generations i.e. 0, 1 and 2 were merged to form generation 0 and the last two i.e. 6 and 7 were merged to form generation 4. Data for the resultant five generations are shown as stacked column bars for each tested compound in Figure 4.6.

The concentrations of compounds tested were those that resulted in >60% viability (PBMCs) in the MTS assay and were similar to those used in determining viability by flow cytometry (Figure 4.4). Proliferation monitoring was done from a “live gate” which was obtained by excluding PI positive events (cells) on a SSC versus PerCp-Cy5.5 dot plot.

The proportion of cells in generation 0 of the untreated sample (cells) was chosen as a reference point (indicated as a grey line spanning across compound treated cells, Figure 4.6) for determining compounds that had anti-proliferative effects on PHA-P stimulated PBMCs. The percentage anti-proliferative effect was calculated using the formula:

$$\% \text{ anti-proliferative effect} = \frac{(\text{Treatment \% in generation 0} - \text{control \% in generation 0}) \times 100}{(\text{Control \% in generation 0})}$$

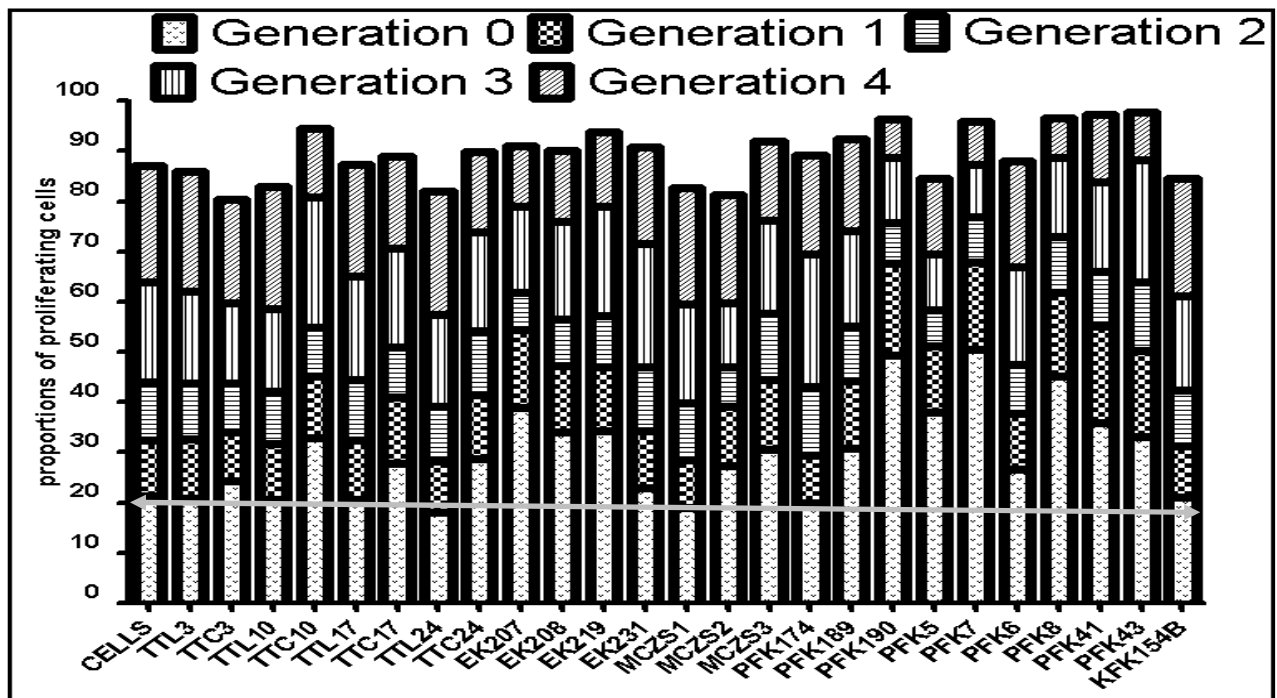


Figure 4.6: The effect of the compounds on PBMC proliferation. CFSE stained PBMCs stimulated with 2 $\mu\text{g/mL}$ of PHA-P were treated with the compounds for 72 h. The cells were harvested and proliferation monitored on a FACSaria flow cytometer. The phosphine(I) complex TTC10, the BPH gold(I) complexes, EK207, EK208, EK 219 , gold(I) thiolate complex PFK190 and the gold(III) thiosemicarbazonate complexes PFK7, PFK8, PFK41 and PFK43 prevented the proliferation of >50% of the initial number of cells in generation 0 compared to the untreated control suggesting these compounds had anti-proliferative effects.

Anti-proliferative effects of >50% caused by the compounds on cells in generation 0 was considered relevant and was applicable to complexes TTC10 (55%), EK207 (83%), EK208 (60%), EK219 (61%), PFK190 (132%), PFK5 (79%), PFK7 (137%), PFK8 (112%), PFK41 (69%) and PFK43 (56%). Compounds that were the least anti-proliferative were ligands TTL3 (1.9 %), TTL10 (2.9%) and TTL17 (2.5%), and gold complexes EK231 (8.1%), PFK174 (6.7%) and KFK154b (1%), a finding which was in agreement with the observed $\text{CC}_{50\text{s}}$ for these compounds (Table 4.2). Only two compounds; TTL24 and MCZS1 appeared to have a minor stimulatory effect with slightly less cells in generation 0 (below grey line). Generally the proportion of cells in generation 0 translated to the 1st, 2nd, 3rd and 4th generations i.e. treatments with less cells in generation 0 had more cells in either generation 1, 2, 3 or 4 and vice versa (Figure 4.6). For example, PFK7 which had the highest percentage of cells in generation 0 (137%) had far fewer cells in generation 4 compared to the untreated control. With regards to class, class IV (Tscs-based) compounds were the most anti-proliferative followed by class II (BPH-based) and finally I, III and V which were the least.

By monitoring the effect of the compounds on the proliferation of T-cells, drug mechanisms can be deduced (Brenchley and Douek, 2004). For example compounds with mitogenic (e.g. PHA-P-like compounds) tendencies which stimulate cellular proliferation or those that inhibit cell proliferation can be identified through the proliferation patterns observed.

Stimulation and therefore proliferation although beneficial in the sense that important bio-molecules and cells such as CD8+ needed by the host (especially during HIV infection)

are elevated, could also be detrimental. The increase in the proliferation of CD8⁺ cells is associated with the production of perforin which aids in the destruction of infected CD4⁺ cells, a phenomenon seen in long term non progressors (Migueles *et al.*, 2002). In HIV infection, activation or stimulation of cells also leads to proliferation and is directly linked to viral pathogenesis (Douek *et al.*, 2009) since it accelerates viral replication (Mcdougal *et al.*, 1985, Folks *et al.*, 1986, Biancotto *et al.*, 2008). These reports suggest that stimulatory and anti-proliferative effects have advantages and disadvantages suggesting that an optimal state (in which there is a balance between the two) should be the ideal.

None of the compounds caused increases in PBMCs proliferation, suggesting that the compounds did not result in cell activation or stimulation, a situation which is usually associated with disease progression e.g. in rheumatoid arthritis (Lampa *et al.*, 2002). This also means that the compounds (if eventually used as drugs), should not demonstrate the type of hypersensitive adverse effects (lymphocyte proliferation resulting from stimulation) usually observed as dermatitis for gold drugs (Verwilghen *et al.*, 1992, Lampa *et al.*, 2002).

None of the gold complexes on their own stimulated cell proliferation (like PHA-P, Figure A4.8C), but when cells were stimulated with PHA-P; it was possible to observe the compounds' anti-proliferative effects (Figure 4.6). This finding was not surprising for these complexes since gold salts have previously been reported to inhibit PHA-P stimulated proliferation of PBMCs (Sfikakis *et al.*, 1993, Lipsky and Ziff, 1977).

The proliferation studies were performed on uninfected cells and so it is not clear if the anti-proliferative effects of the compounds may be related to the ability to lower viral replication. If these assumptions could be made, then the ten complexes which inhibited the proliferation of the PHA-P stimulated cells (Figure 4.6) may be capable of modulating and suppressing viral replication through the ability to prevent T cell activation. However, in the multiparametric flow cytometry assays, the effect of the compounds on the frequency of HIV+CD4⁺ cells could be used to deduce this.

4.3.2.2 Monitoring proliferation using a RT-CES device

Cell proliferation was also monitored using a modified HeLa cell line (TZM-bl) to determine the compounds' effects on the kinetics of cell growth using an RT-CES device. Unlike standard end point assays such as MTT, the ability to monitor cytotoxicity start time, cell recovery and cell response patterns (Xing *et al.*, 2005) in real time make this technique unique. Following titration experiments, 10,000 cells were chosen as the optimum seeding density per well for the TZM-bl cells (Figure 4.7A shows a typical titration profile). This density resulted in an average cell index of 1.5 which was ideal for the assay since over confluency (100%) or under confluency (< 60%) prior to compound addition at about the 24th hour was avoided. The ideal confluency range should be between 70 and 85%.

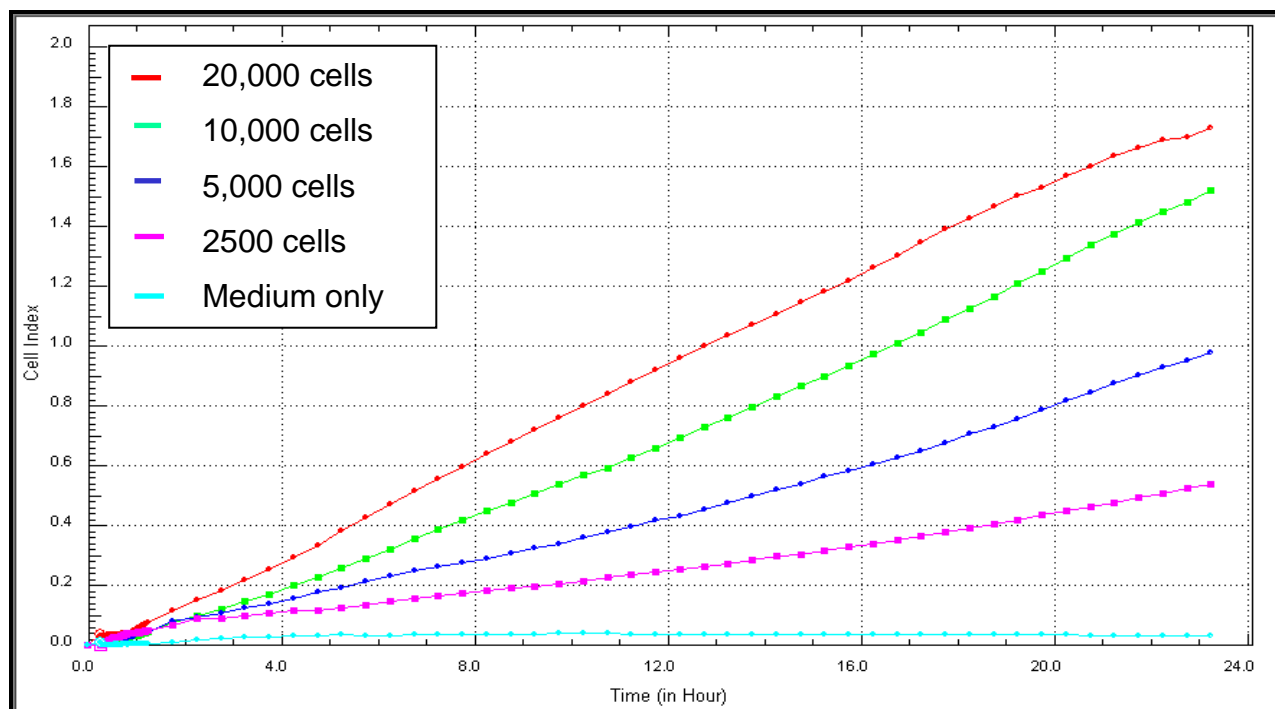


Figure 4.7A: Typical titration profile of TZM-bl cells. The proliferation of the cells was monitored for 23 h at concentrations of 2500, 5000, 10000 and 20,000 cells. A titre of 10,000 cells was chosen for experiments since it resulted in approximately 80% confluency between 22 and 24 h (time range at which test agents were added).

Selected compounds from each class were tested at 3 different concentrations. Representative profiles for all tested compounds are shown in Figure 4.7B while experimental repeats are presented in the appendix (Figure A4.11 and A4.12). The plots were constructed from normalized cell index (CI normalized against the time point when the compounds were added to the cells ~ 22-24 h post seeding) on the y-axis against time in hour on the x-axis. The normalisation is set to 1 and corrects for any small differences between cells before the addition of compounds such that only compound effects are visible. Upon the addition of compounds, the cells could either continue proliferating (increasing CI), stopped proliferating (stable CI) or started dying (decreasing CI). The assay was monitored for 7 days.

Various profiles were observed for the different compounds but there was generally a dose dependent change in CI index. As expected, the phosphine ligand, TTL3, had no adverse effect on the proliferation of these cells compared to the corresponding complex, TTC10, which at 10 μM demonstrated a cytostatic effect. The BPH gold(I) complex, EK207, initially demonstrated a significant increase in CI at 10 μM (probably as a result of compound uptake and swelling of the cells) and then after 24 h of addition (45th h on graph), a steady decrease was observed suggesting toxicity which continued until the assay was stopped at the 168th hour. A similar phenomenon was observed at 5 μM but the cytotoxicity start time was at the 98th h i.e. 72 h after compound addition. The profile for the gold(I) phosphine thiolate complex, MCZS2, suggested that the complex was much more cytotoxic than the rest of the complexes with cell indices steadily dropping until they approached zero within hours of complex addition. For this compound, only the 0.1 μM concentration was non-toxic.

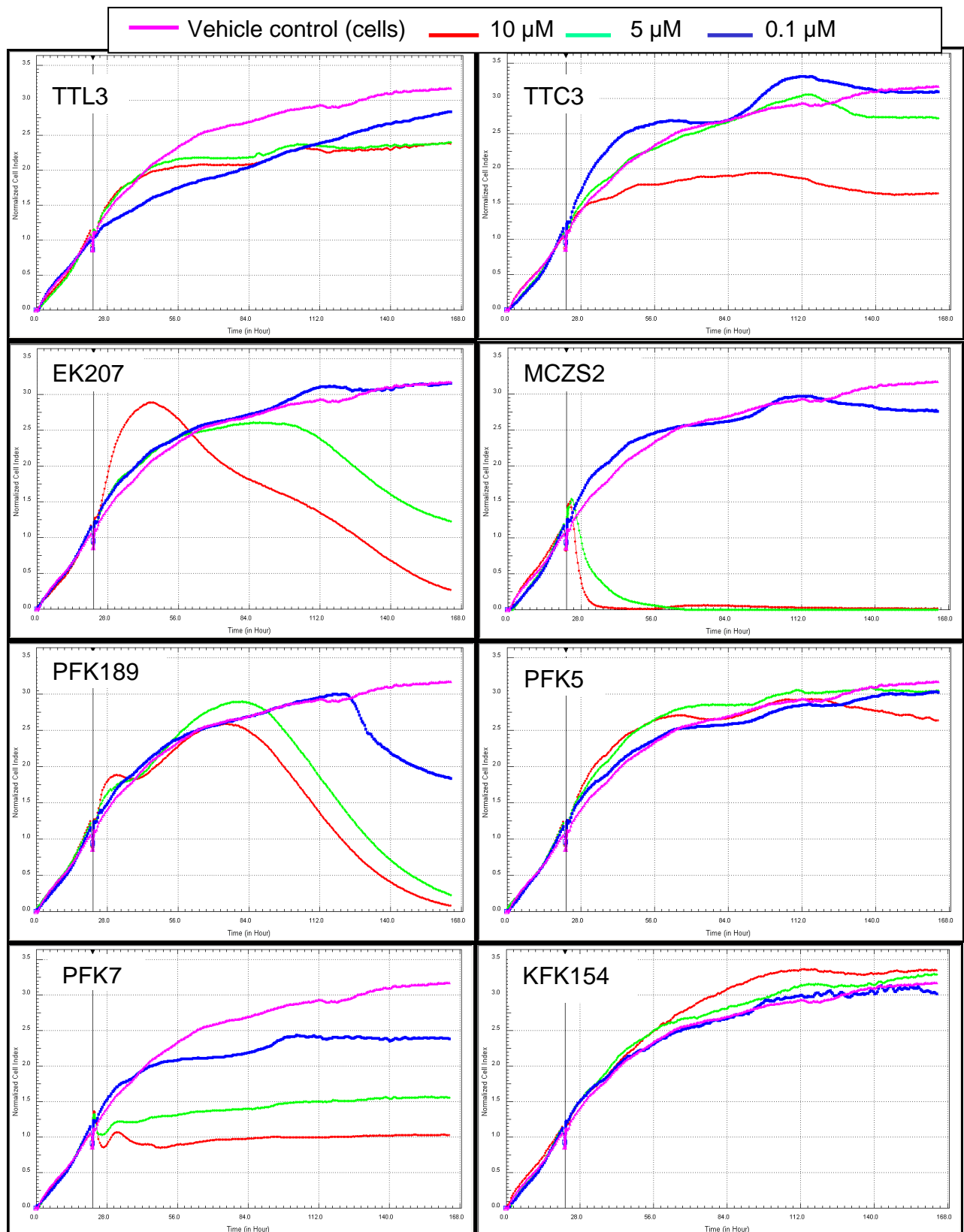


Figure 4.7B: Effect of compounds on TSM-bl cell growth pattern monitored by an RT-CES analyser. Cells were seeded into an E-plate and allowed to adhere for at least 20 h followed by treatment with compounds. Three concentrations of each compound were tested and are represented on each graph as normalized CI (y-axis) against time (h) alongside the vehicle control (cells with 0.5% DMSO, minimum DMSO concentration present in treatment, included exclude vehicle effect on cells). Compounds TTL3, PFK5 and KFK154b did not cause CI decreases. EK207 and PFK189 induced a dose dependent decrease in CI days after addition. TTC3 was cytostatic at 10 μ M while PFK7 displayed a dose dependent cytostasis at all 3 concentrations which was absent for the complementary ligand, PFK5. Significant decreases in CI were observed for complex MCZS2 within hours of addition suggesting toxicity.

PFK189, on the other hand had a similar profile to that of EK207 causing significant CI decreases after 72 h (10 μ M) and 94 h (5 μ M). Some of the possible reasons why the cell indices for EK207 and PFK189 started dropping after an initial phase of increase could be because the cells had reached 100% confluency and were dying as a result of overcrowding. Alternatively cell death could have been triggered after the accumulation of toxic doses of the compounds. The similarity in behaviour between EK207 and PFK189 may be because both compounds are bimetallic gold complexes. These findings were not surprising considering that in the drug-likeness studies, these complexes had been predicted to have extremely higher lipophilic tendencies (outside the ideal limit, Table 3.8A). It is possible that these two complexes bind tightly and accumulate at the cell membrane and likely disrupt it over time as seen in the profiles (Figure 4.7A). TTL3, PFK5 and KFK154b, as expected (from MTS data Table 4.2), were not toxic to these cells at $\leq 10 \mu$ M.

A notable observation was the dose dependent cytostasis observed for the gold(III) thiosemicarbazonate complex, PFK7, which was absent for the complementary ligand, PFK5 (Figure 4.7B, Figure A4.11 and A4.12). The same phenomenon was noted for complex PFK8 (Figure 4.7C), also a thiosemicarbazonate complex. A similar effect was noted for the gold(I) phosphine chloride complex, TTC3 at 10 μ M (Figure 4.7B) but not upon subsequent analysis (Figure A4.11 and A4.12). In an end point assay, such observations could easily have gone unnoticed and the assumption would have been that PFK7 and PFK8 were cytotoxic especially at 5 and 10 μ M, which was apparently not the case as seen from these real time studies. Gold(III) complexes have been shown to have anti-cancer activity (Casini *et al.*, 2008, Che *et al.*, 2003) and thus cytotoxic and anti-proliferative effects (Gabbiani *et al.*, 2007). The cytostatic or anti-proliferative effect noted here for PFK7 and PFK8 may mean that these complexes have potential anti-cancer activity. With regards to HIV, cytostasis has been reported as a mechanism by which some anti-viral drugs e.g. HU, trimidox and didox (Lori *et al.*, 2005, Mayhew *et al.*, 2005, Lori *et al.*, 2007, Clouser *et al.*, 2010) function. Combining optimal doses of cytostatic compounds with drugs that directly inhibit virus, e.g. didanosine, leads to an overall beneficial effect in HIV treatment (Lori, 1999, Lori *et al.*, 2005, Clouser *et al.*, 2010). PFK7 and to a lesser extent PFK8 were some of the complexes which significantly prevented the proliferation of PBMCs in the CFSE assay, retaining as much as 137% and 112% of the cells in generation 0 respectively at 5 μ M (Figure 4.6). The RT-CES analysis for these complexes (Figure 4.7B and C) was therefore in agreement with the CFSE findings (Figure 4.6). These outstanding observations of cytostasis were compiled in a manuscript that was accepted for publication in the Journal of Inorganic Biochemistry (Fonteh *et al.*, 2011) as the possible mechanism by which these compounds inhibited viral infectivity (discussed in the next section). To the best of our knowledge this is the first time a cytostatic mechanism for gold-based drugs has been demonstrated using the impedance-based technology of the RT-CES analyser. The fact that these thiosemicarbazonate gold(III) complexes also demonstrated

outstanding drug-like properties when shake flask (section 3.4.3) and *in silico* ADMET predictions (Table 3.8A) were compared makes these observations significant for HIV (and probably anti-cancer) drug discovery.

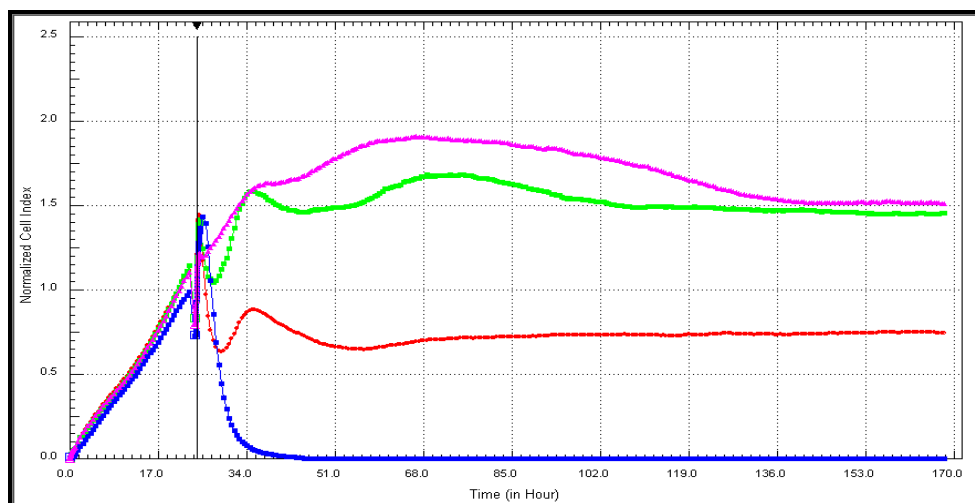


Figure 4.7C: The effect of complex PFK8 on the proliferation of TZM-bl cells monitored by RT-CES analysis. Here the vehicle control is represented by a pink line, green is 5 μM and red is 10 μM concentrations of PFK8 respectively. Auranofin (10 μM) is represented in this figure by the blue line. The cells (vehicle control) appeared to have entered the dead phase earlier (cell index was gradually decreasing after 68 h).

4.3.3 Inhibition of Viral Infectivity by Determining Luciferase Gene Expression from TZM-bl Cells

Inhibition of pseudovirus (Du 151.2) infectivity by the compounds was measured as a reduction in luciferase reporter gene expression after a single round of infection of TZM-bl cells. There was a dose dependent decrease in infection from 0.8 to 25 μM (Figure 4.8A). Viability assessment (using MTT at the same concentrations) was performed to determine whether the observed inhibition of infection was specific and not due to compound-induced cell death (Figure 4.8B).

For the analysis, a cut-off of >80% viability was considered a good point for excluding compounds which might influence infectivity through toxicity (i.e. compounds with <80% viability) since this assay is highly sensitive to toxicity. Based on this criterion, three complexes were inhibitory at non-cytotoxic concentrations. These were the gold(I) phosphine chloride complex TTC24 which only caused 10% toxicity (90% viability) at 12.5 μM with an associated inhibition of infectivity of 94% ($\text{CC}_{50} = 18.6 \pm 4 \mu\text{M}$ and a 50% inhibitory concentration or IC_{50} of $7 \pm 1.8 \mu\text{M}$), two BPH gold(I) complexes EK207 with an 88% viability at 6.25 μM where viral inhibition was 84% ($\text{CC}_{50} = 27 \pm 1.3 \mu\text{M}$ and $\text{IC}_{50} = 3.6 \pm 1.1 \mu\text{M}$) and EK231 which inhibited infectivity by 98 and 104% at 12.5 and 25 μM respectively with viability > 80% in both cases ($\text{CC}_{50} > 25 \mu\text{M}$, $\text{IC}_{50} = 6.8 \pm 0.8 \mu\text{M}$). MTT viability data for the gold(III) thiosemicarbazonate complex, PFK7, suggested that the compound was toxic from 6.25 μM and higher (experimentally tested up to 25 μM). This presumed toxicity was observed as a dose dependent cytostatic effect noted especially for 0.1, 5 and 10 μM (discussed in section 4.3.2.2).

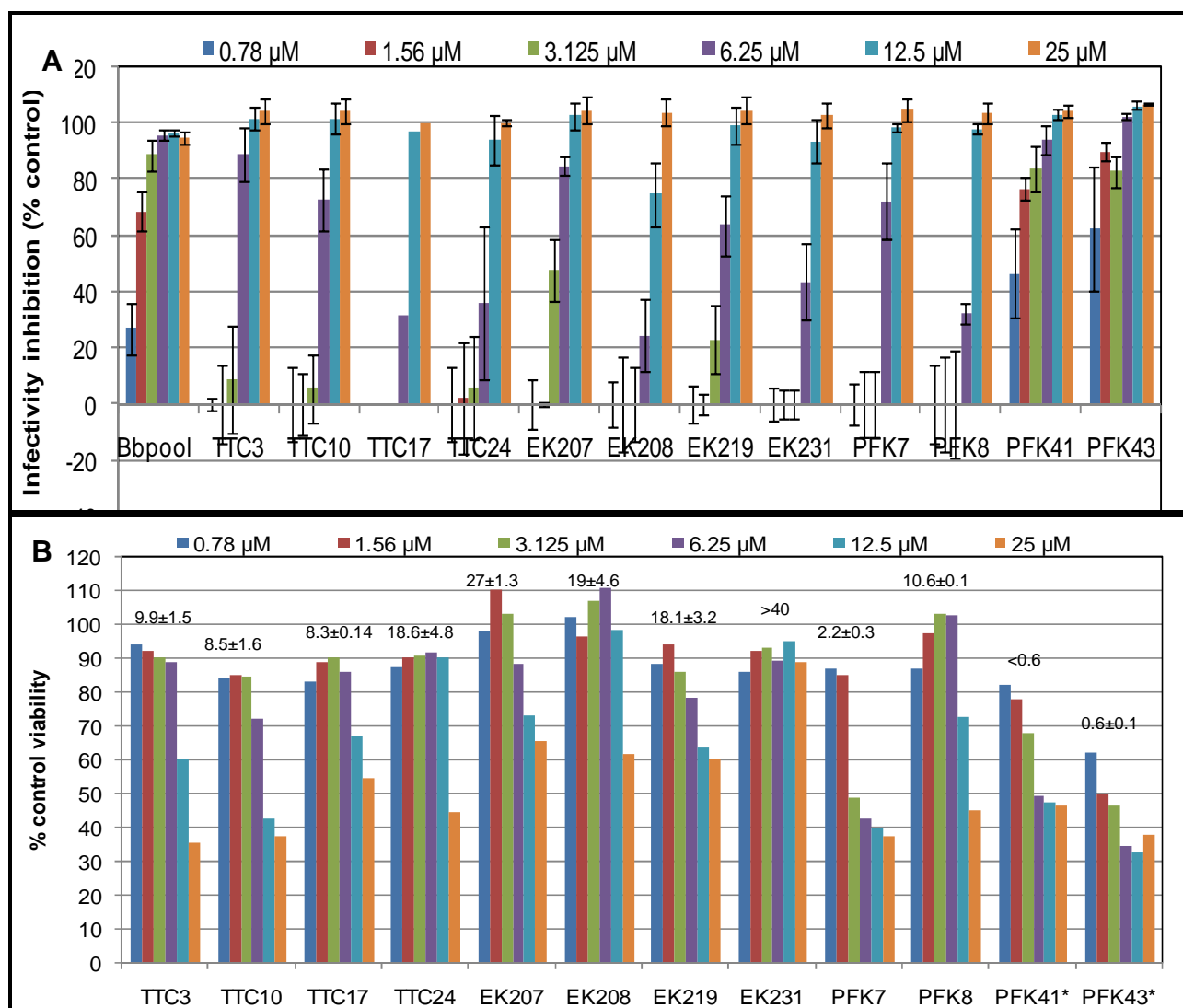


Figure 4.8: The effect of the compounds on the infectivity (A) and viability (B) of TZM-bl cells. A dual subtype C viral isolate (DU151.2) was pre-treated with the compounds and its ability to infect TZM-bl cells was monitored by determining luciferase gene expression after 48 h (A). Cell viability was monitored at the same concentrations (B). TTC24, EK207 and EK231 significantly inhibited viral replication while maintaining cell viability at >80%. Inhibition by PFK7 and PFK8 was seen at cytostatic concentrations. Bbpool was used as a positive control for inhibition of infectivity. The asterisk (*) indicates tested concentrations which were 0.04, 0.08, 0.16, 0.31, 0.625 and 1.25 μ M for PFK41 and PFK43. The concentrations tested for the rest of the complexes are shown on the graph. Concentrations with negative inhibitory values were rounded up and plotted as 0% (A). In B, inserts representing the CC_{50} s of the complexes are shown.

With the RT-CES analysis data in mind, a closer look at Figure 4.8B revealed that for PFK7 (and PFK8 to a lesser extent) cytostasis played a role since viability did not significantly change for concentrations 6.25, 12.5 and 25 μ M. Over this concentration range, viability was only moderately and insignificantly decreasing with percentages of 49.5, 47.5 and 46.4% respectively further confirming the cytostasis seen in Figure 4.6 for PFK7. Not only did PFK7 inhibit viral infection of the TZM-bl cell line by 72 and 98% at 6.25, and 12.5 μ M respectively (Figure 4.8A) with an IC_{50} of 5.3 ± 0.4 μ M (Table A4.2), but it appeared to do so as a result of its cytostatic nature. The same principle could be applicable to PFK8 but this compound demonstrated a lower potency than PFK7. Viral infectivity inhibition by PFK8 was 98% at a non-toxic (67% viability) concentration of 12.5 μ M with an IC_{50} 6.8 ± 0.6 μ M and this compound was cytostatic at 5 and 10 μ M suggesting possible cytostasis at 12.5 μ M. PFK7 was more

effective than PFK8 with the main difference between the two compounds being the presence of methyl groups in place of ethyl groups for latter (Table 3.4) which appear to confer unique properties to this compound. This difference led to a slightly higher lipophilicity value for PFK7 over PFK8 with the former having an AlogP prediction of 1.5 and the latter of 0.8 (Table 3.8A). The same trend was seen in the shake flask data with PFK7 having a log P value of 2.42 ± 0.6 and PFK8 of 0.97 ± 0.5 respectively (Section 3.4.3).

Compounds that inhibit viral infectivity through cytostasis have been extensively covered in the literature and shown to lead to better resistance profiles in clinical tests when combined with drugs that inhibit the virus directly such as didanosine (Lori *et al.*, 1997, Frank, 1999, Rutschmann *et al.*, 1998, Federici *et al.*, 1998). The anti-viral activity of Tscs has been postulated (Easmon *et al.*, 1992) and shown (Spector and Jones, 1985) to be through the lowering of nucleotide pools (needed by the virus) through inhibition of ribonucleotide reductase, an enzyme known to be inhibited by cytostatic agents such as HU (Lori *et al.*, 2005, Clouser *et al.*, 2010). PFK7 and PFK8 being Tscs-based compounds therefore show potential as anti-HIV agents through the observed cytostatic activity. Since cytostatic agents are known to inhibit RNR, as a confirmatory test, the effect of PFK7 and the complementary ligand were tested for this ability using the human ribonucleotide reductase M1, RRM1 ELISA kit from EIAab (USCNLIFE™, Wuhan, China). PBMCs were isolated from blood obtained from four HIV- donors and treated with the compounds for 3 days. The cells were then lysed by repeated freeze thawing and the RNR concentrations (from the lysate) determined from a standard curve after measuring absorbance at 450 nm. The results are shown in Figure 4.9. A dose dependent inhibition was observed for PFK7 with a significant p value of 0.003 at 10 μ M but not for PFK5. This finding further supported the cytostatic ability of this complex. Inhibition of RNR by HU-like compounds such as PFK7 means this compound will be less susceptible to resistance since RNR is not prone to mutations like viral proteins are (Lori, 1999).

PFK41 and PFK43 (both gold(III) thiosemicarbazonate complexes as well) seemed to have cytostatic effects on the TZM-bl cell line at concentrations from 0.31 to 1.25 μ M (Figure 4.8B). Unfortunately this was not confirmed with RT-CES as the initial assumption was that these two complexes were toxic. The IC_{50} and CC_{50} for all tested compounds in Figure 4.8 are shown in the appendix (Table A4.1).

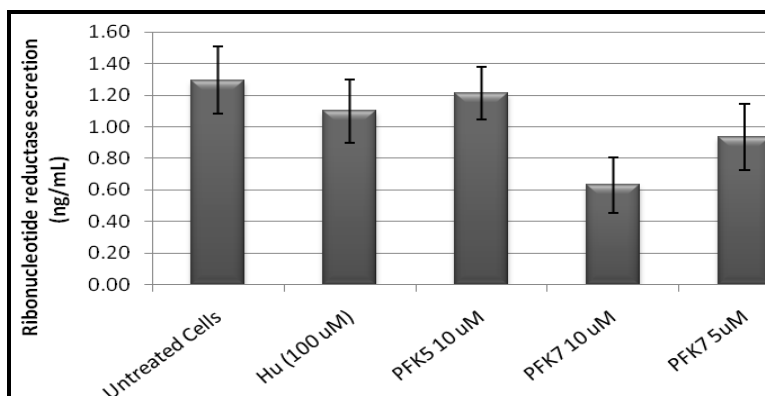


Figure 4.9: The effect of complex PFK7 on RNR production from PBMCs. PFK7 significantly ($p=0.003$) inhibited RNR production at 10 uM but not the complementary ligand, PFK5 at the same concentrations when compared to untreated cells. HU was used as a positive control but the concentration inhibited RNR tested only slightly.

To verify whether inhibition of infection by the compounds was through interaction with components on the surface of the virus (since the virus was pre-treated with the compounds), time of addition studies were performed for selected complexes which included; TTC24, EK231, PFK7 and PFK8. The TZM-bl cells were pre-treated with the compounds prior to addition of virus and the rest of the assay performed as previously described in section 3.2.4. The IC_{50} values obtained (5.6 ± 0.9 , 5.8 ± 0.4 , 6.2 ± 0.5 and 6 ± 1.3 μ M respectively) were not significantly different from when virus was pre-treated with compounds (7 ± 1.8 , 6.8 ± 0.8 , 6.8 ± 0.6 and 5.3 ± 0.4 μ M respectively). This finding suggests that the inhibition of infection was not a direct effect of the complexes on viral surface components but that it could have been by another mechanism probably at the entry or post entry steps (within the cells). Inhibition of infectivity resulting from a compound targeting multiple steps of infection has been seen in an infectivity assay for amphotericin B methyl ester (Waheed *et al.*, 2006). The fact that PFK7 for example was cytostatic at inhibitory concentrations further supports the idea that the complex exhibited inhibition at the entry or post entry steps. The positive control for infectivity inhibition (Bbpool) always presented a dose related inhibition (Figure 4.8A).

4.3.4 Effects of Compounds on T Cell Frequency and on Inflammation

Using a six colour multi-parametric ICCS assay, we investigated the effect of the compounds on both phenotypic markers (cell surface markers specific for T cell subsets to determine frequencies) and cytokine production from the same cells to determine the compounds' effect on HIV inflammation. ICCS is superior over ELISAs because it allows for individual characterization of large numbers of cells and can fully display the heterogeneity of cell populations (Pala *et al.*, 2000). Although ELISA assays were also performed, they were done primarily to determine any correlations with the ICCS assays since the latter measures intracellular cytokines while the former measures secreted cytokines. The ELISA assays were also performed as a precautionary measure in case there was a situation where ICCS was unable to detect cytokines because these proteins may have been released into the culture

supernatant before the addition of the protein transport inhibitor (BD GolgiStop™) to block cytokine secretion.

In Figure 4.10 (A-G), smooth dot plots displaying the hierarchical representative gating strategy that was used in determining ICC levels of IFN- γ and TNF- α within CD4+ and CD8+ cells is shown. The plots were obtained using FlowJo Software Version 7.6.1 (TreeStar Inc., Oregon, USA).

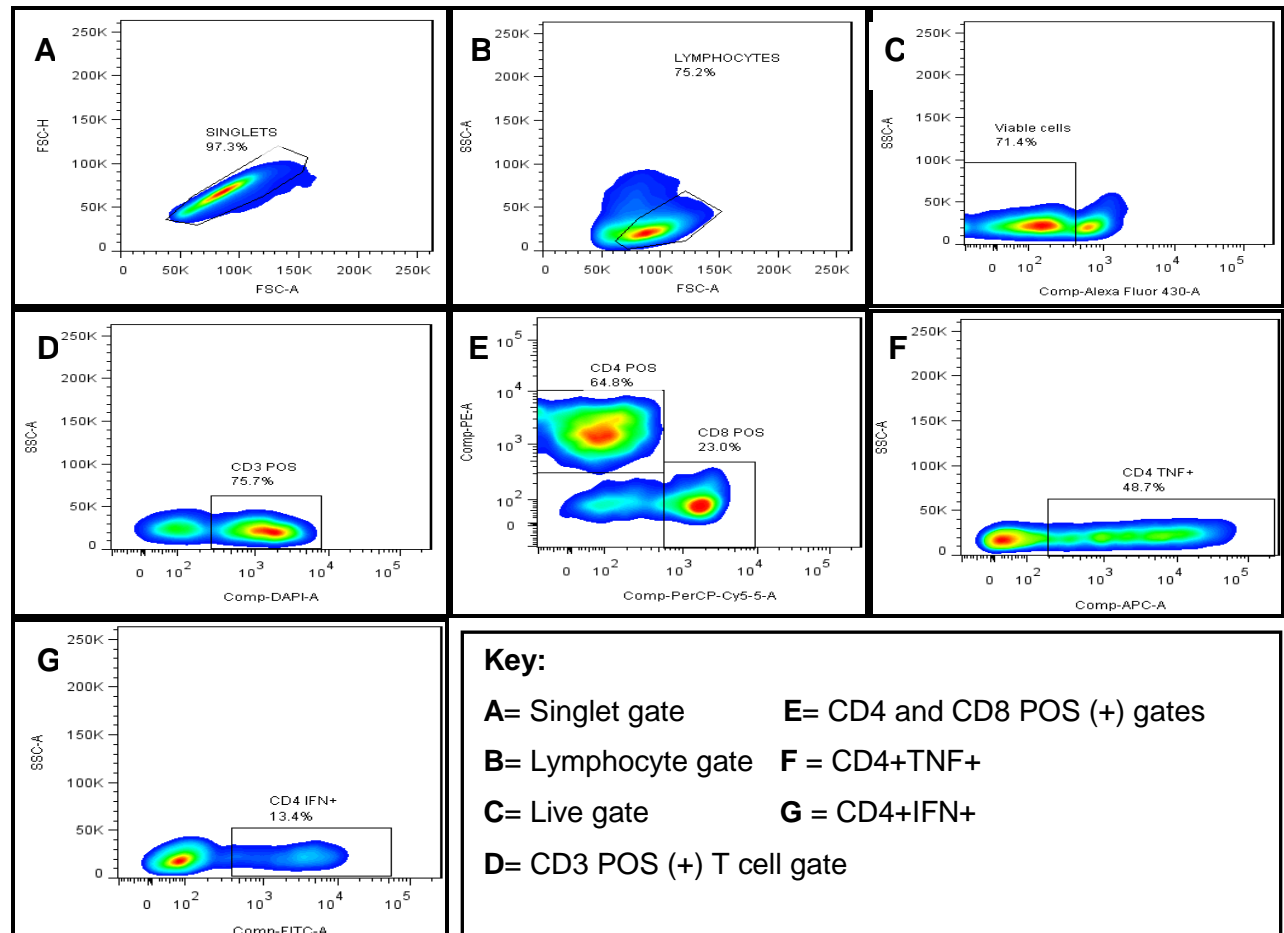


Figure 4.10: Representative FACS plots showing the hierarchical gating strategy for IFN- γ and TNF- α detection. A singlet gate (A), the lymphocyte gate (B), viable cell gate (C), T cell gate (D), T cell subset (CD4+, CD8+) gates (E), CD4+ TNF- α + gate (F) and CD4+IFN- γ + gate (G) are shown. Percentages of the frequencies of the cells in each gate are represented. The figures which represent smooth dot plots were obtained using FlowJo (TreeStar Inc., Oregon, USA).

In A, a singlet population consisting of single cells was obtained on an FSC height (H) and an FSC-area (A) plot followed by the gating of lymphocytes (B). This lymphocyte gate was identified using a CD45 marker so as to exclude neutrophils and monocytes. From the lymphocyte gate, a “live gate” was obtained by excluding cells positive for the aqua fluorescent fixable amine reactive dye (C) while in Figure 4.10D, T cells consisting of cells positive for the CD3+ marker were isolated. This was followed by the gating of the T subsets including CD4+ and CD8+ cells as seen in Figure 4.10E. Subsequently the percentage of TNF- α producing CD4+ cells (F) and IFN- γ producing CD4+ cells (G) were obtained. Cytokine producing CD8+ cells were also obtained in a similar manner as shown for CD4+ cells F and G. The gates were defined based on FMOs after fluorescent spillover subtraction.

The pooled data (after analysis using FlowJo) for all 12 HIV+ and 13 HIV- donors from whom samples were obtained was statistically analysed for significant differences using Graphpad Prism® (San Diego, California, USA). The effect of the compounds on the frequency of CD4+ expressing cells and on the frequency of IFN- γ and TNF- α producing CD4+ cells was analysed separately for HIV+ and HIV- donors (Figure 4.11). This was done using the Wilcoxon's matched pairs signed rank test with untreated cells as controls in each case (Figure 4.11). A similar analysis was done for the CD8+ T cell subset (Figure 4.12).

Effect of compounds on the frequency of IFN- γ and TNF- α from HIV+ and HIV- CD4+ cells: Two complexes, a BPH gold(I) complex, EK207 and the gold(III) thiosemicarbazonate complex (PFK7) significantly reduced the frequency of CD4+ cells from HIV+ donors with p-values of 0.0269 and 0.0049 respectively as seen in the box and whiskers plot (Figure 4.11A) but no such effect was observed for CD4+ cells from HIV- donors (D). A reduction of CD4+ cells has been shown to lead to AIDS in progressors since these are crucial immune system cells required by both the humoral and cell mediated arms of the immune system (Fan *et al.*, 2000). On the other hand cytostatic agents such as HU (in addition to inhibiting RNR, Meyerhans *et al.*, 1994) also exert anti-HIV effect through the lowering of CD4+ count resulting in a decrease in immune activation (Frank, 1999, Rutschmann *et al.*, 1998, Lori *et al.*, 1997). Trimidox and didox (Lori, 1999, Lori *et al.*, 2005, Mayhew *et al.*, 2005, Clouser *et al.*, 2010) are also examples of cytostatic agents which like HU, at optimal non-toxic doses in combination with anti-viral agents such as ddl or indinavir (virostatics) have shown superior efficacy over regimens that did not incorporate them (Lori *et al.*, 2005) in clinical trials (Lori *et al.*, 1997, Frank, 1999, Rutschmann *et al.*, 1998, Federici *et al.*, 1998).

While lowering of CD4+ cells is not such a good quality for a drug that should potentially be administered to immunocompromised (HIV+) persons, significant benefits have been observed when cytostatic drugs (that lower CD4 cells) are combined to form virostatics. These are a decrease in the incidences of drug resistance (compared to current anti-HIV agents) and an overall increase in CD4 cell numbers (Lori *et al.*, 2007). The mechanism of this action is reportedly through the inhibition of RNR thereby reducing dNTP pools required by the virus to make copies of itself (Meyerhans *et al.*, 1994, Lori *et al.*, 1994). When combined with a NRTI (ddl, a dNTP analogue) there is a relative increase in ddl with a resultant synergistic anti-viral effect since the natural substrate of DNA synthesis (dNTP) is lowered (Meyerhans *et al.*, 1994, Lori *et al.*, 1994). Accordingly, complexes EK207 and PFK7 which lowered CD4+ cell frequencies in HIV+ donors might be beneficial in virostatic combinations. In addition, this cytostatic effect (Figure 4.6, Figure 4.7 and Figure 4.9) and lowering of CD4+ cells from HIV+ donors (Figure 4.11) may play a role in the observed anti-HIV effect of these complexes (Figure 4.8). The link between inhibition of infectivity, the lowering of CD4+ cell frequencies and the cytostatic effect observed for PFK7 and its analogues forms part of a manuscript compiled from this study (Fonteh *et al.*, 2011).

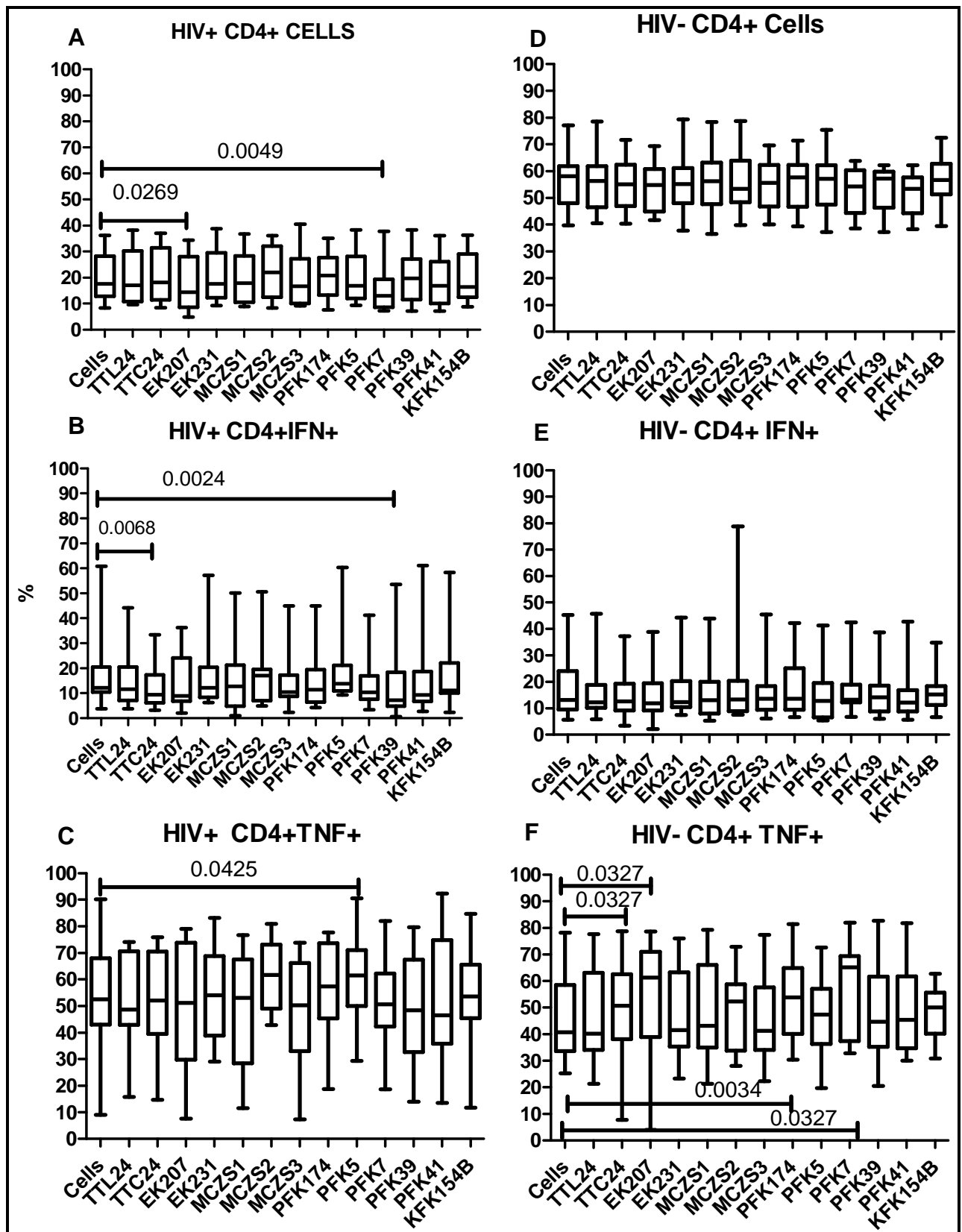


Figure 4.11: The effect of the compounds on CD4+ cells frequency and cytokine production. PBMCs from 12 HIV+ and 13 HIV- donors were treated with the compounds and the frequency of CD4+ cells as well as IFN- γ and TNF- α production from the HIV+ (A, B, C respectively) and HIV- (D, E, F respectively) donors determined. The Wilcoxon matched-pairs signed rank test was used in determining statistical significance while correlations were tested using the nonparametric Spearman correlation test. A p value of <0.05 was considered significant. Complexes EK207 and PFK7 significantly reduced the frequency of CD4+ cells from HIV+ individuals (A). TTC24 and PFK39 significantly reduce the frequency of IFN- γ producing cells while PFK5 caused an increase in the frequency of TNF- α producing cells from the HIV+ group. None of the compounds had an effect on the frequency of CD4+ cells from HIV- donors (D) or on the frequency of these cells producing IFN- γ . TTC24, EK207, PFK174 and PFK7 caused an increase in the number of CD4+ cells producing TNF- α from HIV- donors (G).

None of the compounds tested had a significant effect on frequency of CD4+ cells from HIV- individuals (Figure 4.11D) suggesting that the suppression of CD4+ cells by EK207 and PFK7 was specific for infected cells and would not occur in the absence of an infection.

The effect of the compounds on the frequency of IFN- γ and TNF- α producing cells from both HIV+ (Figure 4.11B and C respectively) and HIV- donors (Figure 4.11E and F respectively) was also investigated. TTC24 and PFK39 suppressed the production of IFN- γ from HIV+CD4+ cells (Figure 4.11B) but none of the compounds altered its production from the HIV- group (Figure 4.11E). IFN- γ is an anti-inflammatory cytokine which has been associated with a decrease in HIV disease progression and pathogenesis (Ghanekar *et al.*, 2001, Francis *et al.*, 1992) such that an increase in its production should be beneficial. Unfortunately, none of the compounds significantly increased the frequency of cells producing IFN- γ . Although IFN- γ was chosen as a representative anti-inflammatory cytokine in this study, this cytokine is known to have a bimodal role in HIV (both enhancement and suppression of HIV replication, Alfano and Poli, 2005) and is sometimes labelled as a pro-inflammatory cytokine because it can augment TNF- α activity and induces nitric oxide production (Dinarello, 2000). Therefore, if IFN- γ was labelled a pro-inflammatory cytokine, then the fact that TTC24 and PFK39 suppressed its production from HIV+CD4+ cells meant these compounds have potential anti-inflammatory abilities.

PFK5 which is the complementary ligand of PFK7 caused an increase in the frequency of TNF- α producing CD4+ cells (C), $p=0.04$. This effect was not seen for PFK7 and appeared to have been lost as a result of complexation. Four of the complexes namely: TTC24, EK207, PFK174 and PFK7 caused an increase in the frequency of HIV+CD4+ cells producing TNF- α (Figure 4.11F). Low circulating levels of the pro-inflammatory cytokine, TNF- α , has been correlated with lower viral load and slower disease progression in HIV (Than *et al.*, 1997) while increases have been associated with HIV disease progression *in vivo* (Caso *et al.*, 2001). The fact that TTC24, EK207, PFK174 and PFK7 caused an increase in TNF- α producing HIV-CD4+ cells is fortunately not critical since these compounds if potentially used as drugs will not be administered to uninfected people.

Effect of compounds on the frequency of IFN- γ and TNF- α from HIV+ and HIV- CD8+ cells: The effect of the compounds on the frequency of CD8+ cells, IFN- γ and TNF- α from PBMCs obtained from HIV+ and HIV- donors was also determined (Figure 4.12). EK207 also significantly ($p= 0.002$) reduced the frequency of CD8+ cells from PBMCs obtained from the HIV+ population (Figure 4.12A) which is not a good property considering that CTLs are required for killing activated CD4+ cells when the latter present antigen.

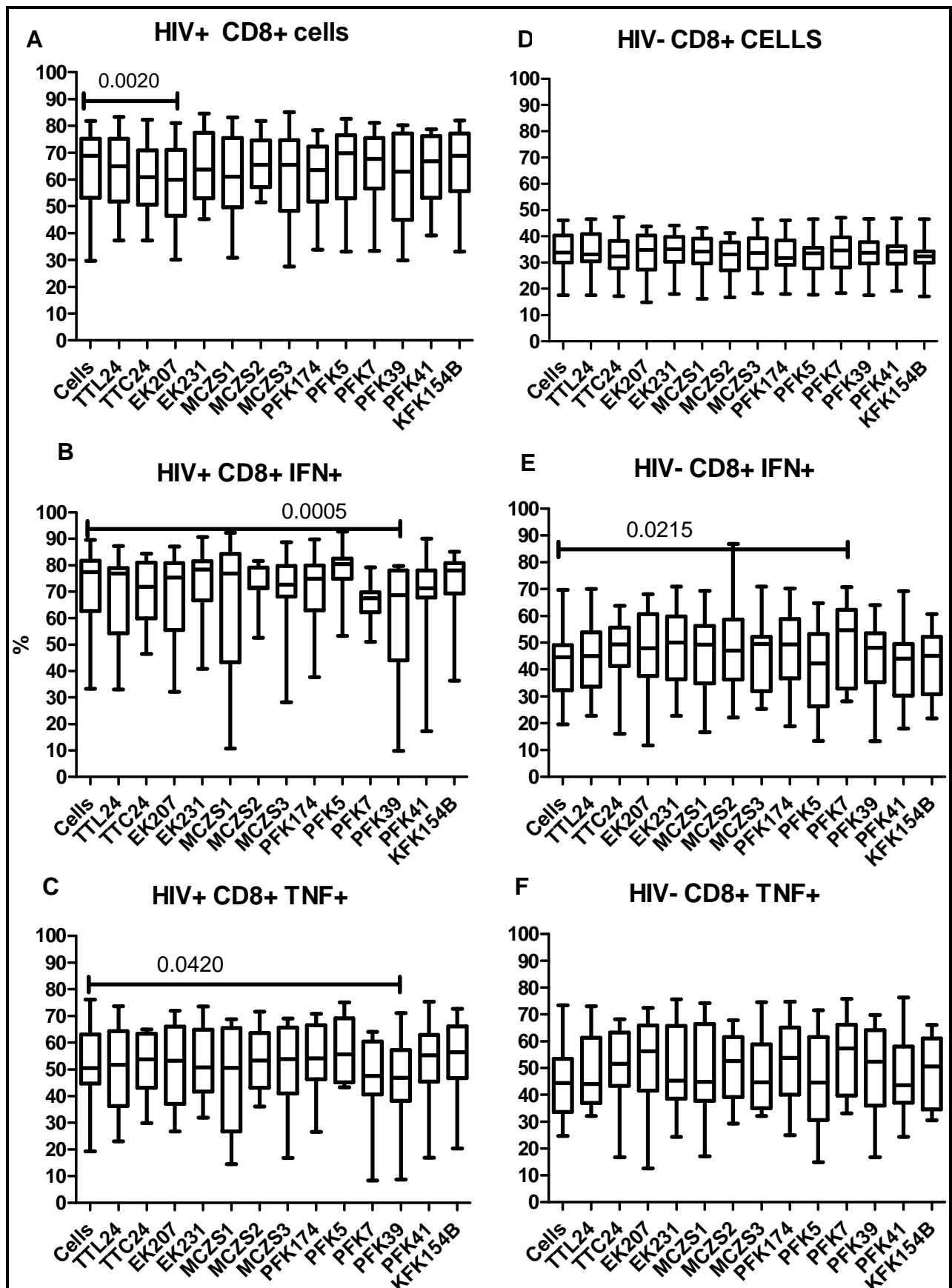


Figure 4.12: The effect of the compounds on CD8+ cell cytokine production. PBMCs from 12 HIV+ and 13 HIV- donors were treated with the compounds and the frequency of CD8+ cells as well as IFN- γ and TNF- α production from the HIV+ (A, B, C respectively) and HIV- (D, E, F respectively) donors determined. Statistical analysis was performed as for Figure 4.11. Complex EK207 significantly reduced the frequency of CD8+ cells from HIV+ individuals (A). PFK39 significantly suppressed the frequency of IFN- γ (B) and TNF- α (C) producing cells from HIV+ individuals. None of the compounds had an effect on the frequency of CD8+ cells from HIV- donors (D) or on the frequency of these cells producing TNF- α . PFK7 enhanced the production of IFN- γ from HIV-CD8+ cells with a p value of 0.022 (E).

PFK39 caused a decrease in the frequency of CD8+ cells producing both IFN- γ and TNF- α from HIV+ donors (Figure 4.12B and C respectively). A reduction in the frequency of CD8+ cells and CD8+TNF- α producing cells was not seen for the HIV- group (Figure 4.12D and F respectively). PFK7 stimulated the production of IFN- γ from the HIV- cells (Figure 4.12E), which is a good sign considering that IFN- γ is an anti-inflammatory cytokine. Compounds that suppress TNF- α production (such as PFK39, Figure 4.12C) will slow down disease progression while those that augment its production e.g. TTC24, EK207, PFK174 and PFK7 (Figure 4.11F) may be detrimental to immune function.

Interestingly though, the increase in the number of TNF- α producing cells caused by these compounds was not observed in the HIV+ group (Figure 4.11C) and appeared to have been removed for PFK7 upon complexation of PFK5 with gold. The use of anti-TNF- α drugs has had some success in limiting RA progression (Stern *et al.*, 2005) and other inflammatory diseases and may play a role in lowering the inflammation caused by HIV. A summary of the effects of compounds that altered ICC production is shown in Table 4.3.

Table 4.3: A summary of the effect of the compounds on immune cell function. CD4+ and CD8+ cell frequency and that of the anti-inflammatory cytokine IFN- γ and the pro-inflammatory TNF- α frequency was assessed. Only compounds that altered the frequency of cells and cells producing cytokines are shown. \uparrow represent increase while \downarrow represents decreases. Complexes are representative from the different classes and there was the expectation that other members would respond the same.

Status	Cell type	Molecule	TTC24	EK207	PFK174	PFK5	PFK7	PFK39
HIV+	CD4+	CD4+		\downarrow			\downarrow	
		IFN- γ +	\downarrow					\downarrow
		TNF- α +				\uparrow		
	CD8+	CD8+	\downarrow					
		IFN- γ +						\downarrow
		TNF- α +						\downarrow
HIV-	CD4+	TNF- α +	\uparrow	\uparrow	\uparrow		\uparrow	
	CD8+	IFN- γ +					\uparrow	

Some notable general observations were the fact that the median CD4+ count in the HIV+ group was lower (Figure 4.11A) than that of the HIV- group (Figure 4.11D) while median CD8+ cells in the HIV+ group was higher (Figure 4.12A) than for the HIV- group (Figure 4.12D). These are hallmarks of HIV infection (Forsman and Weiss, 2008, Musey *et al.*, 1997, Koup *et al.*, 1994) suggesting that these two groups were indeed different with regards to HIV status. The levels of the pro-inflammatory cytokine TNF- α and the anti-inflammatory cytokine IFN- γ from CD4+ cells were similar in both the HIV+ group (Figure 4.12B and C respectively) and the negative group (Figure 4.12E and F respectively). This was not the case in the CD8+ cell populations (Figure 4.12). Here IFN- γ production was generally higher in the HIV+ group (Figure 4.12B) than in the HIV- group (Figure 4.12E). The observed differences are probably because of the immune reactions mounted as a result of the infection in the HIV+ group. TNF- α levels from CD8+ cells from both groups were similar (Figure 4.12C and F). These general observations which support the fact that there are differences in systemic activation of immune

responses (Forsman and Weiss, 2008) provides further evidence that the donors in different groups were correctly assigned with respect to HIV status. This is because in HIV- individuals CD4+ cells numbers are higher than CD8+ cells and this ratio changes in HIV+ patients where CD4+ cells drop as CD8+ cells increase (Musey *et al.*, 1997, Koup *et al.*, 1994). Supporting data for the differences in the immunological state of the donors is shown in the appendix (Figure A4.13).

The ELISA data and detailed explanations are provided in Table A4.2 and subsection 8.3.6.2 of the appendix respectively. Although relatively fewer donors were tested, there was a pattern observed. In the absence of phenotypic identification in ELISAs, the compounds (TTC24, PFK174, PFK5 and PFK7) mostly demonstrated both anti-inflammatory and pro-inflammatory tendencies (except for PFK5 which lowered TNF- α production). In the ICCS assay, only two complexes altered cytokine production i.e. TTC24 and PFK5 (Table A4.3). TTC24 lowered IFN- γ production while PFK5 caused an increase in TNF- α suggesting poor anti-viral tendencies for both complexes with respect to the CD4+ subset that was analysed (Table A4.3). However, because phenotypic identification of the relevant subset of PBMCs (in this case T cells) was important in order that associations could be made with regards to cytokine production and cell phenotype, the ICCS data was considered more representative. The above mentioned conclusions were deduced from only six of the twelve HIV+ donors as a way of determining if cytokines had been secreted prior to the addition of the protein transport inhibitor and for checking if compound effects on cytokine production patterns were similar when ELISA and ICCS methods were compared.

4.4 CONCLUSION

Most of the gold complexes had CC₅₀s in the low micromolar range (between 1 and 20 μ M) in both PBMCs and the PM1 cell line (Table 4.2). An overall summary of the effects of the compounds on the viability/proliferation of the different cell types when monitored using the different assays is provided in Table 4.3. The ligands were generally non-toxic with >20 μ M CC₅₀s (Table 4.2 and 4.3) suggesting that complexation of gold to ligands resulted in increased toxicity except for ligands PFK41 and PFK43 which were more toxic than the corresponding complexes (PFK39 and PFK43). The MTS findings were confirmed for most of the compounds (except for complexes PFK189 and 190) when the annexin V and apoptosis kit was used (Figure 4.4, Table 4.3).

Table 4.4: Summary of the various effects caused by the compounds to the different cell types. In the MTS and MTT assays, compounds with $CC_{50} < 1 \mu\text{M}$ are rated toxic (yes), those with CC_{50} between $1 \mu\text{M}$ and $10 \mu\text{M}$ inclusive were rated as moderately toxic while those with CC_{50} above $10 \mu\text{M}$ were rated as not toxic (no). In the annexin/PI assays, compounds either caused an apoptotic effect (% apoptotic cells > 10 % of control value), a necrotic effect (% necrotic cells > 10% control) or no effect (viability \geq cells). In the CFSE studies, yes represents anti-proliferative and no means no effect while for the impedance measurements, no means no effect and yes means cytostatic. # same []s like in the Ann/PI study. The ligands are coloured in grey. The asterisk (*) on TTC3 refers to the fact that cytostasis was only seen once for this complex at $10 \mu\text{M}$. Superscript (a) represent cytotoxic compounds.

Compound	PBMCs			PM1	TZM-bl	
	MTS (Toxicity)	Annexin/PI [] with >60% viability in MTS	CFSE Anti-proliferative [#]	MTS (Toxicity)	MTT (Toxicity)	RT-CES Cytostasis/cytotoxic ^a
Cells only	No	Viable (100%)	No	No	No	No
TTL3	No	Viable	No	No		No
TTC3	Moderate	Viable	No	ND	Moderate	No*
TTL10	No	Viable	No	No		
TTC10	Moderate	Viable	Yes	<3.1	Moderate	
TTL17	No	Viable	No	No		
TTC17	Moderate	Viable	yes	No		
TTL24	No	Viable	No	ND		
TTC24	Moderate	Viable	No	Moderate	No	
EK207	Moderate	Viable	Yes	Moderate	No	^a over days
EK208	Moderate	Viable	Yes	Moderate	No	
EK219	Moderate	Viable	Yes	Moderate	No	
EK231	moderate	Viable	No	No	No	
MCZS1	No	Viable	No	No		
MCZS2	Moderate	Viable	No	Moderate		^a within hours
MCZS3	No	Viable	No	No		
PFK174	No	Viable	No	No	No	
PFK189	No	Apoptotic Necrotic	No	Moderate	No	^a over days
PFK190	No	Apoptotic Necrotic	Yes	Yes		
PFK5	No	Viable	Yes	No		No
PFK7	No	Viable	Yes	Moderate	Moderate	Yes
PFK6	No	Viable	No	ND		
PFK8	No	Viable	Yes	ND	No	Yes
PFK39	Yes	Viable		ND		
PFK41	Yes	Viable	Yes	ND	Yes	
PFK38	Yes	Viable		ND		
PFK43	Yes	Viable	Yes	No	Yes	
KFK154b	No	Viable	No	No		No

With regards to cell proliferation, ten compounds inhibited proliferation of PHA-P stimulated PBMCs by >50% with Tscs-based compounds>BPH gold(I) chloride complexes > phosphine chloride compounds> gold(I) phosphine thiolate>gold(III) pyrazolyl complex (Figure 4.6). Except for PFK5 which appeared to slow down cell proliferation, the rest of the ligands did not affect PBMC proliferation. Anti-proliferative compounds have the potential of lowering immune activation in asymptomatic patients and can reduce viral loads to undetectable levels and prevent progression to AIDS (Lori, 1999).

In the RT-CES analysis to determine the effect of the compounds on TZM-bl cell proliferation profiles, it was evident that two of the gold(III) Tscs-based complexes, PFK7 and PFK8 had cytostatic effects on this cell line (Figure 4.7B and C) and appeared to display cytostatic effects irrespective of cell type i.e. in PBMCs (Figure 4.6) and in the TZM-bl cell line (Figure 4.7B and C). Cytostasis is an important anti-HIV mechanism which when combined with an antiviral mechanism results in immune boosting capabilities and a reduction in drug resistance not seen for current HAART cocktails. The use of the impedance-based technology of a RT-CES analyser to observe the cytostatic mechanism of gold-based drugs was demonstrated here for the first time to the best of our knowledge.

The different complementary assays that were performed for determining cell viability and proliferation led to results which supported the importance of testing more than one marker in viability studies (Kepp *et al.*, 2011). In the MTS and MTT assay, either toxic or non-toxic responses were obtained while in the CFSE and RT-CES assay, anti-proliferative and cytostatic conclusions were reported for some compounds initially thought to be cytotoxic when MTT and MTS assays were performed e.g. PFK7 (Figure 4.7B and 4.8A).

The gold(I) phosphine chloride complex TTC24 and two BPH gold(I) phosphine chloride complexes (EK207 and EK231) inhibited viral infectivity of the TZM-bl cell line at non-toxic concentrations (Figure 4.8A and B) while PFK7 and PFK8 (to a lesser extent) did so at cytostatic concentrations (Figure 4.7B and C and Figure 4.7A). Time of addition studies suggested that inhibition might have been as a result of the compounds inhibiting multiple targets either on the virus, on or within the cell since viral pre-treatment and cell pre-treatment resulted in similar IC_{50} values (Table A4.1). According to this finding, the differences in the exposure time appeared to have had nothing to do mechanistically. All compounds appeared to inhibit virus especially at high concentrations, this could obviously not be true and was confirmed through TZM-bl viability testing in concert with infection inhibition where cytotoxicity appeared to be the cause of the presumed infectivity inhibition responses that were observed (Figure 4.8). In the case of the cytostatic complexes (PFK7 and PFK8), where inhibition of infectivity was as a result of cytostasis (Figure 4.7B and C and Figure 4.9) the observed cytotoxicity in the MTT assay was not relevant. Although complexes TTC24, EK207 and EK231 inhibited viral infectivity at non-toxic concentrations (>80% viability), the fact that these complexes (especially EK207 and EK231) were predicted to have very poor drug-like properties (unlike PFK7 and PFK8) means to be used as drugs, structural modifications (e.g. the addition of NH groups) to increase aqueous solubility will be required. TTC24 on the other hand (with a drug score of 3/7) may stand a better chance of being developed to a drug without significant structural modifications.

Notable observations with regards to the effects of the compounds on immune cell function were the findings from ICCS assays that EK207 and PFK7 could decrease the frequency of CD4+ cells from HIV+ and not in HIV- donors (Figure 4.11). These findings

correlated with the anti-proliferative and cytostatic (PFK7 only) findings observed for these compounds (Figure 4.6 and 4.7B). The ICCS and ELISAs techniques used for determining cytokine production did not correlate (Table A4.3) since opposite trends were observed.

The most outstanding findings from experiments in this chapter are those observed for complex PFK7 and PFK8 to a lesser extent (Fonteh *et al.*, 2011). These thiosemicarbazonate complexes proved to be cytostatic when data from CFSE for PBMCs (Figure 4.6) and RT-CES for TZM-bl cells were compared (Figure 4.7B and C) and inhibited viral infectivity at these cytostatic concentrations ($IC_{50}=5.3\pm 0.4$ and 6.8 ± 0.6 μ M respectively). In addition, PFK7 caused a decrease RNR levels (Figure 4.9) and in the frequency of CD4+ cells from 12 HIV+ donors ($p=0.0049$) and the two complexes demonstrated very favourable drug-like properties when the shake-flask and *in silico* ADMET methods were compared (Table 3.8A and Table 3.9). We suggest that these gold complexes could potentially be combined with viral inhibitory agents such as ddl to form part of the new and emerging class of anti-viral agents known as virostatics (Lori *et al.*, 2005, Lori *et al.*, 2007). Cytostatic drugs are not prone to the resistance issues associated with HAART and may become the combination of choice to curb the resistance associated with HAART. No evidence of cellular resistance has been revealed for HU, a cytostatic agent with more than 40 years of clinical usage (Donehower, 1992). In addition, HU has been shown to compensate for resistance that arises from the use of NRTIs when it is used in combination with ddl (Lori, 1999, Lori *et al.*, 1997). The possibility that PFK7 and PFK8 could limit drug resistance is further supported by findings that the coordination of organic ligands with metals could lead to significant reduction in drug resistance (West *et al.*, 1991) probably because of the stabilisation that the metal confers to the ligand. Other advantages that metal-based drugs have over organic ones are improved stability and the fact that they form covalent interactions (leading to longer lasting interactions with their active site). This may mean that PFK7 and PFK8 could be better cytostatic inhibitors than HU. A 10 μ M concentration of HU inhibited cell proliferation and suppressed HIV-1 replication *in vitro* (Lori *et al.*, in 2005) which is within the concentration range of viral infectivity inhibition and cytostasis that was seen for PFK7 and PFK8 (a concentration that is clinically relevant for gold compounds). The mechanism by which a cytostatic agent such as HU and potentially HU-like agents e.g. PFK7 function in a virostatic combination to curb viral replication is demonstrated in Figure 2.15.

To further investigate the potential of using these thiosemicarbazonate compounds (PFK7 and PFK8) in virostatic cocktails, the effect of PFK7 on RNR secretion was tested. PFK7 but not the complementary ligand significantly ($p = 0.003$) inhibited RNR secretion from PBMCs at 10 μ M. However, *in vitro* combination studies with ddl must still be performed to determine if there would be a synergistic anti-viral or immunomodulatory effect.

CHAPTER 5

COMPOUND EFFECTS ON VIRAL ENZYMES

SUMMARY

Background: A lot of success (in clinical use) has been achieved with inhibitors that target HIV enzymes, RT, PR and IN. To investigate the effect of the gold-based compounds on these viral targets, direct enzyme assays and computer aided *in silico* analysis were performed. In the direct enzyme RT and PR bioassays, the eleven new compounds (the three bimetallic phosphine thiolate complexes in class III and the thiosemicarbazone-based complexes and complementary ligands in class V) were tested while for the IN assay a preliminary study was performed for all twenty seven compounds. Compounds analysed in the *in silico* tests were mostly those which had demonstrated $\geq 50\%$ inhibition in the direct enzyme inhibitory assays.

Materials and Methods: The direct enzyme assays for RT were performed using a colorimetric kit and recombinant RT enzyme by ELISA while the PR assay was done using an HIV protease substrate and recombinant PR enzyme in a fluorogenic substrate assay. For the IN assay, ELISAs were performed using two different kits; a dual kit consisting of both 3' processing and strand transfer components and a second strand transfer specific kit. *In silico* studies were performed using the CDOCKER protocol in Discovery Studio®.

Results and Discussion: None of the eleven compounds from class III and V inhibited RT while PFK7 inhibited PR by 55.5% at a concentration (toxic to cells) of 100 μM ($p=0.03$). In a preliminary screen four complexes (EK231, PFK7, PFK8 and PFK174) inhibited IN by $\geq 50\%$ but not upon subsequent repeats. All twenty seven compounds were tested using the dual IN ELISA kit. For repeats, attempts were made to access additional kits but the manufacturer reported difficulties in developing kit components. The kit was again available several months later and the initial data was not reproducible. In the *in silico* docking studies favourable binding free energy predictions were obtained for five of the gold complexes in the RNase H site of RT, none for the PR site and five for the lens epithelium derived growth factor binding site of IN. Although favourable enthalpic contributions were noted for the RNase H site, size-shape complementarity and thus good binding affinity was lacking; the flatness of the RNase H binding pocket and the fact that the complexes lacked metal chelating groups (required by substrates binding to this site) may be responsible for this. PFK7 was predicted to interact more favourably with hotspot residues in the LEDGF binding site of IN and with better complementarity than the corresponding ligand or its analogues. Structure activity relationships were observed in the *in silico* studies for both the RNase H and the LEDGF site.

Conclusions: The binding affinities from the *in silico* predictions studies did not appear to represent stable interactions. This finding appeared to support findings from the direct

enzymes assays where inhibition was noted at toxic concentrations e.g. PFK7's inhibition of PR or the inconsistent results seen for IN. Although the RNase H site of RT and the LEDGF site of IN were favoured in the overall predictions, the favoured compounds would not in the current form inhibit or bind to these enzymes appreciably and will require structural optimisation through rational drug design to increase activity.

Keywords: enzyme inhibition, RT, PR, IN, direct enzyme bioassays, docking, mechanism of inhibition.

5.1 INTRODUCTION

The virally encoded RT, PR and IN are crucial enzymes in the life cycle of HIV and have been successfully targeted for ARV therapy. The combination of drugs that inhibit these enzymes especially RT and PR were the earliest to be used in HAART and lately IN inhibitors have been approved for clinical use and for inclusion in HAART or as salvage therapy for patients who have already developed resistance to existing combinations (McColl and Chen, 2010). The development of resistance by HIV to these drugs is the driving force for research towards the identification of novel inhibitors of these enzymes while efforts to identify new viral targets are also being pursued. A total of twelve RT inhibitors including eight NRTIs and four NNRTIs, have been approved for clinical use (de Bethune, 2010), nine PR inhibitors have been approved (Wensing *et al.*, 2010) and the most recent addition in terms of class being the IN inhibitor raltegravir which was approved by the US FDA in 2007 (McColl and Chen, 2010). HAART has led to significant declines in morbidity and mortality associated with HIV infection especially in countries where ARV medications are widely accessible (Bartlett *et al.*, 2007). Despite all the progress that has been made in terms of delaying disease progression, prolonging survival and improving the quality of life of patients (Antiretroviral Therapy Cohort collaboration, 2008), ARV therapy still fails to suppress HIV completely for both existing and even the newer classes of drugs (Marcelin *et al.*, 2009). The failure is mostly associated with the development of resistant viral strains leading to the accumulation of mutant forms (Ceccherini-Silberstein *et al.*, 2007, Cozzi-Lepri *et al.*, 2005, Clavel *et al.*, 2004, Hanna *et al.*, 2000). A troubling concern is the fact that there are few treatment options and strategies in the case of drug failure and/or cross resistance to the same class of compounds e.g. NNRTIs (Johnson *et al.*, 2005). Cross resistance has also been shown for the recently approved IN inhibitor raltegravir, and eltragravir (an IN inhibitor still in clinical trials, Marinello *et al.*, 2008). This rapid rate of drug resistance development by the virus and the associated cross resistance to drugs within the same class makes the quest for identifying novel therapy imperative while at the same time pursuing research on novel targets and vaccines. The toxicity associated with HAART and uncomfortable side effects (Yeni, 2006, Montessori *et al.*, 2004, Montaner *et al.*, 2003) are also some of the reasons driving the search for new and hopefully safer drugs.

In this study, enzyme assays were used in high throughput screening (96 well plate format) methods for identifying compounds that could directly inhibit RT, PR and IN experimentally in bioassays. However, because data from such experimental studies does not say much about the type of binding interactions made by the compound with the enzyme, computer aided studies were used to decipher this information (specifically molecular modelling or docking). Molecular modelling as defined by Richon, (1994), is the science or art of representing molecular structures numerically and simulating their behaviour with the equations of quantum and classical physics. It is important to note that both experimental and computational techniques have important roles in drug development and represent complementary approaches (Kapetanovic, 2008). The popularity of computer aided drug design goes beyond mechanistic exploration. It has been used in target identification and validation, in streamlining the drug discovery and development process, for optimisation of experimental findings as well as to eliminate compounds with undesirable characteristics using *in silico* filters (Kapetanovic, 2008, Tang *et al.*, 2006). Although recent trends in rational drug design studies begin with *in silico* analysis before synthesis and biological testing as proposed by Tarbit and Berman (1998), it should be noted that *in silico* studies are mainly predictions and must be validated experimentally. The approach in this study was synthesis based on the history of gold and complementary ligands as possible anti-HIV agents and on literature accounts on drug-likeness of the various ligands e.g. lipophilicity of the phosphine ligands (Shaw *et al.*, 1994) and the anti-viral activity of Tscs-base ligands (Easmon *et al.*, 1992, Spector and Jones, 1985). This was followed by HTS *in vitro* analysis and the *in silico* work was performed as a complementary approach to corroborate bioassay findings.

Gold compounds have previously been reported to inhibit HIV RT (Fonteh *et al.*, 2009, Fonteh and Meyer 2008, Sun *et al.*, 2004, Tepperman *et al.*, 1994, Okada *et al.*, 1993, Blough *et al.*, 1989) and to interact with proteins by undergoing ligand exchange reactions with sulfhydryl groups of cysteine residues (Shaw III, 1999, Sadler and Guo, 1998). The chrysotherapeutic effect of gold compounds was also reported in the inhibition of the lysosomal cysteine PRs (a family of proteases responsible for joint destruction in rheumatoid arthritis) through ligand exchange reactions with sulfhydryl group of cysteine (Gunatilleke *et al.*, 2008, Chircorian and Barrios 2004), making these compounds possible PR inhibitors. Although HIV PR is an aspartic PR, it was tempting to speculate that the presence of cysteine residues in the dimerisation interface of HIV PR (Zutshi and Chmielewski, 2000) could result in interactions with the gold ion. Inhibition of IN has not been reported for gold compounds but because the integration process involves viral cDNA, it is possible that gold complexes could intercalate with it since gold compounds have been reported to interact with DNA (Mirabelli *et al.*, 2002). This interaction could possibly result in the inhibition of IN activity.

Overall, the expectation for all three viral enzymes in addition to possible ligand exchange reactions and DNA intercalation was that since complexation has been reported to

lead to more stable compounds which stay at enzyme active sites longer and to increased drug efficacy (Navarro, 2009, Beraldo and Gambino, 2004), the gold complexes should be better inhibitors compared to the ligands.

In the next sections, findings obtained for the effect of the compounds on RT, PR and IN from both the direct enzyme and *in silico* binding predictions will be provided.

5.2 MATERIALS AND METHODS

Some of the compounds currently being investigated in this project have previously inhibited HIV RT and PR in direct enzyme assays (Fonteh *et al.*, 2009, Fonteh and Meyer 2009). The RT inhibitors were tested again as controls in the bioassays and *in silico* predictions of the binding modes with this enzyme were also done using molecular modelling. Compounds that inhibited PR in the direct enzyme bioassays were also analysed to predict potential binding modes using molecular modelling. The eleven new compounds that had not been tested before in both the RT and PR direct enzyme assays were also screened for the inhibition of these enzymes prior to molecular modelling of successful candidates. IN bioassays were initiated for all the compounds and repeated for compounds that showed promise in the pre-screen followed by molecular modelling.

5.2.1 Direct Enzyme-Based Assays

The direct enzymes assays included either sandwich ELISAs (RT and IN) or a fluorogenic substrate assay (PR). These are assays in which the compounds were allowed to interact with the enzymes in the presence of substrate and enzyme activity monitored in endpoint analysis either by determining absorbance or fluorescence.

5.2.1.1 RT inhibition assay

The Reverse Transcriptase Colorimetric kit (Roche Diagnostics, Mannheim, Germany) was used (assay principle pictured in Figure 5.1). This assay gives a quantitative measure of the RT activity and takes advantage of the ability of RT to synthesise DNA, starting from the template/primer hybrid poly (A) x oligo (dT)₁₅. Digoxigenin and biotin labelled nucleotides are incorporated into the same DNA molecule as it is freshly synthesized by RT. The detection and quantification of newly synthesized DNA as a parameter for RT activity follows a sandwich ELISA protocol where biotin-labelled DNA binds to the surface of streptavidin-coated microplate modules. An antibody to digoxigenin, conjugated to peroxidase (anti-DIG- POD) is then added and binds to the digoxigenin-labelled nucleotides. Finally, a peroxidase substrate, 2, 2'-azino-di-[3-ethylbenzthiazoline sulfonate (6)] diammonium salt crystals (ABTS), is added. The peroxidase enzyme catalyzes the cleavage of the substrate to produce a coloured reaction product. The absorbance of the samples is determined using a microplate (ELISA) reader, and is directly correlated to the level of RT activity in the sample.

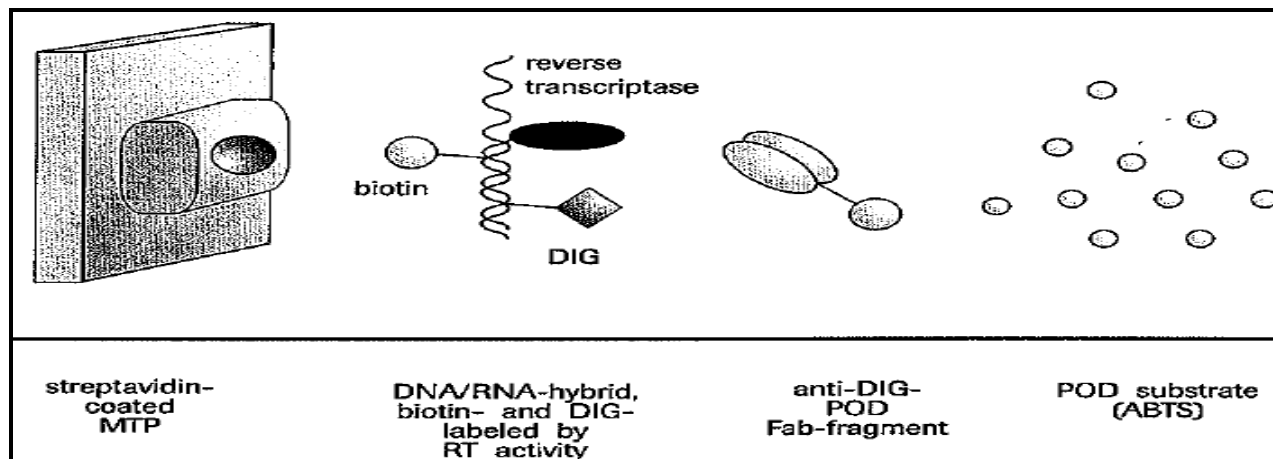


Figure 5.1: Reverse transcriptase colorimetric test principle. The test follows a sandwich protocol. The figure was adapted from the Roche Diagnostics colorimetric reverse transcriptase assay brochure (Version 13, 2010).

Procedure: The assay was performed according to the manufacturer's instructions and as previously described (Fonteh and Meyer, 2008). Briefly, 20 μ L (0.2U) of purified recombinant HIV RT (Merck, Darmstadt-Germany) and 20 μ L of reaction mixture consisting of reconstituted template-template/primer hybrid poly (A).Oligo (dT)₁₅ and diluted nucleotide (Tris-HCl, 50 mM, pH 7.8, with DIG-dUTP, biotin-dUTP and dTTP) were transferred to microfuge tubes containing 20 μ L of pre-determined concentrations of the compounds dissolved in DMSO and diluted with lysis buffer. This was followed by 1 h of incubation at 37 °C. The samples were then transferred to appropriate wells of a streptavidin-coated plate followed by another hour of incubation at 37 °C. The plate was washed 5 times with 250 μ L of wash buffer and blotted on paper towels to completely remove buffer before adding 200 μ L of anti-DIG-POD working solution (200 mU/mL). A further 1 h incubation at 37 °C followed by 5 rinses using wash buffer was performed. An ABTS substrate solution (200 μ L) was transferred into all wells of the plate and the plate(s) incubated at room temperature (15-25 °C) until sufficient green colour development for photometric detection was attained (approximately 15 min). Controls included RT only with an equivalent amount of DMSO used in the test samples (1.5%, v/v) while a positive control was a plant extract (designated known inhibitor or KI) for which anti-HIV data exists. The plate was read on a Multiskan Ascent[®] plate reader (Labsystems, Helsinki, Finland) at 405 nm and a reference wavelength of 492 nm. Data analysis was performed using Microsoft[®] Office Excel[®] 2007 (Microsoft Corporation, Washington, USA) with inhibition expressed as percentages and calculated based on the formula: $100 - [(Test\ reagent\ absorbance - Blank\ absorbance) / (untreated\ DIG\ control\ absorbance - blank\ absorbance) \times 100]$.

5.2.1.2 PR inhibition assay

This assay makes use of a fluorogenic HIV PR substrate 1 with structure: Arg-glu-(EDANS)-Ser-Gln-Asn-Tyr-Pro-Ile-Val-Gln-Lys-(DABCYL)-Arg (Sigma Aldrich, Missouri USA). This substrate is a synthetic peptide that contains a cleavage site (Tyr-Pro) for HIV PR as well as two covalently modified amino acids for the detection of cleavage (Matayoshi *et al.*, 1990).

One of the modifications involves the attachment of the fluorophore 5-(2-aminoethylamino)-1-naphthalene sulfonate (EDANS) to the glutamic residue. The other modification is the addition of an acceptor chromophore 4'-dimethylaminoazobenzene-4-carboxylate (DABCYL) to the lysine residue. The modified amino acids are on opposite sides of the cleavage site. Spatial orientation and overlap of the DABCYL absorbance with the EDANS emission permits resonance energy transfer between the two moieties and quenching of the EDANS fluorescence at 490 nm occurs. However, when HIV PR cleaves the peptide, the DABCYL group is no longer proximal to the fluorophore and emission at 490 nm cannot be detected. A compound that inhibits HIV PR therefore prevents this cleavage thus allowing quenching to occur such that the EDANS fluorescence signal is diminished.

Procedure: The assay was performed according to procedures by Lam *et al.*, (2000) using a 1 mM stock of HIV PR substrate 1 dissolved in DMSO and diluted to 20 μ M with assay buffer (0.1M sodium acetate, 1 M NaCl, 1 mM EDTA, 1mM DTT and 1 mg/mL BSA, pH 4.7). An aliquot of the substrate (20 μ M, 49 μ L) and 1 μ L of HIV PR solution (1 μ g/mL; Bachem, Switzerland) were added directly into Costar[®] black 96 well fluorescence assay plates (Corning Incorporated, New York, USA) in the presence or absence (untreated control) of the compounds to a final reaction volume of 100 μ L. This mixture was incubated at 37 °C for 1 h. Ten microlitres of acetyl pepstatin designated AP (Bachem BioScience Inc. PA, USA) at a concentration of 10 μ g/mL was used as a positive control for inhibition of HIV PR while a blank treatment consisted of assay buffer and the substrate only. The fluorescence intensity was measured at an excitation wavelength of 355 nm and an emission wavelength of 460 nm using a Fluoroskan Ascent[®] plate reader (Labsystems, Helsinki, Finland). The data was analysed using Microsoft[®] Office Excel[®] 2007 (Microsoft Corporation, Washington, USA) and the percentage inhibition calculated based on the formula: $100 - [(Test\ reagent\ RFU - blank\ RFU) / (untreated\ control\ RFU - blank\ RFU) \times 100]$ where RFU = relative fluorescence units.

5.2.1.3 IN inhibition assay

Two different direct enzyme assay kits were used for determining the effect of the compounds on HIV IN and thus on the integration process. The Xpress Bio HIV IN kit (Thurmont, Maryland, USA) which contains unprocessed viral DNA (due to the presence of dinucleotides at the 3' ends) such that both the 3'P and ST reactions can be executed (referred to as dual IN kit) and the Auro pure kit (Mintek, Johannesburg, South Africa) which was specifically designed for detecting ST IN inhibitors. Both assays mimic the integration process except for the fact that the target DNA in the Auro pure kit is modified to exclude the 3'P reaction (contains processed viral DNA with the dinucleotides at the 3' ends excluded) making it specific for determining ST IN inhibitors. The motivation for specifically targeting ST inhibition is because IN drugs currently in clinical use are the ST inhibitors unlike 3'P inhibitors (3'PIs) which have shown activity *in vitro* but not *in vivo* (Mouscadet *et al.*, 2010).

Procedure: The dual IN inhibitor kit (Thurmont, Maryland, USA) assay was performed according to the manufacturers' instructions. Streptavidin-coated 96 well plates were further coated with a double stranded HIV LTR U5 donor substrate oligonucleotide or donor DNA containing an end-labelled biotin for 1 h. This was followed by 3 washes and then by blocking with blocking buffer for 1 h. After 3 additional wash steps, full-length recombinant IN protein (200 nm, purified from bacteria) was loaded onto the oligo substrate and the plate incubated for 30 min at 37 °C. Non-toxic concentrations of the compounds were added in triplicate to the plate after 3 further washes and the plate was incubated for 5 min at room temperature. A different double-stranded target substrate oligo containing 3'-end modifications was added directly to the plate containing the compounds. The IN enzyme cleaves the terminal two bases from the exposed 3'-end of the HIV LTR donor substrate (3'P) and then catalyzes a ST reaction to integrate the donor substrate into the target substrate. The products of the reactions were detected colorimetrically using a horse radish peroxidase (HRP)-labelled antibody directed against the target substrate 3'-end modification and a tetramethylbenzidine (TMB) peroxidase substrate. A blank treatment without enzyme or test compounds and a control containing 10% (v/v) sodium azide (NaA₃) as positive inhibitor of IN activity were included in the analysis. The plate was read at 450 nm using a Multiskan Ascent® plate reader (Labsystems, Helsinki, Finland).

The Auro Pure kit (Mintek, Johannesburg, South Africa) assay was performed according to the manufacturer's specifications at the AuTEK Biomed Laboratory (Mintek, Johannesburg, South Africa). Briefly, biotin labelled donor DNA or donor substrate (processed) was added to streptavidin coated microwell strips and incubated for 1 h at 22 °C. The plates were washed 3 times with wash buffer followed by the addition of bacterially expressed recombinant HIV IN enzyme (1 µM). After 30 min of incubating at 22 °C and 2 wash steps, the test compounds and controls were added to the plate and allowed to interact for a further 30 min. The target DNA or target substrate was then added to the mix and after another hour of incubation at 37 °C, the plates were washed 3 times and a detection antibody added to the wells and incubated (2 h, 25 °C). Three last washes were performed and a substrate reagent added into each well. The plate was sealed and incubated at 37 °C for 1 h followed by absorbance measurements at 620 nm on an xMark™ Microplate Absorbance Spectrophotometer (Bio-Rad Laboratories Inc., California, USA). Inhibition percentage calculations for both IN assays were done using Microsoft® Office Excel® 2007 (Microsoft Corporation, Washington, USA) and the formula: $100 - [(Test\ absorbance - blank\ absorbance) / (control\ abs - blank - absorbance)] \times 100$.

5.2.2. Molecular Modelling to Predict Potential Binding Sites

In this section, the term receptor will be used to represent the target enzyme also known as “receiving” molecule or protein i.e. RT, PR or IN. Ligand (a computational

terminology) will be used to refer to both the gold complexes and precursors (free or uncomplexed compounds) and is defined as the complementary partner molecule, which binds to the receptor.

To perform a direct or protein-based docking study where the active site is known, unlike indirect or ligand-based docking where the active site is not known (Vaidyanathan *et al.*, 2009), one of the first requirements is to obtain 3D crystal structures of the receptor which must have been solved by x-ray crystallography or NMR (Raha *et al.*, 2007). The next important requirement is a database of the ligands to serve as inputs in the docking program. The crystal structures of RT, PR and IN were obtained from the protein data bank (<http://pubchem.ncbi.nlm.nih.gov/>) and the ligands were compounds, which had inhibited these enzymes in direct enzyme assays. After docking (also known as searching), scoring functions are usually employed to help in predicting the binding affinity of the ligands to the receptor (Wu *et al.*, 2003).

Molecular modelling studies were done using Discovery Studio® version 2.5.5 (Accelrys®, California, USA). All simulations were performed on an Intel® Core™ 2 Duo CPU 2.2 GHz processor, 1.97 GB RAM with Windows XP professional version 2002 operating system. These specifications were the minimum recommended for DS® installation and performance. Higher specifications should lead to lower computational costs and thus faster run rates. The next subsections will outline the steps that were performed in order to simulate the interactions of the ligands with the receptors and to determine binding affinity.

5.2.2.1 Ligand preparation

Ligand preparation involved obtaining molecular structures, which had to be in the structural data file (.sdf) or molecular file (molfile) chemical format and these were obtained using the ChemDraw software (CambridgeSoft, PerkinElmer Inc., USA). Considering that molecular modelling greatly depends on molecular properties, for modelling to be useful, it must readily and reliably reproduce properties that resemble those of experimentally obtained data (Comba and Hambley, 1995). One of the commonly applied models for determining molecular properties is molecular mechanics (MM), which calculates the structure and strain (deformation of a molecule resulting from stresses) of a molecule based on known reference structures and properties to give it a geometry with minimum strain energy. An example of such a model is the Chemistry at Harvard Macromolecular mechanics or CHARMM force field.

Unlike in the ADMET prediction studies where the only required preparative phase was the application of CHARMM force fields and minimization of the ligands, for the docking studies, a further ligand preparative step was involved. This is because the CHARMM force field in the docking algorithm that was used in Discovery Studio® does not have force fields assigned for gold or other transition metals. This complication arises from the fact that these transition metal ions have partially filled d-orbitals (Comba and Hambley, 1995, Hay, 1993).

These partially filled orbitals result in the diverse structures of coordination compounds with a large variety of possible coordination numbers and geometries (Comba and Hambley, 1995, Hay, 1993). Developing reference structural and strain energy values for metal complexes is a daunting task (Comba *et al.*, 2006) and is therefore not feasible. Instead, a combined quantum mechanics and molecular mechanics (QUANTUMm also designated QM/MM) computation was performed to calculate all-atom force fields for each ligand. In this approach, some atoms were treated by classical MM (CHARMm) and others treated by QM (DMol3) thereby combining the advantages of the two approaches. QM is significant in describing chemical interactions that involved the breaking and formation of covalent bonds and unlike MM, does not assume that the nature of the bonding does not change with the structure and is thus applicable to metal complexes (Höltje *et al.*, 2003, Comba and Hambley, 1995). For the calculation, the gold atom was ionised by deleting the covalent bonds, then assigning formal charges, followed by constraining bond angle distances thus simulating a covalent bond while calculating the force fields. CHARMm normally omits from the nonbonded lists any interactions that include only fixed atoms and would therefore not proceed with docking if these unknown atoms were not fixed through the addition of constraints, restraints and QM/MM minimisation. The QM/MM minimisation also gives the ligands better geometries and removes steric overlap that could produce bad contacts before the dynamics (heating and cooling) process that is involved in docking. For all QM/MM calculations the parameters sets included a QM/MM boundary set to a nonbond list radius of 10.0-12.0 Å, where the electronic embedding method was to neglect boundary charges. The type of DFT exchange-correlation potential chosen was the gradient-corrected (PBE) potentials. The atomic spin state were treated such that the spin was restricted if the number of electrons in the system was even. A medium quality of the Dmol3 calculation was set. After minimisation, the constraints and restraints on the gold and bonded atoms e.g. P-Au-Cl were removed, the bonds and the formal charges restored. Although constraints followed by QM/MM calculations could have been applied to gold and bonded atoms for the compounds in the ADMET studies, it was not necessary since CHARMm and Dmol3 force fields are not included in the ADMET prediction protocol.

5.2.2.2 Receptor preparation

Published crystallographic structures of the respective receptors (HIV RT, PR and IN) in complex with active site identification ligands were obtained from the PDB. The receptors were either wild type or mutant forms. Where possible, subtype C crystal structures were used to increase the relevance and specificity of potential inhibitor(s) to the South African/Sub Saharan African context where subtype C is prevalent. Crystal structures of subtype C receptors were unfortunately not readily available just as was the case for the recombinant enzymes used in the direct enzyme assays since research has focused largely on the subtype B viral strain. In the case of RT, It was important to determine whether the compounds

inhibited the enzyme by binding to the RNase H site or the NNRTI site. Binding at the NRTI site was not sought since these compounds are not dNTP analogues (e.g. zidovudine and ddI, Figure 2.8). Therefore, only crystal structures of receptors complexed to known inhibitors of the RNase H and NNRTIs sites were obtained. Docking was also done on a third site of RT recently shown by Su *et al.*, (2010) to be an allosteric inhibitory site close to the NNRTI pocket. The PDB identification codes for the RT receptors are 3LP2 (Su *et al.*, 2010) for the NNRTI allosteric site and 3LP3 (Su *et al.*, 2010) in complex with naphthyridinone-containing RNase H inhibitor site while the 2WON PDB structure (Corbau *et al.*, 2010) was used for predicting binding to the NNRTI site. The RT crystal structures were of wild type strains. In the case of HIV PR, two crystal structures were used; 1HXW in complex with ritonavir (Kempf *et al.*, 1995) coding for a subtype B strain and 2R5P (Coman *et al.*, 2008) coding for a subtype C viral strain. The crystal structures employed for predicting binding interactions with IN were the 2B4J structure which is the crystal structure of the CCD of IN complexed to LEDGF/p75 (Cherepenov *et al.*, 2005) at the dimer interface of the enzyme. This site has been used by Christ *et al.*, (2010) to determine small molecule inhibitors of protein-protein (IN-LEDGF) interactions. Other sites that were used for predicting IN inhibition were the ISQ4 site complexed to the 5-CITEP inhibitor found in the Asp64, Asp116 and Glu152 motif of IN (Goldgur *et al.*, 1999) and the binding site for sucrose identified in 3L3V (Wielens *et al.*, 2010) both in the CCD of IN. A summary of all the receptors used is provided in Table 5.1. The PDB identification codes, resolution and information on whether the structure is a mutant or wild type are provided. The smaller the resolution, the better the crystal structure is. Resolutions of 2.8 Å and below were considered sufficient for this study.

Table 5.1: A summary of the protein data bank crystal structures used for molecular modelling. Three crystal structures were used for RT, one with an allosteric binding site, another with an RNase H and a third with a polymerase or NNRTI binding site, two for PR consisting of a clade B and a C variant, and three for the IN consisting of an allosteric binding site in complex with sucrose, one in the LEDGF binding site at the dimer interface of IN and a third in the DNA binding site (3'P and ST site).

Protein	PDB code	Notes	Wild type/mutant	Resolution (Å)
HIV RT	3LP2	Allosteric site near NNRTI site	Wild type	2.8
	3LP3	RNase H site	Wild type	2.8
	2WON	NNRTI site	Wild type	2.8
HIV PR	1HXW	Subtype B	Wild type	1.8
	2R5P	Subtype C	Mutant (Q7K, L33I, L63I)	2.3
HIV IN	3L3V	CCD in complex with sucrose (allosteric site to LEDGF site)	Mutant (C56S, W131D, W139D, F185H)	2
	2B4J	CCD bound to LEDGF (at dimer interface)	Mutant (F185K)	2.02
	ISQ4	CCD (DNA binding site)	Mutant F185K, W131E	2.1

Binding site sphere definition: Before the docking simulations could be initiated, a protein clean process was performed and a binding site sphere defined on the receptor. The protein clean process involves the addition of hydrogen atoms to the amino acid residues of the

receptor and the removal of unnecessary groups e.g. water molecules. Decisions on maintaining groups such as cofactors, active site crystal water molecules, and catalytic metal ions had to be made. Ultimately the importance of these molecules or ions in the activity of the enzyme had to be considered and usually such groups were maintained. Docking with active site waters for example has been shown to result in increased accuracy of docking (Höltje *et al.*, 2003). A ribbon structure of the receptor was then displayed followed by the application of a CHARMM force field and partial charges (charges on polar molecules due to differences in electronegativity), Momany and Rone (1992). The co-crystallised ligand or active site identification ligand was used in defining the binding site sphere which is an area around the bound inhibitor in the three axis direction (xyz) with a minimum radius of 5 Å (see Figure 5.2 for a typical binding site sphere). Once the active site sphere had been defined, the co-crystallised ligand within the sphere was removed by highlighting and deleting using keyboard commands.

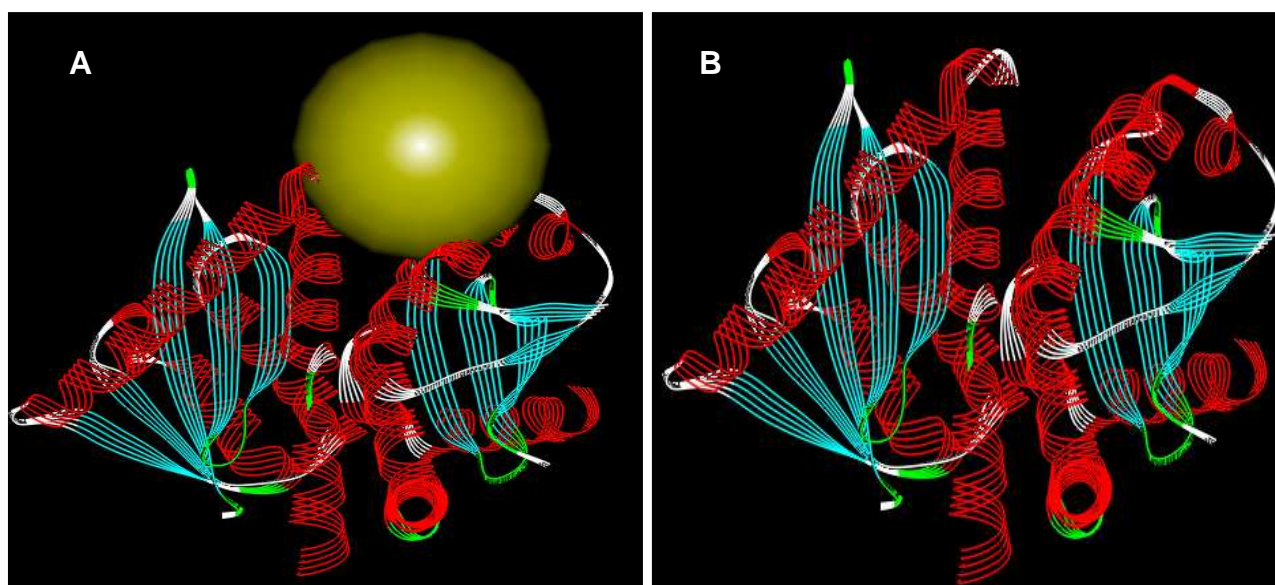


Figure 5.2: Binding site sphere (yellow ball in A) in the catalytic core domain of IN (2B4J). In (B) sphere has been removed. The sphere radius is 11 and the xyz coordinates with respect to the active site are 12.08, -18.587 and -11.632. This sphere was generated within one of the catalytic dimer interfaces specifically in the IN-LEDGF binding site (also shown in figure 2.17). Here the IN binding domain (depicted in Figure 2.17) of LEDGF has been removed and replaced with the binding site sphere in preparation for docking. This figure was obtained from Discovery Studio (Accelrys®, California, USA).

5.2.2.3 Docking with CDOCKER

The next step after ligand and receptor preparation was for docking to be initiated. This was done using CDOCKER (CHARMM-based DOCKER, Wu *et al.*, 2003), a grid-based molecular docking algorithm that employs CHARMM molecular dynamics in DS® (Accelrys®, California, USA). It allows one to run refinement docking of any number of ligands with a single protein receptor. The receptor is held rigid while the minimized ligands are allowed to flex during the refinement. Ligand placement in the active site was specified using the binding site sphere and the grid method helps to reduce computation time while facilitating molecular dynamics interactions between receptor and ligand atoms. The calculated QM/MM force fields

for the ligands (with the gold atom accounted for) were used in the docking and not the default CHARMM-based force fields. Random ligand conformations (poses) are generated from the initial ligand structure through high temperature molecular dynamics, followed by random rotations. The random conformations are refined by grid-based simulated annealing which involves intermittent cooling by decreasing simulation temperature. The final energy minimization during docking was set as “off” and a separate minimization step (below) was performed instead.

5.2.2.4 Ligand minimization

A separate minimisation step was launched which minimizes the series of ligand poses (a pose being a unique target bound orientation and conformation of the ligand after docking) using CHARMM and helps to filter the poses and ensure diversity while improving on the docking accuracy (Krovat *et al.*, 2005, Wu *et al.*, 2003). Generally, minimization (performed before and after docking) reduces the energy of a structure through geometry optimization. The minimization of the poses was done in the presence of the receptor. In the protocol, the receptor is held rigid and residues with atoms inside the minimization sphere of flexible atoms are allowed to be move. This strategy helps minimise computational costs (time) involved when the entire receptor is flexible (Krovat *et al.*, 2005). The protocol used was customized to include an implicit solvent model (generalized born with molecular volume) which allows for the calculation of the binding free energy between the receptor and ligand while mimicking solvent effect (Mohan *et al.*, 2005). This is because protein surface interactions occur in aqueous solution making the description of solvation forces and energies due to solute-solvent effect critical in modelling (Sun and Latour, 2006).

5.2.2.5 Energy calculations and analysis of minimized poses (Scoring)

Docking is usually performed together with scoring functions to predict the binding affinity of the ligands (Wu *et al.*, 2003). This was done by calculating the energy of binding represented as binding free energy and given in kcal/mol followed by analysis of the docked poses. The “calculate binding energy” protocol was used and the calculated QM/MM force fields employed for the ligands. The protocol estimates binding free energy between each ligand pose and the receptor using CHARMM implicit solvation models. The free energy of binding for a receptor-ligand complex is calculated from subtracting the energy of the ligand and that of the receptor from the energy of the complex and is given by the formula:

$$\text{Energy of binding} = \text{energy of complex} - \text{energy of ligand} - \text{energy of receptor}.$$

Energy calculations were done for each pose, and the binding free energies ranked from the lowest to highest with the former representing the most favourable receptor-ligand interaction in terms of binding affinity (Muegge and Rarey, 2001).

Further scoring analysis was done using, the “analyse ligand poses” protocol in DS[®]. It helps in determining heat maps, short distances between atoms, electrostatic interactions and generally aids in further interpreting the binding modes between the ligand and the receptor as realistic or not. The pose predicted to have the most favourable binding free energy with the receptor was then mapped using 2D drawings, molecular surface diagrams (depicting hydrophobicity) followed by molecular graphics generation.

Docking controls: To ensure that the ligand orientations and positions predicted by the docking studies were likely to represent valid and reasonable potential binding modes, the active site identification ligands (co-crystallised ligand) were docked using the customised CDOCKER docking parameters and the prepared sphere selections for each of the binding sites. The interactions were considered acceptable when the predicted binding orientations were comparable to the expected orientation and position of the inhibitor observed in the crystal structures.

5.2.2.6 Summary of methods used

A flow diagram of the methods that were used in determining the interactions of the compounds with HIV enzymes is depicted in Figure 5.3. Both “wet lab” and *in silico* (docking) methods were followed.

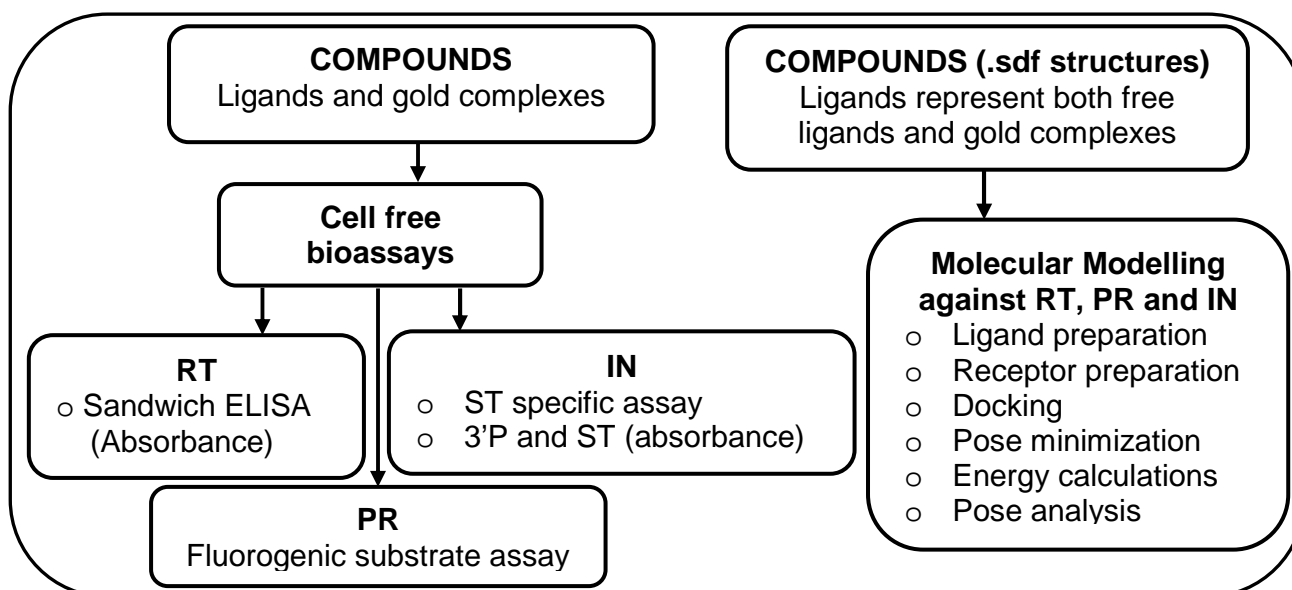


Figure 5.3: Summary of methods used in determining the effect of the compounds on viral enzymes.

5.3 RESULTS AND DISCUSSION

5.3.1 Direct Enzyme Assays

5.3.1.1 HIV RT and PR activity

Compounds tested for RT and PR inhibition included the Tscs-based compounds; PFK5, PFK7, PFK6, PFK8, PFK39, PFK41, PFK38 and PFK43 and the gold(I) phosphine thiolate complexes; PFK174, PFK189 and PFK190. No inhibition of RT was recorded at 25 and 100 μM (only 25 μM is shown, Table 5.2) and only one compound significantly inhibited

HIV PR activity by >50% (Table 5.2). This was the gold(III) thiosemicarbazonate complex, PFK7, which inhibited the enzyme by 55% at 100 μM ($p = 0.03$). Its free ligand PFK5 had no effect on PR's activity. Unfortunately 100 μM (which is the same concentration at which compounds tested in the prior study inhibited PR, Fonteh and Meyer, 2009) is toxic to all the cell types for which cytotoxicity measurements were performed suggesting poor specificity. PFK7 is cytostatic (at 5 and 10 μM , Figure 4.7B) and was not really expected to have a direct anti-viral effect (for either RT or PR) since cytostatic agents target cellular components (Lori *et al.*, 2005). While the higher concentration of PFK7 appears to have a direct anti-viral effect, this ability is not of any value since this concentration was also very toxic (the CC_{50} of this compound was 5.6 in PBMCs and 1.7 in PM1 cells, Table 4.2). However the compound can interfere with viral replication through its effect on the host cell at non-toxic but cytostatic concentrations (Figure 4.6, 4.7B, 4.8A).

Table 5.2: The effect of the compounds on HIV RT and PR activity. None of the compounds inhibited RT's activity while PFK7 inhibited PR at 100 μM by 55.5%. KI represents a known inhibitor which inhibited RT by 94.7% and PR by 100%. PFK7 inhibited PR by 55% at 100 μM ($p=0.03$). Ligands are shaded in grey.

HIV RT Inhibition		HIV PR Inhibition	
Compound	% inhibition at 25 μM	Concentration (μM)	% inhibition
KI	94.7	16	100.2
H ₂ AuCl ₄ ·4H ₂ O	-14.0		30.43
PFK189	23.7		35, 49
PFK190	10.5		34, 48.7
PFK5	9.55	2.5, 100	14, 15.4,
PFK7	14.7	2.5, 25, 100	-5, 5.8, 55.2
PFK6	9.36	5, 100	-8.8, 0.14
PFK8	5.35	5, 25, 100	1.3, 5.3, 16.7
PFK39	7.86		ND
PFK41	6.39	0.2, 100	-12., 12.9
PFK38	-8.68		ND
PFK43	11.26	0.04, 100	-9, 2.8

Eight gold complexes (TTC3, TTC10, TTC17, TTC24, EK207, EK219, EK231 and KFK154b) previously shown to inhibit RT at a concentration range of 6.25 to 250 μM (Fonteh and Meyer, 2009, Fonteh *et al.*, 2009, Fonteh and Meyer, 2008) were re-tested as controls in the present study. None of the compounds inhibited RT's activity at 25 and 100 μM (only 25 μM is shown, Table A5.1). These unexpected results triggered a search for reasons and explanations. The most serious of these was the possibility that degradation products not visible on NMR spectra (when stability studies were performed, chapter 2 in section 3.4.1) were present in addition to storage, compound age and dissolution related concerns. All the compounds previously published as active were freshly synthesised and tested in the same manner. These compounds were now re-tested after three years of storage at -20 °C in powder form and sometimes dissolved in DMSO (used within a week, for KFK154b, storage

was at room temperature for a year and a half prior to testing). These storage conditions were obviously not optimal and the inherent hygroscopic abilities observed for some of these complexes (e.g. TTC3 and possibly its analogues, Table 3.7) could have potentiated solubility issues. Newly synthesised compounds (eleven in total) did not have similar storage issues and may simply have no RT/PR inhibitory abilities. When taking into account docking predictions which resulted in limited active site binding (full discussion in section 5.3.2) as well as the low ADMET solubility predictions for some of these previously active compounds, the absence of activity is somewhat confirmed. Possible additional reasons for the loss of RT activity are provided in the appendix (section 8.4)

5.3.1.2 HIV IN activity

Inhibition of HIV IN activity was performed using two different kits, one involving both 3^{P} and ST inhibitor steps and the other specific for ST inhibitors. In a preliminary assay using the dual IN kit, all 27 compounds including the gold starting material ($\text{HAuCl}_{4.4}\text{H}_2\text{O}$) were tested in triplicate at one concentration (Figure A5.1A). Four compounds inhibited HIV IN by >50% at non-toxic concentrations when this assay was done and included the BPH gold(I) complex, EK231 (50.8%), the gold(III) thiosemicarbazonate complexes PFK7 (54.5%) and PFK8 (58.6%) and the gold(I) phosphine thiolate complex PFK174 (78%). Ligands PFK5 and PFK6 inhibited the enzyme in this assay by 47.5 and 47% respectively suggesting that the ligands contributed in the inhibition. New kits were purchased to perform repeat experiments and the problems mentioned in the abstract were experienced. In the repeat experiments, percentage inhibitions were mostly negative values at three different concentrations (2.5, 5, 10, and 25 μM) and were all rounded off to 0% (Figure A5.1B). The assay was performed 3 times with similar results each time. The positive control inhibited the enzyme by $99.9 \pm 0.3\%$. The reason for this change in results between kits is not clear and might have been poor performance of the kits. For both the initial and subsequent kits, the positive control worked very well. The company from which the kit was obtained had manufacturing problems for some time and we had to wait for up to 8 months to be able to repeat the assay. Communication with the manufacturers did not lead to clarification of the discrepancies and the assumption was that the manufacturing problems might have been the cause. While these concerns are valid, one could postulate that some of the same reasons that were attributed to the compounds that inhibited RT previously and which subsequently lost the inhibitory ability may be applicable here (particularly poor aqueous solubility, aging, the presence of degradation products not detectable by NMR and solvent effects, see section 8.4.1). The first concern (poor aqueous solubility) does not apply to the gold(III) bithiosemicarbazonate complexes since these compounds had good prediction values in the ADMET study and in the experimental shake flask method but are applicable to complexes EK231 and PFK174 (Table 3.8A, section 3.4.3). The eleven additional compounds had only been stored for a year and a

half (in the course of analysis). While solvent effects could have played a part, it is important to note that cytostasis was not affected. The same sample of PFK7 which inhibited IN in the pre-screen was also cytostatic at the time and remained cytostatic when additional repeats were recently (close to the time of writing) performed.

In the ST specific assay, representative compounds (consisting of those that had initially inhibited IN in the dual inhibitor assay pre-screen) from each class i.e. TTL24, TTC24, EK231, MCZS1, KFK154b, PFK5, PFK7, PFK8, $\text{HAuCl}_4 \cdot 4\text{H}_2\text{O}_4$ and a positive control for IN inhibition (NaA_3) were tested (Figure 5.4). None of the compounds inhibited the ST activity of HIV IN including those that had inhibited IN by > 50% in the dual IN inhibitor assay pre-screen. NaA_3 (6%) inhibited the enzyme by 77.5%. Although both 3'P and ST inhibitors have been reported in *in vitro* tests, only the latter have been successful *in vivo* and have subsequently been approved for clinical use (Mouscadet *et al.*, 2010, Chirch *et al.*, 2009) making their identification important. The fact that none of the compounds that had inhibited IN in the dual assay did so in the ST specific study suggests that inhibition of the enzyme in the former could have been at the 3'P step. Considering that subsequent testing in the dual assay resulted in no inhibition, it is likely that the compounds were neither 3'P nor ST inhibitors. Failure of 3'P inhibitors to inhibit *in vivo* was the reason why the inconsistent data was not investigated further. The ST specific data was therefore considered more significant and the conclusion was that no IN inhibition was exhibited by the compounds.

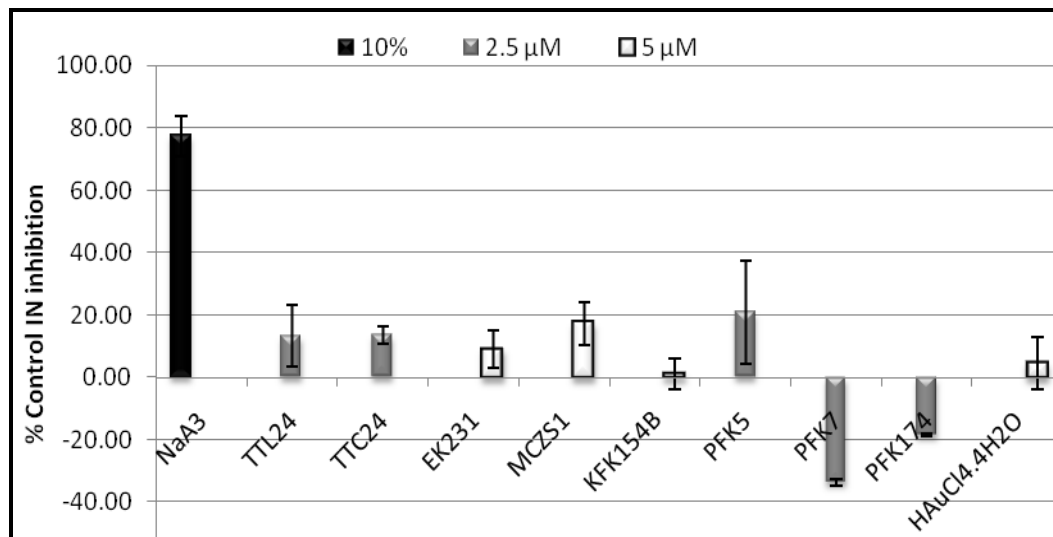


Figure 5.4: HIV IN inhibitory activity of representative compounds from different classes. The effect of the compounds on the enzyme was determined using the ST specific IN assay kit. None of the compounds significantly inhibited the enzyme (all p values were > 0.05). NaA_3 was used as a positive control for IN inhibition and inhibited the enzyme 77.5%. Concentrations tested here are those which resulted in >60% viability in the viability assays.

5.3.2. Molecular Modelling for Predicting Binding Interactions with Enzyme Active Site.

The selection criterion for the ligands (gold complexes and free ligands) chosen for molecular modelling studies was the fact that the latter had inhibited the enzyme in the respective direct enzyme bioassays. In the case of RT and PR these were compounds reported by Fonteh *et al.*, (2009), Fonteh and Meyer (2009) and herein (Table 5.2) as having

inhibitory activity while for IN, those which inhibited in the preliminary dual inhibitor assay (Figure A5.1) were tested. The respective ligands for each receptor are shown in Table 5.3. The phosphine gold(I) complexes; TTC3, TTC10, TTC17, TTC24 and the BPH gold(I) complexes EK219 and EK231 inhibited RT while one phosphine gold(I) complex TTC24, the BPH gold(I) complex, EK208, two phosphine gold(I) thiolate-based complexes (MCZS1 and MCZS3) and a gold(III) thiosemicarbazone complex (PFK7) inhibited HIV PR. Four Tscs-based ligands (PFK5, PFK7, PFK6, PFK8) and a phosphine gold(I) thiolate complex PFK174 were also tested based on preliminary findings which showed that these ligands could inhibit IN by at least 48% when the xPressbio dual inhibition assay kit (Thurmont, MD, USA) was used (data is in the appendix Figure A5.1). Although subsequent screening with the same dual assay kit resulted in 0% inhibition (Figure A5.1B), it was important that these findings be further confirmed by an alternative method such as molecular modelling. This was also the rationale for docking the compounds that had previously shown RT inhibitory ability but which had later lost this property upon re-test (section 8.4.1, Table A5.1). This is because for compounds with favourable interactions in the *in silico* study, structural modifications can be recommended to enhance drug-likeness through rational drug design. In addition the *in silico* studies obviate the need for investing in new synthesis while at the same time determining if there was a correlation between experimental data and docking findings.

Table 5.3: Summary of compounds that inhibited HIV RT, PR and IN in direct enzyme bioassays. Compounds which inhibited previously (Fonteh and Meyer 2009, Fonteh *et al.*, 2009) and those for which inhibition was observed here (grey) are represented. Except for PFK5 and PFK6 with inhibitions of 45≥50%, the rest of the complexes inhibited by >50%.

RT inhibitory ability		PR inhibitory ability		IN inhibitory ability	
TTC3	EK231	TTC24	MCZS3	EK231	PFK7
TTC10	KFK154b	EK208	PFK7	PFK174	PFK6*
TTC17	EK207	MCZS1	KFK154b	PFK5*	PFK8
TTC24	EK219				

The binding of a ligand to a receptor depends on ionic interactions, hydrogen bonds, hydrophobic interactions, van der Waals and dipole interactions that can be established between the two (Sahu *et al.*, 2008). Other defining conditions for the interaction of a ligand with a receptor are its three dimensional characteristics which include size, stereochemical orientation of functional groups as well as physical and electrochemical properties. After the docking process, various numbers of unique conformations were generated for each ligand and this occupancy rate indicates ligand flexibility (Purohit *et al.*, 2008). In addition to giving some perception of the flexibility of the different ligands in each receptor site, differences in the variation between classes of ligands for a particular receptor site compared to the variation within a class could be observed. The variation within classes was usually less compared to that between classes probably because of the structure similarity of the latter. The more flexible a ligand is, the greater the ensemble of ligand-receptor conformations that it can have and the more likely it is to have good overall size-shape complementary and thus more

favourable enthalpic contributions to the binding free energy. Such inhibitors have a higher chance of remaining active in the event of a mutation (although with lower efficacy) since an alternative binding conformation is easily attainable. Flexibility is also linked to the number of rotatable bonds that a ligand has. A summary of all the docked poses for each of the receptor sites for successfully docked compounds is shown in the appendix (Table A5.2).

Further investigation of the binding affinity of the ligands to the receptors was based on the binding free energy. Generally the more negative the binding energy, the greater the affinity between an inhibitor and its receptor (Sadiq *et al.*, 2010).

Not all compounds for which docking was initiated was successful. In some cases, either the binding free energies predicted were too high, depicting unfavourable interactions while in others, refined poses were not possible probably because of very poor stereochemical orientation or size-shape complementarity. While such a problem could be addressed by scaling the receptor site to accommodate the ligand, it is usually advisable to maintain the default parameters (Friesner *et al.*, 2004), which was the case in this study. A summary of the most favourable binding free energies of the successfully docked ligands in the various receptor active sites are shown in Table 5.4. Binding free energies below 100 kcal/mol are shown for the gold complexes with the exception of gold complex TTC3 and free ligands TL17 and TTL24 (Table 5.4) whose energies are provided for comparison purposes. Although amino acid atoms within 4 Å of the ligand were identified as those interacting with the latter, bond distances of relevant dipole interactions beyond 4 Å (particularly those of cation- π and π - π interactions) were also identified and are represented in Table 5.4. A majority of the binding free energy values shown in Table 5.4 were not negative suggesting that the reactions were not spontaneous or self driven. The ranking and further discussions are meant to serve as aids in describing the affinity of the compounds with the various receptors with the intention that these might serve as guides for optimising SAR for these compounds.

A table representing the twenty amino acids is shown in the appendix to aid in their identification. The three and one letter identification codes as well as classification based on hydrophobicity (non polar), polarity, polar acidic and polar basic properties are represented (Table A5.3). In the following subsections the interactions and binding affinities of the ligands with the various active site amino acid residues will be elaborated on.

5.3.2.1 Binding modes between ligands and RT sites

Docking was done for three different sites of RT namely the RNase H site (3LP3), a second site close to the NNRTI site (3LP2) and the NNRTI site (2WON). Very unfavourable binding energies were predicted for the NNRTI site suggesting poor binding affinity and for this reason no further analysis were done. This finding was not surprising considering that traditional structure-based design of NNRTIs has generally been complicated by the fact that

RT has considerable conformational flexibility (Hsiou *et al.*, 1996, Kroeger *et al.*, 1995, Jäger *et al.*, 1994).

Table 5.4: Summary of predicted binding free energy values and relevant bond distances obtained after molecular modelling. The lowest binding energies for the respective ligands are shown and represent the most favourable binding poses for each receptor site. The most favourable binding predictions for RT were with the RNase H site (3LP3) while those for IN were with the LEDGF binding site (2B4J). The free ligands are colour coded in a darker grey. The superscript (^a) represents a pi-pi stacking interaction.

HIV RT							
Compound	3LP2			3LP3+ Mn ²⁺		3LP3- Mn ²⁺	
	Energy	H-bond	Cation-pi	Energy	Cation/pi-pi	Energy	Cation-pi
TTC3	243			18.7		-9.4	
TTL10	84.2			76.6			
TTC10	87.7		3.5, 3.8	10.9	6	0.21	2.8
TTL17	299						
TTC17	85.9			25.7		5.1	
TTL24	182			78.6			
TTC24	57.2	2.3, 1.9	3.8, 5.4	12.3	4.6 ^a	0.52	
KFK154B	86.3			10.4			
HIV IN							
Compound	3L3V			2B4J			
	Energy	H-bonds		Energy	H-bonds		
PFK5	40.1	2.9, 1.7, 2.4, 2.2		8.9	2.2, 2.5		
PFK7	42.3	2.4, 2		13.2			
PFK8	42.1			15.7			
PFK41	40.4			18.2	2.4, 1.7		
PFK174				7.2			

Figure 5.5 represents annotated structures of ligands TTC3 and TTC24 which will subsequently be important in describing binding predictions with the RNase H and the 3LP2 receptor sites for which much more favourable binding free energies were obtained. The phenethyl amine portion of TTC3 also present in TTC17 (a), the *N,N*-dimethyl-ethane-1,2-diamine group of TTC24 also present in TTC10 and (b) the diphenylphosphanyl-benzyl portion common to all the ligands in this group are shown as inserts.

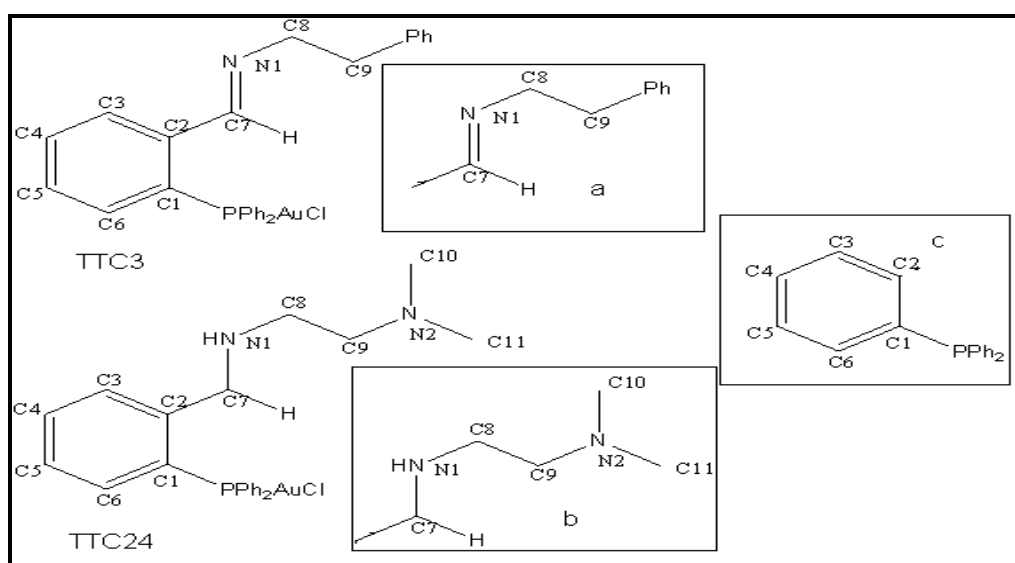


Figure 5.5: Annotated structures of TTC3 and TTC24 and important groups. The figure also shows the phenethyl-amine group of TTC3 (a), the *N,N*-dimethyl-ethane-1,2-diamine group of TTC24 (b) and the diphenylphosphanyl-benzyl portion present in all the ligands and complexes in this class as inserts.

Predicted binding interactions with the RNase H site: The RNase H site contains two metal ions (Mn^{2+}) that are ligated to active site carboxylate residues of Asp443, Glu478, Asp498 and Asp549 which are both needed in binding the substrates of this site and catalyzing the phosphodiester bond hydrolysis (Jochmans, 2008). The crystal structure used for this study (3LP3) was recently derived by Su *et al.*, (2010) into which the authors predicted the binding interactions of the metal binding naphthyridinone compounds (compounds that contain groups that can bind to the active site metal ions) designated MK1, MK2 and MK3. Docking in this site resulted in lower binding free energies compared to the 3LP2 site (Table 5.4). The lowest binding free energy of 10.4 kcal/mol was noted for the gold(III) pyrazolyl complex (KFK154b). This was followed by the gold(I) phosphine chloride complexes in the order TTC10<TTC24<TTC3<TTC17 with binding free energies of 10.9, 12.3, 17.8, and 25.7 respectively (Table 5.4). The order here did not correspond with that noted for the bioassays, where TTC24 was the most potent inhibitor followed by TTC10 and then TTC17 and TTC3 (Table 5.3). However, preference for the *N,N*-dimethyl-ethane-1,2-diamine group present in TTC10 and TTC24 over the phenethyl-amine group in TTC17 and TTC3 was observed.

Predicted interactions with the RNase H site in the presence of Mn^{2+} ions: In Figure 5.6 A and B, the interactions of TTC10 and TTC24 with the RNase H site in the presence of the Mn^{2+} ions are shown. The receptor in Figure 5.6 and those in the rest of this report are coloured according to the Kyte and Doolittle (1982) hydrophobicity profile.

A cation- π (6 Å distance) interaction was predicted between the phosphate group of the 2-diphenylphosphanyl-benzyl portion of TTC10 and the imidazole ring of His539 (Figure 5.6A). Hydrophobic interactions were also predicted in the binding between the ligand and Ala538. The significance of the interaction with Ala538 is that it could confer specificity in the binding affinity of the compound since in human RNase H1 this group is replaced by Gly538 (Su *et al.*, 2010). In addition, Ala538 has been reported to interact with Asp549 which forms a critical hydrogen bond with water facilitating RNase H function (Di Grandi *et al.*, 2010). The predicted cation- π interactions with His539 may therefore play a significant role in inhibiting RNase H activity. A molecular surface diagram of the receptors' hydrophobicity depicting the binding interactions of TTC10 with this site is shown in Figure A5.2, which unfortunately did not show great size-shape complementarity. Unlike the ribbon structure of the receptor shown in Figure 5.6 where it is easier to visualise H-bonds and other interactions (in addition to the hydrophobic interactions) unlike in a molecular surface map, which presents a different view of the overall hydrophobicity and hydrophilicity of the ligand-complex.

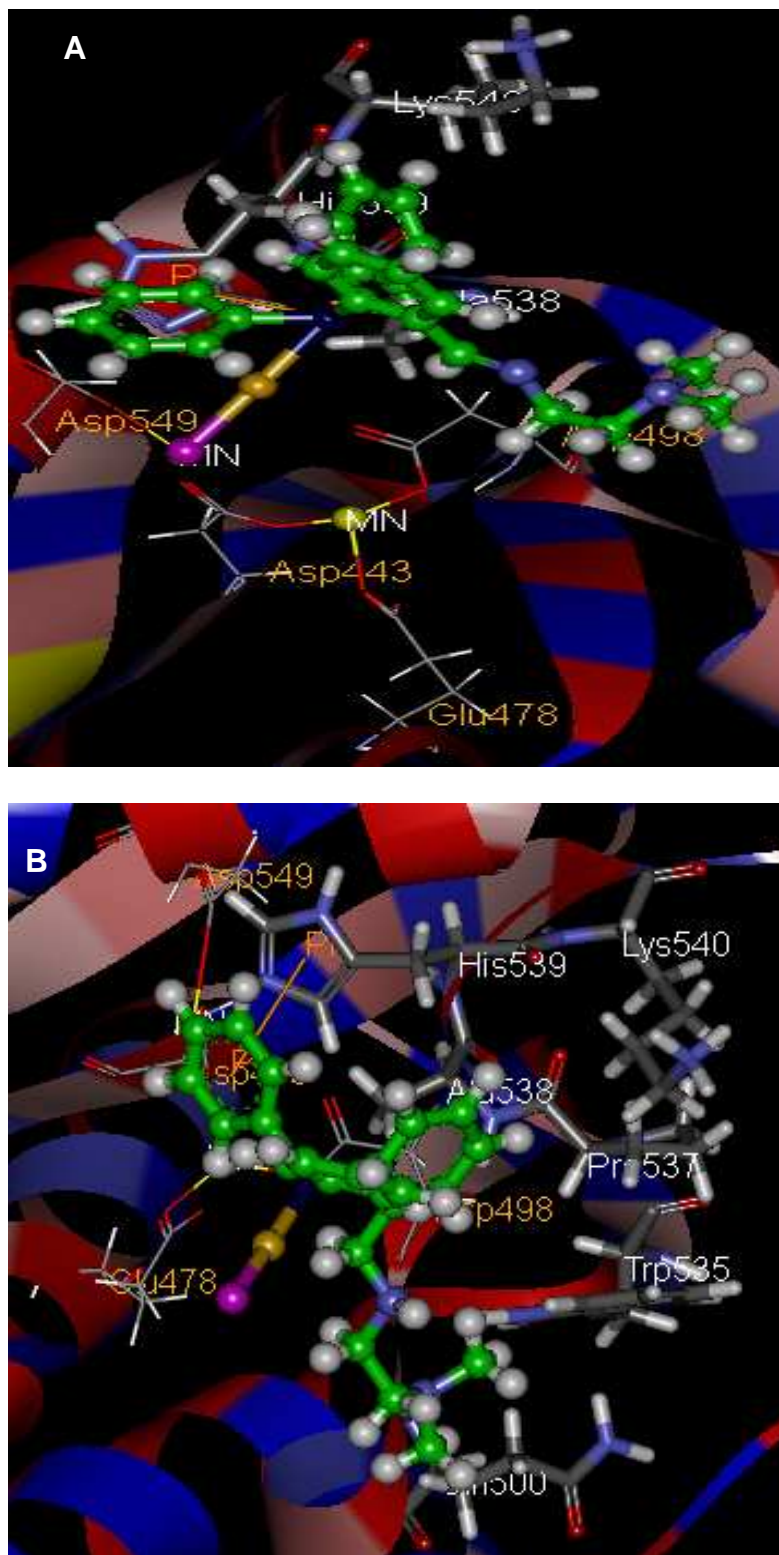


Figure 5.6: Predicted binding predictions of TTC10 and TTC24 (green ball and stick models) to the RNase H site in the presence of Mn^{2+} (yellow balls). Prominent amino acids are shown as stick models. Both compounds did not interact with the Mn^{2+} ions present in this site but formed crucial interactions with His539. A cation-pi interaction was formed between the phosphate group of TTC10 and the imidazole ring of His539 (A). Hydrophobic interactions were also observed between Ala538 and the side chain (CH₂)₃ group of Lys540. (B) TTC24 on the other hand formed a crucial pi-pi stacking interaction between one of its phenyl groups and the imidazole ring of His539. Hydrophobic interactions were also observed between Ala538, Pro537, Trp535 and the side chain group of Lys540 (CH₂)₃ and Gln500 (CH₂)₂. Active site carboxylate residues of Asp443, Glu478, Asp498 and Asp549 which are coordinated to the Mn^{2+} ions are represented with line diagrams and labelled in orange while the active site residues with which the ligands were predicted to interact are labelled white and represented as stick diagrams. Red balls or sticks = O, blue = N, white = H, orange=Au, purple = Cl, grey = C on receptor and green on ligand, P = dark blue.

Predicted interactions of TTC24 with this site (Figure 5.6B) included a pi-pi stacking interaction (4.6Å) between one of the phenyl rings attached to the phosphanyl-benzyl moiety (insert C, Figure 5.5) of the compound with the imidazole ring of His539 and hydrophobic interactions with Pro537, Trp535 and side chain residues of Gln500. In the same manner like TTC10, TTC24 was also predicted to interact with Lys540 through hydrophobic interactions with side chain (CH₂)₃ groups. It appears the *N,N*-dimethyl-ethane-1,2-diamine group present in TTC10 and TTC24 confers better interactions between these ligands and the RNase H site than the phenethyl-amine moiety of TTC3 and TTC17. These findings are obviously related to structure and suggest a SAR. In terms of H-bond donors, TTC10, TTC17 and TTC24 each have one while TTC3 has none and in terms of H-bond acceptors, TTC10 and TTC24 each have two while TTC3 and TTC17 each have one. The H-bond donors and acceptors are contributed by either the *N,N*-dimethyl-ethane-1,2-diamine of TTC10 and TTC24 or from the phenethyl-amine moiety of TTC3 and TTC17. In the experimental data reported by Fonteh and Meyer (2009), a similar trend with respect to inhibition of RT was observed. TTC24 which has the highest number of H-bond acceptors and donors (total of 3, Table 3.6) inhibited RT by > 74 % at 6.25 μM, TTC10 with two H-bond acceptors by > 34 % at 6.25 μM while complexes TTC3 and TTC17 resulted in <2% inhibition at 6.25 μM.

In the validation docking with the naphthyridinone-containing compound, MK3, a crucial pi-pi (5.5 Å) stacking interaction between one of its phenyl groups and the imidazole ring of His539 in addition to three H-bonds contacts were also predicted in conformity with Su *et al*'s findings. The interactions between His539 therefore appear to be very important in the binding of these ligands with the RNase H site.

Predicted docking interactions for the free ligands of TTC10 and TTC24 i.e. TTL10 and TTL24 respectively (which were tested as controls to determine the significance of complexation) resulted in binding free energies, which were seven fold higher than for the corresponding complexes. The predicted binding free energies of TTL10 and TTL24 were 76.6 and 78.6 kcal/mol compared to 10.9 and 12.3 kcal/mol for TTC10 and TTC24 respectively (Table 5.4). In the bioassays (early screening done in 2007 and reported in Fonteh and Meyer 2009), these ligands had no inhibitory activity and it is therefore not surprising that while the complexes were predicted to interact more favourably with the RNase H site of RT, the free ligands did not. These differences suggests that the gold complexes are more stable in binding to the RNase H site than the free ligands, a finding which supports the concept of increased stability and activity when organic compounds are complexed with metals (Navarro, 2009).

The binding affinity predictions for the gold(III) pyrazolyl compound KFK154b which had also previously inhibited HIV RT in cell free assays (Fonteh *et al.*, 2009) resulted in energetically feasible binding predictions with the RNase H site (binding free energy of 10.4 kcal/mol). Different portions of the compound i.e. the tetra-chloro gold portion, the bis-(3,5-

dimethylpyrazolyl)methane portion and the Cl⁻ ion interacted with different sites of the receptor. The interaction of the Cl⁻ and the tetra-chloro gold portion were outside the sphere that was defined as the active site (Figure A5.3). No conclusions could be made on the binding interactions of this compound with the RNase H site as a result.

Although favourable binding predictions were observed for the gold(I) phosphine chloride complexes (TTC10, and TTC24) in the RNase H site, there was unfortunately poor size-shape complementarity. The addition of chemical substituents that have metal binding groups (e.g. carbonyl groups) could aid in sandwiching these ligands better in the active site pocket while increasing the binding affinity and thus efficacy. A poor fit to the RNase H site has also been attributed to the flatness or absence of a deep pocket which makes it difficult for the development of RNase H inhibitors (Himmel *et al.*, 2009, Davies *et al.*, 1991). Another limitation to the interaction of the complexes with this site could have stemmed from the fact that metal-based docking parameters have not been incorporated into DS[®] and other docking software. As a result, expected covalent interactions that could have occurred between gold and the receptor (particularly with sulfhydryl groups of cysteine residues) were not possible. Unfortunately, this could not be assessed since docking algorithms were designed for organic molecules which form non covalent bonds such as hydrogen bonding and van der Waal forces unlike metallodrugs which form covalent bonds and ionic forces (Navarro, 2009).

Predicted binding interactions with the RNase H site in the absence of Mn²⁺: Docking to the 3LP3 site was also performed in the absence of Mn²⁺ ions for TTC3, TTC10, TTC17 and TTC24 in an attempt to determine the influence of these metal ions on the binding. The predictions suggested better binding affinities than in the presence of Mn²⁺ in the order of TTC3<TTC10<TTC24<TTC17 with binding free energies of -9.4, 0.2, 0.5 and 5.2 kcal.mol respectively (Table 5.4). Surprisingly TTC3 had the highest affinity for this site compared to TTC10 or TTC24 which were the most favoured both in the bioassays and for this same site in the presence of Mn²⁺ (Table 5.4). It appears that there were repulsive forces between the ligands and the receptor when docking was done in the presence of Mn²⁺ (Figure 5.6) possibly because the ligands do not have metal binding groups that could interact with the active site Mn²⁺ ions. In the absence of the metal ions, there was better size-shape complementarity (Figure 5.7) with the ligands interacting with active site residues that were otherwise not within 4 Å of the ligand when docking was done in the presence of Mn²⁺ (Figure 5.6).

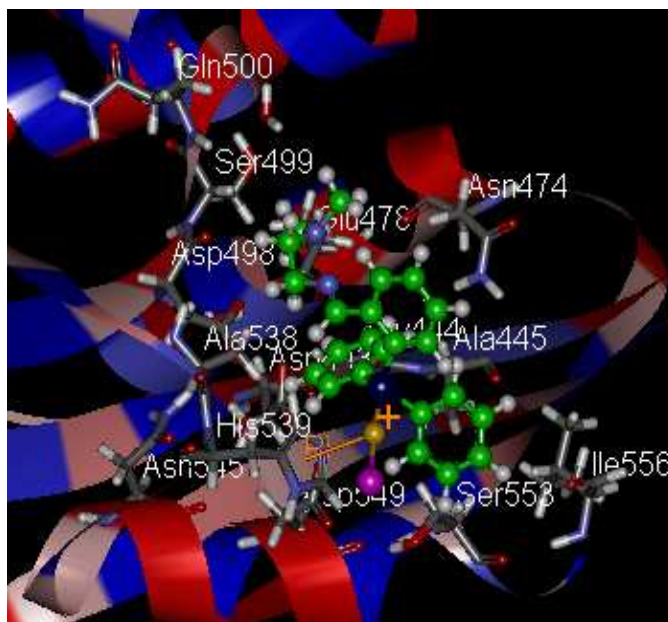


Figure 5.7: Predicted binding interactions of TTC10 to the RNase H site in the absence of Mn^{2+} . The ligand fits more snugly into the active site making contact with many more residues including those normally bonded to Mn^{2+} (Asp443, Glu478, Asp498 and Asp549) it also interacted with hydrophobic residues Ala445, Ala538, Ile556 and polar residues Gly444, Asn474, Ser 499, Gln500, Asn545, Ser 553 and two water molecules. Red balls or sticks=O, blue=N, white =H, orange=Au, purple=Cl, grey=C on receptor and green ball on ligand, P=dark blue

Although favourable interactions were observed in the absence of Mn^{2+} , the two metal ions are important in the activity of RNase H and both are needed in binding the substrates of this site and catalyzing phosphodiester bond hydrolysis (Jochmans, 2008). The data however corroborates the fact that repulsive forces were present when docking with Mn^{2+} was done because the ligands lacked metal binding groups. In addition, the observed interactions of the ligands with the RNase H site in the absence of Mn^{2+} could aid in the design of compounds that would interact more favourably with this site in the presence of Mn^{2+} by including groups which should hopefully interact with the additional amino acid contacts present when docking was done in the absence of Mn^{2+} . Compound TTC10 for example (Figure 5.7) was predicted to form a cation-pi interaction (2.8 Å) between gold and the imidazole ring of His539 and in addition to interacting with the amino acids normally coordinated to Mn^{2+} (i.e. Asp443, Glu478, Asp498 and Asp549), also made hydrophobic contacts with residues Ala445, Ala538, Ile556 and polar residues Gly444, Asn474, Ser 499, Gln500, Asn545, Ser 553 and two water molecules (all residues within 4 Å of the ligand). These interactions were absent when docking was done in the presence of Mn^{2+} (Figure 5.6). The lower binding energy could therefore be attributed to a better fit which also correlated with a decrease in the cation-pi distance from 6 Å in the presence of the Mn^{2+} ions to 2.8 Å in their absence. The data suggests that the binding of these ligands to this site did not require coordination to the metal ion when comparing the binding free energies predicted in the absence or presence of the metal ions (Table 5.4). In the former case the probable reason lack metal chelating moieties such as carbonyl groups in the ligands. Unfortunately these metal ions are required for the activity of the enzyme making

their chelation necessary for the inhibition of RNase H (Kirschberg *et al.*, 2009). A modification of the compounds to contain metal chelating groups so as to enhance the activity of the gold-containing ligands might prove promising for improving the binding predictions and possibly reproducibility and efficacy in bioassays.

Predicted interactions with the NNRTI allosteric site (3LP2): Eight ligands were successfully docked into the 3LP2 site. These were the phosphine gold(I) complexes (TTC3, TTC10, TTC17 and TTC24, free ligands of TTL10, TTL17, TTL24) and the gold(III) pyrazolyl complex, KFK154b (Table 5.4). The binding free energies predicted were not in the single digit or negative range but some very interesting interactions that could be optimised were observed. TTC24 will be used as a model (Figure 5.8) for elaborating the binding predictions that were seen for the phosphine gold(I) complexes since its interactions resulted in the lowest binding free energy of 57 kcal/mol (Table 5.4). The predicted interactions of the compounds with this site showed SAR that correlated with the biological data (Fonteh and Meyer 2009). TTC24 inhibited RT the most (prior to loss of activity, Table 5.2) in the direct enzyme assays with a >50% inhibition at 6.25 μM (Table 5.3).

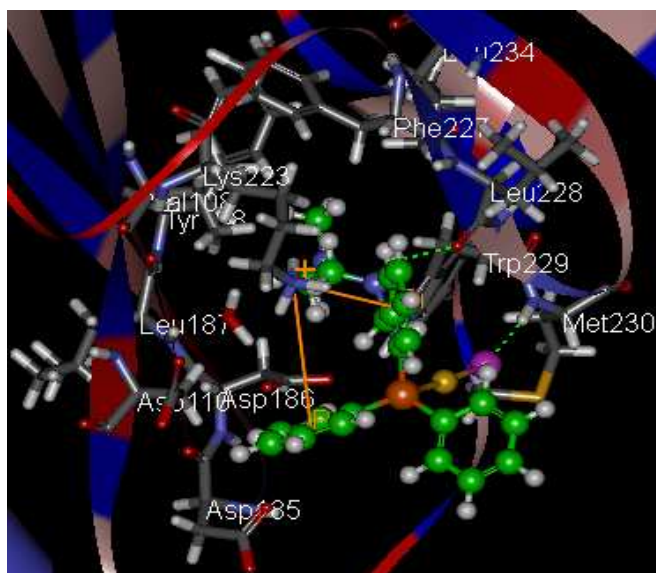


Figure 5.8: Predicted binding interactions of TTC24 with the site close to the polymerase/NNRTI site (3LP2). The interactions of TTC24 with this site showed the *N,N*-dimethyl-ethane-1,2-diamine group being inserted in a hydrophobic pocket and two cation-pi interactions occurring between two of the phenyl groups of TTC24 and Lys223. Two H-bonds were seen between one of the amine groups of the ligand and Leu228 (2.3 Å) and the other between the Cl⁻ ion and the backbone NH₃⁺ group of Met230 (1.9 Å). One of the phenyl groups not involved in cation-pi interactions is solvent exposed. Red balls or sticks=O, blue=N, white =H, orange=Au, purple=Cl, grey=C on receptor and green balls on ligand, P=dark blue. H-bonds are shown as green dotted lines. Cation-pi interactions=orange lines

The *N,N*-dimethyl-ethane-1,2-diamine portion of TTC24 (Figure 5.5) led the inhibitors into a predominantly hydrophobic pocket lined by numerous residues which include Val108, Asp110, Asp185, Asp186, Leu187, Tyr188, Lys223, Phe227, Leu228, Trp229, Met230, Leu234 and a water molecule (Figure 5.8). In addition to two cation-pi interactions (3.8 and 5.4 Å respectively) predicted between the NH₃⁺ group of Lys223 and two of the phenyl groups (attached to C1 of the diphenylphosphanyl benzyl portion, Figure 5.5) of TTC24, two H-bonds

interactions were also predicted between the H-bond donor (N1, Figure 5.5) and Leu228 (2.3 Å) and the other between the Cl⁻ ion and the backbone NH₃⁺ group of Met230 (1.9 Å). Two cation-pi interactions were predicted between two of the phenyl groups of TTC10 and Lys223 (3.5 and 3.8 Å respectively). TTC10 was also predicted to interact with similar residues lining the binding pocket as seen for TTC24 (with the exception of Tyr181, Gln182, Phe226, Gly231, Gln242). The absence of the two H-bond interactions between TTC10 and the receptor is probably responsible for the higher binding free energy (87.7 kcal/mol) making TTC24 (57.kcal/mol) a better inhibitor. Although cation-pi interactions are known to be strong non-covalent bonds (Dougherty, 1996) which could have easily increased the binding affinity of TTC24 to this site, one of the two phenyl rings attached to phosphorous (at the PPh₂ position, Figure 5.5) not involved in cation-pi interactions appeared to be predominantly solvent exposed and could be the contributing factor for the high binding free energy. This solvent exposed phenyl group possibly contributed unfavourably to the overall entropy of binding and hence reduced the stability of binding. The interaction of TTC17 with this site is similar to that of TTC10 but better than that of TTC3 which had the highest binding free energy prediction of 243 kcal/mol (Table 5.4). The only difference between compounds TTC17 and TTC3 is the presence of an H-bond donor in TTC17.

The overall binding interactions of the compounds with this site presented similar orientations as reported by Su *et al.*, (2010) for the diethylaminophenoxy group of the naphthyridinone-containing inhibitors. Although the interactions were not spontaneous nor in the single digit range in terms of energy rankings, these findings suggests that modifying the dimethyl-ethane-1,2-diamine portion of TTC10 and TTC24 could result in better binding predictions for these ligands. In addition, the solvent exposed phenyl ring might need to be replaced with a smaller group to reduce solvent effects. These findings also provide useful information that can aid in the design of new gold-based complexes targeting this site and should be of interest to medicinal chemists involved in rational drug design.

It has not been determined whether the 3LP2 site is a biologically relevant inhibitory site but the binding of one of the naphthyridinone compounds that was probed by Su *et al.*, (2010) was able to sufficiently bind and displace nevirapine from its NNRTI pocket making it a potential allosteric inhibition site.

5.3.2.2 Binding modes of ligands to the HIV PR site

Unlike RT for which structure-based drug design took a longer time to materialize because the crystal structural information database was lacking, structure-based design for PR inhibitors has been central to the development of many of the drugs that target this enzyme (Ren and Stammers, 2005). Docking for the HIV PR site was performed on two crystal structures; a wild type with pdb code, 1HXW, which like the rest of the crystal structures used in this study, is a subtype B strain and another coded 2R5P which is a subtype

C strain. Very poor binding free energies were predicted for the successfully docked ligands. These were compounds that had previously inhibited PR activity in direct enzyme bioassays at a high 100 μM concentration (Table 5.3). The poor binding free energies predicted in the *in silico* studies are thus suggestive of the fact that the inhibitions observed at 100 μM (in the direct enzyme assays) were non specific especially because these concentrations were also toxic to cells. Based on these findings, no further analyses of the docked poses were done.

5.3.2.3 Binding modes of the ligands with HIV IN sites

Docking studies for IN were done for the compounds that had inhibited HIV IN in the dual 3'P and ST assay pre-screen (Figure A5.1A). The ligands analysed included the Tscs compounds PFK5, PFK7, PFK8 and PFK41 and the gold(I) phosphine thiolate compound, PFK174. Docking was done on the LEDGF binding site (pdb coded 2B4J). LEDGF functions in targeting IN to the chromosome of infected cells and enhances the integration process (Maertens *et al.*, 2003). Cherepanov *et al.*, (2005), speculated that the binding of small molecule inhibitors to the LEDGF binding site is likely to induce defects in HIV replication similar to those seen in mutant viruses. Docking was also done on the ISQ4 site complexed to 5-CITEP (Goldgur *et al.*, 1999) and the 3L3V site in complex with sucrose (Wielens *et al.*, 2010) both in the CCD of IN. The sucrose binding site located 10 Å from the LEDGF binding site was identified by Wielens *et al.*, (2010) as an allosteric inhibitory binding site that can be exploited for developing inhibitors that target LEDGF. Other investigators (Du *et al.*, 2008, Shkriabai *et al.*, 2004) have also identified this site as a putative IN binding site.

Binding predictions for the 1SQ4 site were enthalpically unfavourable suggesting very poor complementarity and hence binding affinity. This site contains only one of the two Mg^{2+} ions that should ideally be found in the enzyme (Cox and Nair, 2006, Bujacz *et al.*, 1997) and because the ligands do not contain metal chelating moieties (also noted for the RNase H site), unfavourable repulsive forces prevailed. This finding is not surprising given that this site is also the DNA binding site since no significant inhibition was observed in the direct enzyme assays that mimicked the integration process. This was the case in the dual inhibitor assay and ST specific assay, except for the once off findings in the dual assay pre-screen (Figure A5.1). Inhibitors of 3'P are known to target the unbound enzyme while IN ST inhibitors target the enzyme/DNA complex in cell-based assays (Hazuda *et al.*, 2000). With regards to docking, there is supporting evidence (Johnson *et al.*, 2006) that suggest that 3' processor inhibitors dock at the HIV DNA site of the enzyme while IN ST inhibitors occupy the position of acceptor DNA (Johnson *et al.*, 2007, Pommier *et al.*, 2005). Based on these theories (which was corroborated by both the bioassays and docking studies on the 1SQ4 sites), one could conclude that the ligands were neither 3' processors nor ST inhibitors.

Binding interactions of the ligands with the LEDGF and the sucrose binding sites on the other hand resulted in significantly lower binding free energy predictions. Interactions with the

LEDGF site were favoured over those of the sucrose binding site as seen from the binding free energies in Table 5.4.

Binding of the ligands to the LEDGF site was in the order of PFK174<PFK5<PFK7<PFK8<PFK41 with corresponding binding free energies of 7.2<8.9<13.2<15.2<18.2 kcal/mol respectively. Only the interactions with the Tscs-based ligands will be discussed since PFK714 is one of the three complexes whose structure cannot be described in detail. The annotated structures of PFK5 and PFK7 depicted in Figure 5.9 will aid in the description of predicted interactions with the LEDGF and the sucrose binding sites.

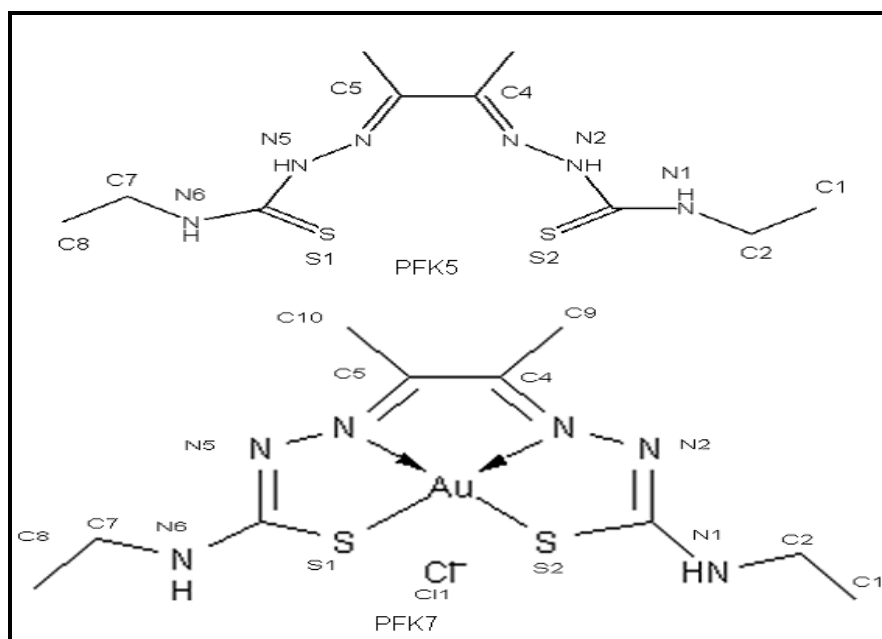


Figure 5.9: Annotated structures of ligands PFK5 and PFK7. Numbers are assigned to the various atoms to facilitate description of ligand-receptor interactions

Predicted interactions with LEDGF binding site: The predicted binding of PFK5 with this site which resulted in a binding free energy of 8.9 kcal/mol for the most favoured pose consisted of two H-bond interactions; one between the backbone NH_3^+ group of Glu170 in chain B (flat ribbon) and a sulphate ion (S2) of PFK5 (2.2 Å) and the other between the backbone carbonyl group of Gln168 of chain B and an H-bond donor (N2) of PFK5 (2.5 Å, Figure 5.10A). One of the sulphate atoms (S1) of PFK5 was however not satisfied since it was not involved in H-bonding.

Binding predictions for the corresponding gold complex of PFK5 (PFK7) resulted in better size-shape complementarity (Figure 5.10B) than the free ligand (PFK5) but with a slightly higher binding free energy (13.2 kcal/mol). Mostly hydrophobic interactions were predicted with both receptor chain A consisting of Ala98, Leu102, Ala128, Ala129, Trp131, Trp132 and Met178 of Chain B (Figure 5.10B). Other amino acid residues (polar residues) within close proximity (4 Å) of the side chain methyl groups of PFK7 were Gln95, Thr125, Gln168, His171 and Thr174. The modification of PFK7 to contain polar groups at points close to these amino acid residues may improve binding affinity for this site.

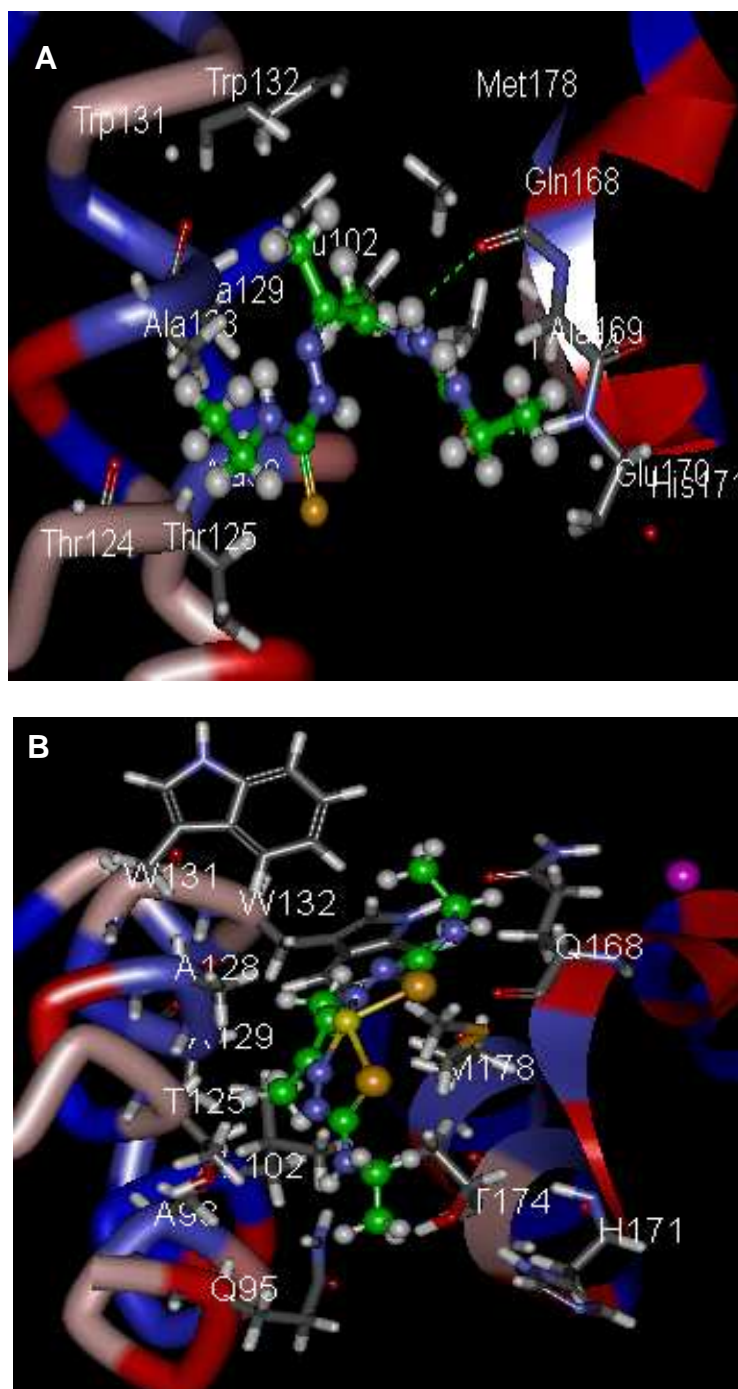


Figure 5.10: Predicted interactions of ligands PFK5 and PFK7 with the LEDGF binding site. Chain A of IN is represented by a tube model while chain B is represented by a flat ribbon model. Better size-shape complementarity was observed for PFK7 (B) with this site than with the free ligand, PFK5 (A). The complex formed mostly hydrophobic interactions with residues Ala98, Leu102, Ala128, Ala129, Trp131, Trp132 of chain A and Met178 of Chain B. PFK5 makes two H-bond contacts with the receptor. Red balls or sticks=O, blue=N, white =H, yellow=Au, orange = S, purple=Cl, grey=C on receptor and green ball on ligand, H-bonds are shown as green dotted lines.

The contacts made by PFK7 with this site are also LEDGF hotspot residues (Wielens *et al.*, 2010). The chloride ion of PFK7 (purple ball in Figure 5.10B) was free floating and made no contact with the receptor. Although PFK5 formed two H-bonds with the receptor and was predicted to have a slightly lower binding free energy than PFK7, it unfortunately had very poor size-shape fit compared to PFK7 which fitted more complementarily with this site. Molecular surface diagrams of the receptor with PFK5 and PFK7 depicting hydrophobic interactions are shown in Figure A5.4.

The interaction of PFK8 with this site resulted in a binding free energy of 15.2 kcal/mol. This compound however did not fit into the active site as snugly as PFK7. The probable reason for this poor fit is because unlike PFK7 this compound has two CH₂ groups less (Table 3.4) and could therefore not make appropriate hydrophobic interactions similar to those observed for PFK7. This observation suggests a structure activity relationship.

PFK41, which differs from PFK7 by having two CH₃ groups less also did not interact with this site as favourably as PFK7. The most favourable pose was predicted to have a binding free energy of 18.2 kcal/mol and made two H-bond contacts, one with Lys173 and the Cl⁻ ion (2.4 Å) and the other between Gln168 and H-bond donor (N1) of PF41 (1.7 Å). These interactions appeared not to compensate for the poor fit hence the higher binding free energy. The predicted interactions of these gold(III) Tscs-based compounds with the 2B4J or LEDGF binding site demonstrated SAR. IN on its own does not exhibit the same integration activity observed for the IN/LEDGF complex (Michel *et al.*, 2009) making compounds which bind and alter LEDGF interactions potential IN inhibitors.

Prediction interactions with the sucrose binding site: Binding free energies predicted for the sucrose binding site were in the order: 40.1 < 40.4 < 42.1 < 42.3 for PFK5, PFK41, PFK8 and PFK7 respectively. Since these enthalpic contributions were poor, and generally presented similar values for the various ligands, only those of PFK5 and PFK7 (Figure 5.11) as representatives are discussed.

The lowest binding free energy for this site (40.1 kcal/mol) was for PFK5 which formed four H-bonds; one between Lys103 and one of the sulphate ions (S1) of PFK5 (2.9 Å), another between H of NH₃⁺ group of Lys173 and N3 of PFK5 (1.7 Å), a third with another H of NH₃⁺ group of Lys173 and N3 of PFK5 (2.4 Å), and a fourth with the carboxylate group of Glu96 and the H-bond donor (N1) of PFK5 (2.2 Å) shown in Figure 5.11A. PFK7 on the other hand with a binding free energy of 42.3 kcal/mol was predicted to form two H-bonds with this receptor (Figure 5.11B). One was between the backbone carbonyl group of Val88 and H-bond donor N6 (2 Å) of PFK7 and the other between the floating Cl⁻ and Gly94 (2.4 Å). The H-bond between the Cl⁻ and the receptor as well as other predicted interactions with the receptor (Thr93, Gly94, Asn120 and Ser123) were outside the defined sphere for docking. This site may represent a putative binding site.

There appeared to be some fit for PFK7 in this site which is comparable to that observed for the LEDGF site (Figure 5.10) but was clearly not as compatible for this ligand as it was for the LEDGF binding. This is further supported by the differences that were seen in the predicted binding free energies and from the molecular surface diagrams (Figure A5.4B and A4.5 respectively). These findings suggest that the compounds do not have allosteric binding ability and will not displace LEDGF from its binding pocket which is 10 Å away.

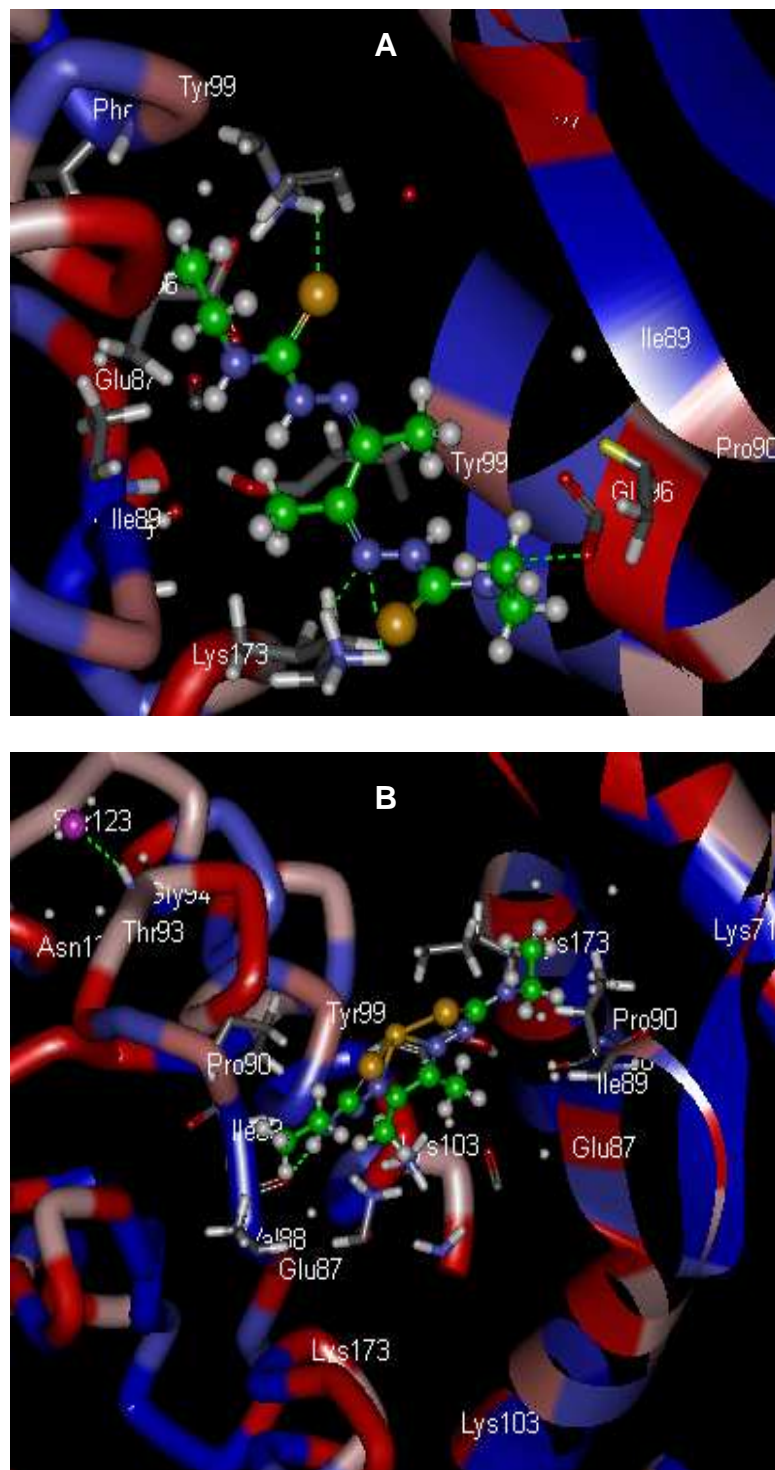


Figure 5.11: Predicted binding interactions of ligands with the sucrose binding site of IN. Prediction interactions of PFK5 and PFK7 are shown. Four H-bonds interactions were predicted between PFK5 and the receptor (A) and two between PFK7 and the receptor (B). The interactions of the ligands with this site showed poor complementarity and thus poor allosteric binding effect. Red balls or sticks=O, blue=N, white=H, yellow=Au, orange=S, purple=Cl, grey=C on receptor and green on ligand, H-bonds=dotted green lines.

The type of inhibition exhibited by IN inhibitors could either be 3'P or ST specific. New targets such as the IN cofactor or LEDGF binding site (Adamson and Freed, 2010), have been identified. In a pre-screen with a dual inhibitor kit, four compounds exhibited >50% inhibition of IN (Figure A5.1A) but this was absent upon subsequent testing (Figure A5.1B) while in the ST specific assay, no significant inhibition was observed. Even though both 3'P and ST inhibitors have been reported in *in vitro* tests, only ST ones have been successful *in vivo* and

subsequently approved for clinical use (Mouscadet *et al.*, 2010, Chirch *et al.*, 2009). Therefore, if the observed inhibition in the pre-screen was due to 3'P, then there is unfortunately no IN therapeutic potential for these compounds since *in vivo* inhibition is unlikely.

With respect to the docking data, the compounds were neither 3'P inhibitors or ST inhibitors, a finding supported by literature (Johnson *et al.*, 2007, Pommier *et al.*, 2005) since interactions with the DNA binding site (1SQ4) were unfavourable. The gold(III) Tscs-based complexes however displayed favourable interactions with the LEDGF binding site of IN in the virtual screening prediction studies. These findings must be confirmed experimentally by using assays specific for determining the effect of these ligands on IN-LEDGF interactions.

5.4 CONCLUSION

Direct enzyme bioassays for RT, PR and IN were performed. Compounds which demonstrated inhibition of these enzymes both in this study and in previous studies (Fonteh and Meyer 2009, Fonteh *et al.*, 2009) were further analysed using complementary *in silico* molecular modelling techniques for the respective receptor binding sites.

In the direct enzyme assays, none of the eleven new compounds inhibited RT while one (PFK7) inhibited PR but at a toxic concentration of 100 μ M. Compounds with previous anti-RT activity when tested as controls three years later appeared to have lost this ability (Table A5.1). This loss of activity in the direct enzyme assay was thought to have resulted from one or more of a number of limitations; poor aqueous solubility seen in the ADMET studies and during wet lab studies for some of the compounds (Table 3.8A) and compound age (activity was noted earlier when compounds were freshly prepared soon after synthesis but absent after three years of storage) and the presence of degradation products not detectable by NMR. In addition, the poor complementarity in binding to the RNase H site due to the lack of metal chelating groups was also thought to be one of the possible reasons. The poor stereochemical orientation of ligands with the active site and the high flexibility associated with protein molecules (Mohan *et al.*, 2005, Höltje *et al.*, 2003) meant the ligands could easily be dislodged. This latter possibility together with the mentioned poor aqueous solubility limitation, and the possibility of the presence of degradation products (not detectable by NMR) makes these compounds poor RT inhibitors and poor drug-like candidates in the current form. The inconsistencies in the bioassay findings were therefore not surprising. The inclusion of metal chelating groups (e.g. carbonyl groups) which can bind to the metal ions found in the active sites of RNase H might prove useful in the binding and inhibition of this important viral enzyme and in enhancing the activity of these ligands in the bioassays. Overall, there was SAR in docking studies which appeared to correspond with RT bioassay findings (Fonteh and Meyer, 2009) where the *N,N*-dimethyl-ethane-1,2-diamine containing ligands

(TTC10 and TTC24) were favoured over the phenethyl-amine containing ligands (TTC3 and TTC17, Table 5.4).

Binding affinity to both a subtype B and C variant of HIV PR for compounds which had previously inhibited the enzyme at 100 μM (Table 5.3) was very poor and in some cases refined poses could not be obtained (Table A5.2 in the appendix). It is thought that the inhibition of the enzyme by these compounds was not specific especially considering the high and toxic concentrations (the CC_{50} of the complexes were mostly below 20 μM , Table 4.2) at which enzyme inhibition was detected. It was therefore not surprising that the binding affinity in the molecular modelling studies was very low.

Binding affinity predictions for HIV IN for the Tscs compounds showed favourable binding interactions with the LEDGF binding site (2B4J) but not with the allosteric sucrose binding site (3L3V) or the DNA binding site (1SQ4). The poor binding to the 1SQ4 site confirms the bioassay studies where the compounds were shown to be neither 3'P nor ST specific inhibitors

The interactions of PFK5 and its corresponding complex, PFK7, with the LEDGF binding site were the most favoured with PFK7 making contact with LEDGF hotspots and with better complementarity than the corresponding free ligand (PFK5, Figure 5.10).

Gold complexes have been reported to undergo ligand exchange reactions with sulfhydryl groups of cysteine residues present in the active site of receptors (Shaw III, 1999, Sadler and Guo, 1998). This was not observed in the *in silico* docking assays performed here possibly because the docking program has not been parameterised to include metals in its atom base such that binding interactions of gold complexes with the receptor could not be simulated. Complexation however appeared to confer stability and led to better binding affinity predictions than those seen for the free ligands (Table 5.4). Differences in the binding free energies of free ligands TTL10 and TTL24 which were 76.6 and 78.6 kcal/mol respectively compared to those of corresponding gold complexes, TTC10 and TTC24 which were 10.9 and 12.3 kcal/mol respectively for the RNase H binding site (Table 5.4) are some examples.

Although favourable interactions were observed for the ligands with the RNase H site of RT and the LEDGF binding site of IN, the binding orientations were poor especially with respect to the RNase H site. The binding predictions of the ligands with these sites can however provide crucial information for the design of gold-based compounds that could potentially attain better inhibition in bioassays and *in silico* with energetically favourable interactions.

CHAPTER 6

CONCLUDING DISCUSSION & FUTURE WORK

Three decades following the discovery of the link between HIV and AIDS, the best option for long-lasting viral suppression which eventually leads to a reduction in morbidity and mortality is the use of HAART (Simon *et al.*, 2006). Unfortunately, latent reservoirs of the virus, which persist within the host's genome, re-emerge and start replicating once treatment is stopped (Finzi *et al.*, 1997). So far, there is no viable cure for HIV/AIDS (the stem cell transplantation report of Hutter *et al.*, in 2009 came close) and advances in vaccine development still require significant research effort to improve safety and efficacy.

HAART continues to play a vital role in sustaining the lives of people infected with HIV but unfortunately, the virus develops resistance to these drug cocktails (Simon *et al.*, 2006, Svarovskaia *et al.*, 2003). In addition, toxicity to the host is also a major problem together with uncomfortable side effects of the drugs (Yeni, 2006, Montessori *et al.*, 2004, Montaner *et al.*, 2003). These limitations greatly affect treatment options, which are further complicated by the fact that therapy has to be life-long. The need to increase the repertoire of drugs available for treatment therefore remains a priority. These new drugs should inhibit both wild type and resistant viral strains or should be capable of targeting different points of the life cycle or points of host cell interactions which had hitherto not been explored. Recent findings by the HIV Prevention Trials Network that early initiation of ARV therapy can curb transmission of HIV to partners of men and women infected by the virus by 96% (www.hptn.org, accessed 5/6/2011) is a finding that further supports the importance for identifying new drugs.

Twenty seven compounds (nineteen gold complexes and eight free ligands, synthesized by chemists from the Project AuTEK consortium) were screened for potential inhibition of HIV. *In silico* and *in vitro* drug-likeness (ADMET) studies of the compounds were performed, interactions with host cells and whole virus as well as the compounds' effects on viral enzymes were also evaluated.

Eight (Table 3.9) of the nineteen gold complexes demonstrated drug-like properties that were similar to those of auranofin (an anti-arthritic gold drug in clinical use) and in some cases better than that of the currently available anti-viral agent, nevirapine (Table 3.8B). The gold(III) thiosemicarbazone complexes, PFK7 and PFK8, had very good drug-like qualities and presented as cytostatic complexes through RT-CES and flow cytometry evidence. According to bioassay studies, none of the compounds (some recently synthesised and others older) had any usable RT or PR inhibitory ability; a finding that was supported by *in silico* docking studies. No inhibition of IN was observed when both dual (3'P and ST) and ST specific assays were performed. However, *in silico* predictions studies, favourable size-shape

complementarity predictions were obtained for the binding of PFK7 to the LEDGF binding pocket of IN. The data so far suggests that PFK7 and PFK8 which had favourable drug-like properties (Table 3.8A), inhibited viral infectivity (Figure 4.8), demonstrated cytostatic effects (Figure 4.7B and C) and lowered the frequency of CD4+ cells in HIV+ donors (PFK7 only, Figure 4.10), are possible lead compounds. PFK7's cytostatic effect was supported by RNR inhibitory effects (Figure 4.9). TTC24 had a drug score of 3/7 and inhibited viral infectivity at non-toxic concentrations. This compound could be a potential lead compound after structural modification to improve drug-likeness. With regards to class, the Tscs class of complexes (class IV) was superior in drug-likeness and in the inhibition of HIV (infectivity and enzyme inhibition) followed by the gold(I) phosphine chloride containing class (class I) with TTC24 being the most favoured. Although the gold(I) phosphine thiolate class (class III, except the bimetallic complexes) and the gold(III) pyrazolyl complex of class V had very favourable ADMET properties, no significant inhibition of HIV was observed. The BPH gold(I) phosphine chloride class (II) of complexes were the least drug-like.

In the following sections, a summary of the major findings for each of the main topics will be provided followed by answers to the research questions that were posed as well as recommendations for future directions. A highlight of the novel contribution of the project and an overall conclusion section will then follow.

6.1 COMPOUNDS: STRUCTURE AND DRUG-LIKE PROPERTIES

Drug-likeness predictions were done using *in silico* computer simulations and by *in vitro* viability studies. The ^1H and ^{31}P NMR chemical shifts of six complexes (from each of the classes) on day zero, 24 h and 7 days after dissolution and storage at -20 and at 37 °C in DMSO suggested that the backbone structure of all the complexes tested were intact (summarised in section 3.4.1.5, Table 3.7). The main difference was the presence of water peaks (in the ^1H NMR at 3.33 ppm, Gottlieb *et al.*, 1997) in the day zero spectrum of four of the complexes (i.e. TTC3, MCZS3, PFK174 and PFK7, Table 3.7), suggesting hygroscopic tendencies. In three of these complexes (except MCZS3 which was only analysed on day zero), the water peak became more prominent after 24 h and at 7 days but was absent in the ^1H spectrum complex KFK154b over time. The increase in the water peak area and the new water peak in the spectrum of complex EK231 after 24 h and later were supposedly as a result of DMSO's hygroscopic nature.

Although compounds dissolved in DMSO can degrade when water is present (Ellson *et al.*, 2005), the main problem usually encountered is the precipitation of compounds out of solution (Ellson *et al.*, 2005) which could result in concentration discrepancies in bioassays. To minimise such problems in this study, DMSO stocks were aliquoted and together with the dissolved compounds, stored in single use vials. In addition, the compounds were stored desiccated at -20 °C and samples were prepared fresh and used within a week. In this form,

compounds from classes I, II, III and V which were analysed for stability approximately 4 years after synthesis, maintained relevant chemical shifts (but not inhibitory activity, see RT studies in Table A5.1) with the only noticeable impurity being a water peak on day zero (Table 3.7). Gold complexes EK231 and KFK154b appeared very stable on day zero but subsequently (24 h and 7 days) both spectra had a water peak (EK231) and a D₂O peak (in KFK154b) as impurities. The ³¹P chemical shifts of complexes TTC3 and EK231 remained intact which was in agreement with the idea that covalent interactions with S, P or C containing ligands lead to stabilising interactions with gold (Parish and Cottrill, 1987). While the backbone structure of all the complexes were represented, the presence of water in the ¹H spectra of complexes TTC3, MCZS3, PFK174 and PFK7 (on day zero) is suggestive of inherent hygroscopic abilities. This means that bioassay activity (as seen in the RT studies) could potentially be affected through compound precipitation in DMSO solutions with the end result being concentration differences. Alternatively, H-bond donors and acceptors present in the compounds with inherent hygroscopic abilities may form interactions with water molecules and hence not be available for interacting with enzyme active sites (even when freshly prepared). Although degradation products were not detectable in the NMR spectra, there is the possibility that this could have occurred. This is because NMR can be limited in sensitivity and there is the possibility of spectral overlap where chemical shifts of degradation products are masked by those of backbone compounds. This may explain why some of these compounds inhibited RT when freshly prepared and analysed after synthesis but not after three years even though NMR analysis presented presumably stable structures (chapter 3 in section 3.4.1).

In the ADMET prediction studies, eight of the nineteen gold complexes had drug-like properties which were comparable to known drugs. These predictions were confirmed for two complexes when the traditional shake flask method was used (section 3.4.3).

6.2 EFFECTS OF COMPOUNDS ON HOST CELLS AND WHOLE VIRUS

A variety of assays were performed to determine the interaction of the compounds with host cells ranging from viability, proliferation, infectivity and the immunomodulatory assays (specifically on T cell frequency and inflammation). The *in vitro* ADMET studies showed physiologically relevant CC₅₀s in the range of 1 and 20 μM for most of the complexes (except for complexes PFK41 and PFK43 whose CC₅₀s values were < 1 μM, Table 4.2). The ligands were less toxic than the gold complexes suggesting that complexation increased toxicity, a finding likely more significant in cancer studies where gold is considered for this property (Che *et al.*, 2003, Marcon *et al.*, 2002, Messori *et al.*, 2000).

Ten complexes inhibited the proliferation of PBMCs by >50% in the CFSE proliferation assay with PFK7 being the most prominent (Figure 4.6). The data correlated with the RT-CES analysis where significant cytostasis was observed for PFK7 and PFK8 (Figure 4.7B and C). None of the compounds stimulated T cell proliferation suggesting that the compounds will not

be potentially antigenic which is the case for some clinically available gold complexes (a situation that is also linked to the side effects that gold complexes have, Lampa *et al.*, 2002, Verwilghen *et al.*, 1992).

Inhibition of viral infectivity was observed at non-toxic concentrations (>80% viability) of complexes TTC24, EK207 and EK231 (Figure 4.8) and cytostatic concentrations of PFK7 (seen by RT-CES analysis, Figure 4.8 and 4.7B respectively). Unfortunately, the very poor drug-likeness predictions for complexes EK207 and EK231 (Table 3.8A) limits their potential as infectivity inhibitory agents. Time of addition studies suggested that inhibition of infectivity was either due to interactions of the compounds with entry or post entry steps as seen from similarities of the IC_{50} values (Table A4.1) implying that differences in exposure time did not affect mechanism of action.

In the immunomodulatory assays (summarised in Table 4.3), the most significant findings were the observed decreases in the frequency of CD4+ cells from 12 HIV+ treatment-naive patients caused by complexes EK207 and PFK7 ($p=0.03$ and 0.005 respectively). TNF- α production was elevated from the same cells by PFK5 and this effect appeared to be removed upon complexation since it was not observed in the complementary complex (PFK7). Cytokine detection by ELISAs from culture supernatant indicated that most of the compounds had stimulatory effects (causing increases in both anti-inflammatory and pro-inflammatory cytokines). However, because these were integrated cytokines from all PBMCs, the ICCS assay findings were considered over the latter because of phenotypic relatedness to T cell type.

None of the ligands demonstrated anti-viral activity supporting the importance of gold complexation in these potential drugs. PFK7 was noted as a lead compound which inhibited viral infectivity at cytostatic concentrations and lowered the frequency of CD4+ cells (and hence activation) without altering cytokine production. These finding suggests that this compound (which also had a good ADMET score, Table 3.9) could be incorporated into the emerging class of anti-HIV agents known as virostatics, a combination which has been found to lead to long term anti-viral efficacy (Lori *et al.*, 2002). Other compounds with potential were PFK8 (an analogue of PFK7) and TTC24 which also inhibited viral infectivity at non-toxic concentrations and had ADMET scores of 6/7 and 3/7 (close to 50%) respectively (Table 3.8A). Although the ADMET score of TTC24 was slightly below average, it will be easier to enhance the drug-likeness of this compound compared to its analogues for which overall drug scores of 0 or 1/7 were noted (Table 3.9). The solubility of this complex could be improved by adding H-bond donors and acceptors such as OH and NH₂ groups, and by reducing the lipophilicity (Kerns and Di, 2008).

6.3 EFFECTS OF COMPOUNDS ON VIRAL ENZYMES

None of the eleven new compounds tested for inhibited RT in the direct enzyme assays (Table 5.2). Eight compounds which previously inhibited RT (Fonteh and Meyer, 2009, Fonteh *et al.*, 2009) were re-tested as controls. It was found that these complexes had lost their RT inhibitory abilities (Table A5.1). This finding was attributed to a number of possible factors such as poor aqueous solubility which is known to affect the reproducibility of bioassay data (Di and Kerns, 2006), degradation, aged compounds and to the possibility that solvents used in the synthetic process (see section 8.4.1 of the appendix for more details) may have contributed to compound effect. The poor size shape complementarity observed for the compounds which interacted favourably with the RNase H site was also thought to be a contributing factor since any conformation change by the receptor to accommodate the ligand could have led to the latter being dislodged. These compounds also lack metal-chelating groups (e.g. carbonyl groups) and therefore could not interact with the crucial active site Mn^{2+} ions such that repulsive forces possibly prevailed.

Except for PFK7 which inhibited PR at a cytotoxic concentration, PR and IN inhibitory activities were absent. The gold(III) thiosemicarbazone complexes (particularly PFK7) interacted favourably with the LEDGF-IN site but these findings must be confirmed using *in vitro* assays.

In silico predictions suggested that the binding of the ligands to RT was at the RNase site while for IN, the ligands interacted more with the LEDGF binding site. Although the enthalpic contributions for both sites were overall not very favourable (negative binding energies are considered favourable), the size-shape complementarity that was observed for PFK7 with this site may play a role in the infectivity inhibition that was observed for this compound but this must still be confirmed experimentally.

The representative gold starting material, $HAuCl_4 \cdot H_2O$ that was tested in this study showed no outstanding inhibition. This was not surprising since it has generally been reported that it is the gold complex and not the ligand or gold starting material that is involved in the biological activity noted for gold complexes (Sun *et al.*, 2004, Traber *et al.*, 1999).

6.4 ANSWERS TO RESEARCH QUESTIONS

In this study, it was hypothesized that “gold-containing compounds could inhibit HIV replication directly through action on viral enzymes and indirectly through action on host cells (e.g. immune modulation) and could serve as drug leads for further analysis and development”. In order to verify this hypothesis, three main research questions were posed. In the following subsections, quick responses will be provided for these questions and other secondary questions that arose.

6.4.1 Were the Compounds Drug-like?

Eight of the nineteen complexes had drug-like properties which were similar to those of auranofin, a gold compound in clinical use for rheumatoid arthritis treatment. Some complexes appeared to have inherent hygroscopic abilities as seen from ^1H NMR spectra but overall the backbone structure of all the analysed compounds were intact for both ^1H and ^{31}P NMR spectra (for compounds dissolved in DMSO and analysed immediately and at 24 h and 7 days later following storage at -20 and 37 °C respectively).

6.4.2 What Were the Effects of the Compounds on Host cells and Whole Virus?

Except for two of the complexes which had CC_{50}s below 1 μM , most of the complexes had CC_{50}s between 1 and 20 μM which were within the physiologically relevant concentration for gold compounds. At these same concentrations, ten of the complexes inhibited T cell proliferation (a mechanism by which gold compounds are thought to exhibit their anti-inflammatory effect (Matsubara and Ziff, 1987). Inhibition of viral infectivity at non-toxic concentrations was observed for complexes TTC24, EK207 and EK231. The gold(III) thiosemicarbazone complexes, PFK7 and PFK8, inhibited viral infectivity at cytostatic concentrations and also lowered the frequency of HIV+CD4+ cells (shown for PFK7 only, $p=0.005$) suggesting potential for incorporation into virostatic cocktails.

6.4.3 Were the Compounds Capable of Inhibiting Viral Enzymes and How?

None of the compounds inhibited RT while one inhibited PR but at a toxic concentration. Compounds with prior anti-RT activity were predicted to bind with the enzyme by interacting with the RNase H site. These interactions unfortunately resulted in poor size-shape fit and poor binding free energies.

None of the compounds inhibited INs' $3'\text{P}$ or ST activities but predictions for the interaction of the gold(III) thiosemicarbazone complexes (particularly PFK7) with LEDGF hotspots on IN were observed.

6.4.4 Other Questions

Answers to some of the secondary questions are provided in the next subsections.

6.4.4.1 Did complexation enhance anti-viral activity?

The advantages of complexation (detailed in Chapter 2), were observed across the chapters. None of the free ligands tested in this study inhibited virus both in the infectivity inhibition assays and in the direct enzyme assays. In the CFSE assay, anti-proliferative effects were noticed more for the complexes than for the ligands e.g. PFK7 retained 137% cells in generation 0 while the complementary ligand retained only 79% (Figure 4.6). Cytostasis was observed for PFK7 and not for PFK5 (Figure 7B) which also lowered the frequency of CD4+

cell presence in HIV+ PBMCs. In the *in silico* docking studies, ligand binding energies were usually higher (suggesting poor binding affinity) than those of complementary complexes. Some examples are the binding free energies obtained for TTL10 and TTL24 (76.6 and 78.6 kcal/mol respectively) and TTC10 and TTC24 (10.9 and 12.3 kcal/mol respectively) in the RNase H studies (Table 5.4). In all, complexation enhanced biological activity and improved binding mode interactions of the gold complexes with host cells in cell-based assays and in *in silico* predictions. Since toxicity checks were implemented in all bioassays, the observed differences in activity were considered not toxicity related.

6.4.4.2 Was activity class and oxidation state related?

The five different classes of compounds (I-V, Table 3.6) that were assayed showed class dependent similarities possibly because of the interclass similarities in precursor structures. With regards to drug-likeness, the gold(I) thiolate complexes of class III, the gold(III) thiosemicarbazone complexes and the gold(III) pyrazolyl complexes were the most drug-like with ADMET scores of 6/7 each. The gold(I) phosphine chloride complexes and corresponding ligands and the BPH gold(I) chloride complexes were the least drug-like and the most lipophilic. With regards to oxidation state, the gold(III) complexes were the most favoured in terms of drug-likeness with all four complexes in class IV and one in class V having drug scores of 6 out of 7 compared to the gold(I) complexes. Cytostasis was observed for the gold(III) thiosemicarbazone complexes and not for any of the other class representatives in the RT-CES studies.

6.4.4.3 What was the effect of complexation on drug-likeness?

With regards to *in silico* ADMET predictions, there were no differences in the ADMET scores of ligands and complementary complexes e.g. TTL24 and TTC24 had similar drug scores (Table 3.9). The same applied to PFK5 and PFK7 and the other ligand-complex pairs.

With regards to *in vitro* ADMET studies (particularly in the cytotoxicity studies), toxicity was observed to increase upon complexation. CC_{50} values for the complexes were generally lower than for the free ligands (Table 4.2). The stability that comes with complexation, although advantageous in improving binding affinity to active sites, is known to be detrimental in the sense that the drug accumulates more in the cells and ends up affecting cell viability. This is the more reason why potential drugs need to be fine tuned to obtain ideal lipophilicity levels and overall drug-like properties.

In the absence of the *in vitro* cytotoxicity studies, the differences in toxicity between ligands and complexes would otherwise not have been obvious from the *in silico* ADMET prediction studies further suggesting the need for complementing both approaches.

6.5 RECOMMENDATIONS

6.5.1 Bioassays should be Complemented with *In Silico* Molecular Modelling Studies

In this study, traditional drug design methods (based on literature and structure) followed by biological screenings were performed. *In silico* predictions studies (although introduced a little latter) helped in the optimisation and filtering of potential drug-like candidates. Their importance as complementary methods to the experimental assays was observed. *In silico* data provided additional explanations for the RT bioassay inconsistencies (the predicted binding site studies suggested poor binding affinity to the RNase H active site). In addition, the observed differences in cytotoxicity patterns between ligands and complexes would not have been noticed. It is therefore recommended that where possible, *in silico* ADMET predictions always be performed alongside high throughput experimental assays or used for eliminating compounds with very poor aqueous solubility properties prior to biological screening. This should increase hit rate and potential drug candidates can be prioritized (Hou and Xu, 2003, Pirard, 2004) which should hopefully lead to a reduction in late-stage drug failures (O'Brien and Groot, 2005). This approach supports the “fail fast” “fail cheap” concept that has been adopted over the past decade by pharmaceutical companies (Egan *et al.*, 2000).

6.5.2 Incorporate Real Time Techniques in Drug Discovery Studies

The use of real time assays such as the RT-CES analysis (which is non invasive) in this study was very valuable in the identification of the mechanism of action of the thiosemicarbazone complexes, PFK7 and PFK8. Although the CFSE studies (endpoint) suggested that PFK7 and other complexes had anti-proliferative effects on PBMCs, it was the RT-CES studies with the TZM-bl cell line, which provided convincing evidence on the cytostatic effect (for PFK7, Figure 4.7B). With the MTT study, also endpoint, the only deduction that could be made was that the compounds were toxic at concentrations which were also inhibiting infectivity. The absence of an additive in the RT-CES analysis eliminates the shortcomings usually associated with MTT making the former data more reliable.

6.5.3 The Need for Therapies to Inhibit Immune Activation

In HIV infected people, activated CD4+ cells presenting virus are primed for killing by CTLs leading to a decrease in CD4+ cells. Concerns regarding cytostatic compounds like HU and the HU-like compound, PFK7, which suppresses CD4+ cell frequency and limit HIV infectivity through a cytostatic mechanism have been raised since these cells are needed by immunocompromised individuals. Several clinical trials (Lori *et al.*, 1997, Frank, 1999, Rutschmann *et al.*, 1998, Federici *et al.*, 1998) have however shown that the use of an optimal cytostatic dose of HU in combination with anti-viral agents such as ddI results in superior efficacy over clinical trial arms that did not incorporate it (Lori *et al.*, 2005). The explanation for

this is that, when a compound suppresses the activity of CD4+ cells, it is likely that activated cells (antigen presenting) and bystander cells (which are mostly affected by HIV apoptosis, Veazey *et al.*, 2000) are reduced in numbers. The result is that these cells are not primed for killing by HIV leading to an overall steady state that is beneficial to the host. Therapies aimed at targeting immune activation have thus been recommended as a remedy for the severe chronic immune activation noted throughout the course of infection (Forsman and Weiss, 2008).

6.5.4 Test the Prodrug in Bioassays

Although auranofin has been reported to demonstrate anti-HIV activity *in vivo* (Lewis *et al.*, 2011, Shapiro and Masci, 1996), it did not exhibit this property in the inhibitory assays that were performed in this study. Most drugs and particularly metal-based compounds such as gold drugs are known to be prodrugs (Tiekink, 2003, Shaw III, 1999, Parish and Cottrill, 1987), and it is therefore possible that the active component of auranofin in the *in vivo* findings was not the one administered and that instead, its metabolites were. In fact metabolites of gold compounds such as diacyanogold(I), Au(CN)₂, have demonstrated anti-RT activity *in vitro* (Tepperman *et al.*, 1994). Some authors have therefore suggested that for *in vitro* studies, the drug metabolites should be tested (Parish and Cottrill, 1987). While this suggestion may be valid theoretically, in practice, it is not easy to comply with since the exact metabolic format of each drug may not be easy to determine without *in vivo* analysis which unfortunately have ethical limitations.

6.5.5 Management of DMSO Compound Stocks

Compounds for HTS are usually dissolved in DMSO and stored frozen. The hygroscopic nature of DMSO could however affect bioassay performance significantly because water in DMSO can accelerate degradation and in many cases, cause compound precipitation thereby affecting concentration (Ellson *et al.*, 2005). Additionally, in the absence of water, compounds dissolved in DMSO could precipitate out of solution within three weeks (Waybright *et al.*, 2009). These limitations can result in underestimated activity, variable data, inaccurate SAR, discrepancies in enzyme and cell-based assays and inaccurate *in vitro* ADMET data (Di and Kerns, 2006). To avoid this problem, DMSO and compounds dissolved in DMSO should be stored in single use aliquots. In addition, short term working stocks should be prepared and DMSO dissolved compounds should not be used for assays after > one week while undissolved compounds should be stored desiccated at -20 °C. The significance of this is to limit or avoid the uptake of water (except in the case where the compounds themselves were hygroscopic e.g. MCZS3) before dissolution for use in assays (Janzen and Popa-Burke, 2009). Alternatively where possible, the compounds should be dissolved and used fresh since compounds prepared fresh maintain activity better (Kerns and Di, 2008).

6.5.6 Structural Modification of the Gold(I) Phosphine Chloride Complexes

Compounds with poor ADMET predictions require structural modification to enhance drug-likeness. The most important of the drug-like properties is lipophilicity since it influences the rest of the parameters such as tissue distribution, receptor binding, cellular uptake, metabolism and bioavailability (Ghose *et al.*, 1998). Compounds in class I, II and the bimetallic complexes of class III (Table 3.6) are those requiring such modifications since the overall drug scores were below 4 (Table 3.9). These compounds had very high lipophilicity values and it would therefore be important to include groups that would result in the reduction of the log P or AlogP98 to the ideal range ($0 \leq 3$, Di and Kerns, 2006). In other words the hydrophilicity or aqueous solubility of the compounds needs to be enhanced. Some suggestions for improving aqueous solubility include the addition of ionisable groups such as a basic amine and carboxylic acid moieties (which will be charged in pH buffers with a resultant increase in solubility), a reduction in log P, introduction of H-bond donors and acceptors, adding polar groups (e.g. ester group and carboxylic acid group) and reducing molecular weight (Kerns and Di., 2008). By improving aqueous solubility, compound toxicity can be reduced while the addition of metal chelating groups to TTC24 for example could enhance interactions with the RNase H site of RT both *in silico* and in direct enzyme assays.

6.5.7 Solvent Effect on Enzyme Activity should be considered During Synthesis

One of the reasons suggested for the absence of RT activity after 3 years for compounds previously shown to inhibit the enzyme when freshly prepared after synthesis was the possibility that solvents used during the synthetic process may have contributed to the inhibition. Solvents such as DMSO, methanol and ethanol have been reported to inhibit RT (Tan *et al.*, 1991). Tan *et al.*, (1991) showed that ethanol inhibited RT activity more than methanol and DMSO, with the latter being the least inhibitory when concentrations from 2-10% (v/v) were tested. In the study, 6 % (v/v) ethanol inhibited RT by up to 50%. For our assays, DMSO concentrations were always kept to the minimum (≤ 0.5 % in cell-based assays) and in the RT assays concentrations of 1.5% had no effect on RT activity (Fonteh and Meyer, 2008). In the synthetic processes, chemists used various solvents either in the complexation process or in the synthesis of gold starting material e.g. dichloromethane and ethanol (Kriel *et al.*, 2007). Synthetic products sometimes resulted in different colours (e.g. TTC3 was cream white at one point and white at another and TTC24 was purple at some point and yellow at another) which the chemists indicated had no effect on analytical data but was mostly linked to the solvent used. While this is true (since backbone NMR chemical shifts were maintained), the fact that these compounds inhibited RT when freshly made up after synthesis and not subsequently may suggest solvent effect and not compound effect may have been at play. We postulate that the loss of activity over time may have resulted from the fact that

inhibitory solvents had evaporated and that the absence or minimal concentrations left had no inhibitory effect on RT.

6.6 NOVEL CONTRIBUTIONS

In this study, the anti-HIV activity of nineteen gold complexes and eight ligands were evaluated. Assays performed were focused towards determining the effect of the compounds on viral infectivity of host cells and on viral targets (RT, PR and IN). Inhibition of viral infectivity was observed for three of the compounds at non-toxic concentrations and for two compounds at cytostatic concentrations. No direct anti-viral activity was noted in direct enzymes assays but favourable predictions were observed for the RNase H site of RT and the LEDGF binding site of IN when computer aided simulations were performed.

Intensive literature review revealed that cytostasis was an anti-viral mechanism in which compounds inhibited viral replication by inhibiting the enzyme, ribonucleotide reductase, thereby reducing dNTP pools required by the virus for replication. Based on the knowledge that gold(III) compounds have anti-cancer activity through cytostatic or anti-proliferative effects (Casini *et al.*, 2008, Che *et al.*, 2003), we postulated and showed for the first time (to the best of our knowledge) that inhibition of HIV-infectivity by the novel group of gold(III) thiosemicarbazone compounds was related to cytostasis. This cytostatic mechanism was determined in both an adherent cell line using impedance-based technology (RT-CES) and in primary cells using CFSE dye dilution technology. Further confirmation of the cytostatic effect for PFK7 was observed where the frequency of CD4+ cells from twelve treatment-naive HIV+ donors was significantly reduced ($p = 0.0049$) as well as in the inhibition of RNR ($p = 0.003$). These findings were in accordance with reports documented for HU which is also a cytostatic anti-HIV agent with both *in vitro* and *in vivo* activity (Lori *et al.*, 1997, Frank, 1999, Rutschmann *et al.*, 1998, Federici *et al.*, 1998). Cytostatic agents also prevent viral replication by reducing cell activation caused by HIV thereby lowering CD4+ cell frequency. This inhibition of immune activation by cytostatic agents such as HU is known to reduce viral replication and we postulate this to be the possible mechanism by which PFK7 (and PFK8) inhibited DU 151.2s' infectivity of the TZM-bl cell line. While this is not the ideal scenario for anti-HIV agents since an increase in CD4+ cell count is usually recommended (Lori *et al.*, 2005), clinical trials have shown that the combination of cytostatic agents such as HU with drugs that directly target the virus such as ddI in virostatics combinations result in longer term efficacy (Lori *et al.* 2002). Some of the benefits are a decrease in immune activation and a reduction in immunodeficiency with an overall increase in CD4+ cell numbers. Additionally the incidence of drug resistance in such combinations is limited compared to current HAART combinations because cytostatic agents target a cellular protein and not a viral one. Since dNTP pools are reduced when cytostatic agents are administered, it means there is a relative

increase in the dNTP analogue (ddl) and an overall longer sustainable efficacy in such combinations (Lori *et al.* 2002).

These postulations were further supported by literature confirming that the anti-viral effects of thiosemicarbazones are as a result RNR inhibition (Easmon *et al.*, 1992, Spector and Jones, 1985). Complexes PFK7 and PFK8 are both thiosemicarbazone-based complexes. The thiosemicarbazone ligands tested here did not inhibit viral infectivity but upon complexation with gold, an overall synergistic anti-viral effect was observed.

Other novel contributions were the findings that the modification of Au(DPPE)₂Cl through the use of nitrogen heteroatoms to increase hydrophilicity in the ethane bridge was not sufficient to render the compounds drug-like as seen from the *in silico* lipophilicity predictions (AlogP98 was >5, Table 3.8A). This finding supports reports by Kriel *et al.*, (2007) that the addition of the hydrazine bridge in synthesizing analogues of Au(DPPE)₂Cl did not result in increased specificity for these compounds as anti-cancer agents.

6.7 FUTURE WORK

6.7.1 Structural Modification To Improve Solubility and Activity

The gold(I) phosphine chloride complex (TTC24) which had a drug-likeness score of 3 out of 7 and inhibited viral infectivity at non-toxic concentrations could be structurally modified to enhance its drug score by increasing aqueous solubility. This same complex and its analogues TTC3, TTC10 and TTC17 also interacted favourably with the RNase H site of RT but will require the addition of metal chelating moieties to increase the affinity of the compounds for this site which contains two Mn²⁺.

The phosphine complexes, the BPH complexes and the bimetallic gold(I) phosphine thiolate ligands were not sufficiently soluble in biological media (precipitating), also seen in the aqueous solubility predictions. This means these compounds will not readily enter cells but may instead assemble at the cell membrane (high lipophilicity) and cause cell death due to irreversible damage to the membrane. Moderating the lipophilicity of these complexes which had AlogP98 predictions of >5 might improve the bioassay activity especially in cell culture. This could potentially solve the problem of inconsistencies in bioassay data (if aqueous solubility was the cause) that was obtained for these complexes especially in the RT assays.

Solubility also appeared to be influenced by geographical location. Compounds with previous anti-RT activity were tested soon after synthesis at the University of Johannesburg, Auckland Park Campus in Johannesburg (1753 m above sea level). The re-tests were done at the University of Pretoria, Pretoria (1271 m above sea level). Differences in geographical location are known to affect air pressure and thus solubility. These differences might have been the cause of the discrepancies in the RT data. To manage this, CO₂/O₂ levels in the dissolved compounds could be altered to improve solubility.

6.7.3 Determine the Oxidation State of Gold Within Cells

The gold complexes that were tested here were either gold(I) or gold(III) complexes. Uptake studies have previously been shown for some of these compounds using ICP-AES (Fonteh and Meyer, 2009). It will be of interest to determine what the oxidation states of the complexes are after uptake using mössbauer spectroscopy. Gold(III) compounds are prone to reduction by thiols in biological media (Fricker, 1996). Gold(I) complexes are more stable than gold(III) complexes when soft ligands such as the phosphine gold and triethylphosphine thiol ligands are used for coordinating the gold nucleus. For gold(III), the use of hard donor ligands containing N and O enhances stability in the biological environment, which was the case in this study. By determining the oxidation states, information on the stability of the complexes and the active form (prodrug form) can be deduced.

6.7.4 RT-CES Analysis

The proliferation profiles of each compound especially the remaining thiosemicarbazone complexes (PFK41 and PFK43), should be determined using RT-CES. These compounds showed considerable toxicity in the MTT assay and very high inhibitory effects on viral infectivity (Figure 4.8). It will be interesting to verify if these complexes perhaps had a cytostatic effect on these cells since the analogues, PFK7 and PFK8 did.

6.7.5 Combination Studies of PFK7 and PFK8 with dNTP Analogues.

The anti-viral activity of the cytostatic agent, HU, was potentiated when combined with dNTP analogues such as ddl and indinavir both *in vitro* (Lori *et al.*, 2005) and *in vivo* (Lori *et al.*, 1997, Frank, 1999, Rutschmann *et al.*, 1998, Federici *et al.*, 1998). Complex PFK7 inhibited viral infectivity of TZM-bl cells at cytostatic concentrations (Figure 4.8 and 4.7 respectively), and like HU lowered the frequency of CD4+ cells from HIV+ donors (Figure 4.11). Combinations studies of PFK7 with ddl or indinavir should hopefully result in synergistic effects both in anti-viral activity and in improving immune responses.

6.7.6 Determine if Compounds with Anti-proliferative Effects can Prevent T Cell Activation

Not all the compounds which had anti-proliferative effects on PBMCs were tested in the immunomodulatory assays where compound effects on virus was assessed with regards to T cell frequency and cytokine production. These were complexes EK208, EK219, PFK190, PFK8 and PFK43. It would be interesting to know if these complexes (particularly PFK8 and PFK43 which are drug-like and structurally similar the gold(III) compound, $\text{KAu}^{\text{III}}\text{Cl}_4$, known to prevent T cell activation, De Wall *et al.*, 2006) can affect T cell frequency and alter the chronic inflammatory effect caused by HIV. Immune activation by HIV leads to clonal expansion and proliferation of T cells. Compounds with anti-proliferative effects may be capable of preventing

this activation and as a result alter T cell frequency and possibly cytokine production. The incorporation of activation markers such as CD69 to monitor these effects will thus be useful.

6.7.7 Determine Viral Core Protein (p24) Secretion as Measure for Viral Infectivity

Viral core protein (p24) was not directly analysed in this study but the expectation was that inhibition of infectivity by the cytostatic complexes such as PFK7 should lead to a reduction of p24 antigen secretion. It would be important to verify this assumption by assessing the level of p24 antigen secretion from infected cells treated with the promising compounds.

6.7.8 Cell Cycle Analysis to Determine the Phase Affected by Cytostatic Compounds

Cells treated with the cytostatic agent, HU, are arrested between the G₁ and S phases or enter and accumulate in the S phase (Maurer-Schultze *et al.*, 1988). It will be useful to determine if the HU-like compounds (PFK7 and 8) inhibit cell proliferation by arresting growth in the same phase as HU does. This will further confirm whether the compounds block dNTP production thereby impairing DNA synthesis (Lori, 1999).

6.7.9 Preselect T Cells Prior to Treatment

The heterogeneous nature of PBMCs together with interperson differences means using these cells for viral quantification can result in data variation (Trkola *et al.*, 1999). For the immunomodulatory studies, cells were tagged with Mabs and cell frequencies and cytokine production levels monitored. The heterogeneous nature of the cell population means compound action could be limited for the cells of interest due to interactions with cells from the different subpopulations prior to analysis. To alleviate this and increase specificity for the immunomodulatory assays, the cells should be pre-sorted using the sorting function on a flow cytometer such as the FACSAria (Becton Dickinson or BD BioSciences, California, USA) or using other cell separating tools such as magnetic beads prior to treatment.

6.7.10 Docking Considerations

Since metals form covalent bonds with ligands and gold complexes are known to undergo ligand exchange reactions, it is possible that a putative inhibitor in a docking study might bind to the protein covalently (Höltje *et al.*, 2003). This could be possible especially for the gold(I) phosphine chloride complexes which have a chloride ion since this ion is a good leaving group (Allaudeen *et al.*, 1985) that would potentially leave the gold atom ionised. Determining the binding affinity of the complexes in the ionised form might result in different outcomes from those that were obtained and might prove more promising for the gold complexes considering that gold could easily form covalent bonds with sulhydryl groups of cysteine residues in receptor active sites. Unfortunately *in silico* docking strategies for such

situations are still being developed and as mentioned in Chapter 5, most *in silico* packages have not yet incorporated metals into their atom base. This is because of the enormous diverse structure of coordination compounds available making it difficult for the development of reference values for such packages (Comba and Hambley, 1995, Hay, 1993).

The modification of the subtype B crystal structures through site directed mutagenesis to include amino acid mutations found in the subtype C strain prior to docking should be considered. While direct enzyme assays for RT inhibition for subtype C and B viral strains have been reported to result in similar susceptibilities for commonly used NRTIs and NNRTIs (Xu *et al.*, 2010), such modifications might lead to different outcomes for the gold-based compounds both in direct enzyme and *in silico* studies.

In the docking studies, metal-based drugs which have previously inhibited viral enzymes should be used as controls.

6.8 CONCLUSION

While finding new medication for HIV remains a major concern for researchers and the pharmaceutical industry, identifying an ideal drug is never easy (Joshi, 2007). A list of criteria has to be met for a lead candidate to successfully navigate through the drug discovery time line phases (Figure 2.18) which can be up to 10 years or more. This has been clearly demonstrated in this study where in an attempt to answer some major research questions, more questions were raised.

A total of 27 compounds were analysed from several angles to determine toxicity, effect on cell proliferation and antiviral abilities. Three promising candidates were singled out; TTC24 which inhibited viral infectivity at non-toxic concentrations with a fairly reasonable drug score and PFK7 and PFK8 which inhibited viral infectivity at cytostatic concentrations and had drug scores similar to clinically available drugs. The latter two (both gold(III) Tscs-based compounds) can be incorporated into virostatic combinations but assays to show favourable responses in immune parameters (e.g. CD4+ cell increases) upon combination with direct viral inhibitory agents must first be done to determine usefulness in such cocktails.

CHAPTER 7

REFERENCES

- Abassi, Y. A., Xi, B., Zhang, W., Ye, P., Kirstein, S.L., Gaylord, M.R., Feinstein, S.C., Wang, X., Xu, X., (2009). Kinetic cell-based morphological screening: prediction of mechanism of compound action and off-targets effects. *Chem. Biol.* 16, 712-723.
- Abdool Karim, Q., Abdool Karim, S.S., Frohlich, J.A., Grobler, A.C., Baxter, C., Mansoor, L.E., Kharsany, A.B., Sibeko, S., Mlisana, K.P., Omar, Z., Gengiah, T.N., Maarschalk, S., Arulappan, N., Mlotshwa, M., Morris, L., Taylor, D., CAPRISA 004 Trial Group, 2010. Effectiveness and safety of tenofovir gel, an antiretroviral microbicide, for the prevention of HIV infection in women. *Science* 329, 1168-1174.
- Abdou, H.E., Mohamed, A.A., Fackler Jr., J.P., Burini, A., Galassi, R., López-de-Luzuriaga, J.M., Olmos, M.E., 2009. Structures and properties of gold(I) complexes of interest in biochemical applications. *Coord. Chem. Rev.* 253, 1661-1669.
- Adamson, C.S., Freed, E.O., 2010. Novel approaches to inhibiting HIV-1 replication. *Anti-viral Res.* 85, 119-141.
- Ahmad, S., 2004. The chemistry of cyano complexes of gold(I) with emphasis on the ligand scrambling reactions. *Coord. Chem. Rev.* 248, 231-243.
- Alfano, M., Poli, G., 2001. Cytokine and chemokine based control of HIV infection and replication. *Curr. Pharm. Des.* 7, 993-1013.
- Alfano, M., Poli, G., 2005. Role of cytokines and chemokines in the regulation of innate immunity and HIV infection. *Mol. Immunol.* 42, 161-182.
- Allaudeen, H.S., Snyder, R.M., Whitman, M.H., Crooke, S.T., 1985. Effects of coordinated gold compounds on in vitro and in situ DNA replication. *Biochem. Pharmacol.* 34, 3243-3250.
- Allen, D.D., Caviades, R., Cardenas, A.M., Shimahara, T., Segura-Aguilar, J., Caviades, P.A., 2005. Cell lines as in vitro models for drug screening and toxicity studies. *Drug Dev. Ind. Pharm.* 31, 757-768.
- Antiretroviral therapy Cohort collaboration. Life expectancy of individuals on combination antiretroviral therapy in high-income countries: a collaborative analysis of 14 cohort studies. 2008. *The Lancet* 372, 293-299.
- Appay, V., Sauce, D., 2008. Immune activation and inflammation in HIV-1 infection: causes and consequences. *J. Pathol.* 214, 231-241.
- Arnesano, F., Natile, G., 2009. Mechanistic insight into the cellular uptake and processing of cisplatin 30 years after its approval by FDA. *Coord. Chem. Rev.* 253, 2070-2081.
- Arrode-Bruses, G., Sheffer, D., Hegde, R., Dhillon, S., Liu, Z., Villinger, F., Narayan, O., Chebloune, Y., 2010. Characterization of T-cell responses in macaques immunized with a single dose of HIV DNA vaccine. *J. Virol.* 84, 1243-1253.
- Baldwin, E.T., Bhat, T.N., Liu, B., Pattabiraman, N., Erickson, J.W., 1995. Structural basis of drug resistance for the V82A mutant of HIV-1 proteinase. *Nat. Struct. Biol.* 2, 244-249.
- Baran, J., Kowalczyk, D., Ozog, M., Zembala, M., 2001. Three-color flow cytometry detection of intracellular cytokines in peripheral blood mononuclear cells: comparative analysis of phorbol myristate acetate-ionomycin and phytohemagglutinin stimulation. *Clin. Diagn. Lab. Immunol.* 8, 303-313.
- Barrera, P., Boerbooms, A.M., van de Putte, L.B., van der Meer, J.W., 1996. Effects of antirheumatic agents on cytokines. *Semin. Arthritis Rheum.* 25, 234-253.
- Bartlett J.A., Chen SS., Quinn J.B., 2007, Comparative efficacy of nucleoside/nucleotide RT inhibitors in combination with efavirenz: results of a systemic overview. *HIV Clinical trials*, 8; 221-226.
- Beraldo, H., Gambino, D., 2004. The wide pharmacological versatility of semicarbazones, thiosemicarbazones and their metal complexes. *Mini Rev. Med. Chem.* 4, 31-39.
- Berners-Price S.J. and Sadler P.J. (1996). Coordination chemistry of metallodrugs: insights into biological speciation from NMR spectroscopy. *Coord. Chem. Rev.* 151:1-40.
- Berners-Price, S.J., Mirabelli, C.K., Johnson, R.K., Mattern, M.R., McCabe, F.L., Faucette, L.F., Sung, C.M., Mong, S.M., Sadler, P.J., Crooke, S.T., 1986. In vivo antitumor activity and in vitro cytotoxic properties of bis[1,2-bis(diphenylphosphino)ethane]gold(I) chloride. *Cancer Res.* 46, 5486-5493.
- Best, S.L, Sadler, P.J. 1996. Gold drugs: mechanism of action and toxicity. *Gold Bulletin* 29, 87-93.

- Betts, M.R., Nason, M.C., West, S.M., De Rosa, S.C., Migueles, S.A., Abraham, J., Lederman, M.M., Benito, J.M., Goepfert, P.A., Connors, M., Roederer, M., Koup, R.A., 2006. HIV nonprogressors preferentially maintain highly functional HIV-specific CD8+ T cells. *Blood* 107, 4781-4789.
- Bianchi, V., Pontis, E., Reichard, P., 1986. Changes of deoxyribonucleoside triphosphate pools induced by hydroxyurea and their relation to DNA synthesis. *J. Biol. Chem.* 261, 16037-16042.
- Biancotto, A., Iglehart, S.J., Vanpouille, C., Condack, C.E., Lisco, A., Ruecker, E., Hirsch, I., Margolis, L.B., Grivel, J.C., 2008. HIV-1 induced activation of CD4+ T cells creates new targets for HIV-1 infection in human lymphoid tissue ex vivo. *Blood* 111, 699-704.
- Block, B.P., 1953. Gold powder and potassium tetrabromoaurate(III). *Inorg. Synth.* 4, 14-17.
- Blough H, Ricchetti M, Montagnier L, Buc H (1989) Organic gold compounds are effective against HIV-1 reverse transcriptase, vol 5. International conference on AIDS, Jun 4–9, p 559.
- Bottenus, B.N., Kan, P., Jenkins, T., Ballard, B., Rold, T.L., Barnes, C., Cutler, C., Hoffman, T.J., Green, M.A., Jurisson, S.S., 2010. Gold(III) bis-thiosemicarbazonato complexes: synthesis, characterization, radiochemistry and X-ray crystal structure analysis. *Nucl. Med. Biol.* 37, 41-49.
- Boyd MR, (1989). Status of the NCI preclinical antitumour drug discovery screen. *Principles and Practices of Oncology*, 1989, 3(10) 1-12
- Boyd, J.M., Huang, L., Xie, L., Moe, B., Gabos, S., Li, X.F., 2008. A cell-microelectronic sensing technique for profiling cytotoxicity of chemicals. *Anal. Chim. Acta* 615, 80-87.
- Breen, E.C., 2002. Pro- and anti-inflammatory cytokines in human immunodeficiency virus infection and acquired immunodeficiency syndrome. *Pharmacol. Ther.* 95, 295-304.
- Brenchley, J.M., Douek, D.C., 2004. Flow cytometric analysis of human antigen-specific T-cell proliferation. *Methods Cell Biol.* 75, 481-496.
- Brenchley, J.M., Price, D.A., Douek, D.C., 2006. HIV disease: fallout from a mucosal catastrophe? *Nat. Immunol.* 7, 235-239.
- Bruni, B., Guerri, A., Marcon, G., Messori, L., Orioli, P., 1999. Structure and Cytotoxic Properties of Some Selected Gold(III) Complexes. *Croat. Chem. Acta* 72, 221-229.
- Bujacz, G., Alexandratos, J., Wlodawer, A., Merkel, G., Andrade, M., Katz, R.A., Skalka, A.M., 1997. Binding of different divalent cations to the active site of avian sarcoma virus integrase and their effects on enzymatic activity. *J. Biol. Chem.* 272, 18161-18168.
- Burdall, S.E., Hanby, A.M., Lansdown, M.R., Speirs, V., 2003. Breast cancer cell lines: friend or foe? *Breast Cancer Res.* 5, 89-95.
- Buttke, T.M., McCubrey, J.A., Owen, T.C., 1993. Use of an aqueous soluble tetrazolium/formazan assay to measure viability and proliferation of lymphokine-dependent cell lines. *J. Immunol. Methods* 157, 233-240.
- Campbell, E.M., Hope, T.J., 2008. Live cell imaging of the HIV-1 life cycle. *Trends Microbiol.* 16, 580-587.
- Carr, A., Cooper, D.A., 2000. Adverse effects of antiretroviral therapy. *Lancet* 356, 1423-1430.
- Carr, J. K., B. T. Foley, T. Leitner, M. O. Salminen, B. Korber, and F. E. McCutchan. 1998. Reference sequences representing the principal genetic diversity of HIV-1 in the pandemic, p. 10–19. In B. Korber, C. L. Kuiken, B. Foley, B. Hahn, F. McCutchan, J. W. Mellors, and J. Sodroski (ed.), *Human retroviruses and AIDS: a compilation and analysis of nucleic acid and amino acid sequences*. Los Alamos National Laboratory, Los Alamos, N.Mex.
- Casini, A., Hartinger, C., Gabbiani, C., Mini, E., Dyson, P.J., Keppler, B.K., Messori, L., 2008. Gold(III) compounds as anticancer agents: relevance of gold-protein interactions for their mechanism of action. *J. Inorg. Biochem.* 102, 564-575.
- Caso, G., Garlick, P.J., Gelato, M.C., McNurlan, M.A., 2001. Lymphocyte protein synthesis is increased with the progression of HIV-associated disease to AIDS. *Clin. Sci. (Lond)* 101, 583-589.
- Castilho, L.R., Moraes A.M., Augusto, E.F.P., Butler, M., 2008. *Animal cell technology: from biopharmaceuticals to gene therapy*. Taylor and Francis e-Library, New York, USA.
- Ceccherini-Silberstein, F., Svicher, V., Sing, T., Artese, A., Santoro, M.M., Forbici, F., Bertoli, A., Alcaro, S., Palamara, G., d'Arminio Monforte, A., Balzarini, J., Antinori, A., Lengauer, T., Perno, C.F., 2007. Characterization and structural analysis of novel mutations in human immunodeficiency virus type 1 reverse transcriptase involved in the regulation of resistance to nonnucleoside inhibitors. *J. Virol.* 81, 11507-11519.
- Champion, G.D., Graham, G.G., Ziegler, J.B., 1990. The gold complexes. *Baillieres Clin. Rheumatol.* 4, 491-534.
- Che, C.M., Sun, R.W., Yu, W.Y., Ko, C.B., Zhu, N., Sun, H., 2003. Gold(III) porphyrins as a new class of anticancer drugs: cytotoxicity, DNA binding and induction of apoptosis in human cervix epitheloid cancer cells. *Chem. Commun. (Camb)* (14), 1718-1719.

- Chen, R., Quinones-Mateu, M.E., Mansky, L.M., 2004. Drug resistance, virus fitness and HIV-1 mutagenesis. *Curr. Pharm. Des.* 10, 4065-4070.
- Cheng, A., Dixon, S.L., 2003. In silico models for the prediction of dose-dependent human hepatotoxicity. *J. Comput. Aided Mol. Des.* 17, 811-823.
- Cheng, A., Merz, K.M., Jr, 2003. Prediction of aqueous solubility of a diverse set of compounds using quantitative structure-property relationships. *J. Med. Chem.* 46, 3572-3580.
- Cherepanov, P., Ambrosio, A.L., Rahman, S., Ellenberger, T., Engelman, A., 2005. Structural basis for the recognition between HIV-1 integrase and transcriptional coactivator p75. *Proc. Natl. Acad. Sci. U. S. A.* 102, 17308-17313.
- Chirch, L.M., Morrison, S., Steigbigel, R.T., 2009. Treatment of HIV infection with raltegravir. *Expert Opin. Pharmacother.* 10, 1203-1211.
- Chircorian, A., Barrios, A.M., 2004. Inhibition of lysosomal cysteine proteases by chrysotherapeutic compounds: a possible mechanism for the antiarthritic activity of Au(I). *Bioorg. Med. Chem. Lett.* 14, 5113-5116.
- Choe, H., Farzan, M., Sun, Y., Sullivan, N., Rollins, B., Ponath, P.D., Wu, L., Mackay, C.R., LaRosa, G., Newman, W., Gerard, N., Gerard, C., Sodroski, J., 1996. The beta-chemokine receptors CCR3 and CCR5 facilitate infection by primary HIV-1 isolates. *Cell* 85, 1135-1148.
- Christ, F., Voet, A., Marchand, A., Nicolet, S., Desimmie, B.A., Marchand, D., Bardiot, D., Van der Veken, N. J., Van Remoortel, B., Strelkov, S.V., De Maeyer, M., Chaltin, P., Debyser, Z., 2010. Rational design of small-molecule inhibitors of the ledgF/p75-integrase interaction and HIV replication 1. *Nat. Chem. Biol.* 6, 442-448.
- Clavel, F., Hance, A.J., 2004. HIV drug resistance. *N. Engl. J. Med.* 350, 1023-1035.
- Clouser, C.L., Patterson, S.E., Mansky, L.M., 2010. Exploiting drug repositioning for discovery of a novel HIV combination therapy. *J. Virol.* 84, 9301-9309.
- Coetzer, M., Cilliers, T., Papathanasopoulos, M., Ramjee, G., Karim, S.A., Williamson, C., Morris, L., 2007. Longitudinal analysis of HIV type 1 subtype C envelope sequences from South Africa. *AIDS Res. Hum. Retroviruses* 23, 316-321.
- Coffin, J.M., Hughes, S.H., Varmus, H.E., 1997. The Interactions of Retroviruses and their Hosts, in: Coffin, J.M., Hughes, S.H., Varmus, H.E. (Eds.), *Retroviruses*. Cold Spring Harbor Laboratory Press, Cold Spring Harbor (NY).
- Coman, R.M., Robbins, A.H., Fernandez, M.A., Gilliland, C.T., Sochet, A.A., Goodenow, M.M., McKenna, R., Dunn, B.M., 2008. The contribution of naturally occurring polymorphisms in altering the biochemical and structural characteristics of HIV-1 subtype C protease. *Biochemistry* 47, 731-743.
- Comba, P., Daubinet, A., Martin, B., Pietzsch, H., Stephan, H., 2006. A new molecular mechanics force field for the design of oxotechnetium(V) and oxorhenium(V) radiopharmaceuticals. *J. Organomet. Chem.* 691, 2495-2502.
- Comba, P., Hambley, T.W., 1995. *Molecular modeling of Inorganic compounds*. VCH Weinheim, Germany.
- Corbau, R., Mori, J., Phillips, C., Fishburn, L., Martin, A., Mowbray, C., Panton, W., Smith-Burchnell, C., Thornberry, A., Ringrose, H., Knochel, T., Irving, S., Westby, M., Wood, A., Perros, M., 2010. Lersivirine, a nonnucleoside reverse transcriptase inhibitor with activity against drug-resistant human immunodeficiency virus type 1. *Antimicrob. Agents Chemother.* 54, 4451-4463.
- Cox, A.G., Nair, V., 2006. Novel HIV integrase inhibitors with anti-HIV activity: insights into integrase inhibition from docking studies. *Antivir. Chem. Chemother.* 17, 343-353.
- Cozzi-Lepri, A., Ruiz, L., Loveday, C., Phillips, A.N., Clotet, B., Reiss, P., Ledergerber, B., Holkmann, C., Staszewski, S., Lundgren, J.D., EuroSIDA Study Group, 2005. Thymidine analogue mutation profiles: factors associated with acquiring specific profiles and their impact on the virological response to therapy. *Antivir Ther.* 10, 791-802.
- Crilly, A., Madhok, R., Watson, J., Capell, H.A., Sturrock, R.D., 1994. Production of interleukin-6 by monocytes isolated from rheumatoid arthritis patients receiving second-line drug therapy. *Br. J. Rheumatol.* 33, 821-825.
- Danielsson and Zhang, 1996. Methods for determining n-octanol - water partition constants. *Trends in Anal. Chem.* 15, 188-196.
- Davies, J.F. 2nd, Hostomska, Z., Hostomsky, Z., Jordan, S.R., Matthews, D.A., 1991. Crystal structure of the ribonuclease H domain of HIV-1 reverse transcriptase. *Science* 252, 88-95.
- de Bethune, M.P., 2010. Non-nucleoside reverse transcriptase inhibitors (NNRTIs), their discovery, development, and use in the treatment of HIV-1 infection: a review of the last 20 years (1989-2009). *Anti-viral Res.* 85, 75-90.

- De Clercq, E., 1995. Toward improved anti-HIV chemotherapy: therapeutic strategies for intervention with HIV infections. *J. Med. Chem.* 38, 2491-2517.
- De Clercq, E., 2009. Anti-viral drug discovery: ten more compounds, and ten more stories (part B). *Med. Res. Rev.* 29, 571-610.
- De Wall, S.L., Painter, C., Stone, J.D., Bandaranayake, R., Wiley, D.C., Mitchison, T.J., Stern, L.J., DeDecker, B.S., 2006. Noble metals strip peptides from class II MHC proteins. *Nat. Chem. Biol.* 2, 197-201.
- Deboucq, C., 1992. The HIV-1 protease as a therapeutic target for AIDS. *AIDS Res. Hum. Retroviruses* 8, 153-164.
- Denizot, F., Lang, R., 1986. Rapid colorimetric assay for cell growth and survival. Modifications to the tetrazolium dye procedure giving improved sensitivity and reliability. *J. Immunol. Methods* 89, 271-277.
- Derdeyn, C.A., Decker, J.M., Sfakianos, J.N., Wu, X., O'Brien, W.A., Ratner, L., Kappes, J.C., Shaw, G.M., Hunter, E., 2000. Sensitivity of human immunodeficiency virus type 1 to the fusion inhibitor T-20 is modulated by coreceptor specificity defined by the V3 loop of gp120. *J. Virol.* 74, 8358-8367.
- Desai, P.V., Patny, A., Gut, J., Rosenthal, P.J., Tekwani, B., Srivastava, A., Avery, M., 2006. Identification of novel parasitic cysteine protease inhibitors by use of virtual screening. 2. The available chemical directory. *J. Med. Chem.* 49, 1576-1584.
- Di Grandi, M., Olson, M., Prashad, A.S., Bebernitz, G., Luckay, A., Mullen, S., Hu, Y., Krishnamurthy, G., Pitts, K., O'Connell, J., 2010. Small molecule inhibitors of HIV RT Ribonuclease H. *Bioorg. Med. Chem. Lett.* 20, 398-402.
- Di, L., Kerns, E.H., 2003. Profiling drug-like properties in discovery research. *Curr. Opin. Chem. Biol.* 7, 402-408.
- Di, L., Kerns, E.H., 2006. Biological assay challenges from compound solubility: strategies for bioassay optimization. *Drug Discov. Today* 11, 446-451.
- Dictionary.com <http://dictionary.reference.com/>
- Dinarello, C.A., 2000. Proinflammatory cytokines. *Chest* 118, 503-508.
- Dixon, S.L., Merz, K.M., Jr, 2001. One-dimensional molecular representations and similarity calculations: methodology and validation. *J. Med. Chem.* 44, 3795-3809.
- Dolan, J., Chen, A., Weber, I.T., Harrison, R.W., Leis, J., 2009. Defining the DNA substrate binding sites on HIV-1 integrase. *J. Mol. Biol.* 385, 568-579.
- Donato, M.T., Lahoz, A., Castell, J.V., Gomez-Lechon, M.J., 2008. Cell lines: a tool for in vitro drug metabolism studies. *Curr. Drug Metab.* 9, 1-11.
- Donehower, R.C., 1992. An overview of the clinical experience with hydroxyurea. *Semin. Oncol.* 19, 11-19.
- Douek, D.C., Roederer, M., Koup, R.A., 2009. Emerging concepts in the immunopathogenesis of AIDS. *Annu. Rev. Med.* 60, 471-484.
- Dougherty, D.A., 1996. Cation- π interactions in chemistry and biology: a new view of benzene, Phe, Tyr, and Trp. *Science* 271, 163-168.
- Dragic, T., Litwin, V., Allaway, G.P., Martin, S.R., Huang, Y., Nagashima, K.A., Cayanan, C., Maddon, P.J., Koup, R.A., Moore, J.P., Paxton, W.A., 1996. HIV-1 entry into CD4+ cells is mediated by the chemokine receptor CC-CKR-5. *Nature* 381, 667-673.
- Du, L., Zhao, Y.X., Yang, L.M., Zheng, Y.T., Tang, Y., Shen, X., Jiang, H.L., 2008. Symmetrical 1-pyrrolidineacetamide showing anti-HIV activity through a new binding site on HIV-1 integrase. *Acta Pharmacol. Sin.* 29, 1261-1267.
- Easmon, J., Heinisch, G., Holzer, W., Rosenwirth, B., 1992. Novel thiosemicarbazones derived from formyl- and acyldiazines: synthesis, effects on cell proliferation, and synergism with anti-viral agents. *J. Med. Chem.* 35, 3288-3296.
- Egan, W.J., Lauri, G., 2002. Prediction of intestinal permeability. *Adv. Drug Deliv. Rev.* 54, 273-289.
- Egan, W.J., Merz, K.M., Jr, Baldwin, J.J., 2000. Prediction of drug absorption using multivariate statistics. *J. Med. Chem.* 43, 3867-3877.
- Eijkelenboom A.P.A., Sprangers, R., Hard, K., Puras Lutzke, R.A., Plasterk R.H.A., 1999. Refined solution structure of the c-terminal DNA-binding domain of human immunovirus-1 integrase. *Proteins: Struct. Funct. Bioinf.* 36, 556-564.
- Elder, R.C., Zhao, Z., Zhang, Y., Dorsey, J.G., Hess, E.V., Tepperman, K., 1993. Dicyanogold (I) is a common human metabolite of different gold drugs. *J. Rheumatol.* 20, 268-272.

- Ellson, R., Stearns, R., Mutz, M., Brown, C., Browning, B., Harris, D., Qureshi, S., Shieh, J., Wold, D., 2005. In situ DMSO hydration measurements of HTS compound libraries. *Comb. Chem. High Throughput Screen.* 8, 489-498.
- Engelman, A., Bushman, F.D., Craigie, R., 1993. Identification of discrete functional domains of HIV-1 integrase and their organization within an active multimeric complex. *EMBO J.* 12, 3269-3275.
- Engelman, A., Mizuuchi, K., Craigie, R., 1991. HIV-1 DNA integration: mechanism of viral DNA cleavage and DNA strand transfer. *Cell* 67, 1211-1221.
- Enting, R.H., Hoetelmans, R.M., Lange, J.M., Burger, D.M., Beijnen, J.H., Portegies, P., 1998. Antiretroviral drugs and the central nervous system. *AIDS* 12, 1941-1955.
- Fan H., Conner R.F., and Villarreal L.P., 2000. *The biology of AIDS*, 4th Edition John and Barlett Publishers, Boston: 46-47.
- Federici ME, Lupo S., Cahn P., Cassetti I., Pedro R., Ruiz-Palacios G et al., Hydroxyurea in combination regimens for the treatment of antiretroviral naïve, HIVinfected adults. XII International Conference on AIDS. Geneva, June 1998 [abstract 287/12235]
- Fields B.N., Knipe D.M., Howley P.M., (1996), *Fields Virology*. 3rd Ed. Lippincott-Raven Publishers, Philadelphia, PA.
- Finzi, D., Hermankova, M., Pierson, T., Carruth, L.M., Buck, C., Chaisson, R.E., Quinn, T.C., Chadwick, K., Margolick, J., Brookmeyer, R., Gallant, J., Markowitz, M., Ho, D.D., Richman, D.D., Siliciano, R.F., 1997. Identification of a reservoir for HIV-1 in patients on highly active antiretroviral therapy. *Science* 278, 1295-1300.
- Fiorentini, S., Giagulli, C., Caccuri, F., Magiera, A.K., Caruso, A., 2010. HIV-1 matrix protein p17: a candidate antigen for therapeutic vaccines against AIDS. *Pharmacol. Ther.* 128, 433-444.
- Fishman, M.C., Porter, J.A., 2005. Pharmaceuticals: a new grammar for drug discovery. *Nature* 437, 491-493.
- Folks, T., Kelly, J., Benn, S., Kinter, A., Justement, J., Gold, J., Redfield, R., Sell, K.W., Fauci, A.S., 1986. Susceptibility of normal human lymphocytes to infection with HTLV-III/LAV. *J. Immunol.* 136, 4049-4053.
- Fonteh P, Meyer D, Chrysotherapy: Evaluating Gold Compounds For Anti-Hiv Activity, April 2008, MSc Dissertation, University of Johannesburg (Former Rand Afrkaans University).
- Fonteh P., Meyer D. 2009. Novel gold(I) phosphine compounds inhibit HIV-1 enzymes. *Metallomics*; 1: 427-433.
- Fonteh, P.N., Keter, K.K., Meyer D., 2011. New Bis(thiosemicarbazone) gold(III) complexes inhibit HIV replication at cytostatic concentrations: potential for incorporation into virostatic cocktails. *J. Inorg. Biochem.* 105, 1173-1180.
- Fonteh, P.N., Keter, F.K., Meyer, D., 2010. HIV therapeutic possibilities of gold compounds. *Biometals* 23, 185-196.
- Fonteh, P.N., Keter, F.K., Meyer, D., Guzei, I.A., Darkwa, J., 2009. Tetra-chloro-(bis-(3,5-dimethylpyrazolyl)methane)gold(III) chloride: An HIV-1 reverse transcriptase and protease inhibitor. *J. Inorg. Biochem.* 103, 190-194.
- Ford, N., Calmy, A., von Schoen-Angerer, T., 2007. Treating HIV in the developing world: getting ahead of the drug development curve. *Drug Discov. Today* 12, 1-3.
- Forrestier J., 1935. Rheumatoid arthritis and its treatment by gold salts. *J. Lab clin Med* 1935, 20 827
- Forsman, A., Weiss, R.A., 2008. Why is HIV a pathogen? *Trends Microbiol.* 16, 555-560.
- Francis, M.L., Meltzer, M.S., Gendelman, H.E., 1992. Interferons in the persistence, pathogenesis, and treatment of HIV infection. *AIDS Res. Hum. Retroviruses* 8, 199-207.
- Frank, I., 1999. Clinical use of hydroxyurea in HIV-1 infected patients. *J. Biol. Regul. Homeost. Agents* 13, 186-191.
- Fricker, S.P., 1996. Medical uses of gold compounds: past, present and future. *Gold bulletin*, 29(2):53-59.
- Fricker, S.P., 2007. Metal based drugs: from serendipity to design. *Dalton Trans.* (43), 4903-4917.
- Friesner, R.A., Banks, J.L., Murphy, R.B., Halgren, T.A., Klicic, J.J., Mainz, D.T., Repasky, M.P., Knoll, E.H., Shelley, M., Perry, J.K., Shaw, D.E., Francis, P., Shenkin, P.S., 2004. Glide: A New Approach for Rapid, Accurate Docking and Scoring. 1. Method and Assessment of Docking Accuracy. *J. Med. Chem.* 47, 1739-1749.
- Gabbiani, C., Casini, A., Messori, L., 2007. Gold(III) compounds as anticancer drugs. *Gold Bulletin* 40, 73-81.
- Gabbiani, C., Messori, L., Cinellu, M.A., Casini, A., Mura, P., Sannella, A.R., Severini, C., Majori, G., Bilia, A.R., Vincieri, F.F., 2009. Outstanding plasmodicidal properties within a small panel of

- metallic compounds: Hints for the development of new metal-based antimalarials. *J. Inorg. Biochem.* 103, 310-312.
- Gambari, R., Lampronti, I., 2006. Inhibition of immunodeficiency type-1 virus (HIV-1) life cycle by medicinal plant extracts and plant-derived compounds. *Adv. Phytomed.* 2, 299-311.
- Gandin, V., Fernandes, A.P., Rigobello, M.P., Dani, B., Sorrentino, F., Tisato, F., Bjornstedt, M., Bindoli, A., Sturaro, A., Rella, R., Marzano, C., 2010. Cancer cell death induced by phosphine gold(I) compounds targeting thioredoxin reductase. *Biochem. Pharmacol.* 79, 90-101.
- Garcia, F., Climent, N., Assoumou, L., Gil, C., Gonzalez, N., Alcamí, J., Leon, A., Romeu, J., Dalmau, J., Martinez-Picado, J., Lifson, J., Autran, B., Costagliola, D., Clotet, B., Gatell, J.M., Plana, M., Gallart, T., DCV2/MANON07- AIDS Vaccine Research Objective Study Group, 2011. A therapeutic dendritic cell-based vaccine for HIV-1 infection. *J. Infect. Dis.* 203, 473-478.
- Garcia, S., Fevrier, M., Dadaglio, G., Lecoœur, H., Riviere, Y., Gougeon, M.L., 1997. Potential deleterious effect of anti-viral cytotoxic lymphocyte through the CD95 (FAS/APO-1)-mediated pathway during chronic HIV infection. *Immunol. Lett.* 57, 53-58.
- Ghanekar, S.A., Nomura, L.E., Suni, M.A., Picker, L.J., Maecker, H.T., Maino, V.C., 2001. Gamma interferon expression in CD8(+) T cells is a marker for circulating cytotoxic T lymphocytes that recognize an HLA A2-restricted epitope of human cytomegalovirus phosphoprotein pp65. *Clin. Diagn. Lab. Immunol.* 8, 628-631.
- Ghose A.K., Viswanadhan, V.N., Wendoloski J.J.. Prediction of Hydrophobic (Lipophilic) Properties of Small Organic Molecules Using Fragmental Methods: An Analysis of ALOGP and CLOGP Methods *J. Phys. Chem. A* 1998, 102, 3762-3772.
- Glynn, S.L., Yazdanian, M., 1998. In vitro blood-brain barrier permeability of nevirapine compared to other HIV antiretroviral agents. *J. Pharm. Sci.* 87, 306-310.
- Goepfert, P.A., 2003. Making sense of the HIV immune response. *Top. HIV. Med.* 11, 4-8.
- Goldgur, Y., Craigie, R., Cohen, G.H., Fujiwara, T., Yoshinaga, T., Fujishita, T., Sugimoto, H., Endo, T., Murai, H., Davies, D.R., 1999. Structure of the HIV-1 integrase catalytic domain complexed with an inhibitor: a platform for anti-viral drug design. *Proc. Natl. Acad. Sci. U. S. A.* 96, 13040-13043.
- Goldsby R.A., Kindt T.J., Osborne B.A., 2000. *Kuby Immunology*. 4th Edition, W.H. Freeman and Company, New York, USA.
- Gombar, V.K., Enslein, K., 1996. Assessment of n-octanol/water partition coefficient: when is the assessment reliable? *J. Chem. Inf. Comput. Sci.* 36, 1127-1134.
- Gonzalez, V.D., Landay, A.L., Sandberg, J.K., 2010. Innate immunity and chronic immune activation in HCV/HIV-1 co-infection. *Clin. Immunol.* 135, 12-25.
- Gotte, M., 2006. Effects of nucleotides and nucleotide analogue inhibitors of HIV-1 reverse transcriptase in a ratchet model of polymerase translocation. *Curr. Pharm. Des.* 12, 1867-1877.
- Gotte, M., Li, X., Wainberg, M.A., 1999. HIV-1 reverse transcription: a brief overview focused on structure-function relationships among molecules involved in initiation of the reaction. *Arch. Biochem. Biophys.* 365, 199-210.
- Gottlieb, H.E., Kotlyar, V., Nudelman, A., 1997. NMR chemical shifts of common laboratory solvents as trace impurities. *J. Org. Chem.* 62, 7512-7515.
- Gougeon, M.L., 2005. To kill or be killed: how HIV exhausts the immune system. *Cell Death Differ.* 12 Suppl 1, 845-854.
- Graziano, M., St-Pierre, Y., Beauchemin, C., Desrosiers, M., Potworowski, E.F., 1998. The fate of thymocytes labeled in vivo with CFSE. *Exp. Cell Res.* 240, 75-85.
- Gunatilleke, S.S., de Oliveira, C.A., McCammon, J.A., Barrios, A.M., 2008. Inhibition of cathepsin B by Au(I) complexes: a kinetic and computational study. *J. Biol. Inorg. Chem.* 13, 555-561.
- Hamid, R., Rotshteyn, Y., Rabadi, L., Parikh, R., Bullock, P., 2004. Comparison of alamar blue and MTT assays for high through-put screening. *Toxicol. In Vitro.* 18, 703-710.
- Hanna, G.J., Johnson, V.A., Kuritzkes, D.R., Richman, D.D., Brown, A.J., Savara, A.V., Hazelwood, J.D., D'Aquila, R.T., 2000. Patterns of resistance mutations selected by treatment of human immunodeficiency virus type 1 infection with zidovudine, didanosine, and nevirapine. *J. Infect. Dis.* 181, 904-911.
- Hansen, J., Schulze, T., Mellert, W., Moelling, K., 1988. Identification and characterization of HIV-specific RNase H by monoclonal antibody. *EMBO J.* 7, 239-243.
- Hansen, S.G., Vieville, C., Whizin, N., Coyne-Johnson, L., Siess, D.C., Drummond, D.D., Legasse, A.W., Axthelm, M.K., Oswald, K., Trubey, C.M., Piatak, M., Jr, Lifson, J.D., Nelson, J.A., Jarvis, M.A., Picker, L.J., 2009. Effector memory T cell responses are associated with protection of rhesus monkeys from mucosal simian immunodeficiency virus challenge. *Nat. Med.* 15, 293-299.

- Haselsberger, K., Peterson, D.C., Thomas, D.G., Darling, J.L., 1996. Assay of anticancer drugs in tissue culture: comparison of a tetrazolium-based assay and a protein binding dye assay in short-term cultures derived from human malignant glioma. *Anticancer Drugs* 7, 331-338.
- Hay, B.P., 1993. Methods for molecular mechanics modeling of coordination compounds. *Coord. Chem. Rev.* 126, 177-236.
- Hazuda, D.J., Felock, P., Witmer, M., Wolfe, A., Stillmock, K., Grobler, J.A., Espeseth, A., Gabryelski, L., Schleif, W., Blau, C., Miller, M.D., 2000. Inhibitors of strand transfer that prevent integration and inhibit HIV-1 replication in cells. *Science* 287, 646-650.
- Heagarty, M. C. (2003) AIDS: The battle rages on. *Issues in Science and Technology Online*, Summer 2003, <http://www.nap.edu/issues/19.4/heagarty.html#top>
- Heeney, J.L., Plotkin, S.A., 2006. Immunological correlates of protection from HIV infection and disease. *Nat. Immunol.* 7, 1281-1284.
- Hertel, C., Hauser, N., Schubengel, R., Seilheimer, B., Kemp, J.A., 1996. Beta-amyloid-induced cell toxicity: enhancement of 3-(4,5-dimethylthiazol-2-yl)-2,5-diphenyltetrazolium bromide-dependent cell death. *J. Neurochem.* 67, 272-276.
- Higby G.J. (1982). Gold in medicine. A review of its use in the west before 1900. *Gold bulletin*; 15(4): 130-140.
- Himmel, D.M., Maegley, K.A., Pauly, T.A., Bauman, J.D., Das, K., Dharia, C., Clark, A.D., Jr, Ryan, K., Hickey, M.J., Love, R.A., Hughes, S.H., Bergqvist, S., Arnold, E., 2009. Structure of HIV-1 reverse transcriptase with the inhibitor beta-Thujaplicinol bound at the RNase H active site. *Structure* 17, 1625-1635.
- Hogg, R.S., Yip, B., Kully, C., Craib, K.J., O'Shaughnessy, M.V., Schechter, M.T., Montaner, J.S., 1999. Improved survival among HIV-infected patients after initiation of triple-drug antiretroviral regimens. *CMAJ* 160, 659-665.
- Hoke, G.D., Macia, R.A., Meunier, P.C., Bugelski, P.J., Mirabelli, C.K., Rush, G.F., Matthews, W.D., 1989. In vivo and in vitro cardiotoxicity of a gold-containing antineoplastic drug candidate in the rabbit. *Toxicol. Appl. Pharmacol.* 100, 293-306.
- Holmes, E.C., Zhang, L.Q., Simmonds, P., Ludlam, C.A., Brown, A.J., 1992. Convergent and divergent sequence evolution in the surface envelope glycoprotein of human immunodeficiency virus type 1 within a single infected patient. *Proc. Natl. Acad. Sci. U. S. A.* 89, 4835-4839.
- Höltje H.-D., Sippl W., Rognan D., Folkers, G. *Molecular: basic principles and applications*. 2nd Edition, 2003, Wiley-VCH, Weinheim, Germany.
- Hou T., Xu X. *Recent Development and Application of Virtual Screening in Drug Discovery: An Overview*, 2003, *Curr Pharm Des*, 10, 1011-1033.
- Hsiou, Y., Ding, J., Das, K., Clark, A.D., Jr, Hughes, S.H., Arnold, E., 1996. Structure of unliganded HIV-1 reverse transcriptase at 2.7 Å resolution: implications of conformational changes for polymerization and inhibition mechanisms. *Structure* 4, 853-860.
- Huang, C.C., Lam, S.N., Acharya, P., Tang, M., Xiang, S.H., Hussan, S.S., Stanfield, R.L., Robinson, J., Sodroski, J., Wilson, I.A., Wyatt, R., Bewley, C.A., Kwong, P.D., 2007. Structures of the CCR5 N terminus and of a tyrosine-sulfated antibody with HIV-1 gp120 and CD4. *Science* 317, 1930-1934.
- Hutter, G., Nowak, D., Mossner, M., Ganepola, S., Mussig, A., Allers, K., Schneider, T., Hofmann, J., Kucherer, C., Blau, O., Blau, I.W., Hofmann, W.K., Thiel, E., 2009. Long-term control of HIV by CCR5 Delta32/Delta32 stem-cell transplantation. *N. Engl. J. Med.* 360, 692-698.
- Janzen, W.P., Popa-Burke, I.G., 2009. Advances in improving the quality and flexibility of compound management. *J. Biomol. Screen.* 14, 444-451.
- Jäger, J., Smerdon, S.J., Wang, J., Boisvert, D.C., Steitz, T.A., 1994. Comparison of three different crystal forms shows HIV-1 reverse transcriptase displays an internal swivel motion. *Structure* 2, 869-876.
- Jochmans, D., 2008. Novel HIV-1 reverse transcriptase inhibitors. *Virus Res.* 134, 171-185.
- Johnson, A.A., Marchand, C., Patil, S.S., Costi, R., Di Santo, R., Burke, T.R., Jr, Pommier, Y., 2007. Probing HIV-1 integrase inhibitor binding sites with position-specific integrase-DNA cross-linking assays. *Mol. Pharmacol.* 71, 893-901.
- Johnson, A.A., Santos, W., Pais, G.C., Marchand, C., Amin, R., Burke, T.R., Jr, Verdine, G., Pommier, Y., 2006. Integration requires a specific interaction of the donor DNA terminal 5'-cytosine with glutamine 148 of the HIV-1 integrase flexible loop. *J. Biol. Chem.* 281, 461-467.
- Johnson, R.P., Glickman, R.L., Yang, J.Q., Kaur, A., Dion, J.T., Mulligan, M.J., Desrosiers, R.C., 1997. Induction of vigorous cytotoxic T-lymphocyte responses by live attenuated simian immunodeficiency virus. *J. Virol.* 71, 7711-7718.

- Johnson, V.A., Brun-Vezinet, F., Clotet, B., Conway, B., Kuritzkes, D.R., Pillay, D., Schapiro, J., Telenti, A., Richman, D., 2005. Update of the Drug Resistance Mutations in HIV-1: 2005. *Top. HIV. Med.* 13, 51-57.
- Johnston, M.I., Fauci, A.S., 2008. An HIV vaccine--challenges and prospects. *N. Engl. J. Med.* 359, 888-890.
- Jones, G., Brooks, P.M., 1996. Injectable gold compounds overview. *Brit. J. Rheumatol.* 35, 1154-1158.
- Joshi, H.N., 2007. Drug development and imperfect design. *Int. J. Pharm.* 343, 1-3.
- Kageyama, S., Anderson, B.D., Hoesterey, B.L., Hayashi, H., Kiso, Y., Flora, K.P., Mitsuya, H., 1994. Protein binding of human immunodeficiency virus protease inhibitor KNI-272 and alteration of its in vitro antiretroviral activity in the presence of high concentrations of proteins. *Antimicrob. Agents Chemother.* 38, 1107-1111.
- Kantor, R., Katzenstein, D., 2004. Drug resistance in non-subtype B HIV-1. *J. Clin. Virol.* 29, 152-159.
- Kapetanovic, I.M., 2008. Computer-aided drug discovery and development (CADD): In silico-chemico-biological approach. *Chem. Biol. Interact.* 171, 165-176.
- Karlsson, A.C., Deeks, S.G., Barbour, J.D., Heiken, B.D., Younger, S.R., Hoh, R., Lane, M., Sallberg, M., Ortiz, G.M., Demarest, J.F., Liegler, T., Grant, R.M., Martin, J.N., Nixon, D.F., 2003. Dual pressure from antiretroviral therapy and cell-mediated immune response on the human immunodeficiency virus type 1 protease gene. *J. Virol.* 77, 6743-6752.
- Kempf, D.J., Marsh, K.C., Denissen, J.F., McDonald, E., Vasavanonda, S., Flentge, C.A., Green, B.E., Fino, L., Park, C.H., Kong, X.P., 1995. ABT-538 is a potent inhibitor of human immunodeficiency virus protease and has high oral bioavailability in humans. *Proc. Natl. Acad. Sci. U. S. A.* 92, 2484-2488.
- Kenseth, J. R., Coldiron, S.J., 2004. High-throughput characterisation and quality control of small-molecule combinatorial libraries. *Curr. Opin. Chem. Biol.* 8, 418-423.
- Kepp, O., Galluzzi, L., Lipinski, M., Yuan, J., Kroemer, G., 2011. Cell death assays for drug discovery. *Nat. Rev. Drug Discov.* 10, 221-237.
- Kerns H., Di, L., 2008. Drug-like properties: concepts, structure design and methods, from ADME to toxicity optimisation. Academic Press, USA.
- Keseru, G.M., Makara, G.M., 2006. Hit discovery and hit-to-lead approaches. *Drug Discov. Today.* 11, 741-748.
- Keter K.K., Fonteh P.N., Little, T., Liles D., Darkwa J., Meyer D., (2011). Palladium(II) and platinum(II) complexes of bis(thiosemicarbazones): syntheses, structures and bioactivity. Manuscript in preparation.
- Khanye, S.D., Smith, G.S., Lategan, C., Smith, P.J., Gut, J., Rosenthal, P.J., Chibale, K., 2010. Synthesis and in vitro evaluation of gold(I) thiosemicarbazone complexes for antimalarial activity. *J. Inorg. Biochem.* 104, 1079-1083.
- Kilby, J.M., 2001. Human immunodeficiency virus pathogenesis: insights from studies of lymphoid cells and tissues. *HIV/AIDS.* 33, 873-884
- Kirschberg, T.A., Balakrishnan, M., Squires, N.H., Barnes, T., Brendza, K.M., Chen, X., Eisenberg, E.J., Jin, W., Kutty, N., Leavitt, S., Licican, A., Liu, Q., Liu, X., Mak, J., Perry, J.K., Wang, M., Watkins, W.J., Lansdon, E.B., 2009. RNase H active site inhibitors of human immunodeficiency virus type 1 reverse transcriptase: design, biochemical activity, and structural information. *J. Med. Chem.* 52, 5781-5784.
- Koff, W.C., 2010. Accelerating HIV vaccine development. *Nature* 464, 161-162.
- Kola, I., Landis, J., 2004. Can the pharmaceutical industry reduce attrition rates? *Nat. Rev. Drug Discov.* 3, 711-715.
- Kostova, I., 2006. Platinum complexes as anticancer agents. *Recent. Pat. Anticancer Drug Discov.* 1, 1-22.
- Koup, R.A., Safrit, J.T., Cao, Y., Andrews, C.A., McLeod, G., Borkowsky, W., Farthing, C., Ho, D.D., 1994. Temporal association of cellular immune responses with the initial control of viremia in primary human immunodeficiency virus type 1 syndrome. *J. Virol.* 68, 4650-4655.
- Kriel F.H., Layh M., Coates J. and Marques H.M., Gold and Silver Complexes of bis(phosphino) hydrazine ligands as potential anti-tumour agents. August 2007, PhD Thesis, University of the Witwatersrand.
- Kroeger Smith, M.B., Rouzer, C.A., Taneyhill, L.A., Smith, N.A., Hughes, S.H., Boyer, P.L., Janssen, P.A., Moereels, H., Koymans, L., Arnold, E., 1995. Molecular modeling studies of HIV-1 reverse transcriptase nonnucleoside inhibitors: total energy of complexation as a predictor of drug placement and activity. *Protein Sci.* 4, 2203-2222.

- Krovat, E.M., Steindl, T., Langer, T., 2005. Recent advances in docking and scoring. *Curr. Comp. Aided Drug. Des.* 1, 93-102.
- Kyte J., Doolittle R. F., 1982. A Simple Method for Displaying the Hydrophobic Character of a Protein. *J. Mol. Biol.* 157, 105-132.
- Lam, T.L., Lam, M.L., Au, T.K., Ip, D.T., Ng, T.B., Fong, W.P., Wan, D.C., 2000. A comparison of human immunodeficiency virus type-1 protease inhibition activities by the aqueous and methanol extracts of Chinese medicinal herbs. *Life Sci.* 67, 2889-2896.
- Lampa, J., Klareskog, L., Ronnelid, J., 2002. Effects of gold on cytokine production in vitro; increase of monocyte dependent interleukin 10 production and decrease of interferon-gamma levels. *J. Rheumatol.* 29, 21-28.
- Lapenta, C., Santini, S.M., Logozzi, M., Spada, M., Andreotti, M., Di Pucchio, T., Parlato, S., Belardelli, F., 2003. Potent immune response against HIV-1 and protection from virus challenge in hu-PBL-SCID mice immunized with inactivated virus-pulsed dendritic cells generated in the presence of IFN- α . *J. Exp. Med.* 198, 361-367.
- Lemey, P., Pybus, O.G., Wang, B., Saksena, N.K., Salemi, M., Vandamme, A.M., 2003. Tracing the origin and history of the HIV-2 epidemic. *Proc. Natl. Acad. Sci. U. S. A.* 100, 6588-6592.
- Lever A.M.L, 2005. HIV: the virus, *Medicine*, 33:6, 1-3.
- Lever A.M.L. 2005b. What's new in HIV? *Infectious Diseases Journal of Pakistan*, 45-50.
- Lewis, M.G., DaFonseca, S., Chomont, N., Palamara, A.T., Tardugno, M., Mai, A., Collins, M., Wagner, W.L., Yalley-Ogunro, J., Greenhouse, J., Chirullo, B., Norelli, S., Garaci, E., Savarino, A., (2011). Gold drug auranofin restricts the viral reservoir in the monkey AIDS model and induces containment of viral load following ART suspension. *AIDS*, 25(11):1347-56.
- Lewthwaite, P., Wilkins, E., 2005. Natural history of HIV/AIDS. *Medicine* 33, 10-13.
- Lin T.S., Fischer, B., Blum, K.A., Brooker-McEldowney, M., Moran, M.E., Andritsos L.A., Flynn, J.M., Phelps, M.A., Dalton, J.T., Johnson A.J., Mitchell, S.M., et al., 2008. Flavopiridol (alvocidib) in chronic lymphocytic leukemia. *Hematology Meeting Reports* 2008;2(5):112-119
- Lipinski, C.A., 2000. Drug-like properties and the causes of poor solubility and poor permeability. *J. Pharmacol. Toxicol. Methods* 44, 235-249.
- Lipinski, C.A., Lombardo, F., Dominy, B.W., Feeney, P.J., 1997. Experimental and computational approaches to estimate solubility and permeability in drug discovery and development settings. *Adv. Drug Deliv. Rev.* 23, 3-25.
- Lipsky, P.E., Ziff, M., 1977. Inhibition of antigen- and mitogen-induced human lymphocyte proliferation by gold compounds. *J. Clin. Invest.* 59, 455-466.
- Lobell, M., Sivarajah, V., 2003. In silico prediction of aqueous solubility, human plasma protein binding and volume of distribution of compounds from calculated pKa and AlogP98 values. *Mol. Divers.* 7, 69-87.
- Loetscher, P., Dewald, B., Baggiolini, M., Seitz, M., 1994. Monocyte chemoattractant protein 1 and interleukin 8 production by rheumatoid synoviocytes. Effects of anti-rheumatic drugs. *Cytokine* 6, 162-170.
- Lombardo, F., Gifford, E., Shalaeva, M.Y., 2003. In silico ADME prediction: data, models, facts and myths. *Mini Rev. Med. Chem.* 3, 861-875.
- Lorber, A., Simon, T.M., Leeb, J., Peter, A., Wilcox, S.A., 1979. Effects of chrysotherapy on parameters of immune response. *J. Rheumatol.* 6, 81-90.
- Lori, F., Foli, A., Maserati, R., Seminari, E., Xu, J., Whitman, L., et al. 2002. Control of HIV during a structured treatment interruption in chronically infected individuals with vigorous T cell responses. *HIV Clin Trials* 3:115–124.
- Lori, F., 1999. Hydroxyurea and HIV: 5 years later--from anti-viral to immune-modulating effects. *AIDS* 13, 1433-1442.
- Lori, F., 2008. Treating HIV/AIDS by reducing immune system activation: the paradox of immune deficiency and immune hyperactivation. *Curr. Opin. HIV. AIDS.* 3, 99-103.
- Lori, F., Foli, A., Groff, A., Lova, L., Whitman, L., Bakare, N., Pollard, R.B., Lisziewicz, J., 2005. Optimal suppression of HIV replication by low-dose hydroxyurea through the combination of anti-viral and cytostatic ('virostatic') mechanisms. *AIDS* 19, 1173-1181.
- Lori, F., Foli, A., Kelly, L.M., Lisziewicz, J., 2007. Virostatics: a new class of anti-HIV drugs. *Curr. Med. Chem.* 14, 233-241.
- Lori, F., Jessen, H., Lieberman, J., Clerici, M., Tinelli, C., Lisziewicz, J., 1999. Immune restoration by combination of a cytostatic drug (hydroxyurea) and anti-HIV drugs (didanosine and indinavir). *AIDS Res. Hum. Retroviruses* 15, 619-624.

- Lori, F., Malykh, A., Cara, A., Sun, D., Weinstein, J.N., Lisziewicz, J., Gallo, R.C., 1994. Hydroxyurea as an inhibitor of human immunodeficiency virus-type 1 replication. *Science* 266, 801-805.
- Lori, F., Malykh, A.G., Foli, A., Maserati, R., De Antoni, A., Minoli, L., Padrini, D., Degli Antoni, A., Barchi, E., Jessen, H., Wainberg, M.A., Gallo, R.C., Lisziewicz, J., 1997. Combination of a drug targeting the cell with a drug targeting the virus controls human immunodeficiency virus type 1 resistance. *AIDS Res. Hum. Retroviruses* 13, 1403-1409.
- Lu, W., Arraes, L.C., Ferreira, W.T., Andrieu, J.M., 2004. Therapeutic dendritic-cell vaccine for chronic HIV-1 infection. *Nat. Med.* 10, 1359-1365.
- Lusso, P., Cocchi, F., Balotta, C., Markham, P.D., Louie, A., Farci, P., Pal, R., Gallo, R.C., Reitz, M.S., Jr, 1995. Growth of macrophage-tropic and primary human immunodeficiency virus type 1 (HIV-1) isolates in a unique CD4+ T-cell clone (PM1): failure to downregulate CD4 and to interfere with cell-line-tropic HIV-1. *J. Virol.* 69, 3712-3720.
- Lyons, A.B., Parish, C.R., 1994. Determination of lymphocyte division by flow cytometry. *J. Immunol. Methods* 171, 131-137.
- Madhok, R., Crilly, A., Murphy, E., Smith, J., Watson, J., Capell, H.A., 1993. Gold therapy lowers serum interleukin 6 levels in rheumatoid arthritis. *J. Rheumatol.* 20, 630-633.
- Maertens, G., Cherepanov, P., Pluymers, W., Busschots, K., De Clercq, E., Debyser, Z., Engelborghs, Y., 2003. LEDGF/p75 is essential for nuclear and chromosomal targeting of HIV-1 integrase in human cells. *J. Biol. Chem.* 278, 33528-33539.
- Mahnke, Y.D., Roederer, M., 2007. Optimizing a multicolor immunophenotyping assay. *Clin. Lab. Med.* 27, 469-485.
- Maino, V.C., Picker, L.J., 1998. Identification of functional subsets by flow cytometry: intracellular detection of cytokine expression. *Cytometry* 34, 207-215.
- Mansfield, K., Lang, S.M., Gauduin, M.C., Sanford, H.B., Lifson, J.D., Johnson, R.P., Desrosiers, R.C., 2008. Vaccine protection by live, attenuated simian immunodeficiency virus in the absence of high-titer antibody responses and high-frequency cellular immune responses measurable in the periphery. *J. Virol.* 82, 4135-4148.
- Marcelin, A.G., Ceccherini-Silberstein, F., Perno, C.F., Calvez, V., 2009. Resistance to novel drug classes. *Curr. Opin. HIV. AIDS.* 4, 531-537.
- Marcon G, Carotti S, Coronello M, Messori L, Mini E, Orioli P, Mazzie T, Cinellu MA, Minghetti G (2002). Gold(III) complexes with bipyridyl ligands: solution chemistry, cytotoxicity, and DNA binding properties. *J. Med. Chem.* 45: 1672-1677.
- Marcon, G., Messori, L., Orioli, P., 2002. Gold(III) complexes as a new family of cytotoxic and antitumor agents. *Expert Rev. Anticancer Ther.* 2, 337-346.
- Marinello, J., Marchand, C., Mott, B.T., Bain, A., Thomas, C.J., Pommier, Y., 2008. Comparison of raltegravir and elvitegravir on HIV-1 integrase catalytic reactions and on a series of drug-resistant integrase mutants. *Biochemistry* 47, 9345-9354.
- Marra, C.M., Booss, J., 2000. Does brain penetration of anti-HIV drugs matter? *Sex. Transm. Infect.* 76, 1-2.
- Mascarenhas B, Granda J, Freyberg R (1972) Gold metabolism in patients with rheumatoid arthritis treated with gold compounds-reinvestigated. *J. Rheumatol.* 23:1818-1820.
- Matayoshi, E.D., Wang, G.T., Krafft, G.A., Erickson, J., 1990. Novel fluorogenic substrates for assaying retroviral proteases by resonance energy transfer. *Science* 247, 954-958.
- Matsubara, T., Ziff, M., 1987. Inhibition of human endothelial cell proliferation by gold compounds. *J. Clin. Invest.* 79, 1440-1446.
- Maurer-Schultze, B., Siebert, M., Bassukas, I.D., 1988. An *in vivo* study on the synchronizing effect of hydroxyurea. *Exp Cell Res.* 174, 230-243.
- Monavi K. 2006, A review on infection with human immunodeficiency virus, *Best Practice & Research Clinical Obstetrics and Gynaecology* Vol. 20, No. 6, pp. 923-940, 2006.
- Mayhew, C.N., Sumpter, R., Inayat, M., Cibull, M., Phillips, J.D., Elford, H.L., Gallicchio, V.S., 2005. Combination of inhibitors of lymphocyte activation (hydroxyurea, trimidox, and didox) and reverse transcriptase (didanosine) suppresses development of murine retrovirus-induced lymphoproliferative disease. *Anti-viral Res.* 65, 13-22.
- McCull, D.J., Chen, X., 2010. Strand transfer inhibitors of HIV-1 integrase: bringing IN a new era of antiretroviral therapy. *Anti-viral Res.* 85, 101-118.
- McDougal, J.S., Mawle, A., Cort, S.P., Nicholson, J.K., Cross, G.D., Scheppler-Campbell, J.A., Hicks, D., Sleigh, J., 1985. Cellular tropism of the human retrovirus HTLV-III/LAV. I. Role of T cell activation and expression of the T4 antigen. *J. Immunol.* 135, 3151-3162.
- McMichael, A., Dorrell, L., 2009. The immune response to HIV. *Medicine* 37, 321-325.

- McMichael, A.J., Dorrell, L., 2005. The immune response to HIV. *Medicine* 33, 4-7.
- Meyerhans, A., Vartanian, J.P., Hultgren, C., Plikat, U., Karlsson, A., Wang, L., Eriksson, S., Wain-Hobson, S., 1994. Restriction and enhancement of human immunodeficiency virus type 1 replication by modulation of intracellular deoxynucleoside triphosphate pools. *J. Virol.* 68, 535-540.
- Merchant, B., 1998. Gold, the noble metal and the paradoxes of its toxicology. *Biologicals* 26, 49-59.
- Messori L, Abbate F, Marcon G, Orioli P, Fontani M, Mini E, Carroti S (2000). Gold (III) complexes as potential anti tumor agents: solution chemistry, cytotoxicity and DNA binding properties. *J. Med. Chem.* 43: 3541-3548.
- Messori, L., Marcon, G., Cinellu, M.A., Coronello, M., Mini, E., Gabbiani, C., Orioli, P., 2004. Solution chemistry and cytotoxic properties of novel organogold(III) compounds. *Bioorg. Med. Chem.* 12, 6039-6043.
- Meyerhans, A. Vartanian, J.P., Hultgren, C., Plikat, U., Karlsson, A., Wang, L., Eriksson, S., Wain-Hobson, S., 1994. Restriction and enhancement of human immunodeficiency virus type 1 replication by modulation of intracellular deoxynucleoside triphosphate pools. *J. Virol.* 68 (1994) 535-540.
- Michel, F., Crucifix, C., Granger, F., Eiler, S., Mouscadet, J.F., Korolev, S., Agapkina, J., Ziganshin, R., Gottikh, M., Nazabal, A., Emiliani, S., Benarous, R., Moras, D., Schultz, P., Ruff, M., 2009. Structural basis for HIV-1 DNA integration in the human genome, role of the LEDGF/P75 cofactor. *EMBO J.* 28, 980-991.
- Migueles, S.A., Laborico, A.C., Shupert, W.L., Sabbaghian, M.S., Rabin, R., Hallahan, C.W., Van Baarle, D., Kostense, S., Miedema, F., McLaughlin, M., Ehler, L., Metcalf, J., Liu, S., Connors, M., 2002. HIV-specific CD8+ T cell proliferation is coupled to perforin expression and is maintained in nonprogressors. *Nat. Immunol.* 3, 1061-1068.
- Milacic, V., Dou, Q.P., 2009. The tumor proteasome as a novel target for gold(III) complexes: implications for breast cancer therapy. *Coord. Chem. Rev.* 253, 1649-1660.
- Mirabelli C.K., Johnson R.K., Hill D.T., Faucette L.F., Girard G.R., Keu G.Y., Sung C.M., Crooke S.T. (1986). Correlation of the in vitro cytotoxic and in vivo antitumor activities of gold(I) coordination complexes. *J. Med. Chem.* 29: 218-223.
- Mirabelli, C.K., Jensen, B.D., Mattern, M.R., Sung, C.M., Mong, S.M., Hill, D.T., Dean, S.W., Schein, P.S., Johnson, R.K., Crooke, S.T., 1986. Cellular pharmacology of mu-[1,2-bis(diphenylphosphino)ethane]bis[(1-thio-beta-D-glucopyranosato-S)gold(I)]: a novel antitumor agent. *Anticancer Drug Des.* 1, 223-234.
- Mirabelli, C.K., Sung, C.M., Zimmerman, J.P., Hill, D.T., Mong, S., Crooke, S.T., 2002. Interactions of gold coordination complexes with DNA. *Biochem. Pharmacol.* 35; 1427-1433.
- Mishra, V., Pandeya, S.N., Pannecouque, C., Witvrouw, M., De Clercq, E., 2002. Anti-HIV activity of thiosemicarbazone and semicarbazone derivatives of (+/-)-3-menthone. *Arch. Pharm. (Weinheim)* 335, 183-186.
- Mohan, V., Gibbs, A.C., Cummings, M.D., Jaeger, E.P., DesJarlais, R.L., 2005. Docking: Successes and Challenges. *Curr. Pharm. Des.* 11, 323-333
- Momany, F. A., Rone, R. J., 1992. Validation of the general purpose QUANTA3.2/CHARMM force field. *Comp. Chem.* 1992, 13, 888-900.
- Montaner, J.S., Cote, H.C., Harris, M., Hogg, R.S., Yip, B., Chan, J.W., Harrigan, P.R., O'Shaughnessy, M.V., 2003. Mitochondrial toxicity in the era of HAART: evaluating venous lactate and peripheral blood mitochondrial DNA in HIV-infected patients taking antiretroviral therapy. *J. Acquir. Immune Defic. Syndr.* 34 Suppl 1, S85-90.
- Montefiori, D.C. Evaluating neutralizing antibodies against HIV, SIV and SHIV in luciferase reporter gene assays. In: Coligan JE, Kruisbeek AM, Margulies DH, Shevach EMW, Strober MW, Coico R, editors. *Curr. Protoc. Immunol.* 2004.
- Montessori, V., Press, N., Harris, M., Akagi, L., Montaner, J.S., 2004. Adverse effects of antiretroviral therapy for HIV infection. *CMAJ* 170, 229-238.
- Mosmann, T., 1983. Rapid colorimetric assay for cellular growth and survival: application to proliferation and cytotoxicity assays. *J. Immunol. Methods* 65, 55-63.
- Mouscadet, J.F., Delelis, O., Marcelin, A.G., Tchertanov, L., 2010. Resistance to HIV-1 integrase inhibitors: A structural perspective. *Drug Resist. Update* 13, 139-150.
- Muegge, I., Rarey, M., 2001. Small molecule docking and scoring. *Rev. Comput. Chem.* 17, 1-60.
- Mueller, H., Kassack, M.U., Wiese M., 2004. Comparison of the usefulness of the MTT, ATP and calcein assays to predict the potency of cytotoxic agents in various human cancer cell lines. *J. Biomol. Screen.* 9, 506-515.

- Musey, L., Hughes, J., Schacker, T., Shea, T., Corey, L., McElrath, M.J., 1997. Cytotoxic-T-cell responses, viral load, and disease progression in early human immunodeficiency virus type 1 infection. *N. Engl. J. Med.* 337, 1267-1274.
- Navarro, M., 2009. Gold complexes as potential anti-parasitic agents. *Coord. Chem. Rev.* 253, 1619-1626.
- Navarro, M., Perez, H., Sanchez-Delgado, R.A., 1997. Toward a novel metal-based chemotherapy against tropical diseases. 3. Synthesis and antimalarial activity in vitro and in vivo of the new gold-chloroquine complex [Au(PPh₃)(CQ)]PF₆. *J. Med. Chem.* 40, 1937-1939.
- Navarro, M., Vasquez, F., Sanchez-Delgado, R.A., Perez, H., Sinou, V., Schrevel, J., 2004. Toward a novel metal-based chemotherapy against tropical diseases. 7. Synthesis and in vitro antimalarial activity of new gold-chloroquine complexes. *J. Med. Chem.* 47, 5204-5209.
- Nkolola, J.P., Essex, M., 2006. Progress towards an HIV-1 subtype C vaccine. *Vaccine* 24, 391-401.
- Nobili S, Mini E, Landini I, Gabbiani C, Casini A, Messori L. Gold compounds as anticancer agents: chemistry, cellular pharmacology, and preclinical studies. *Med Res Rev.* 2010, 30, 550– 580.
- Núñez, M., 2010. Clinical syndromes and consequences of antiretroviral-related hepatotoxicity. *Hepatology* 52, 1143-1155.
- Nylander, S., Kalies, I., 1999. Brefeldin A, but not monensin, completely blocks CD69 expression on mouse lymphocytes: efficacy of inhibitors of protein secretion in protocols for intracellular cytokine staining by flow cytometry. *J. Immunol. Methods* 224, 69-76.
- O'Brien, S.E., de Groot, M.J., 2005. Greater than the sum of its parts: combining models for useful ADMET prediction. *J. Med. Chem.* 48, 1287-1291.
- Ohlstein, E.H., Ruffolo Jr., R.R., Elliott, J.D., 2000. Drug Discovery in the Next Millennium *Annu. Rev. Pharmacol. Toxicol.* 40,177–191.
- Okada, T., Patterson, B.K., Ye, S.Q., Gurney, M.E., 1993. Aurothiolates inhibit HIV-1 infectivity by gold(I) ligand exchange with a component of the virion surface. *Virology* 192, 631-642.
- Orvig C, Abrams MJ. Medicinal inorganic chemistry: introduction. *Chem Rev* 1999; 2201-2204.
- Ostapowicz, G., Fontana, R.J., Schiodt, F.V., Larson, A., Davern, T.J., Han, S.H., McCashland, T.M., Shakil, A.O., Hay, J.E., Hynan, L., Crippin, J.S., Blei, A.T., Samuel, G., Reisch, J., Lee, W.M., U.S. Acute Liver Failure Study Group, 2002. Results of a prospective study of acute liver failure at 17 tertiary care centers in the United States. *Ann. Intern. Med.* 137, 947-954.
- Ott, I., 2009. On the medicinal chemistry of gold complexes as anticancer drugs. *Coord. Chem. Rev.* 253, 1670-1681.
- Paiardini, M., Frank, I., Pandrea, I., Apetrei, C., Silvestri, G., 2008. Mucosal immune dysfunction in AIDS pathogenesis. *AIDS. Rev.* 10, 36-46.
- Pala, P., Hussell, T., Openshaw, P.J., 2000. Flow cytometric measurement of intracellular cytokines. *J. Immunol. Methods* 243, 107-124.
- Parella, F.J., Jr, Delaney, K.M., Moorman, A.C., Loveless, M.O., Fuhrer, J., Satten, G.A., Aschman, D.J., Holmberg, S.D., 1998. Declining morbidity and mortality among patients with advanced human immunodeficiency virus infection. HIV Outpatient Study Investigators. *N. Engl. J. Med.* 338, 853-860.
- Pandeya, S.N., Sriram, D., Nath, G., DeClercq, E., 1999. Synthesis, antibacterial, antifungal and anti-HIV activities of Schiff and Mannich bases derived from isatin derivatives and N-[4-(4'-chlorophenyl)thiazol-2-yl] thiosemicarbazide. *Eur. J. Pharm. Sci.* 9, 25-31.
- Pantaleo, G., Graziosi, C., Demarest, J.F., Butini, L., Montroni, M., Fox, C.H., Oreintin, J.M., Kotler, D.P., Fauci, A.S., 1993. HIV infection is active and progressive in lymphoid tissue during the clinically latent stage of disease. *Nature.* 362, 355–358.
- Parish, R.V., Cottrill, M., 1987. Medicinal gold compounds, *Gold Bulletin*; 20; 3-12.
- Pellegrini, M., Calzascia, T., Toe, J.G., Preston, S.P., Lin, A.E., Elford, A.R., Shahinian, A., Lang, P.A., Lang, K.S., Morre, M., Assouline, B., Lahl, K., Sparwasser, T., Tedder, T.F., Paik, J.H., Depinho, R.A., Basta, S., Ohashi, P.S., Mak, T.W., 2011. IL-7 Engages Multiple Mechanisms to Overcome Chronic Viral Infection and Limit Organ Pathology. *Cell* . doi: 10.1016/j.cell.2011.01.011.
- Pelosi, G., Bisceglie, F., Bignami, F., Ronzi, P., Schiavone, P., Re, M.C., Casoli, C., Pilotti, E., 2010. Antiretroviral activity of thiosemicarbazone metal complexes. *J. Med. Chem.* 53, 8765-8769.
- Perelson, A.S., Neumann, A.U., Markowitz, M., Leonard, J.M., Ho, D.D., 1996. HIV-1 dynamics in vivo: virion clearance rate, infected cell life-span, and viral generation time. *Science* 271, 1582-1586.
- Petsko G.A and Ringe D., 2004. Protein Structure and Function. Printed by Stamford Press PTE Singapore
- Pirard B., 2004. Computational Methods for the Identification and Optimisation of High Quality Leads. *Comb. Chem. High Throughput Screening* 7, 271-280.

- Platt, E.J., Wehrly, K., Kuhmann, S.E., Chesebro, B., Kabat, D., 1998. Effects of CCR5 and CD4 cell surface concentrations on infections by macrophagetropic isolates of human immunodeficiency virus type 1. *J. Virol.* 72, 2855-2864.
- Poeschla, E.M., 2008. Integrase, LEDGF/p75 and HIV replication. *Cell Mol. Life Sci.* 65(9),1403–24.
- Pommier, Y., Johnson, A.A., Marchand, C., 2005. Integrase inhibitors to treat HIV/AIDS. *Nat. Rev. Drug Discov.* 4, 236-248.
- Ponsoda, X., Jover, R., Nunez, C., Royo, M., Castell, J.V., Gomez-Lechon, M.J., 1995. Evaluation of the cytotoxicity of 10 chemicals in human and rat hepatocytes and in cell lines: Correlation between in vitro data and human lethal concentration. *Toxicol. In Vitro.* 9, 959-966.
- Popa-Burke, I.G., Issakova, O., Arroway, J.D., Bernasconi, P., Chen, M., Coudurier, L., Galasinski, S., Jadhav, A.P., Janzen, W.P., Lagasca, D., Liu, D., Lewis, R.S., Mohney, R.P., Sepetov, N., Sparkman, D.A., Hodge, C.N., 2004. Streamlined system for purifying and quantifying a diverse library of compounds and the effect of compound concentration measurements on the accurate interpretation of biological assay results. *Anal. Chem.* 76, 7278-7287.
- Poveda, E., Rodes, B., Labernardiere, J.L., Benito, J.M., Toro, C., Gonzalez-Lahoz, J., Faudon, J.L., Clavel, F., Schapiro, J., Soriano, V., 2004. Evolution of genotypic and phenotypic resistance to Enfuvirtide in HIV-infected patients experiencing prolonged virologic failure. *J. Med. Virol.* 74, 21-28.
- Pozio, E., Morales M.A.G., 2005. The impact of HIV-protease inhibitors on opportunistic parasites. *TRENDS Parasitol.* 21; 59-63.
- Preston, B.D., Poiesz, B.J., Loeb, L.A., 1988. Fidelity of HIV-1 reverse transcriptase. *Science* 242, 1168-1171.
- Purohit, R., Rajasekaran, R., Sudandiradoss, C., George Priya Doss, C., Ramanathan, K., Rao, S., 2008. Studies on flexibility and binding affinity of Asp25 of HIV-1 protease mutants. *Int. J. Biol. Macromol.* 42, 386-391.
- Quah, B.J., Warren, H.S., Parish, C.R., 2007. Monitoring lymphocyte proliferation in vitro and in vivo with the intracellular fluorescent dye carboxyfluorescein diacetate succinimidyl ester. *Nat. Protoc.* 2, 2049-2056.
- Quinn, T.C., Overbaugh, J., 2005. HIV/AIDS in women: an expanding epidemic. *Science* 308, 1582-1583.
- Rafique, S., Idrees, M., Nasim, A., Akbar, H., Athar, A., 2010, Transition metal complexes as potential therapeutic Agents. *Biotechnol. Mol. Biol. Rev.* 5(2) 38-45.
- Raha, K., Peters, M.B., Wang, B., Yu, N., Wollacott, A.M., Westerhoff, L.M., Merz, K.M., Jr, 2007. The role of quantum mechanics in structure-based drug design. *Drug Discov. Today* 12, 725-731.
- Rambaut, A., Posada, D., Crandall, K.A., Holmes, E.C., 2004. The causes and consequences of HIV evolution. *Nat. Rev. Genet.* 5, 52-61.
- Ren, J., Stammers, D.K., 2005. HIV reverse transcriptase structures: designing new inhibitors and understanding mechanisms of drug resistance. *Trends Pharmacol. Sci.* 26, 4-7.
- Reks-Ngarm, S., Pitisuttithum, P., Nitayaphan, S., Kaewkungwal, J., Chiu, J., Paris, R., Prensri, N., Namwat, C., de Souza, M., Adams, E., Benenson, M., Gurunathan, S., Tartaglia, J., McNeil, J.G., Francis, D.P., Stablein, D., Birx, D.L., Chunsuttiwat, S., Khamboonruang, C., Thongcharoen, P., Robb, M.L., Michael, N.L., Kunasol, P., Kim, J.H., MOPH-TAVEG Investigators, 2009. Vaccination with ALVAC and AIDSVAX to prevent HIV-1 infection in Thailand. *N. Engl. J. Med.* 361, 2209-2220.
- Richon A.B., 1994, *Mathematech*, 1, 83 (1994)., An Introduction to Molecular modeling, <http://www.netsci.org/Science/Compchem/feature01.html>
- Roberts, J.R., Xiao, J., Schliesman, B., Parsons, D.J., Shaw, C.F., 3rd, 1996. Kinetics and Mechanism of the Reaction between Serum Albumin and Auranofin (and Its Isopropyl Analogue) in Vitro. *Inorg. Chem.* 35, 424-433.
- Roederer, M., 2008. How many events is enough? Are you positive? *Cytometry Part A* 73A, 384-385.
- Romagnoli, P., Spinaz, G.A., Sinigaglia, F., 1992. Gold-specific T cells in rheumatoid arthritis patients treated with gold. *J. Clin. Invest.* 89, 254-258.
- Rose, R.E., Gong, Y.F., Greytok, J.A., Bechtold, C.M., Terry, B.J., Robinson, B.S., Alam, M., Colonna, R.J., Lin, P.F., 1996. Human immunodeficiency virus type 1 viral background plays a major role in development of resistance to protease inhibitors. *Proc. Natl. Acad. Sci. U. S. A.* 93, 1648-1653.
- Rutschmann, O.T., Opravil, M., Iten, A., Malinverni, R., Vernazza, P.L., Bucher, H.C., Bernasconi, E., Sudre, P., Leduc, D., Yerly, S., Perrin, L.H., Hirschel, B., 1998. A placebo-controlled trial of didanosine plus stavudine, with and without hydroxyurea, for HIV infection. The Swiss HIV Cohort Study. *AIDS* 12, F71-7.

- Sadiq, S.K., Wright, D.W., Kenway, O.A, Coveney, P.V., 2010. Accurate Ensemble Molecular Dynamics Binding Free Energy Ranking of Multidrug Resistant HIV-1 Proteases. *J. Chem. Inf. Model.* 50, 890–905.
- Sadler P.J and Guo Z. (1998). Metal complexes in medicine: design and mechanism of action. *Pure Appl. Chem.* 70(4): 863-871.
- Sahu, V.K., Khan, A.K.R., Singh, R.K., Singh P.P. 2008. Hydrophobic, Polar and Hydrogen Bonding Based Drug-Receptor Interaction of Tetrahydroimidazobenzodiazepinones. *Am. J. Immunol.* 4, 33-42.
- Sam Z., in “Biomedical Applications of gold: Stage 9”, Mintek Communication C4050M, July 2005.
- Sanabani, S., Kleine Neto, W., Kalmar, E.M., Diaz, R.S., Janini, L.M., Sabino, E.C., 2006. Analysis of the near full length genomes of HIV-1 subtypes B, F and BF recombinant from a cohort of 14 patients in Sao Paulo, Brazil. *Infect. Genet. Evol.* 6, 368-377.
- Sanchez-Delgado, R.A., Anzellotti, A., 2004. Metal complexes as chemotherapeutic agents against tropical diseases: trypanosomiasis, malaria and leishmaniasis. *Minrev. Med. Chem.* 4, 23-30
- Sannella, A.R., Casini, A., Gabbiani, C., Messori, L., Bilia, A.R., Vincieri, F.F., Majori, G., Severini, C., 2008. New uses for old drugs. Auranofin, a clinically established antiarthritic metallodrug, exhibits potent antimalarial effects in vitro: Mechanistic and pharmacological implications. *FEBS Lett.* 582, 844-847.
- Sarafianos, S.G., Marchand, B., Das, K., Himmel, D.M., Parniak, M.A., Hughes, S.H., Arnold, E., 2009. Structure and function of HIV-1 reverse transcriptase: molecular mechanisms of polymerization and inhibition. *J. Mol. Biol.* 385, 693-713.
- Savarino, A., 2007. In-Silico docking of HIV-1 integrase inhibitors reveals a novel drug type acting on an enzyme/DNA reaction intermediate. *Retrovirology* 4, 21.
- Schiavone, M., Quinto, I., Scala, G., 2008. Perspectives for a protective HIV-1 vaccine. *Adv. Pharmacol.* 56, 423-452.
- Schultz, S.J., Champoux, J. J., 2008, RNase H activity: Structure, specificity, and function in reverse transcription. *Virus Res.* 134, 86–103.
- Sfikakis, P.P., Souliotis, V.L., Panayiotidis, P.P., 1993. Suppression of interleukin-2 and interleukin-2 receptor biosynthesis by gold compounds in in vitro activated human peripheral blood mononuclear cells. *Arthritis Rheum.* 36, 208-212.
- Shapiro, D.L., Masci, J.R., 1996. Treatment of HIV associated psoriatic arthritis with oral gold. *J. Rheumatol.* 23, 1818-1820.
- Sharp, P.M., Robertson, D.L., Hahn, B.H., 1995. Cross-species transmission and recombination of 'AIDS' viruses. *Philos. Trans. R. Soc. Lond. B. Biol. Sci.* 349, 41-47.
- Shaw III, C.F. 1999. Gold-based therapeutic agents. *Chem. Rev.* 99, 2589-2600.
- Shaw III, C.F., Isab, A.A., Hoeschele, J.D., Starich, M., Locke, J., Schulteis, P., Xiao, J., 1994. Oxidation of the phosphine from the auranofin analogue, triisopropylphosphine (2,3,4,6-tetra-O-acetyl-1-thio-β-D-glucopyranosato-S)gold(I), via a protein-bound phosphonium intermediate. *J. Am. Chem. Soc.* 116, 2254–2260.
- Shkriabai, N., Patil, S.S., Hess, S., Budihis, S.R., Craigie, R., Burke, T.R., Jr, Le Grice, S.F., Kvaratskhelia, M., 2004. Identification of an inhibitor-binding site to HIV-1 integrase with affinity acetylation and mass spectrometry. *Proc. Natl. Acad. Sci. U. S. A.* 101, 6894-6899.
- Sigler, J.W., Bluhm, G.B., Duncan, H., Sharp, J.T., Ensign, D.C., McCrum, W.R., 1974. Gold salts in the treatment of rheumatoid arthritis. A double-blind study. *Ann. Intern. Med.* 80, 21-26.
- Simon, V., Ho, D.D., Abdool Karim, Q., 2006. HIV/AIDS epidemiology, pathogenesis, prevention, and treatment. *Lancet* 368, 489-504.
- Skillman, A.G., Maurer, K.W., Roe, D.C., Stauber, M.J., Eargle, D., Ewing, T.J., Muscate, A., Davioud-Charvet, E., Medaglia, M.V., Fisher, R.J., Arnold, E., Gao, H.Q., Buckheit, R., Boyer, P.L., Hughes, S.H., Kuntz, I.D., Kenyon, G.L., 2002. A novel mechanism for inhibition of HIV-1 reverse transcriptase. *Bioorg. Chem.* 30, 443-458.
- Slabaugh, M.B., Howell, M.L., Wang, Y., Mathews, C.K., 1991. Deoxyadenosine reverses hydroxyurea inhibition of vaccinia virus growth. *J. Virol.* 65, 2290-2298.
- Sluis-Cremer, N., Tachedjian, G., 2008. Mechanisms of inhibition of HIV replication by non-nucleoside reverse transcriptase inhibitors. *Virus Res.* 134, 147-156.
- Soman, G., Yang, X., Jiang, H., Giardina, S., Vyas, V., Mitra, G., Yovandich, J., Creekmore, S.P., Waldmann, T.A., Quinones, O., Alvord, W.G., 2009. MTS dye based colorimetric CTLL-2 cell proliferation assay for product release and stability monitoring of interleukin-15: assay qualification, standardization and statistical analysis. *J. Immunol. Methods* 348, 83-94.

- Spector, T., Jones, T.E., 1985. Herpes simplex type 1 ribonucleotide reductase. Mechanism studies with inhibitors. *J. Biol. Chem.* 260, 8694-8697.
- Stelzer, G.T., Shults, K.E., Loken, M.R., 1993. CD45 gating for routine flow cytometric analysis of human bone marrow specimens. *Ann. New York Acad. Sci.* 677, 265-279.
- Stern, I., Wataha, J.C., Lewis, J.B., Messer, R.L., Lockwood, P.E., Tseng, W.Y., 2005. Anti-rheumatic gold compounds as sublethal modulators of monocytic LPS-induced cytokine secretion. *Toxicol. In Vitro.* 19, 365-371.
- Su, H.P., Yan, Y., Prasad, G.S., Smith, R.F., Daniels, C.L., Abeywickrema, P.D., Reid, J.C., Loughran, H.M., Kornienko, M., Sharma, S., Grobler, J.A., Xu, B., Sardana, V., Allison, T.J., Williams, P.D., Darke, P.L., Hazuda, D.J., Munshi, S., 2010. Structural basis for the inhibition of RNase H activity of HIV-1 reverse transcriptase by RNase H active site-directed inhibitors. *J. Virol.* 84, 7625-7633.
- Sun, R.W., Yu, W.Y., Sun, H., Che, C.M., 2004. In vitro inhibition of human immunodeficiency virus type-1 (HIV-1) reverse transcriptase by gold(III) porphyrins. *Chembiochem* 5, 1293-1298.
- Sun, Y., Lantour, R.A., 2006. Comparison of implicit solvent models for the simulation of protein surface interactions. *J. Comput. Chem* 27; 1908-1922.
- Susnow, R.G., Dixon, S.L., 2003. Use of robust classification techniques for the prediction of human cytochrome P450 2D6 inhibition. *J. Chem. Inf. Comput. Sci.* 43, 1308-1315.
- Sussman, N.L., Walterschied, M., Butler, T., Cali, J.J., Riss, T., Kelly, J.H., 2002. The predictive nature of high-throughput toxicity screening using a human hepatocyte cell line. *Cell Notes* 3, 7-10.
- Sutton, B.M., 1986. Gold compounds for rheumatoid arthritis. *Gold Bulletin*, 19(1): 15-16.
- Sutton, B.M., McGusty, E., Walz, D.T., DiMartino, M.J., 1972. Oral gold anti-arthritic properties of alkylphosphinegold coordination complexes. *J. Med. Chem.* 15, 1095-1098.
- Svarovskaia, E. S., S. R. Cheslock, W. Zhang, W. Hu, and V. K. Pathak. 2003. Retroviral mutation rates and reverse transcriptase fidelity. *Front. Biosci.* 8:d117-d134.
- Takeuchi, Y., McClure, M.O., Pizzato, M., 2008. Identification of gammaretroviruses constitutively released from cell lines used for human immunodeficiency virus research. *J. Virol.* 82, 12585-12588.
- Tan, G.T., Pezzuto, J.M., Kinghorn, A.D., 1991. Evaluation of natural products as inhibitors of human immunodeficiency virus type 1 (HIV-1) reverse transcriptase. *J. Nat. Prod.* 54, 143-154.
- Tanaka, E., 1998. Clinically important pharmacokinetic drug-drug interactions: role of cytochrome P450 enzymes. *J. Clin. Pharm. Ther.* 23, 403-416.
- Tang, Y., Zhu, W., Chen, K., Jiang, H., 2006. New technologies in computer-aided drug design: Toward target identification and new chemical entity discovery. *Drug Discovery Today: Technologies* 3, 307-313.
- Tarbit, M.H., Berman, J., 1998. High-throughput approaches for evaluating absorption, distribution, metabolism and excretion properties of lead compounds. *Curr. Opin. Chem. Biol.* 2, 411-416.
- Taukumova, L.A., Mouravjoy, Y., Gribakin, S.G., 1999. Mucocutaneous side effects and continuation of aurotherapy in patients with rheumatoid arthritis. *Adv. Exp. Med. Biol.* 455, 367-373.
- Telesnitsky, A., Goff, S.P., 1993a. Strong-stop strand transfer during reverse transcription. In: Skalka, A.M., Goff, S.P. (Eds.), *Reverse Transcriptase*. Cold Spring Harbor Laboratory Press, Plainview, New York, pp. 49-83.
- Temesgen, Z., Cainelli, F., Poeschla, E.M., Vlahakis, S.A., Vento, S., 2006. Approach to salvage antiretroviral therapy in heavily antiretroviral-experienced HIV-positive adults. *Lancet Infect. Dis.* 6, 496-507.
- Tepperman K., Zhang Y., Roy P.W., Floyd R, Zhao Z, Dorsey J.G., Elder R.C. (1994). Transport of the diacyanogold (I) anion. *Metal Based Drugs*; 1(5-6): 433-443.
- Than, S., Hu, R., Oyaizu, N., Romano, J., Wang, X., Sheikh, S., Pahwa, S., 1997. Cytokine pattern in relation to disease progression in human immunodeficiency virus-infected children. *J. Infect. Dis.* 175, 47-56.
- Thompson, K.H., Orvig, C., 2003. Boon and bane of metal ions in medicine. *Science* 300, 936-939.
- Tiekink, E.R., 2002. Gold derivatives for the treatment of cancer. *Crit. Rev. Oncol. Hematol.* 42, 225-248.
- Tiekink, E.R.T., 2003. Gold compounds in medicine: Potential anti-tumour agents. *Gold Bulletin* 36, 117-124.
- Tilton, J.C., Doms, R.W., 2010. Entry inhibitors in the treatment of HIV-1 infection. *Anti-viral Res.* 85, 91-100.
- Tosi, S., Cagnoli, M., Guidi, G., Murelli, M., Messina, K., Colombo, B., 1985. Injectable gold dermatitis and proteinuria: retreatment with auranofin. *Int. J. Clin. Pharmacol. Res.* 5, 265-268.

- Traber K.E., Okamoto H., Kurono C., Baba M., Saliou C., Soji T., Parker L., Okamoto T. (1999). Anti-rheumatoid compound aurothioglucose inhibits tumour necrosis- α - induced HIV-1 replication in latently infected OM10.1 and Ach2 cells. *Int. Immunol.* 11(2): 143-150.
- Traoré, H.N., Meyer, D., 2001. Comparing qualitative and quantitative spectroscopic techniques for the detection of the effect of direct iron loading of mammalian cell cultures. *Methods Cell Sci.* 2001;23(4):175-84.
- Traut, T., Williams., B. 2006. "Synthesis And Testing Of Anti-Hiv Gold Compounds : Stage 11", *Mintek Communication*.
- Trkola, A., Pomales, A.B., Yuan, H., Korber, B., Maddon, P.J., Allaway, G.P., Katinger, H., Barbas, C.F., 3rd, Burton, D.R., Ho, D.D., 1995. Cross-clade neutralization of primary isolates of human immunodeficiency virus type 1 by human monoclonal antibodies and tetrameric CD4-IgG. *J. Virol.* 69, 6609-6617.
- Trkola, A., Mathews, J., Gordon, C., Ketas, T., Moore, J.P., 1999. A cell line-based neutralization assay for primary human immunodeficiency virus type 1 isolates that use either CCR5 or CXCR4 coreceptor. *Journal of Virology*, 73:8966-8974.
- Turner, B.G., Summers, M.F., 1999. Structural biology of HIV. *J. Mol. Biol.* 285, 1-32. UNAIDS Report on the global epidemic (December 2010).
- UNAIDS Report on the global epidemic (December 2010).
- Vaidyanathan, J., Vaidyanathan, T.K., Ravichandran, S., 2009. Computer simulated screening of dentin bonding primer monomers through analysis of their chemical functions and their spatial 3D alignment. *J Biomed Mater Res Part B: Appl Biomater* 88B: 447-457.
- van de Waterbeemd, H., Gifford, E., 2003. ADMET in silico modelling: towards prediction paradise? *Nat. Rev. Drug Discov.* 2, 192-204.
- Veazey, R.S., Tham, I.C., Mansfield, K.G., DeMaria, M., Forand, A.E., Shvets, D.E., Chalifoux, L.V., Sehgal, P.K., Lackner, A.A., 2000. Identifying the target cell in primary simian immunodeficiency virus (SIV) infection: highly activated memory CD4(+) T cells are rapidly eliminated in early SIV infection in vivo. *J. Virol.* 74, 57-64.
- Verwilghen, J., Kingsley, G.H., Gambling, L., Panayi, G.S., 1992. Activation of gold-reactive T lymphocytes in rheumatoid arthritis patients treated with gold. *Arthritis Rheum.* 35, 1413-1418.
- von dem Borne, A.E., Pegels, J.G., van der Stadt, R.J., van der Plas-van Dalen, C.M., Helmerhorst, F.M., 1986. Thrombocytopenia associated with gold therapy: a drug-induced autoimmune disease? *Br. J. Haematol.* 63, 509-516.
- Waheed, A.A., Ablan, S.D., Mankowski, M.K., Cummins, J.E., Ptak, R.G., Schaffner, C.P., Freed, E.O., 2006. Inhibition of HIV-1 replication by amphotericin B methyl ester: selection for resistant variants. *J. Biol. Chem.* 281, 28699-28711.
- Walker, L.M., Phogat, S.K., Chan-Hui, P.Y., Wagner, D., Phung, P., Goss, J.L., Wrin, T., Simek, M.D., Fling, S., Mitcham, J.L., Lehrman, J.K., Priddy, F.H., Olsen, O.A., Frey, S.M., Hammond, P.W., Protocol G Principal Investigators, Kaminsky, S., Zamb, T., Moyle, M., Koff, W.C., Poignard, P., Burton, D.R., 2009. Broad and potent neutralizing antibodies from an African donor reveal a new HIV-1 vaccine target. *Science* 326, 285-289.
- Walker, P.R., Worobey, M., Rambaut, A., Holmes, E.C., Pybus, O.G., 2003. Epidemiology: Sexual transmission of HIV in Africa. *Nature* 422, 679.
- Walters, W.P., Murcko, M.A., 2002. Prediction of 'drug-likeness'. *Adv. Drug Deliv. Rev.* 54, 255-271.
- Wang, X.Q., Duan, X.M., Liu, L.H., Fang, Y.Q., Tan, Y., 2005. Carboxyfluorescein diacetate succinimidyl ester fluorescent dye for cell labeling. *Acta Biochim. Biophys. Sin. (Shanghai)* 37, 379-385.
- Watts, C., 1997. Capture and processing of exogenous antigens for presentation on MHC molecules. *Annu. Rev. Immunol.* 15, 821-850.
- Waybright, T.J., Britt, J.R., McCloud, T.G., 2009. Overcoming problems of compound storage in DMSO: solvent and process alternatives. *J. Biomol. Screen.* 14, 708-715.
- Wei, X., Decker, J.M., Liu, H., Zhang, Z., Arani, R.B., Kilby, J.M., Saag, M.S., Wu, X., Shaw, G.M., Kappes, J.C., 2002. Emergence of resistant human immunodeficiency virus type 1 in patients receiving fusion inhibitor (T-20) monotherapy. *Antimicrob. Agents Chemother.* 46, 1896-1905.
- Wensing, A.M., van Maarseveen, N.M., Nijhuis, M., 2010. Fifteen years of HIV Protease Inhibitors: raising the barrier to resistance. *Anti-viral Res.* 85, 59-74.
- West D.X., Padhye S.B., Sonawane P.B., In *Structure and Bonding*, Springer-Verlag:New York, 1991, Vol 76 pp 1-49.

- West, D.X., Ives, J.S., Bain, G.A., Liberta, A.E., Valdés-Martínez, J., Ebert, K.H., Hernández-Ortega, S., 1997. Copper(II) and nickel(II) complexes of 2,3-butanedione bis(N(3)-substituted thiosemicarbazones). *Polyhedron* 16, 1895-1905.
- Wielens, J., Headey, S.J., Jeevarajah, D., Rhodes, D.I., Deadman, J., Chalmers, D.K., Scanlon, M.J., Parker, M.W., 2010. Crystal structure of the HIV-1 integrase core domain in complex with sucrose reveals details of an allosteric inhibitory binding site. *FEBS Lett.* 584, 1455-1462.
- Williams, D.B.G., Traut, T., Kriel, F.H., van Zyl, W.E., 2007. Bidentate amino- and iminophosphine ligands in mono- and dinuclear gold(I) complexes: Synthesis, structures and AuCl displacement by AuC6F5. *Inorg. Chem. Commun.* 10, 538-542.
- Wlodawer, A., Erickson, J.W., 1993. Structure-based inhibitors of HIV-1 protease. *Annu Rev Biochem.* 62, 543-585.
- Wlodawer, A., Vondrasek, J., 1998. Inhibitors of HIV-1 protease: a major success of structure-assisted drug design. *Annu. Rev. Biophys. Biomol. Struct.* 27, 249-284.
- World Bank (1997). *Confronting AIDS: public priorities in global epidemic.* Washington, DC: World Bank.
- Wouter, J., Buvé, A., Nkengasong, J.N., 1997. The puzzle of HIV-1 subtypes in Africa. *AIDS*; 11: 705-712.
- Wu, G., Robertson, D.H., Brooks, C.L., 3rd, Vieth, M., 2003. Detailed analysis of grid-based molecular docking: A case study of CDOCKER-A CHARMM-based MD docking algorithm. *J. Comput. Chem.* 24, 1549-1562.
- Xing, J.Z., Zhu, L., Gabos, S., Xie, L., 2006. Microelectronic cell sensor assay for detection of cytotoxicity and prediction of acute toxicity. *Toxicol. In Vitro.* 20, 995-1004.
- Xing, J.Z., Zhu, L., Jackson, J.A., Gabos, S., Sun, X.J., Wang, X.B., Xu, X., 2005. Dynamic monitoring of cytotoxicity on microelectronic sensors. *Chem. Res. Toxicol.* 18, 154-161.
- Xu, H-T., Quan, Y., Ashchop, E., Oliveira, M., Moisi, D., Wainberg M.A., (2010). Comparative biochemical analysis of recombinant reverse transcriptase enzymes of HIV-1 subtype B and subtype C. *Retrovirology*, 7, 80-91.
- Xu, L., Pozniak, A., Wildfire, A., Stanfield-Oakley, S.A., Mosier, S.M., Ratcliffe, D., Workman, J., Joall, A., Myers, R., Smit, E., Cane, P.A., Greenberg, M.L., Pillay, D., 2005. Emergence and evolution of enfuvirtide resistance following long-term therapy involves heptad repeat 2 mutations within gp41. *Antimicrob. Agents Chemother.* 49, 1113-1119.
- Yamaguchi, K., Ushijima, H., Hisano, M., Inoue, Y., Shimamura, T., Hirano, T., Muller, W.E., 2001. Immunomodulatory effect of gold sodium thiomalate on murine acquired immunodeficiency syndrome. *Microbiol. Immunol.* 45, 549-555.
- Yanni, G., Nabil, M., Farahat, M.R., Poston, R.N., Panayi, G.S., 1994. Intramuscular gold decreases cytokine expression and macrophage numbers in the rheumatoid synovial membrane. *Ann. Rheum. Dis.* 53, 315-322.
- Yeni, P., 2006. Update on HAART in HIV. *J. Hepatol.* 44, S100-3.
- Yoder, K.E., Bushman, F.D., 2000. Repair of gaps in retroviral DNA integration intermediates. *J. Virol.* 74, 11191-11200.
- Yoshida, A., Tanaka, R., Murakami, T., Takahashi, Y., Koyanagi, Y., Nakamura, M., Ito, M., Yamamoto, N., Tanaka, Y., 2003. Induction of protective immune responses against R5 human immunodeficiency virus type 1 (HIV-1) infection in hu-PBL-SCID mice by intrasplenic immunization with HIV-1-pulsed dendritic cells: possible involvement of a novel factor of human CD4(+) T-cell origin. *J. Virol.* 77, 8719-8728.
- Yoshida, S., Kato, T., Sakurada, S., Kurono, C., Yang, J.P., Matsui, N., Soji, T., Okamoto, T., 1999. Inhibition of IL-6 and IL-8 induction from cultured rheumatoid synovial fibroblasts by treatment with aurothioglucose. *Int. Immunol.* 11, 151-158.
- Young, F.M., Phungtamdet, W., Sanderson, B.J., 2005. Modification of MTT assay conditions to examine the cytotoxic effects of amitraz on the human lymphoblastoid cell line, WIL2NS. *Toxicol. In Vitro.* 19, 1051-1059.
- Young, T.P., 2003. Immune Mechanisms in HIV Infection. *Journal of the Association of Nurses in AIDS care* 14, 71-75.
- Yousif, L.F., Stewart, K.M., Horton K.L., Kelley S.O., 2009. Mitochondria-penetrating peptides: sequence effects and model cargo transport. *CHEMBIOCHEM*, 10, 2081-2088.
- Zhang, C.X., Lippard, S.J., 2003. New metal complexes as potential therapeutics. *Curr. Opin. Chem. Biol.* 7, 481-489.
- Zhang, Y., Hess, E.V., Pryhuber, K.G., Dorsey, J.G., Tepperman, K., Elder, R.C., 1994. Interaction of gold with red blood cells. *Met. Based. Drugs* 1, 517.

- Zhang Y., Hess E.V., Pryhuber K.G., Dorsey J.G., Tepperman K., Elder R.C. (1995). Gold binding sites in red blood cells. *Inorganica Chimica Acta*, 229: 271-280.
- Zoete, V., Michielin, O., Karplus, M., 2002. Relation between sequence and structure of HIV-1 protease inhibitor complexes: a model system for the analysis of protein flexibility. *J. Mol. Biol.* 315, 21-52.
- Zutshi, R., Chmielewski, J., 2000. Targeting the dimerization interface for irreversible inhibition of HIV protease. *Bioorg. Med. Chem. Lett.* 10, 1901–1903.

Web References

<http://pubchem.ncbi.nlm.nih.gov/>

<http://www.bbc.co.uk/news/health-13362927>

<http://www.hotindir.com/wp-content/uploads/2010/10/amino-acids.gif>

<http://www.ncbi.nlm.nih.gov/pccompound>

www.htpn.org

www3.bio-rad.com.

CHAPTER 8

APPENDIX

8.1 CHAPTER 2

8.1.1 Statistical Definitions

In Table A2.1, the meanings of the statistical terminology used in this study are provided. Most of the definitions were obtained from web sources such as dictionary.com, answers.com and reference.com and from the Handbook of biological statistics (<http://udel.edu/~mcdonald/statcentral.html>).

Table A2.1: Description of statistics calculations that were implemented in this study.

Analysis	Description
% Standard error of mean (% SEM)	It is the percentage of the standard deviation of the sampling distribution of the mean.
CC ₅₀	This is the concentration of a compound at which 50% of cells are killed.
Correlation coefficient	A statistic representing how closely two variables co-vary; it can vary from -1 (perfect negative correlation) through 0 (no correlation) to +1 (perfect positive correlation).
IC ₅₀	This is the concentration of compound at which 50% inhibitory activity is observed.
Mean	The sum of all observations divided by the number of observations
Median	The middle number or average of two middle numbers in an ordered sequence of numbers.
P values	This is a probability value ranging from zero to one. This value is used to determine the difference between sample means if the means were the same. If the p value is <0.05, then there is a significant difference between two populations but if it is > 0.05 then the differences are not significant.
Percentile or quartile	A percentile is a value at or below which a given percentage or fraction of the variable values lie. Quartiles split the percentage into quarters. The first quarter is the 25 th percentile, the second the 50 th and the 3 rd the 75 th
Standard deviation (SD)	This indicates measures of deviation or spread of values from the mean of treatments in a population or multiset of values.

8.2 CHAPTER 3

8.2.1 NMR chromatograms

8.2.1.1 The effect of water on the NMR spectra of gold complex TTC3

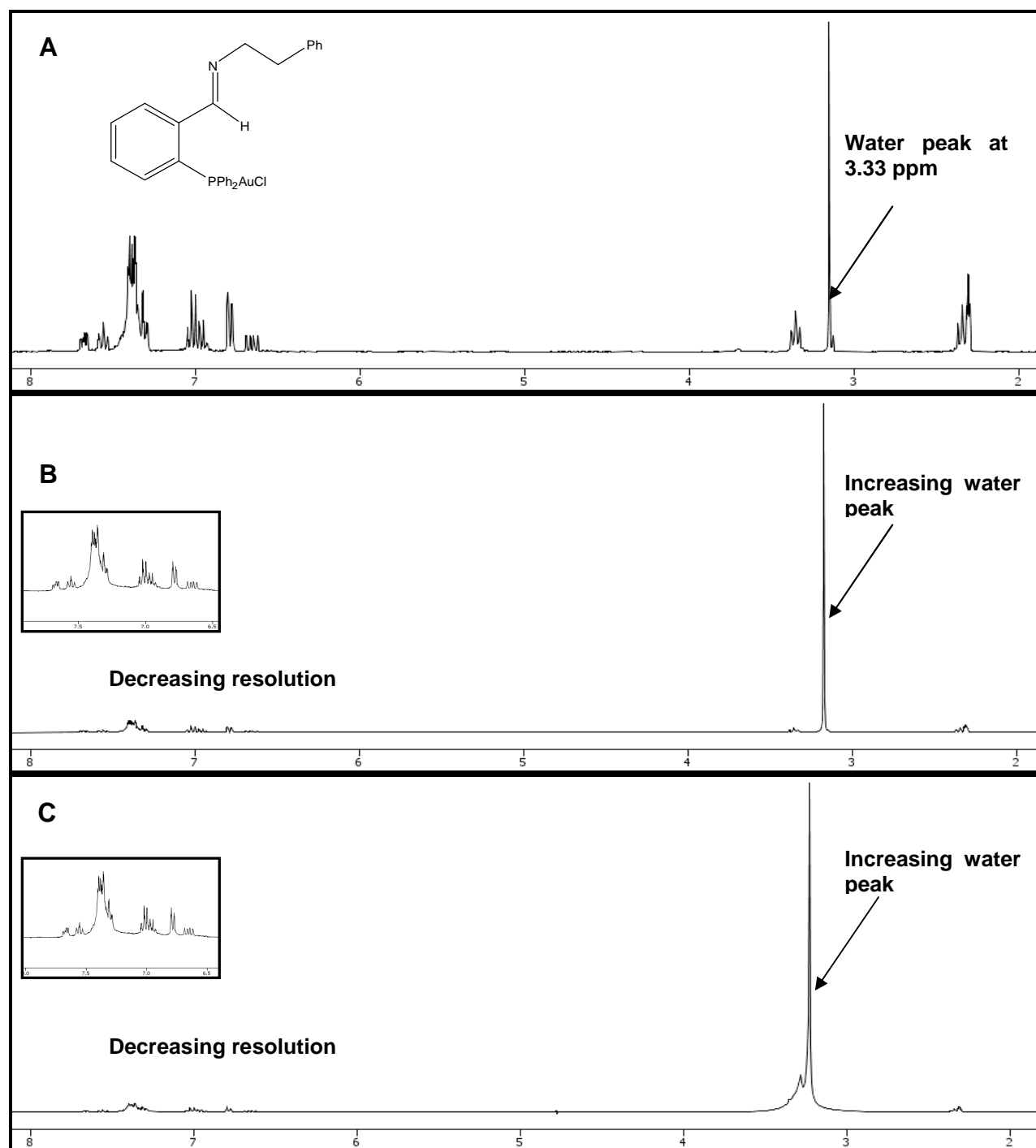


Figure A3.1: The effect of water on the ^1H profile of the gold(I) phosphine chloride complex, TTC3. A water peak was visible on day zero and became more prominent by 24 h and 7 days later causing a decrease in the resolution of proton peaks. TTC3 appeared to have taken up water from the atmosphere shown on day zero. The area of the water peak was seen to increase after 24 h and 7 days due to the additional hygroscopic nature of DMSO. Although the backbone structure of the compound appeared intact on day zero and over time (please see insert showing relevant peaks), the overall chemistry of the compound could ultimately have been affected leading to degradation and precipitation as a result of water. This effect can alter the final concentration of the compound available for biological analysis.

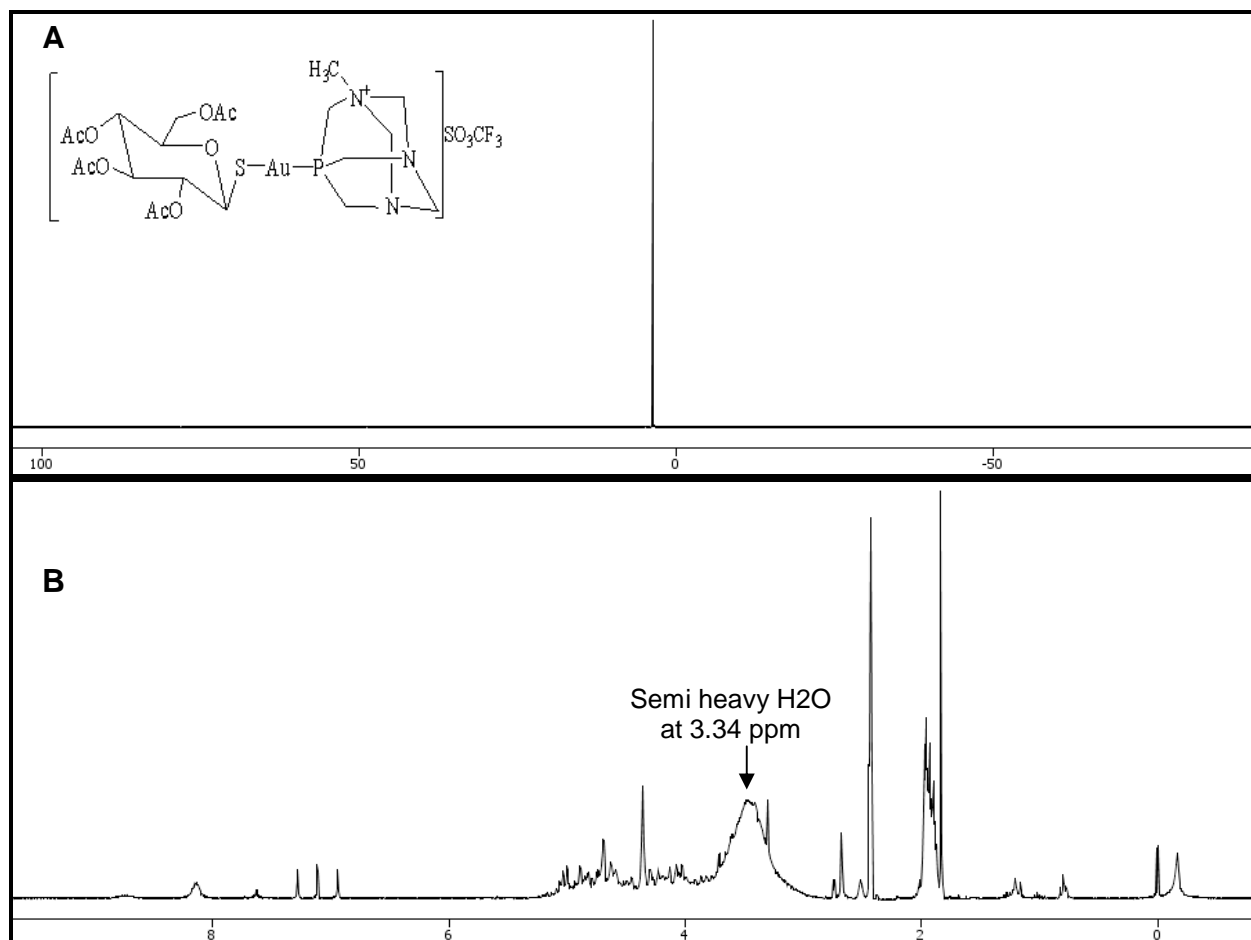
8.2.1.2 The ^{31}P and ^1H NMR spectra of MCZS3

Figure A3.2: The ^{31}P and ^1H NMR of MCZS3 on day zero. The ^{31}P NMR shown in A was referenced to a phosphorous standard (normally at 0 but shifted to 3.8 ppm when spectra was downloaded from Chenomx software for better visibility). No ^{31}P peak was observed in the spectra. This could be because there was insufficient amount of the compound to reach the threshold required for resolved peaks due to poor solubility (hence precipitation) which was evident during sample preparation. In the ^1H NMR spectrum, the broad peak at 3.4 ppm is likely HDO (semi heavy water) resulting from *d6*-DMSO exchanging a deuterium atom with hydrogen atom of water (deuterium exchange). According to the spectrum, the backbone phosphine and acetylated sugar moieties were intact.

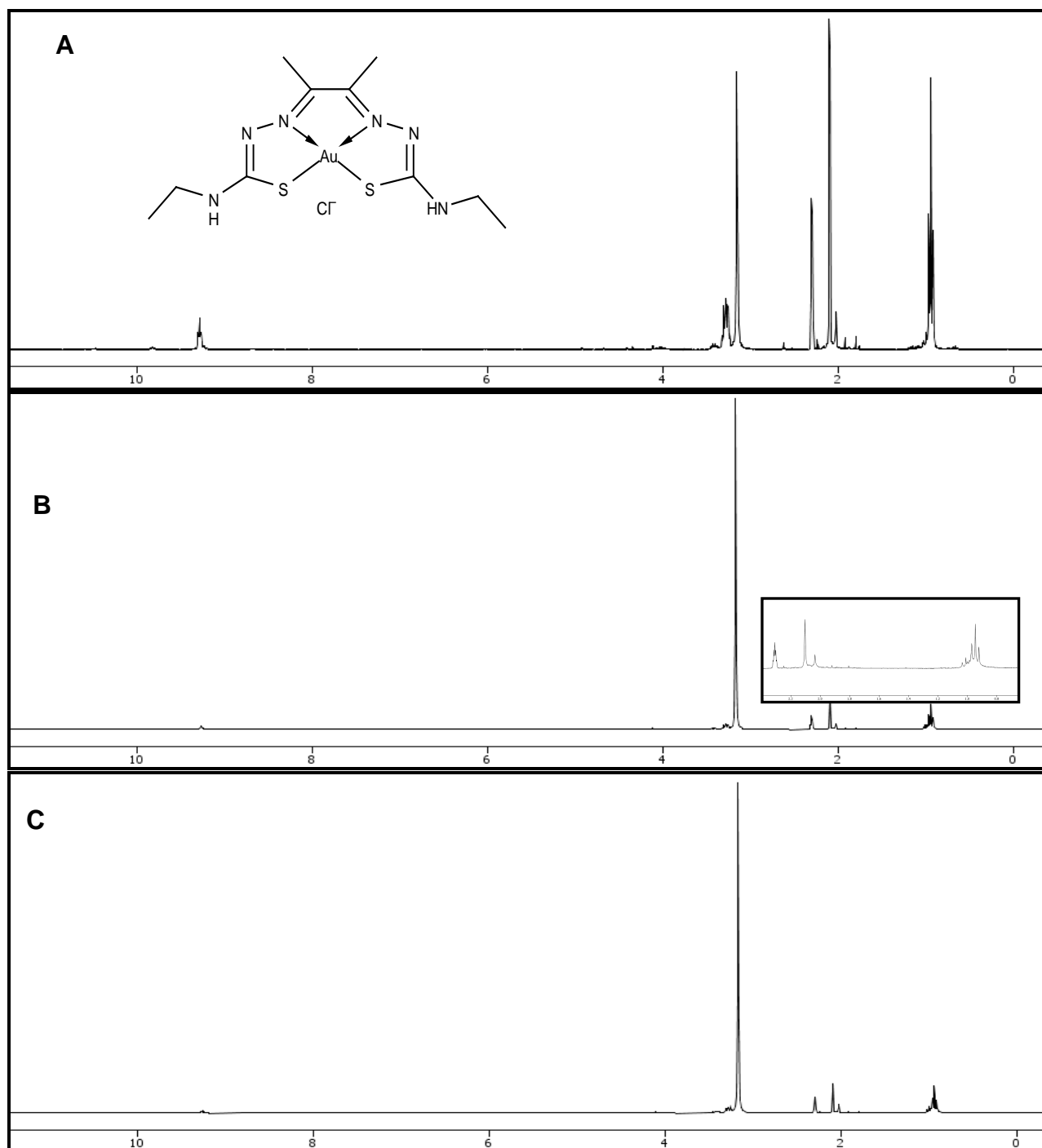
8.2.1.3 The ^1H spectra of PFK7

Figure A3.3: ^1H NMR spectra of PFK7. A is a spectrum taken on day zero, B is a spectrum after 24 h and C is a spectrum taken after 7 days of storage at $-20\text{ }^\circ\text{C}$. Except for a water peak seen on day zero (3.33 ppm, Gottlieb *et al.*, 1997) that became increasingly prominent at 24 h and 7 days later, the compound remained relatively stable although peak resolutions were suppressed by the water peaks. The relevant peaks at 24 h are enlarged in the insert.

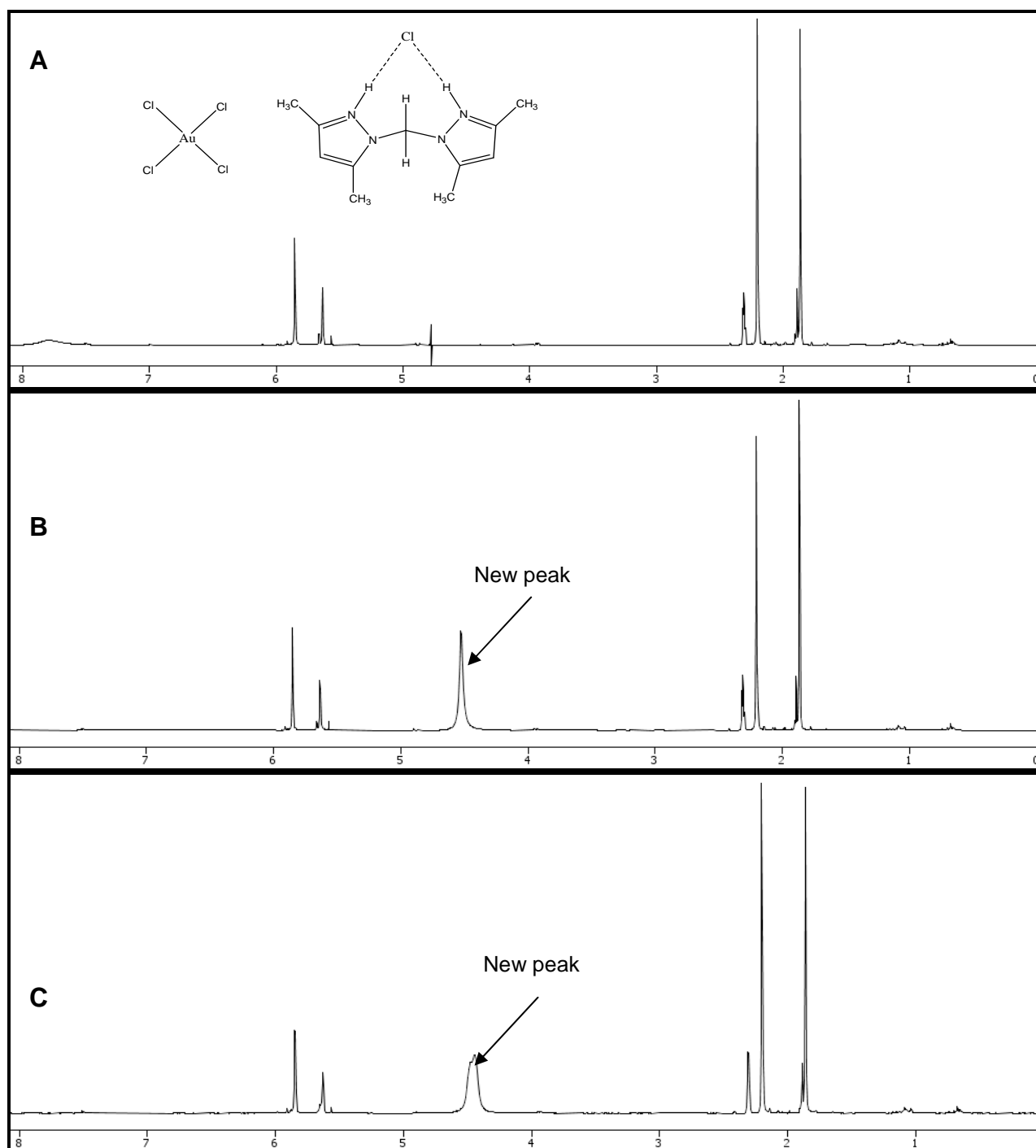
8.2.1.4 The ^1H NMR spectra of KFK154b after 24 h and 7 days

Figure A3.4: ^1H NMR of KFK154b. At day zero (A) the spectrum appears with no peak evident at 4.7 nor was there a water peak at 3.33 ppm but after analysing at 24 h and 7 days following storage at $-20\text{ }^\circ\text{C}$ every other chemical shift remained intact suggestive of a stable compound except for a new peak at 4.7 ppm. This new peak is possibly an impurity resulting from deuterated water (Gottlieb *et al.*, 1997). Since deuterated water was not used in the analysis, it is unclear where it came from and might have been experimental error. It appears the deuterated water peak compensated for the water peak present in the other spectra at 3.33 ppm.

8.3 CHAPTER 4

8.3.1 Viability Assay Optimisations

Sixteen of the compounds (ligands and complexes) consisting of classes I, II, and III shown in Table 3.6 demonstrated different effects on primary and continuous cell lines when analysed with various viability dyes such as MTT and (2,3)-bis(2-methoxyl-4-nitro-5-sulphenyl)-(2H)-tetrazolium-5-carboxanilide (XTT, Fonteh and Meyer, MSc. Dissertation, 2008). The compounds

generally demonstrated higher CC_{50} values of $> 200 \mu\text{M}$ in the primary cells (PBMCs) and CC_{50} s in the low micromolar range in the cell lines (CEM.NKR-CCR5 and PM1). These significant differences in the effect of the compounds on the viability of these two cell types needed explanation and formed part of optimisation assays that were performed in this study.

While toxicity can be species and organ specific (Ponsoda *et al.*, 1995), the fact that both cell lines are T cell lines (CEM.NKR-CCR5 and PM1) and that the PBMCs are predominantly T cells suggested that the known limitations of MTT may have been at play. Alternatively the fact that PBMCs are a mixture of different cell types could have meant the metabolism of MTT (which can be affected by cell type) was irreproducible. This is because interperson variability could affect the results (Trkola *et al.*, 1999) especially if the relative cell populations were not the same in samples from the same or different donors over time. While aqueous solubility problems (postulated to have affected RT assays) could have played a role, this conclusion was not alluded to given that there was consistent toxicity when cell lines were used and not when primary cells were used. To clarify all issues regarding cells types, possible compound effects, and different dyes, optimisation assays were performed using HTS assays. For the optimisation, the MTT (Sigma Aldrich, Missouri USA) and MTS (Promega Corporation, WI, USA) viability dyes, propidium iodide (BD BioScience, California, USA) using flow cytometry and the lactate dehydrogenase (LDH) cytotoxicity assay kit (Roche Diagnostics, Mannheim, Germany) were used.

MTT and MTS (both tetrazolium salts) function on the same principle where mitochondrial dehydrogenases in viable cells convert the yellow water soluble MTT and MTS to a water insoluble product (in the case of MTT, (Young *et al.*, 2005) and a water soluble product (in the case of MTS). The incorporation of an electron coupling reagent (phenazine methosulfate) in MTS leads to the production of a soluble product (Soman *et al.*, 2009). The purple water insoluble formazan product resulting from the use of MTT requires solubilisation, which can be achieved using different solutions such as propanol (Denzizot and Lang, 1986) and 2-propanol and 1M HCl (Mueller *et al.*, 2004). The absorption of the dissolved formazan for both dyes in the visible region of the electromagnetic spectrum correlates with the number of intact live cells (Mueller *et al.*, 2004).

8.3.1.1 MTT data optimisation

In the previous MTT assays (sixteen compounds, Fonteh and Meyer, 2008) and preliminary screening in this study (nine of the sixteen compounds) were analysed. The nine compounds included TTL3, TTC3, TTL10, TTC10, EK207, EK208, EK219, EK231 and MCZS1. The assays for the nine compounds were performed as previously described (Fonteh and Meyer, 2008) with the only variable being a reduction in the incubation time from 7 days to 3 days. After incubating cells (PBMCs, PM1) with compound concentrations ranging from 3.125 -200 μM in a 200 μL final volume, 20 μL of MTT (5 mg/mL) was added directly to the wells and incubated for 24 h. Then 50 μL of solubilisation solution consisting of acidified isopropanol in a 1:9 ratio (i.e. 1 part of 1 M HCl and 9 parts of isopropanol) was added directly into the wells and the plate read immediately at 540/550 nm (690 nm reference wavelength).

The viability data with MTT suggested that the compounds were not toxic to PBMCs (Figure A4.1, also seen previously, Fonteh and Meyer, 2008) at higher concentrations that were otherwise toxic to PM1 cells (Fonteh and Meyer, 2008). The change in incubation time (from 7 days to 3 days) did not appear to have an effect on the viability profiles i.e. no apparent toxicity of the compounds was observed for the primary cells (Figure A4.1A).

Three possible theories for the differences between viability data for PBMCs and PM1 cells were proposed. (1) the possibility that the compounds could be interfering with MTTs' metabolism by forming products with MTT that were being absorbed (only when assays are performed for PBMC), (2) the fact that PBMCs are a mixture of cells unlike the cell lines which are homogenous making the metabolism of MTT different (it has been reported that different cell types metabolise MTT differently, Young *et al.*, 2005, Hertel *et al.*, 1996) and a third consideration (3) was the possibility that the compounds were being absorbed at the same wavelength like MTT. This 3rd possibility was ruled out when compound spectra showed no absorbance at wavelengths used for measuring the MTT and MTS formazan products. The maximum absorbance for all the compounds were <400 nm but MTT absorbs at 540/550 while MTS absorbs at 492.

For the optimisation, the first parameter change involved the removal of 150 μ L of spent medium at the end of the incubation (to exclude any unabsorbed compound). This was replaced with an equal volume of freshly prepared complete RPMI medium. The rest of the protocol was maintained i.e. incubation for 24 h and then adding 50 μ L solubilisation solution followed by reading the plate at 550 nm (690 nm reference λ). This resulted in distinct data differences (Figure A4.1B) when compared to the unoptimised protocol (Figure A4.1A). The CC_{50} s of the compounds were similar to those obtained when viability was determined for PM1 cells using MTT (Fonteh and Meyer, 2008). The fact that the only change in the protocol was the removal of spent medium did not explain why the results now looked similar to the PM1 MTT assay findings in previous studies (Fonteh and Meyer, 2008) since in the previous studies spent medium was not removed for the latter. The conclusion at this point was that in as much as the compounds were playing a role, the differences in the cell types (heterogeneity of PBMCs and homogeneity of PM1) also had an effect on the metabolism of the MTT when analysed in the presence of compounds.

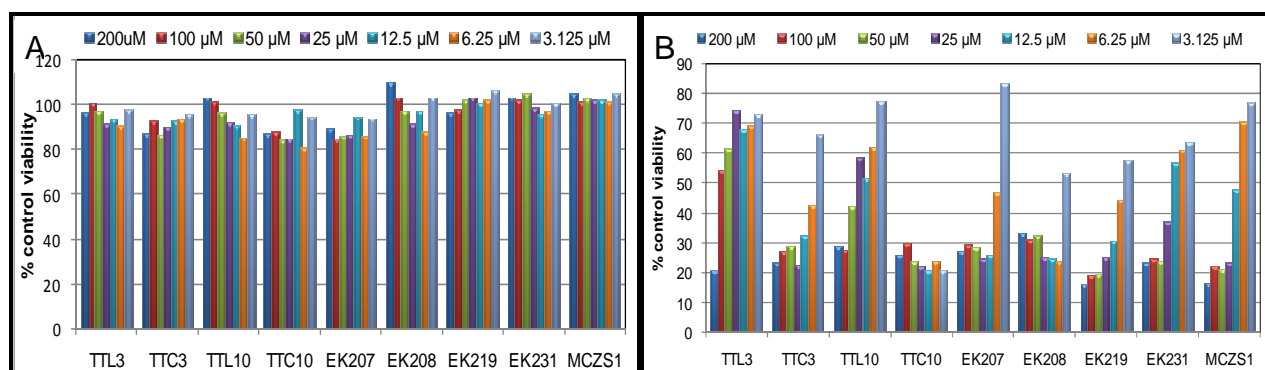


Figure A4.1: MTT viability optimisation assays with PBMCs. In A, the cells were treated with the compounds for 72 h. Twenty microlitres of MTT (5 mg/mL) was added to the cells followed by a 24 h incubation. Solubilisation solution consisting of HCl and isopropanol was added to the wells to dissolve formazan crystals and the plate read at 550 nm on a spectrophotometer. In B, the only difference was that after the 72 h incubation, the plate was centrifuged and the spent media discarded and replaced with an equal volume of freshly prepared complete medium which apparently excluded compound effect seen in A resulting in a dose dependent cytotoxicity. Results are averages of at least three repeats.

8.3.1.2 MTS data optimisation

A second viability dye (MTS) which functions on the same principle as MTT (except for the fact that a solubilisation step is not required and also the fact that the dye absorbs at a different wavelength) was used for comparison purposes. After cells and compounds had been incubated for 3 days, 10 μL of MTS was added to the wells of the plate, incubated for 24 h and absorbance measured at 492 nm (690 nm reference wavelength). Figure A4.2A shows viability data for PBMCs obtained using MTS without excluding compound effect in medium. It appears the compounds were not significantly toxic but this time there was a slight dose dependent toxicity (Figure A4.2A) which was not seen when MTT was used in determining viability in the same manner (Figure A4.1A). This finding suggested that the effect of the compounds on PBMCs could easily be determined with MTS. When an optimisation step (similar to the one employed for MTT) which included the replacement of spent medium with freshly prepared medium before addition of the dye was performed, a pattern different from that seen in Figure A4.2A was observed (suggesting toxicity) shown in Figure A4.2B but similar to that seen for MTT in the optimised assay (Figure A4.1B). This data (MTS/PBMCs/optimised Figure A4.2B) which supported the MTT findings in Figure A4.1B (MTT/PBMCs/optimised) confirmed that fact that the compounds may have been interfering with the metabolism of MTT. As mentioned earlier, compound spectra showed no absorbance at wavelengths used for measuring the MTT and MTS formazan products. The concern here was therefore the fact that the compounds might be capable of reacting with MTT to produce products which interfered with MTT absorbance readings resulting in false conclusions.

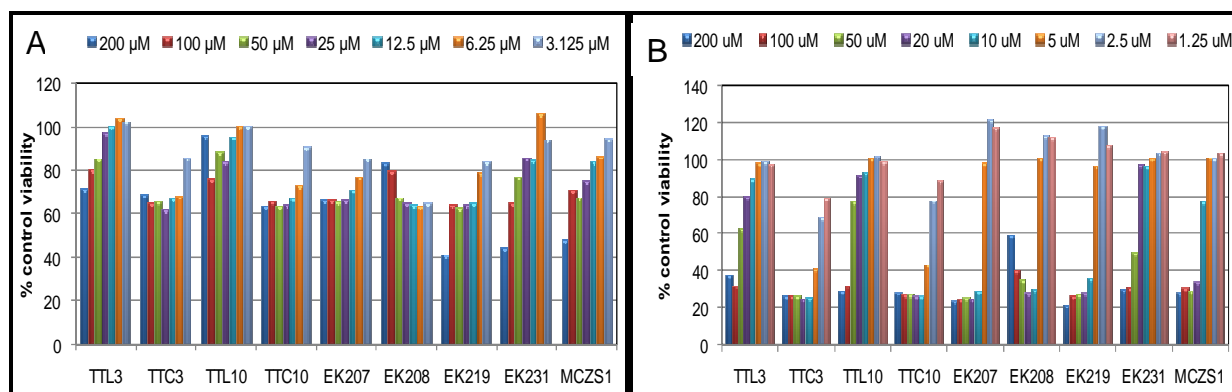


Figure A4.2: MTS viability optimisation assays on PBMCs. In A, the cells were treated with the compounds for 72 h. Ten microlitres of MTS was added to the cells followed by a 24 h incubation. The plate was read at 492 nm on a spectrophotometer. In B, the only difference was that after the 72 h incubation, the plate was centrifuged and the spent media discarded and replaced with an equal volume of freshly prepared complete medium which apparently excluded compound effect seen in A. Results are averages of at least three repeats.

The next concern was whether the unoptimised protocol would still result in different trends (lower CC_{50}) for the cell line compared to primary cells as previously seen (Fonteh and Meyer, 2008). To verify this, MTS was used as the viability dye. When the MTS dye was used in determining viability in the PM1 cell line (in the absence of optimisation), a totally different pattern from that seen in the unoptimised protocol for PBMCs (Figure A4.2A) was observed (Figure A4.3) but similar to PBMCs (Figure A4.2B, optimised). The pattern in Figure A4.2B and that of the PM1 in Figure A4.3 were similar in CC_{50} s suggesting better correlation. This disparity in the data

between the different cell types which was also seen previously (Fonteh and Meyer, 2008) for MTT and observed here for MTS further confirms the fact that the different cell types metabolise the dyes differently. It is however not clear why removing compound effect in the PBMCs assay (by replacing spent medium with freshly prepared medium, Figure A4.2B) led to similar results to that observed for PM1 cells (Figure A4.3, unoptimised). The only logical explanation at this point was that the presence of the compounds in the heterogeneous mixture of cells (PBMCs) affected the cells' metabolism of MTT. Medium components such as serum have been implicated for causing discrepancies in such assays (Denzizot and Lang, 1986) but the same medium (RPMI-1640 medium) was used so the variable could not have been the medium.

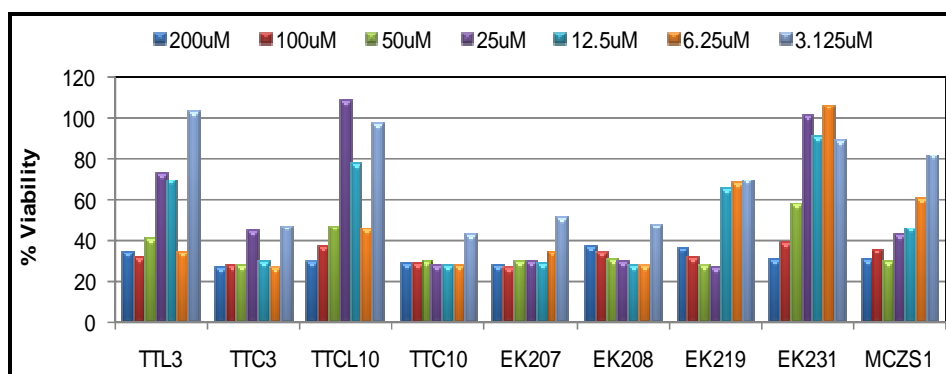


Figure A4.3: Viability pattern of PM1 cells treated with compounds and determined with MTS. PM1 cells were treated with the compounds for 72 h. MTS solution (10 μ L) was added to the cells and the soluble formazan product read at 492 nm after 2 h of incubation.

8.3.1.3 Lactate dehydrogenase assay optimisations

The LDH cytotoxicity detection kit (Roche Diagnostics, Mannheim, Germany) which measures LDH release into culture supernatant as an indication of cytotoxicity was also used in determining toxicity. Figure A4.4 represents the assay principle. The difference between this assay and the MTT and MTS assays is that it measures toxicity and not viability. In addition, incubations with compounds were only done for 24 h since LDH released into the supernatant is not stable after >24 h.

The assay was performed as previously described (Fonteh and Meyer, 2008). Following 24 h of compound exposure to the PBMCs, plates were centrifuged. Fifty microlitres of culture supernatant was carefully aspirated from the plate into corresponding wells of an optically clear 96 well flat bottom microtitre plate. To this, 50 μ l of LDH reaction mixture was added and the absorbance read immediately at 490 nm (reference wavelength 690 nm). Total cellular LDH was obtained by treatment with 0.1% triton x-100 (v/v) and set as 100% cytotoxicity. Background and negative controls were obtained by LDH measurement of assay medium and untreated cell medium respectively. Data from control and treated cells was calculated as percentage cytotoxicity using the following formula:-

$$\text{Cytotoxicity (\%)} = \frac{\text{Absorbance Sample} - \text{Absorbance medium}}{\text{Absorbance 100\%} - \text{Absorbance medium}} \times 100$$

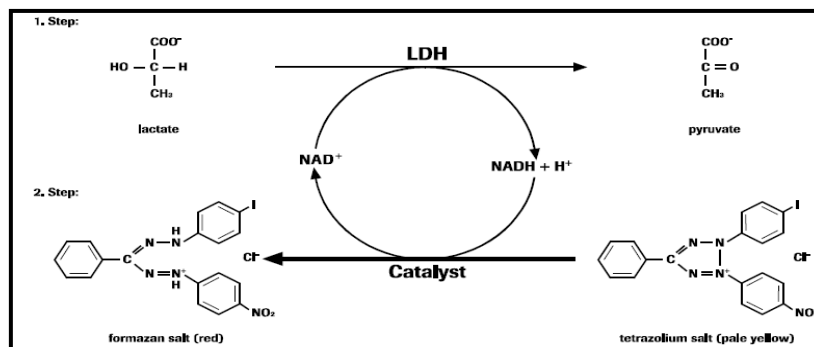


Figure A4.4: LDH cytotoxicity assay test principle. The LDH activity is determined in an enzymatic test where in the first step; NAD⁺ is reduced to NADH/H⁺ by LDH catalysed conversion of lactate to pyruvate. In a second step, the catalyst (diaphorase) transfers H⁺/H⁺ from NADH/H⁺ to the tetrazolium salt INT which is reduced to formazan. An increase in plasma membrane damage leads to an increase in LDH activity in the culture supernatant which is directly proportional to water soluble formazan dye formed. This figure was taken from the LDH cytotoxicity detection kit catalogue (Roche Diagnostics, Mannheim, Germany).

Higher toxic concentrations of compounds were expected to release more LDH in a dose dependent manner which should decrease as dose decreases e.g. for compounds TTL3, TTL10, EK231 and MCZS1 (Figure A4.5). This was however not the case for complexes TTC3, TTC10 (complexes of TTL3 and TTL10 respectively), EK207, EK208 and EK219 with the converse being true i.e. LDH release was lower at higher concentrations. The probable reason for this was the fact that the gold in the gold compounds (especially at the higher concentrations) with the exception of EK231 and MCZS1 may have coordinated with an intermediary product in the reaction. Probably a reduction reaction with the pale yellow tetrazolium salt at the N=N bridge (Figure A4.4) preventing the formation of the formazan product which is indicative of toxicity from the red colour (Figure A4.4). If this suggestion is true, then it is possible that the compounds were capable of reducing MTT and MTS (both tetrazolium salts) to an intermediary product when viability was done for PBMCs. The outcome was false (low) absorbance readings obtained in the unoptimised data (Figure A4.1A and A4.2A respectively) and hence false conclusions about the viability status of the cells. But when the compound effect was excluded through the removal of spent medium, this viability trend changed (observed toxicity, Figure A4.1B and A4.2B). Unfortunately, optimisations like the one done for the MTT and MTS assay (replacement of spent medium with fresh) could not be performed for the LDH assay since the analyte (containing LDH) in this case is the medium and not the cells. As a result, toxicity testing with the LDH cytotoxicity kit was terminated.

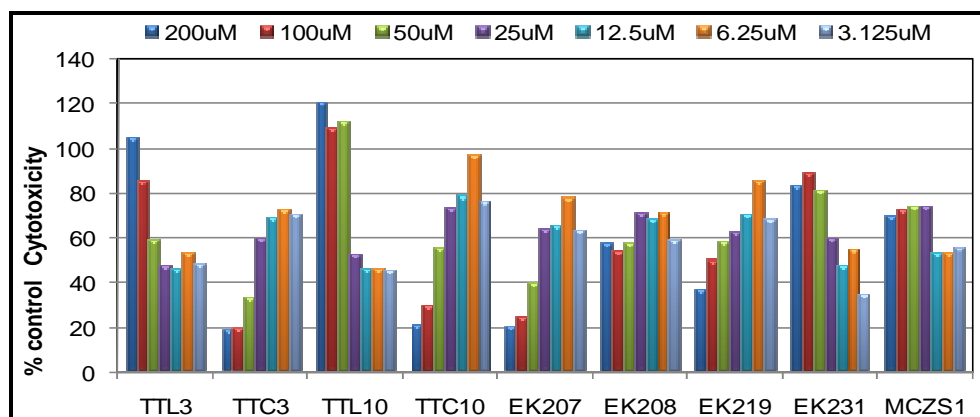


Figure A4.5: Cytotoxicity pattern of compounds on PBMCs determined using the LDH cytotoxicity detection kit. An unusual trend in cytotoxicity was observed for complexes TTC3, TTC10, EK207 and EK219 which tended to be toxic at lower but not higher concentrations.

8.3.1.4 Viability optimisation using flow cytometry and propidium iodide

To confirm the MTT and MTS findings, a more sensitive flow cytometry assay using propidium iodide which stains dead cells was performed for PBMCs (Figure A4.6). It was observed that the presumed CC_{50} s values of the compounds as per Figure A4.1A and A4.2A ($>25 \mu\text{M}$) were in fact very toxic since a $25 \mu\text{M}$ concentration was toxic for most of the compounds except TTL3, TTL10, EK207, EK231 and MCZS1 (Figure A4.6B). These findings corroborated the data obtained from the PBMCs optimised data (Figure A4.1B and A4.2B) for the different dyes and PM1 cell line (unoptimised, Figure A4.3) e.g. according to Figure A4.1B, A4.2B and A4.3, TTC20 was toxic at $25 \mu\text{M}$ while EK231 was not also observed in the flow cytometry analysis (Figure A4.6B). This comparison is applicable to the rest of the compounds.

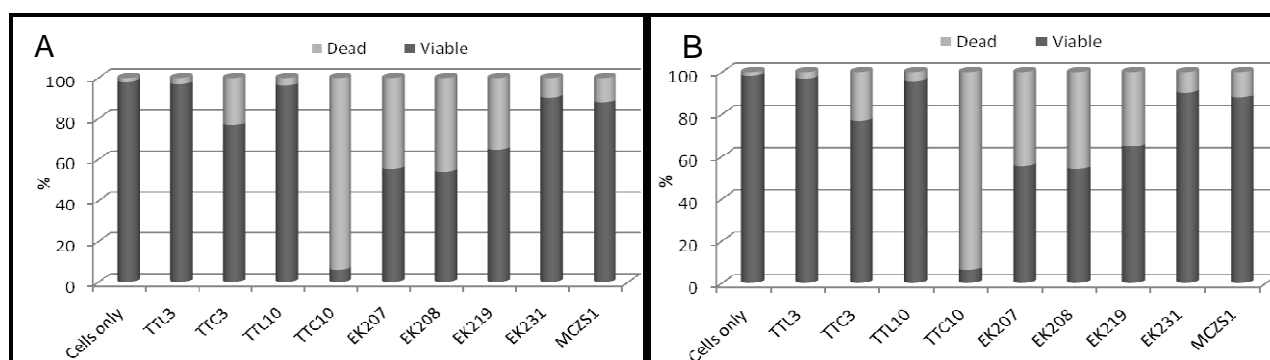


Figure A4.6: The effect of the compounds on the viability of PBMCs. The cells were treated with the compounds for 72 h and stained with propidium iodide. Cells not positive for PI and annexin were considered viable. Compound concentrations of $5 \mu\text{M}$ and $25 \mu\text{M}$ were used in A and B respectively. More viable cells were present at $5 \mu\text{M}$ than at $25 \mu\text{M}$.

Based on all the optimisation findings (MTT, MTS, flow cytometry with annexin V and PI), the MTS dye was chosen as the viability dye of choice for HTS to determine the CC_{50} s of the compounds in the PM1 and PBMCs. This was because of the experience that PBMCs poorly metabolised the MTT dye compared to MTS (Figure A4.1A and A4.2A respectively) and sometimes the data was irreproducible (probably because of the heterogeneity of the cells). Inefficient metabolism of some human cell lines by tetrazolium dyes have previously been reported (Hertel *et al.*, 1996). In the case of the cell lines, the use of either MTT or MTS resulted in similar CC_{50} values. In all cases (PBMCs or PM1), the optimised protocol was used. The optimised assays were employed for all the compounds and the methods and results are incorporated in chapter 4 (sections 4.2.3 and 4.3.1 respectively).

8.3.2 CFSE Incubation Time and Stimulant Optimisation

Incubation strategies included (1) incubation of the compounds with the stained cells for various times ranging from 1 day to 7 days, (2) treatment of stained cells with compounds only and (3) treatment of stained cells with compounds and stimulant (PHA-P or PMA/ION).

8.3.2.1. Time optimisation

CFSE is a dye that is spread equally between daughter cells as they divide allowing for the monitoring of cellular proliferation by fluorescent measurement using flow cytometry. However,

depending on the time point when incubation is stopped, varying results could be obtained and in some cases, the proliferation pattern might be missing after too many divisions. To avoid this, optimisation assays that included quantifying cell division over different time periods were performed (Figure A4.7). Three generations were analysed for this. By day 7, the cells had undergone too many divisions (too many cells in the daughter 2 population) while on day 1 not many cells were present in the daughter 2 population. Based on these findings 3 days of incubation was chosen as incubation time for subsequent analysis.

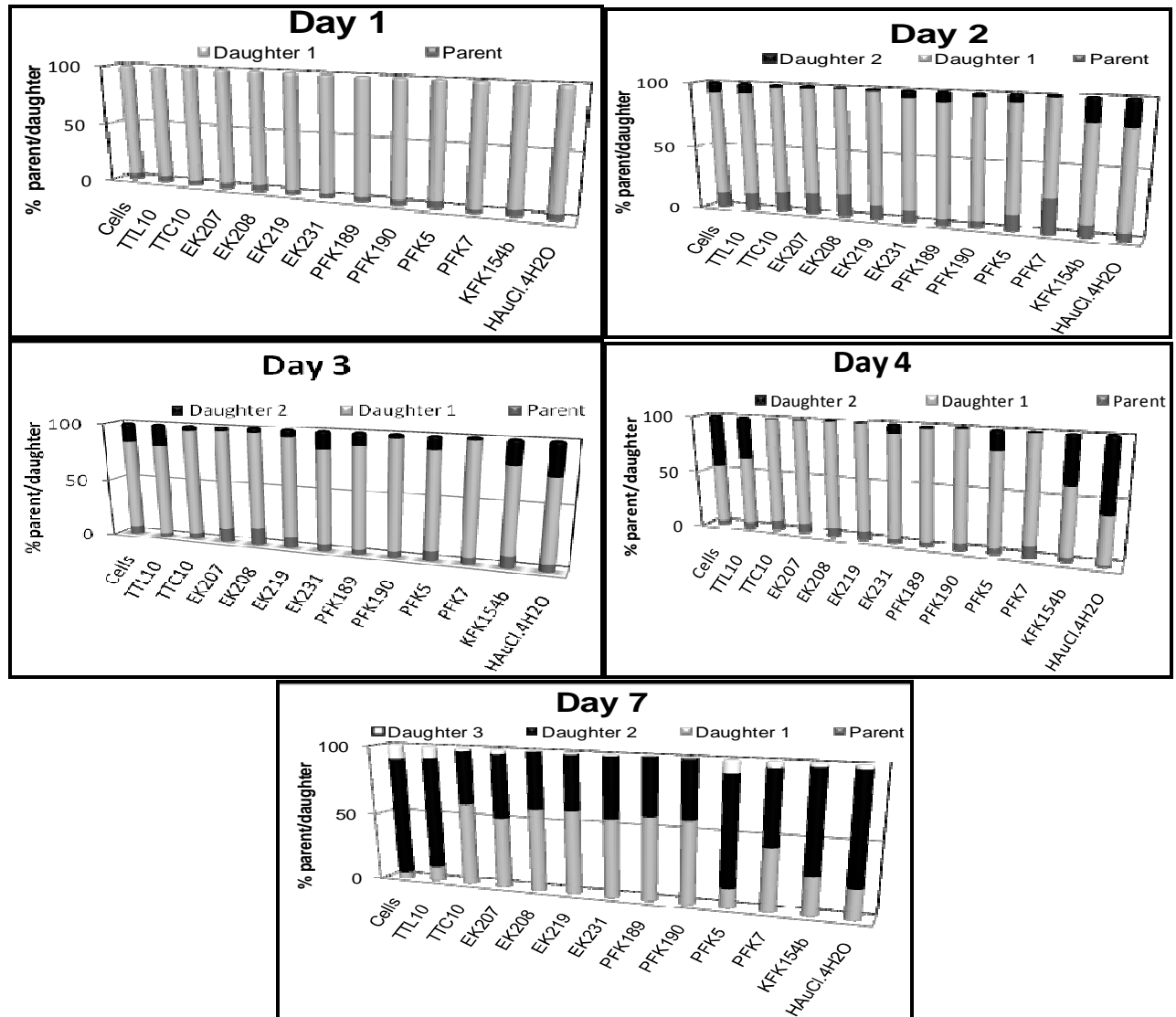


Figure A4.7: Time optimisation experiments for CFSE. Patterns obtained after three and four days were better representations of proliferation. By day 7, most of the CFSE dye had been diluted out resulting in very dim populations.

8.3.2.2 Stimulant optimisation

Stimulation of PBMCs is usually required *in vitro* to initiate proliferation and cytokine production. Stimulants like PHA-P, PMA/ION are usually used. Since the effect of the compounds on the proliferation profiles of PBMCs was being sought, it was important to know the role the stimulants could play in such assays. The proliferation of PHA-P stimulated cells was affected by some compounds e.g. TTC3 and EK207 (Figure A4.8A). Gold compounds have previously been reported to inhibit the proliferation of PHA-P stimulated cells (Sfikakis *et al.*, 1993, Lipsky and Ziff,

1977) making this finding not surprising. Stimulation with PMA/ION had no effect on proliferation (Figure A4.8B). This was only useful for enhancing and monitoring cytokine production. In the absence of stimulants, PBMCs did not proliferate at all (similar finding to when PMA/ION was used) both for compound treated and untreated cells (Figure A4.8 C). This suggests that the compounds had no stimulatory effect and were therefore not mitogenic.

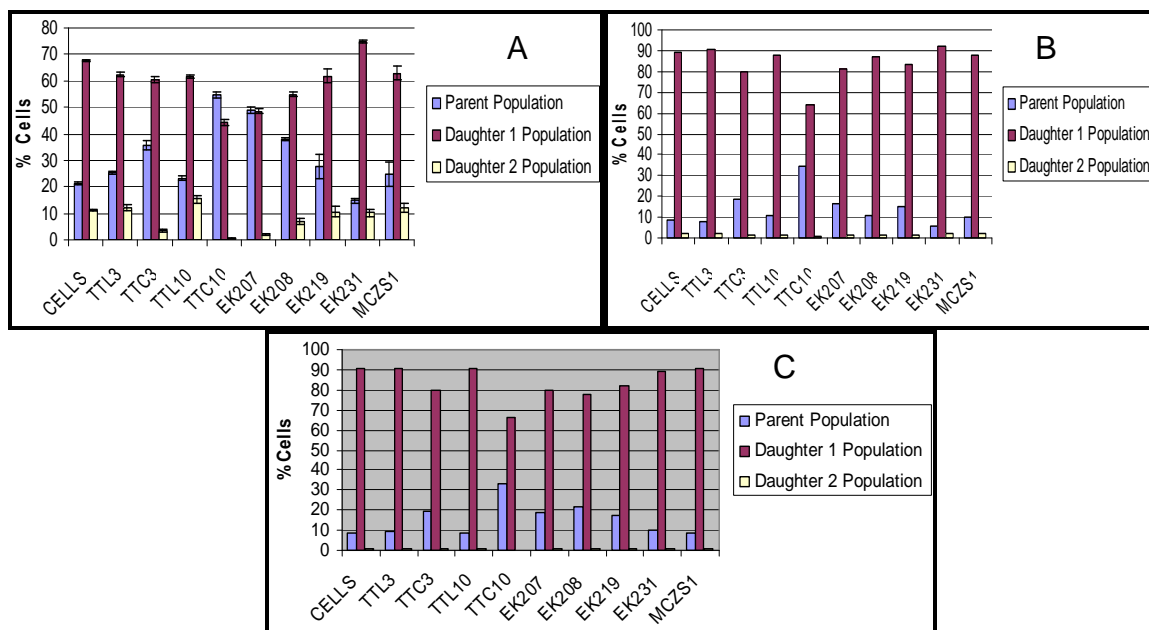


Figure A4.8: Differences in cell proliferation pattern of PBMCs in the presence and absence of stimulant after 3 days of treatment with compounds. In A, PHA-P stimulated cells were shown to proliferate resulting to cells in both the daughter 1 and daughter 2 populations. In B, the use of PMA/ION as stimulant for proliferation was shown to be ineffective as no cells were present in the daughter 2 population. The same was applicable for cells not stimulated with either PHA or PMA/ION (C). Three days of incubation with PHA-P as stimulant was chosen as ideal for proliferation monitoring.

From the optimisation assays, it was observed that in the absence of stimulant, both compound treated and untreated cells did not proliferate and that three or four days was ideal for stopping the assay in the presence of stimulant. Three days and the use of PHA-P as stimulant for monitoring proliferation were used for subsequent testing.

8.3.3 Other Flow Cytometry Optimisations

8.3.3.1 Gating optimisation

Figure A4.9A (P1) represents lymphocytes which were obtained by back gating on the Q4 (CD45–PerCP–Cy5.5 +) population in Figure A4.9B. The P4 gate contains debris, dead cells and might contain other sub populations. Once the lymphocyte gate was positively identified, the effect of the compounds on the viability of PBMCs was subsequently analysed based on this gate. The threshold on the FSC and SSC plot was placed at 5000 to show the other populations and debris (Figure A4.9A). This threshold was increased to 40,000 to eliminate the debris and dead cells when compounds were later tested in cell viability, proliferation or in immunomodulatory assays.

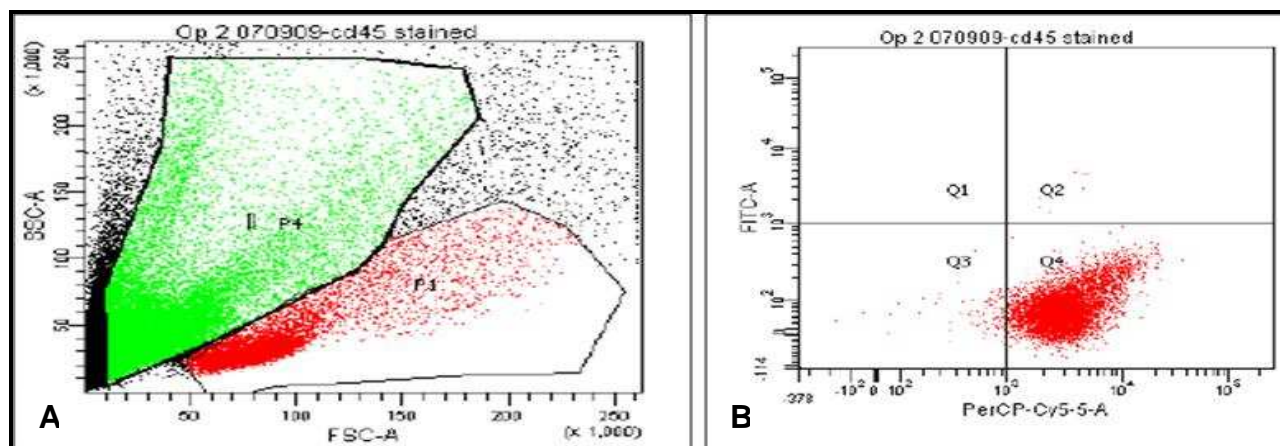


Figure A4.9: Lymphocyte identification gating. CD45 gate – P1 (A) back-gated from the CD45-PerCP-Cy5.5 stain (B). CD45 stains lymphocytes and was used to aid in excluding monocytes and neutrophils. The P4 gate consists mostly of debris and death cells but might also contain another subpopulation.

8.3.3.2 Stimulant optimisation

It has been established that unstimulated cells do not produce cytokines (Nylander and Kalies, 1999) such that appropriate stimulation of cells for cytokine investigation is a necessity. Figure A4.10 shows the different time and stimulant optimisation assays that were done for the PBMCs prior to ICCS assays. Cells treated with gold compounds only, PHA+gold compounds and then PMA/ION+gold compounds were analysed after 24, 48 and 72 h. In the case where PMA/ION were used as stimulants, their addition was done in the last 6 h of incubation because of the toxicity associated with the use of these stimulants for longer periods. As seen in Figure A4.10A, B and C there was no cytokine production for untreated cells and cells treated with gold compounds only after 24, 28 and 72 h. Cytokine production by PHA-P treated and PHA-P + compound treated cells increased but remained minimal (Figure A4.10D, E and F). Cells treated with PMA/ION and PMA/ION+ compound on the other hand (Figure A4.10G, H and I) produced significantly more cytokines. The only limitation in the PMA/ION treatment is the fact that there was a decrease of CD4+ cell frequency, a finding which has been reported for PMA/ION before. However, in the 24 h treatment with the latter, the CD4 frequency and cytokine secretion profiles were sufficient for monitoring the effect of the compounds on cytokine production. PMA/ION was used as stimulant with a 24 h incubation time for subsequent cytokine analysis.

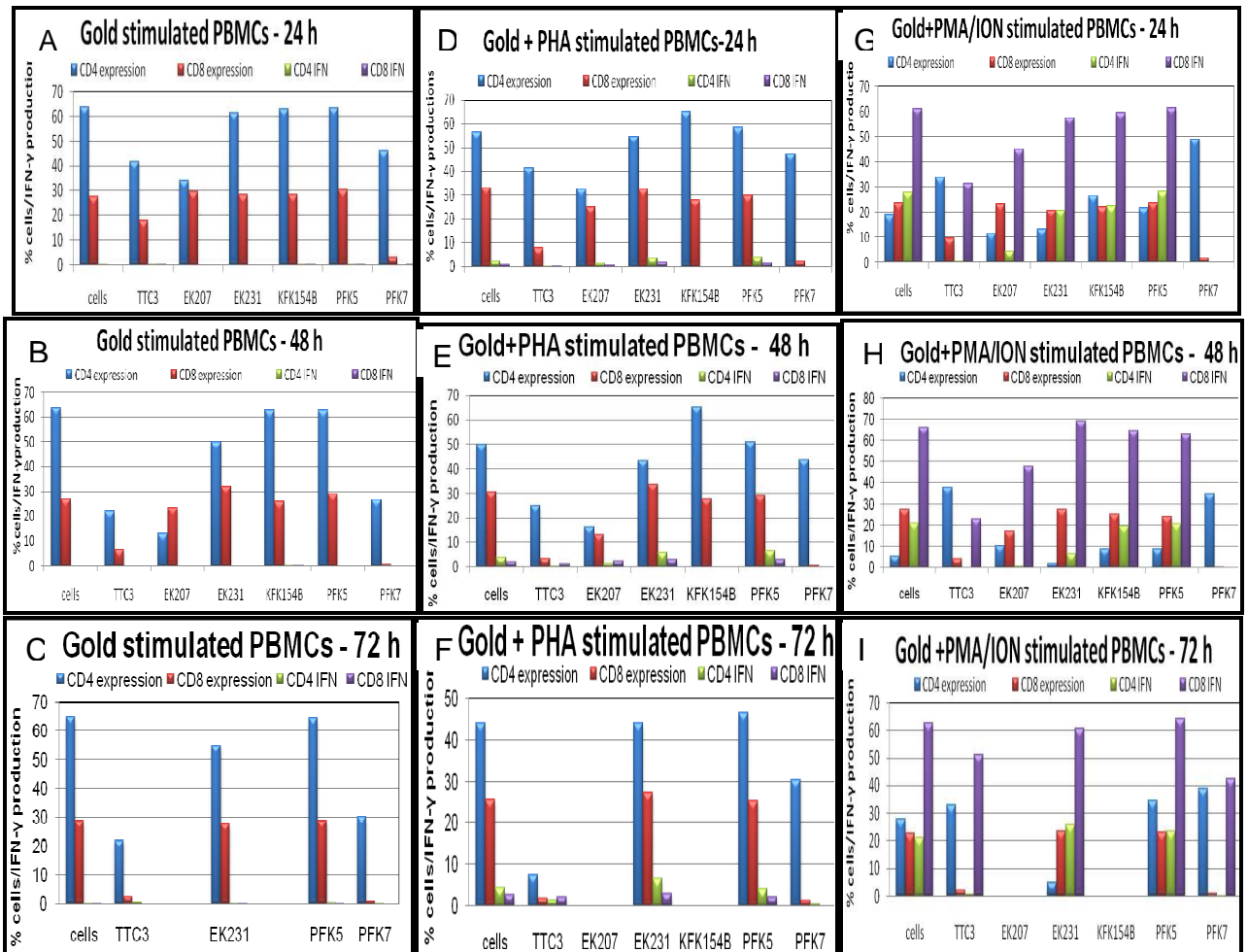


Figure A4.10: Stimulant and time optimisation assays for ICCS experiments. In A, B and C, the PBMCs were treated with compounds only for 24, 48 and 72 h respectively. Under these conditions, no ICC production was observed. In D, E and F, the cells were treated both with compounds and with PHA-P. There was a slight increase in the cytokine level. When the cells were treated with PMA/ION and protein transport inhibitor (golgistop) in the last 6 h of incubating with the compounds (G, H, I), significantly higher levels of cytokines were produced which were easier to quantify and analyse. Based on these three treatments, cells stimulated with PMA/ION and golgistop in the last 6 h of a 24 h incubation period, were used for further analysis.

8.3.4 RT-CES Analyser Repeats

Figure A4.11 and 12 are experimental repeats for the RT-CES analysis shown in Figure 4.7B.

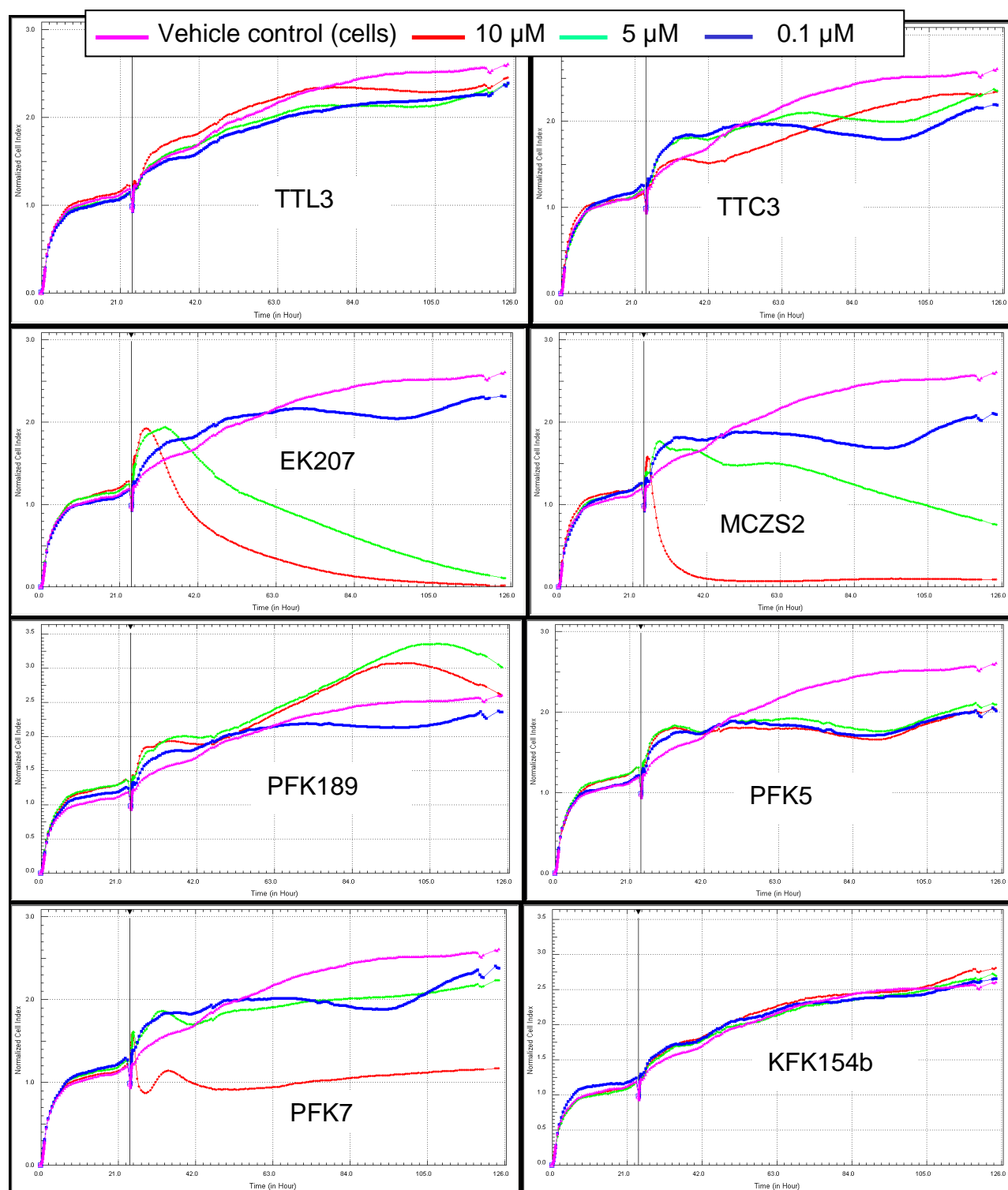


Figure A4.11: The effect of representative compounds on the proliferation of T2M-bl cells using an RT-CES analyser. Cells were seeded into E-plates and allowed to adhere for at least 22 h followed by treatment with the compounds. Three concentrations of each compound were tested and are represented on each graph as normalized CI (y-axis) against time (h) alongside the vehicle control. Compounds TTL3, PFK5 and KFK154b did not cause CI decreases (do not influence proliferation/viability). EK207 and PFK189 induced a dose dependent decrease in CI, days after addition. PFK7 displayed a dose dependent cytostasis at all 3 concentrations tested. MCZS2 induced CI decreases within hours of addition. Proliferation was monitored for 123 h.

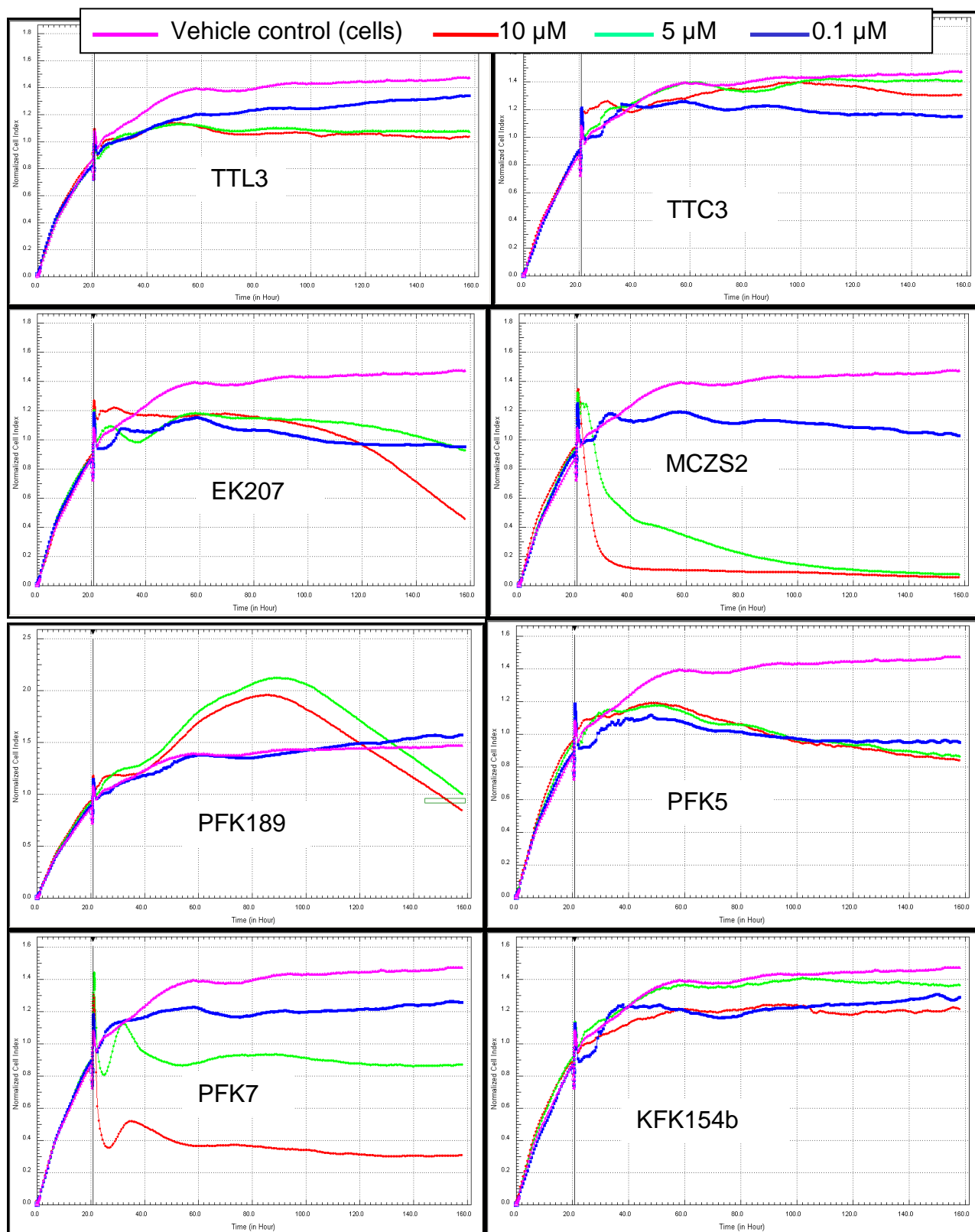


Figure A4.12: The effect of representative compounds on the proliferation of TzM-bl cells using an RT-CES analyser. Cells were seeded into E-plates and allowed to adhere for at least 20 h followed by treatment with the compounds. Three concentrations of each compound were tested and are represented on each graph as normalized CI (y-axis) against time (h) alongside the vehicle control. Compounds TTL3, PFK5 and KFK154b did not cause CI decreases (do not influence proliferation/viability). EK207 and PFK189 induce a dose dependent decrease in CI days after addition. PFK7 was displayed a dose dependent cytostasis at all 3 concentrations. MCZS2 induced CI decreases within hours of addition. Proliferation was monitored for 160 h.

8.3.5 Infectivity Studies, CC₅₀ and IC₅₀

Table A4.1 shows CC₅₀ and IC₅₀ results for viability and infectivity analysis performed on the TZM-bl cells. IC₅₀ values are shown for both virus pre-treatment and cell pre-treatment for compounds TTC24, EK231, PFK7 and PFK8. The fact that the IC₅₀ values for these compounds after these two exposure strategies were used are similar suggests that that inhibition was neither at entry of post entry step but that multiple points may have been involved.

Table A4.1: CC₅₀ and IC₅₀ for infectivity of the compounds in TZM-BL cells. The cells were treated with the compounds and toxicity determined using MTT while infectivity determination was done using the luciferase gene expression assay. ND means not done. % SEM was <20%.

Compound	CC ₅₀	IC ₅₀ (virus pre-treatment)	IC ₅₀ (Cell pre-treatment)
TTC3	9.9±1.5	4.8±0.9	
TTC10	8.5±1.6	4.9±0.9	
TTC17	8.3±0.14	6.9±0.3	
TTC24	18.6±4.8	7±1.8	5.6±0.9
EK207	27±1.3	3.6±1.1	
EK208	19±4.6	8.7±1.7	
EK219	18.1±3.2	4.9±0.7	
EK231	>40	6.8±0.8	5.8±0.4
PFK7	2.2±0.3	5.3±0.4	6±1.3
PFK8	10.6±0.1	6.8±0.6	6.2±0.5
PFK41	<0.2	1.4±0.4	
PFK43	0.6±0.1	1.4±0.2	

8.3.6 Immune System Cells: Function Determination

8.3.6.1 Differences in CD4+ and CD8+ cell frequency.

Infection with HIV is known to lead to a decline in CD4+ cells in infected individuals compared to uninfected people. These differences were also observed in the sample population which was analysed in this study which consisted of 12 HIV+ and 13 HIV- donors (Figure A4.13, p=0.0001). The reverse of this was seen for CD8+ cells where the positive donors had more CD8+ cells compared to the negative (p=0.0004). This data serves as confirmation for the HIV status of the donors in the different groups.

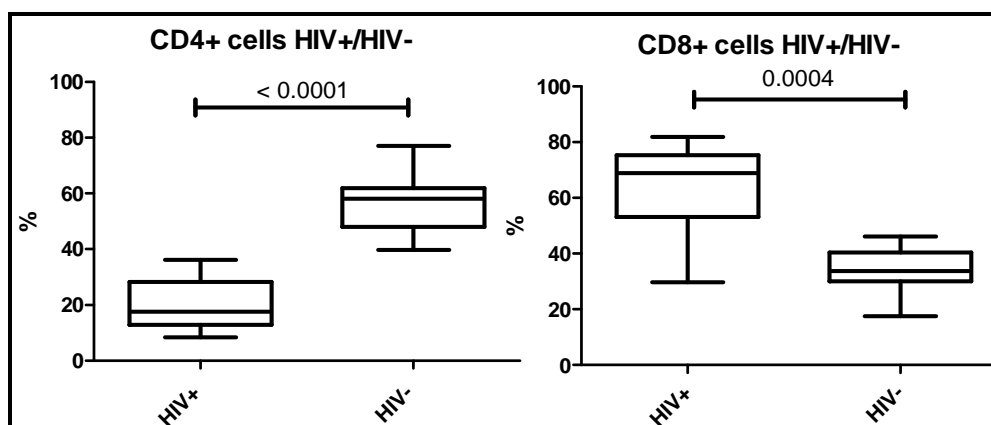


Figure A4.13: Differences in the frequency of production of T lymphocytes from HIV+/- donors. HIV+ subjects had significantly lower CD4+ and higher CD8+ cell frequencies than the negative group. Box and whisker plots show median and range of CD4+ and CD8+ cells in PBMCs cultured for 24 h in the presence of PMA/ION and BD GolgiStop™. Bars show 25th and 75th percentile. Statistical analysis (Wilcoxon matched-pairs signed rank test) revealed significant differences (p=0.0001 and 0.0004 respectively) in the frequency of cells expressing the CD4+ and CD8+ markers from PBMCs in the two groups.

8.3.6.2 ELISA data

To detect cytokines that may have been secreted prior to the addition of protein transport inhibitor (see ICCS protocol in section 4.2.6) in the intracellular cytokine assay, a step where the culture supernatant was collected and analysed for secreted cytokines using ELISAs was included.

Materials and Method: The concentration of IFN- γ and TNF- α in the supernatant collected from PBMCs treated for ICC detection was quantified using ELISA kits (eBioScience Inc., California, USA), according to the manufacturers' protocol. These sandwich ELISAs were initiated by coating 96-well plates with 100 μ L/well of capture antibody and after an overnight incubation (4°C), 200 μ L/well assay diluents were added to block non-specific reaction (25 °C, 1 h). The culture supernatant, reconstituted IFN- γ and TNF- α standards (known concentrations) were added to appropriate wells of 96 well plates. Two fold serial dilutions of standards were performed to make a standard curve. The plates were sealed and incubated overnight at 4 °C for maximal sensitivity. After washing the plates, 100 μ L/well of the detection antibody was added and the plates were incubated at room temperature for a further 1 h. This was followed by the addition of 100 μ L/well of avidin-horse radish peroxidase into each well followed by 30 min incubation at 25 °C. A substrate solution was then added to the wells and the plates incubated for 15 min at room temperature. The reaction was terminated by the addition of a stop solution consisting of 2 N H₂SO₄. Finally, the concentration of cytokines was calculated from the colorimetric absorbance which was read at 450 nm with a 550 nm reference filter using a Multiskan Ascent[®] spectrophotometer (Labsystems, Helsinki, Finland). The sensitivity limit of the assay was 4 pg/mL for IFN- γ and TNF- α with a standard curve range of 4 to 500 pg/mL in each case. ELISA analyses were performed in duplicate and the levels of IFN- γ and TNF- α presented as pg/mL.

Results and Discussion: IFN- γ secretion from six HIV+ and two HIV- donors was assessed (Table A4.2). A twofold decrease in IFN- γ secretion was observed for HIV+ cells treated with PFK41 and a general increase in secretion was observed for cells treated with compounds TTC24, MCZS1, PFK5, PFK7 and PFK174 (Table A4.2). Similar increases were seen for HIV- cells treated with TTC24, MCZS1 and PFK174, while PFK5 and PFK41 suppressed IFN- γ 's secretion by 0.2 and 2 folds respectively.

Table A4.2: The effect of the compounds on IFN- γ and TNF- α secretion from PBMCs. Cytokines concentrations were determined using sandwich ELISAs. The compounds generally increased IFN- γ secretion from PBMCs of both HIV+/- donors except for PFK41 which caused a decrease in its secretion in the HIV+ group and PFK5 which did so in the HIV- group. TNF- α production was also increased by most of the compounds in both HIV+/- donors except in the case of PFK5 which caused a decrease in the HIV+ group. [] represents cytokine concentration, \uparrow an increase and \downarrow a decrease in cytokine levels.

Compounds	HIV+IFN+ [] (pg/mL), n=6		HIV-IFN+ [] (pg/mL), n=2		HIV+TNF+ [] (pg/mL), n=5		HIV-TNF+ [] (pg/mL), n=4	
		\uparrow or \downarrow						
Control	31.5		94.8		43.3		12.5	
TTC24	134.0	4 \uparrow	185.6	2 \uparrow	571.9	13 \uparrow	118.5	9 \uparrow
MCZS1	83.4	3 \uparrow	305.2	3 \uparrow	74.3	2 \uparrow	22.5	2 \uparrow
PFK174	131.9	2 \uparrow	617.6	7 \uparrow	222.7	5 \uparrow	34.8	3 \uparrow
PFK5	64.9	6 \uparrow	77.3	0.2 \downarrow	12.9	3 \downarrow	24.6	2 \uparrow
PFK7	187.3	4 \uparrow	270.5	3 \uparrow	567.4	13 \uparrow	45.9	4 \uparrow
PFK41	14.5	2 \downarrow	44.0	2 \downarrow	221.0	5 \uparrow	27.5	2 \uparrow

In the case of TNF- α , a decrease in secretion was seen for HIV+ cells treated with PFK5 while the rest of the compounds tested generally caused an increase (Table A4.2). The compounds also generally caused an increase in TNF- α secretion from the HIV- cells (Table A4.2) with TTC24 inducing the highest secretion in both HIV+/- donors with an overall 13 fold increase in the HIV+ group. The general trend was that the compounds caused an increase in the secretion of IFN- γ and TNF- α from PBMCs obtained from both infected and uninfected donors.

Conclusion and comparison with ICCS: The observed increases in IFN- γ and TNF- α caused by the compounds as seen in the ELISA assay were thought to be as a result of the fact that integrated cytokines from all the different PBMCs subsets were quantified whereas for the ICCS assay (chapter 4 section 4.3.4), cytokines were measured from T cells only (CD4+ or CD8+ cells). Additionally because data was only collected for 6 donors in the ELISA assay (unlike 12 in the ICCS), it is possible that differences in patients status (for the outstanding 6) e.g. viral load was responsible in the observed differences.

Four compounds (TTC24, PFK174, PFK5 and PFK7) were used to compare cytokine production between the ICCS and ELISA techniques (Table A4.3). For the ICCS assay, only cytokines from CD4+ cells were compared (Table 4.3) to integrated cytokine production from PBMCs in each case from HIV+ donors. When cytokine production was altered by compounds such as TTC24 which lowered IFN- γ levels and PFK5 which caused an increase in TNF- α levels in the intracellular cytokine analysis of CD4+ cells (Table 4.3), the opposite effect was seen in the ELISA assay for PBMCs (Table A4.3). But in the situation where no effect was observed in the ICCS assay (e.g. for complexes PFK174 and PFK7), it appears the cytokines had already been secreted prior to the addition of golgistop since increases in secretion were observed for the ELISA study (Table A4.3). What this means is that in the absence of phenotypic identification (ELISA), complexes TTC24, PFK174, PFK5 and PFK7 had both anti-inflammatory and pro-inflammatory tendencies but when phenotypic identification of the cell subset (in this case CD4+ cells) was performed, only two complexes altered cytokine production i.e. TTC24 and PFK5. For this study, because phenotypic identification of the relevant subset of cells (T cells here) was important for monitoring immunomodulatory effect, the ICCS data was considered relevant over the ELISA.

Table A4.3: Comparison of cytokine production levels between ICCS (CD4+ cells) and ELISAs (PBMCs). Cells were from HIV+ donors only. Except for PFK5 which lowered TNF- α levels from PBMCs when secreted cytokines were measured by ELISA, the rest of the four gold complexes that were compared caused increases in the production of both the IFN- γ and TNF- α . \uparrow represents an increase and \downarrow represents decrease both relative to untreated control.

	ICCS		ELISA	
	IFN- γ	TNF- α	IFN- γ	TNF- α
TTC24	\downarrow	No effect	\uparrow	\uparrow
PFK174	No effect	No effect	\uparrow	\uparrow
PFK5	No effect	\uparrow	\uparrow	\downarrow
PFK7	No effect	No effect	\uparrow	\uparrow

8.4 CHAPTER 5

8.4.1 Anti-RT Inhibitory Ability of Previously Anti-RT Complexes as Controls.

The anti-RT activity of the eight gold complexes (TTC3, TTC10, TTC17, TTC24, EK207, EK219, EK231 and KFK154b) previously shown to inhibit RT at a concentration range of 6.25 to 250 μM (Fonteh and Meyer, 2009, Fonteh *et al.*, 2009, Fonteh and Meyer, 2008) are shown in Table A5.1. The only compound which had close to 50% inhibition was the gold(III) pyrazolyl compound of class V which inhibited RT by 42% at 25 μM . There are a number of possible reasons for the loss in activity and these are enumerated below.

Table A5.1: Anti-RT activity of complexes with prior RT activity. These complexes which inhibited RT previously (when freshly prepared after synthesis) at a concentration range of 6.25- 250 μM appeared to have lost this ability possibly due to aging and other possible factors. KI is a known inhibitor which inhibited the enzyme by 94.7%.

Compound	% Inhibition of RT at 25 μM
KI (2 absorbance units)	94.7
$\text{HAuCl}_{4.4}\cdot\text{H}_2\text{O}$	-14.0
TTL3	15.2
TTC3	5.7
TTC10	17.2
TTC17	26.2
TTC24	-18.6
EK207	-2.78
EK219	-2.27
EK231	2.1
KFK154b	42.6

8.4.1.1 Poor aqueous solubility and solvent (DMSO) associated solubility limitations

The eight complexes that were reported to inhibit RT in the 2009 publications (Fonteh and Meyer, 2009, Fonteh *et al.*, 2009) and MSc. Dissertation (Fonteh and Meyer 2008) were freshly made up soon after synthesis (synthesised late 2006, and early 2007) and significantly inhibited RT at concentrations as low as 6.25 μM (complexes TTC24, EK207 and EK219) and up to 250 μM . For re-testing here (in 2009/2010), no new synthesis was performed and stored compounds (stored at -20 $^{\circ}\text{C}$ for 3 years either as powder/DMSO solutions) were used. Poor aqueous solubility was predicted for most of these complexes (TTC3, TTC10, TTC17, EK207, EK219 and EK231) except for TTC24 and KFK154b when ADMET prediction studies were done. Precipitation in biological media during wet lab studies was also observed. Complexes TTC3, TTC10 and TTC17 had aqueous solubility predictions of 1 (rated as possible) while EK207, EK219 and EK231 had aqueous solubility predictions of 0 (extremely low) and TTC24 and KFK154b were predicted to have aqueous solubility levels of 2 (low) and 4 (optimal) respectively (Table 3.8A). Compounds with poor aqueous solubility can affect bioassays by causing underestimated activity, reduced HTS hit rates, result in variable data, inaccurate SAR, discrepancies between enzyme and cell assays and inaccurate *in vitro* ADMET testing (Di and Kerns, 2006).

While aqueous solubility could have been a limitation, it is possible that freshly synthesised compounds dissolved easily in the solvent used and not after long term storage (particularly if

inherent hygroscopic abilities seen in ^1H NMR spectra for complex TTC3 and possibly the rest of the class I compounds were prevalent) further potentiating aqueous solubility problems. DMSO is the most common solvent used in drug studies (Waybright *et al.*, 2009, Janzen and Popa-Burke, 2009) but it is well known that long term storage in this solvent is detrimental due to precipitation and degradation problems that can ensue, which are further potentiated by uptake of water (Waybright *et al.*, 2009, Ellson *et al.*, 2005).

The predicted aqueous solubility problems and observed precipitation of these compounds in biological media coupled with the possibility of compound precipitation in solvent due to the presence of water (in compound) may therefore have played a role in the observed inconsistencies in the RT data.

8.4.1.2 NMR stability profile

A look at the stability data that was obtained for these complexes in d_6 -DMSO, especially for complexes TTC3, EK231 and KFK154b (with previous RT inhibition) when ^{31}P spectroscopy was performed, suggested that, TTC3 and EK231 remained stable on immediate dissolution, 24 h and 7 days later. However, in the ^1H spectrum of TTC3 (which could be extrapolated for the rest of the class I complexes which also inhibited RT), a water peak was evident on day zero (Figure A3.1), becoming more prominent at 24 h and 7th day. The water peak presumably became more apparent in the spectrum as a result of DMSO's hygroscopic nature. In the case where DMSO solutions of the compounds were used, fears that the compounds could have precipitated out of DMSO solutions were believed to be eliminated by the fact that only single use aliquots of DMSO/compound solutions were involved. In addition DMSO dissolved compounds were used within a week to reduce possible precipitation. While these conditions may prove to not be the best storage/usage methodology, given the nature of DMSO, these have been recommended by other authors (Waybright *et al.*, 2009, Janzen and Popa-Burke, 2009). Although some authors have advocated the use of freshly prepared samples each time (Kerns and Di, 2008) this cannot always be feasible when HTS is involved and when one is faced with limited starting material.

As for complex KFK154b, no water peak was observed in the ^1H NMR spectrum throughout the analysis. What was observed was a new peak after 24 h (4.75 ppm) and later at 7 days (4.6 ppm, slightly broader, See Figure A3.4) that was thought to be an impurity resulting from D_2O . It is not clear exactly how this peak appeared in the spectrum but may have been introduced during sample storage and transfer into NMR tubes (contaminant). Unfortunately re-tests could not be done to verify the source since sufficient quantities of the compound were not available. This new peak (if at all inherent for this complex) may be responsible for the observed RT data fluctuation that was seen for this complex.

NMR is a useful in the identification of a compound and has the capability of allowing for structure elucidation (Kenseth and Coldiron, 2004). However, limitations such as low sensitivity and spectral overlap can prevent the identification of impurities present in a sample (Kenseth and Coldiron, 2004). After three years of storing the gold complexes desiccated at -20 , it is possible

that impurities and breakdown products not detectable by NMR had developed. Such impurities could have altered the effect of the original compounds on RT resulting in the activity loss.

8.4.1.3 Compound age and solvent used at synthesis

Another likely reason for the discrepancy in the data is the fact that the compounds had aged. Three years is a long time and according to the NMR stability data, although the backbone structure of the complexes were maintained, the presence of water in the day zero spectra of complexes TTC3 and MCZS3 suggests inherent hygroscopic abilities which could potentially affect solubility. Additionally, one could speculate that some other component present at synthesis (e.g. residual solvent used in synthesis) may have been responsible for the observed RT inhibitory activity but this possibility still needs to be investigated. As a matter of fact, in 2006, two batches of compounds in class I were received from chemists and three of them had two different colours which the chemists attributed to the solvent used in synthesis and suggested that this would not influence structure (and therefore bioactivity of the active compound) since the analytical data was identical. For the two batches, TTC10 was cream white and then white, TTC17 was orange in colour and then subsequently a white product was received while TTC24 was purple and yellow in another batch. The concern now is if the solvent used during synthesis may have played a part in the observed RT inhibitory activity at the time and whether after 3 years, the solvent had evaporated and the activity was now lost as a result. Solvents such as DMSO, methanol and ethanol have been reported to inhibit RT activity (Tan *et al.*, 1991) with 10% DMSO being the least inhibitory while 10% ethanol inhibited the enzyme by as much as 100%. For the purposes of this study, DMSO concentrations were always kept below 1.5 %, a concentration which had no significant inhibitory ability (Fonteh and Meyer, 2008). Various solvents were used in the synthesis of the complexes e.g. dichloromethane and ethanol (Kriel *et al.*, 2007). Considering that complex colour could be influenced by solvent used, it is therefore not surprising that enzyme activity could also be affected. It is therefore recommended that compounds synthesised for bioactivity testing such as RT inhibitory assays should be devoid of synthetic solvent as much as possible.

8.4.1.4 Poor stereochemical interaction with the RNase H site of RT

From the docking studies, it was observed that the complexes were interacting more favourably with the RNase H site of RT. Since docking only depended on the chemical structure of the complexes, concerns about activity loss were not an issue. Although favourable enthalpic values were obtained for the binding of the ligands with the RNase site, the stereochemistry was very poor. Considering that proteins are very flexible (Mohan *et al.*, 2005, Höltje *et al.*, 2003), in the actual wet lab studies, such poor stereochemical orientations could mean that the ligands are easily displaced from the receptor leading to loss of activity. In a situation where the ligands were anchored to the active site, a presumed inhibitory activity was recorded.

8.4.1.5 Other concerns and future perspectives

Other concerns are how the issues mentioned above could have affected other wet lab assays done with these compounds. The fact that ADMET predictions for these compounds were really poor (except for complex TTC24 which was moderate with a score of 3/7 and KFK154b with a score of 6/7, Table 3.9) means that these compounds will require significant modification to be used as drugs and will potentially be very costly to develop further. TTC24 may still be a lead compound because of the inhibitory activity that was demonstrated in the infectivity studies at non-toxic concentrations (Figure 4.8) and the fact that it interacted with the RNase H site of RT more favourably in the *in silico* studies than any of the other complexes that inhibited RT previously (Table 5.4, Figure 5.6).

No re-tests were done for the compounds that inhibited PR since the concentrations at which the compounds inhibited the enzyme (100 μM) very cytotoxic (CC_{50} s were mostly below 20 μM).

8.4.2 IN 3'P and ST Inhibitory Assay

Bioassays for inhibition of HIV-1 IN were performed using the xPressBio integrase assay kit (Thurmont, MD, USA) for all the compounds at one concentration in triplicate. Four complexes (EK231, PFK7, PFK8 and PFK174) inhibited the enzyme by > 50% at non-toxic concentrations (Figure A5.1) with PFK174 inhibiting by 70% at 5 μM . Subsequent testing led to the results in B which was attributed to manufacturing problems that existed between the time the first kit (used in Figure A5.1A) was obtained to when the second one was (Figure A5.1B). The results obtained below are based on determining inhibition of the DNA integration process (3' P and ST steps). *In silico* predictions (with the Tscs-based compounds) suggested that binding to IN was not due to inhibition of DNA integration (Table 5.4, which was also shown for the ST assay, Figure 5.4) but was as a result of the compounds interacting with hotspot residues in the LEDGF binding sites. Because interactions were more with the LEDGF site and since no activity was observed in the ST specific assay (Figure 5.4), the conclusion was that these compounds were neither 3'P nor ST inhibitors. The data differences from the two kits (same principle, Figure A5.1) may well validate the problems that the kit manufacturer reportedly had when the product was ordered for repeats in the course of this study.

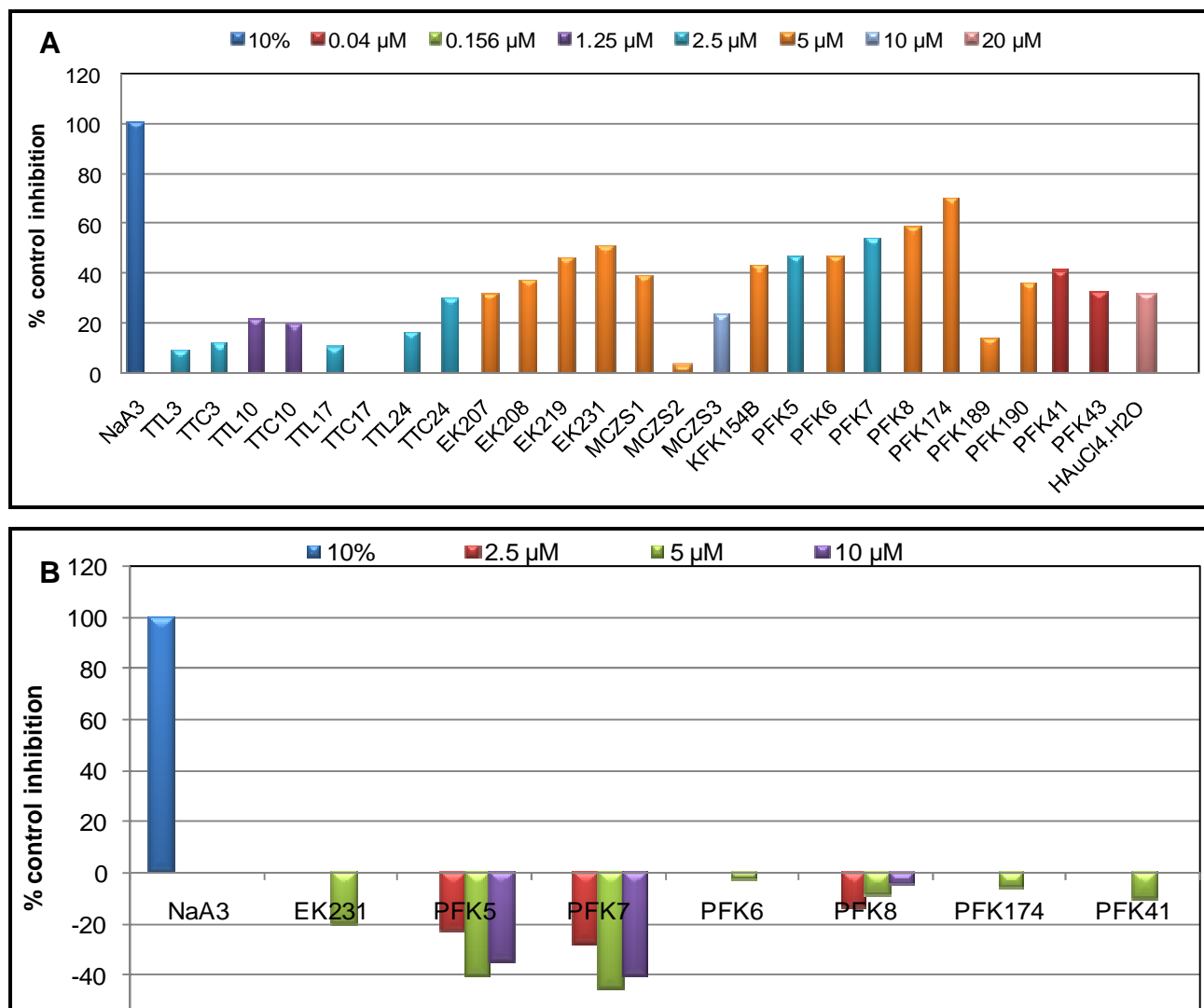


Figure A5.1: Effect of compounds on HIV-1 IN activity. (A) Four complexes (EK231, PFK7, PFK8, and PFK174) inhibited IN by $\geq 50\%$. In B, the assay was repeated for complexes EK231, PFK5, PFK7, PFK6, PFK8, PFK174 and PFK41. Surprisingly, all inhibitory values were negative. This finding was strange and might be related to manufacturing problems raised by manufacturer between the time the first experiment (A) was done and that in B. Inhibition values are relative to untreated control of enzyme only. A positive control sodium azide (NaA₃) inhibited IN by 100%. The most potent compound was PFK174 which inhibited the enzyme by 71% at 5 μ M.

8.4.3 Molecular Modelling

8.4.3.1 Summary of docked poses for each receptor

A summary of the successfully docked poses in the different active sites of the various enzyme targets i.e. RT, PR and IN are shown in Table A5.2. Variation between groups of compounds for a particular receptor site was more compared to that within groups and gave some perception of the flexibility of the different ligands in each receptor site which is represented by the number of possible poses. Inhibitors that are more flexible and which interact with a binding site more have a higher chance of remaining active in the event of a mutation since an alternative conformation assumed. Flexibility was the least for RT in the 3LP2 site compared to the 3LP3 site both in the presence and absence of Mn²⁺ while the 2WON site was intermediary (Table A5.2). KFK154B was the most flexible ligand in all the binding sites. The Tscs ligands docked with similar number of poses in each of the IN active sites and demonstrated relatively high flexibility with a minimum of 21 and a maximum of 49 poses.

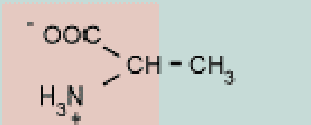
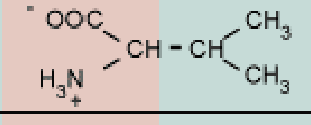
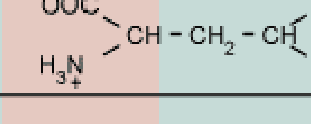
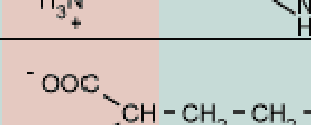
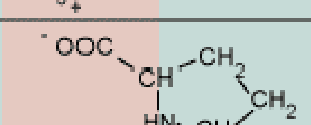
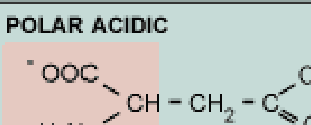
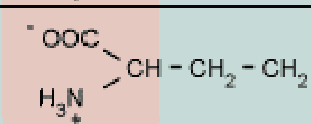
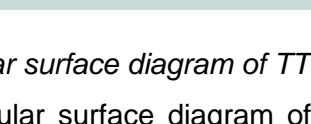
Table A5.2: Number of successfully docked poses of the compound with different enzymes and sites. Except for KFK154b, the 3LP2 site of RT resulted in the lowest number of poses indicating poor flexibility of the ligands in this site. The free ligands are colour coded in grey. The superscript a (^a) represents ligands for which atomic charges could not be read and x represents ligands that had no refined docked poses possibly because of poor complementarity due to ligand stereochemical structure.

Compound	HIV-1 RT				HIV-1 PR		HIV-1 IN		
	3LP2	3LP3 + Mn ²⁺	3LP3- Mn ²⁺	2WON	1HXW	2R5P	ISQ4	3L3V	2B4J
Control		30							
TTC3	16	42	37	24					
TTL10	4	35							29
TTC10	20	48	44	19					41
TTL17	2								
TTC17	11	44	32	23					
TTL24	11	32							
TTC24	11	49	41	25	20	19			
EK207	x	x	x	x					
EK208					x	x			
Ek219	x	x	x	x					
EK231	x	x	x	x				x	49
MCZS1					17	^a			
MCZS3					49	^a			
KFK154B	46	50	47	28 ^a	48	45 ^a			
PFK5							31	21	33
PFK7					10		39	46	46
PFK8							39	29	44
PFK41							27	39	44
PFK174							33	x	49

8.4.3.2 Structure of amino acids

Table A5.3 represents the structure of the 20 amino acids. The three letters and one letter identification codes are shown as well as the classification into non polar or hydrophobic, polar acidic and polar basic.

Table A5.3: Table of amino acid structures. Retrieved from <http://www.hotindir.com/wp-content/uploads/2010/10/amino-acids.gif> (assessed on the 4th February 2011)

NONPOLAR, HYDROPHOBIC		POLAR, UNCHARGED	
Alanine Ala A MW = 89		R GROUPS	Glycine Gly G MW = 75
Valine Val V MW = 117			Serine Ser S MW = 105
Leucine Leu L MW = 131			Threonine Thr T MW = 119
Isoleucine Ile I MW = 131			Cysteine Cys C MW = 121
Phenylalanine Phe F MW = 131			Tyrosine Tyr Y MW = 181
Tryptophan Trp W MW = 204			Asparagine Asn N MW = 132
Methionine Met M MW = 149			Glutamine Gln Q MW = 146
Proline Pro P MW = 115		POLAR BASIC	Lysine Lys K MW = 146
Aspartic acid Asp D MW = 133			Arginine Arg R MW = 174
Glutamine acid Glu E MW = 147			Histidine His H MW = 155

8.4.3.3 Molecular surface diagram of TTC10 in the RNase H site of RT

A molecular surface diagram of TTC10 and the RNase H site is shown in Figure A5.2. Anchored to this site appears to be facilitated as a result of the cation-pi interaction predicted with the imidazole ring of His539. Complementarity was limited as most of the groups were not satisfied (were solvent exposed). This poor complementarity is easily visible in a surface diagram like the one shown here unlike in the ribbon diagram in Figure 5.6 which has the advantage of better visibility of interactions e.g. H-bond and pi-pi interactions.

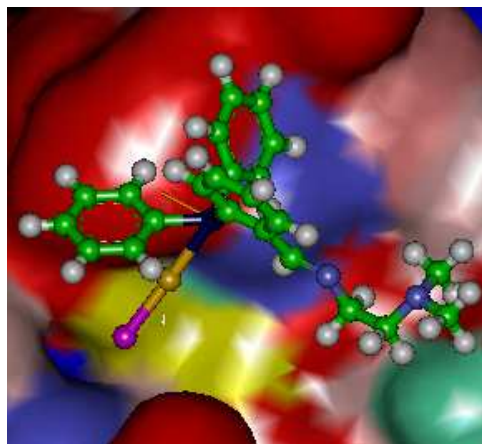


Figure A5.2: Molecular surface diagram of TTC10 in the RNase H active site. Red patches represent totally hydrophilic amino acid residues, blue patches contain totally hydrophobic amino acid residues and the other colours are between the hydrophobic and hydrophilic scale (Kyte and Doolittle, 1982).

8.4.3.4 KFK154B binding to 3LP3 in the presence of Mn^{2+} ions

The flexibility seen for KFK154b (Table A5.2) appears to be detrimental in its binding to a defined active site. Figure A5.3 shows KFK154B binding to regions outside the defined sphere of binding. Although the binding energy for this compound to the RNase H site appears to be comparatively favourable (10.4 kcal/mol), the fact that the compound interacts with more than one site (sites which probably have not been defined as active sites) makes the observed interactions inconclusive with respect to RNase H binding.

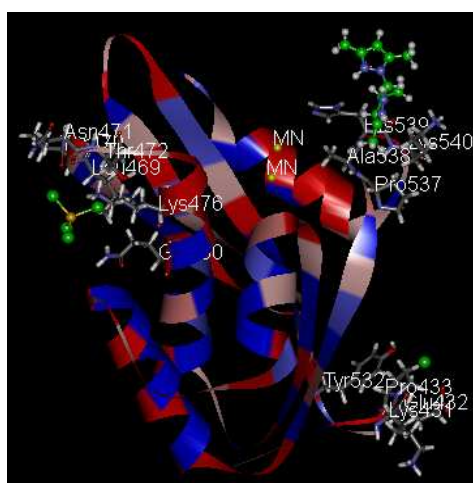


Figure A5.3: Predicted binding interactions between KFK154b and the RNase H binding site of RT. The ligand interacted with three different sites of the receptor. Because two of these sites are out of the defined sphere of binding, the predicted interactions and binding energy of 10 kcal/mol does not represent RNase H binding.

8.4.3.5 Molecular surface diagram of PFK5 and PFK7 with the LEDGF binding site of IN

Molecular surface diagrams of the receptor showing interactions of PFK5 (A5.4A) and PFK7 (A5.4B) with the LEDGF binding site of IN are shown in Figure A5.4. PFK5 which had a lower binding free energy (8.9 kcal/mol compared to 13.2 kcal/mol for PFK7) did not fit into the mostly hydrophobic pocket as snugly as PFK7.

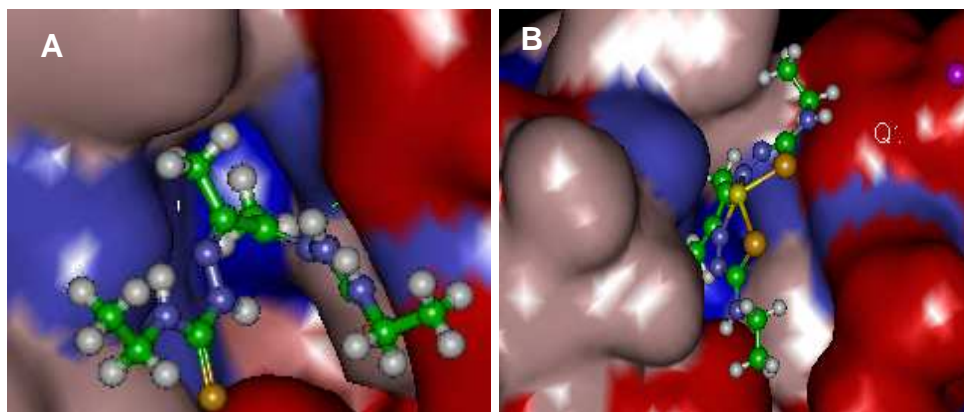


Figure A5.4: Molecular surface diagram of PFK5 (A) and PFK7 (B) with the LEDGF binding site of HIV IN. PFK7 fits more snugly into this site than PFK5 which is the corresponding free ligand. Red patches represent totally hydrophilic amino acid residues, blue patches contain totally hydrophobic amino acid residues and the other colours are between the hydrophobic and hydrophilic scale.

8.4.3.6 Molecular surface diagram of PFK7 with the sucrose binding site of IN

The binding free energy of PFK7 with the sucrose binding site was 42.3 kcal/mol for the most favoured pose. The ligand's interaction with this (which is 10 Å from the LEDGF binding site) evidently shows poor complementarity compared to those with the LEDGF binding site (13.2 kcal/mol). The ligand appears to lie across the dimer interface in an attempt to make hydrophobic interactions with the ethyl groups at N1 and N6 while the hydrophobic diacetyl portion in the groove is not satisfied by the predominantly positively charged and negatively charged amino acids. The presence of H-bond donor or acceptor groups at this point would have been more favoured.

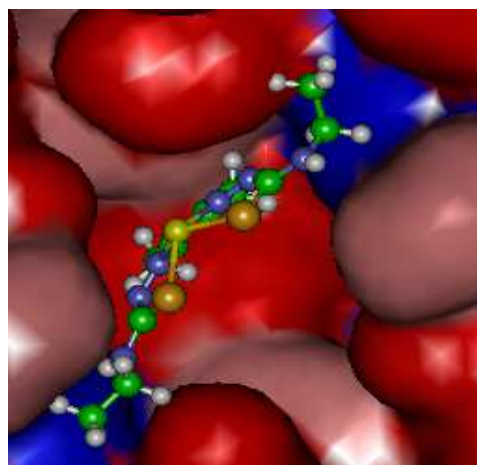


Figure A5.5: Molecular surface diagram of PFK7 in the sucrose binding site (3L3V) of IN. Very poor complementarity was observed for the ligand with this site (binding free energy was 42.3 kcal/mol). Red patches represent totally hydrophilic amino acid residues, blue patches contain totally hydrophobic amino acid residues and the other colours are between the hydrophobic and hydrophilic scale.

GLOSSARY

The following is a list of the meanings of important terminology that was used in this thesis. A majority of the definitions were taken from one of the following sources; Kerns and Di., (2008), Goldsby *et al.*, (2000), Petsko and Ringe (2004), Comba and Hambley, (1993), and Dictionary.com. Specific reference sources are indicated next to the word.

Active site: asymmetric pocket on or near the surface of a macromolecule that promotes chemical catalysis when the appropriate ligand or substrate binds.

Affinity: Tightness of a protein-ligand complex

Allosteric inhibitor: A ligand that binds to a protein and induces a conformation change that decreases the protein's activity.

Allosteric site: A site on an enzyme which is not the substrate site but which reversible binding by another inhibitor can result in conformational changes that alters can alter its catalytic property.

Anti-inflammatory cytokine: Cytokine that prevents systemic inflammation.

Cation- π interaction: This is a strong non covalent force between a cation e.g. Li^+ and the π face of an aromatic ring e.g. benzene ring.

CCR5 antagonists: Small molecule allosteric inhibitors of the human CCR5 chemokine receptor which binds to the CCR5 receptor and is thought to alter the conformational state of the CCR5 receptor.

CD4+: A glycoprotein that serves as a coreceptor on MHC class II restricted T cells, mostly T helper cells.

CDOCKER: Stands for CHARMM-based DOCKER which is a grid-based docking algorithm.

Cell index: Unit for measuring cellular impedance or resistance on a RT-CES analyser which is directly related to the adhering ability of the cells.

Cell line: a population of cultured tumour cells or normal cells that have been subjected to chemical or viral transformation. Cell lines can be propagated indefinitely.

Chemokines: Family of small cytokines or proteins secreted by cells.

Chrysotherapy: Chrysotherapy (from the Greek word for gold-chrysos) or aurotherapy are terms used to describe the treatment of ailments with gold compounds.

Cofactor: A small non protein molecule or ion that is bound in the functional site of a protein and assists in ligand binding or catalysis or both. The may be bound covalently or otherwise.

Complex: In chemistry, a **coordination complex** or **metal complex** is a structure consisting of a central atom or ion (usually metallic), bonded to a surrounding array of molecules or anions (ligands or complexing agents).

Complexation: Chemical reaction involving a metal and an organic ligand.

Constraint: Mathematically precise fixing of internal coordinates

CTL: An effector T cell (usually CD8+) that can mediate the lysis of target cells bearing antigenic peptides complexed with an MHC molecule.

CYP450: A family of isoenzymes that absorb light at 450 nm and oxidise compounds in many tissues (found in high abundance in the liver).

Cytokine: low molecular weight proteins that regulate the intensity and duration of an immune response by exerting a variety of effects on lymphocytes and other immune cells.

Cytostatic: tending to retard cellular activity and multiplication.

Dimer: An assembly of two identical (homo-) or different (hetero-) subunits.

Dmol3: This is a programme used in simulating chemical processes and predicting the properties of materials. It is used in solving quantum mechanical equations.

Donor atom: The atom within a ligand (in coordination chemistry) that is directly bonded to the central atom or ion.

Drug-like: molecules which contain functional groups and or have physical properties consistent with the majority of known drugs.

Electrostatic interactions: Non covalent interactions between atoms or groups of atom due to attraction of opposite charges.

Enthalpy: A form of energy equivalent to work that can be released or absorbed as heat under constant pressure.

Entropy: a measure of the disorder or randomness in a molecule or system.

Esterases: Enzyme that hydrolyses an ester into an alcohol and an acid.

Ex vivo: Outside of a living organism

Force field: The “unstrained” values of bond lengths, angles and torsions plus non-bonded interactions that are used as a reference for the calculation of the total steric energy of a molecule in terms of deviations from the “unstrained” (Höltje *et al.*, 2003)

Free energy: a function designed to produce conditions for a spontaneous change that combined **entropy** and **enthalpy** of a molecule or system. Free energy decreases for a spontaneous process and is unchanged at equilibrium.

H-bond acceptor: Electronegative atom (e.g. N, O, F) that may accept a hydrogen bond.

H-bond donor: hydrogen atom attached to a relatively electronegative atom that may form a hydrogen bond.

H-bond: a non covalent interaction between a donor atom which is bound to a positively polarized hydrogen atom and the acceptor which is negatively polarized holding both the donor and acceptor close together.

Hepatotoxicity: Drug induced liver toxicity.

High throughput screening: Performing assays at a high rate using large compound libraries.

Hit: compound that is active in HTS or in initial screens.

Hydrophilic: Tending to interact with water

Hydrophobic: Tending to avoid water.

Hygroscopic: Absorbs water from the atmosphere

Hypersensitive: Adaptive immune response occurring in an exaggerated or inappropriate form and causing tissue damage. It is a characteristic of an individual and is manifested on second contact with an antigen.

Immunomodulatory: An immunological change in which one or more immune system molecules are altered through suppression or stimulation.

Impedence: Resistance

In silico: Performed using a computer and specially developed software

in vitro: referring to experiments performed in a laboratory vessel (e.g. test tube, well of a microtiter plate), outside the living organism but tissue involved need not be in culture as is the case with *ex vivo* assays.

in vivo: Performed in a living organism.

Lead: compound that is currently the most favourable in a discovery project and that can serve as a template for the design of analogues during lead optimisation

Ligand (a): In computational terms it means the complementary partner molecule which binds to the receptor. Ligands are most often small molecules but could also be another macromolecule or biopolymer. (b): it is a small molecule or macromolecule that recognises and binds to a specific site or a macromolecule.

Ligand (a): In coordination chemistry, it is an ion, molecule or functional group that binds to a central metal atom to form a coordination complex.

Lipophilicity: The affinity of a molecule or a moiety for a lipid or non polar environment.

Metallo drug: chemically synthesized agents containing a metal complexed to a suitable ligand.

MHC: A complex of genes encoding cell-surface molecules and are required for antigen presentation to T cells and for rapid graft rejection. It is called H-2 complex in mouse and HLA complex in humans.

Microbicide: any compound or substance whose purpose is to reduce the infectivity of microbes, such as viruses or bacteria.

Molecular dynamics: In modelling, it is a simulation method where the interaction of atoms is monitored over time using the equations of motion. It follows the equations of classical mechanics or Newton's laws.

Molecular Mechanics: Calculation of the molecular structure and the corresponding strain energy by minimisation of a total energy calculated using functions which relate internal coordinates to energy values (Comba and Hambley, 1995)

Molecular modelling/docking: 1) the science (or art) of representing molecular structures numerically and simulating their behaviour with the equations of quantum and classical physics. **OR 2)** the visualisation and analysis of structures, molecular properties (thermodynamics, reactivity, spectroscopy), and molecular interactions, based on a theoretical means for predicting the structures and properties of molecules and complexes (Comba and Hambley, 1995) **OR 3)** computational simulation of a candidate ligand binding to a receptor.

Molecular structure: Three-dimensional arrangement of atoms in a molecule.

Partial Charge: Charge of an atom in a polar molecule due to differences in electronegativity.

Phosphodiester bond: A covalent bond in RNA or DNA that holds a polynucleotide chain together by joining a phosphate group at position 5 in the pentose sugar of one nucleotide to the hydroxyl group at position 3 in the pentose sugar of the next nucleotide.

Pi-pi interaction: Non-covalent interactions that occur between the faces of phenyl rings.

Plasma: The pale yellow or gray-yellow, clotting factor-containing fluid portion of the blood which unlike serum contain clotting factors.

Pose: A candidate binding mode or a unique target bound orientation or conformation of a ligand.

Pro-inflammatory cytokine: cytokine that would promote systemic inflammation.

Quantum mechanics: This is a branch of physics that provides a mathematical description to the dual particle-like and wave-like behaviour and interaction of matter and energy.

Ranking: the process of classifying which ligands are most likely to interact favourably to a particular receptor on the predicted free-energy of binding.

Receptor: the “receiving” molecule most commonly a protein or other biopolymer.

Rotatable bonds: Rotatable bond is defined as any single non-ring bond, bounded to non terminal heavy (i.e. non-hydrogen) atom. Amide C-N bonds are not considered because of their high rotational energy barrier.

Recombinase: An enzyme that catalyses the exchange of short pieces of DNA between two long DNA strands, particularly the exchange of homologous regions between the paired maternal and paternal chromosomes.

Resolution: The level of detail that can be derived from a given process.

Restraints: Fixation of a structural parameter by artificially large force constants to drive an internal coordinate close to a selected value.

Salvage therapy: A final treatment for people who are nonresponsive to or cannot tolerate other available therapies for a particular condition and whose prognosis is often poor.

Scoring: This is the process of evaluating the strength of the non covalent interactions (or binding affinity) that a particular pose has with a receptor after docking.

Senescence: When a cell loses its ability to divide after a certain number of divisions.

Shake flask: laboratory vessel in which partitioning e.g. Log P or equilibrium solubility experiments are performed.

Strain energy: the energy penalty associated with deforming an internal coordinate (Comba and Hambley, 1995)

Strain: The deformation of a molecule that results from stresses

Synovium: Thin layer of tissue which lines the space between joints.

van der Waal interaction: A weak attractive force between two atoms or groups of atoms arising from the fluctuation in electron distribution around the nuclei. Van der Waals forces are stronger between less electronegative atoms such as those found in hydrophobic groups.

Virostatics: A combination of drugs which includes one directly inhibiting virus (*viro*) e.g. didanosine and one indirectly inhibiting virus (*static*) e.g. hydroxyurea (Lori *et al.*, 2005, 2007).